ACCSCIENCE PUBLISHING

Tumor Discovery

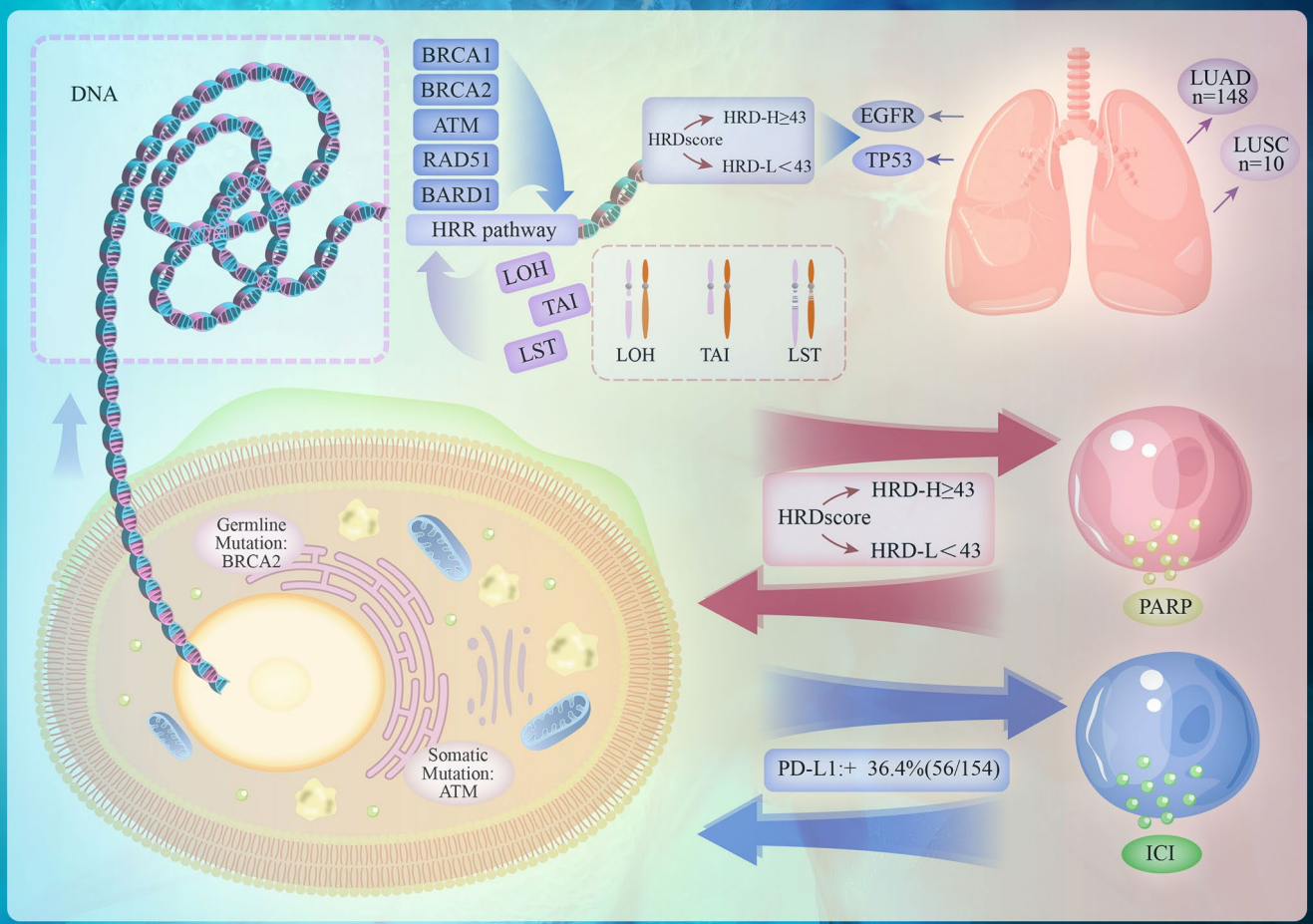

Genomic alterations of homologous recombination deficiency in Chinese NSCLC patients

ISSN: 3060-8597 (Print)
ISSN: 2810-9775 (Online)
Volume 4 • Issue 3
September 2025

Tumor Discovery

Print ISSN: 3060-8597
Online ISSN: 2810-9775

Tumor Discovery is a peer-reviewed and open-access journal that aims to present new cancer research with strong emphasis on fundamental and translational studies. *Tumor Discovery* covers topics such as etiology and pathogenesis of cancer, mechanisms and molecular pathways underlying cancer initiation and progression, tumor metastasis, etc.

Scan to access website:

Scan to submit papers:

About the Publisher

AccScience Publishing is a publishing company based in Singapore. We publish a range of high-quality, open-access, peer-reviewed journals and books from a broad spectrum of disciplines.

Contact Us

Managing Editor
td.office@accscience.sg

AccScience Publishing
9 Raffles Place, Republic Plaza 1 #06-00 Singapore 048619.

Volume 4 • Issue 3 • September 2025
ISSN 3060-8597 (print) ISSN 2810-9775 (online)

TUMOR DISCOVERY

ACCSCIENCE PUBLISHING

Access Science Without Barriers

TUMOR DISCOVERY

ISSN: 3060-8597 (print)
ISSN: 2810-9775 (online)

Editorial and Production Credits

Publisher: AccScience Publishing
Managing Editor: Alice Liu
Production Editor: Sharmila Velapasamy
Article Layout and Typeset: Sinjore Technologies (India)

For all advertising queries, contact td.office@accscience.sg.

Supplementary file

Supplementary files of articles can be obtained at https://accscience.com/journal/TD/4/3.

Disclaimer

AccScience Publishing is not liable to the statements, perspectives, and opinions contained in the publications. The appearance of advertisements in the journal shall not be construed as a warranty, endorsement, or approval of the products or services advertised and/or the safety thereof. AccScience Publishing disclaims responsibility for any injury to persons or property resulting from any ideas or products referred to in the publications or advertisements. AccScience Publishing remains neutral with regard to jurisdictional claims in published maps and institutional affiliations.

Tumor Discovery

Editorial Board

Youth Editorial Board Members

*Editorial Board Members as of September 23, 2025

ACCSCIENCE PUBLISHING

Volume 4 | Issue 3 | September 2025 | Page 1 – 112 |

Tumor Discovery

https://accscience.com/journal/TD

CONTENTS

REVIEW ARTICLES

1 **FBXW7 in leukemia: A critical regulator of oncogenic stability and a potential therapeutic target**
Xiuming Li, Bin Liu

16 **Emerging immunomodulatory effects of CDK4/6 inhibitors in breast cancer therapy: A comprehensive review**
Yuling Zhang, Bingfeng Chen, Siyue Lin, Rendong Zhang, Jundong Wu, Chunfa Chen

ORIGINAL RESEARCH ARTICLES

32 **Genomic alterations of homologous recombination deficiency in Chinese NSCLC patients**
Shuang Xiang, Changqiong Shen, Chun Huang, Ya-ting Yang, Jing Guo, Yi Liu, Mingzhu Yin, Song Duan

46 **Prognostication in palliative cancer care: Both probabilities and uncertainties must be taken into account**
Erik Torbjørn Løhre, Ragnhild Hansdatter Habberstad, Tora Skeidsvoll Solheim, Pål Klepstad, Gunnhild Jakobsen, Morten Thronæs

58 **Highly specific and sensitive gene panels for cancer screening: First application of only-normal and only-tumor genes**
Gabriel Gil, Claudia Carricarte, Julio C. Drake-Pérez, Yasser Perera, Augusto Gonzalez

70 **Magnesium-28: A theorical novel self-theranostic strategy targeting metabolic enzyme disruption and intracellular irradiation**
Tran Van Luyen

SHORT COMMUNICATION

81 **Sorafenib generates microvesicle particles in non-small cell lung cancer**
Yevgeniy Gladkiy, Anita Thyagarajan, Morgann Hendrixson, Ravi P. Sahu

CASE REPORTS

92 **Complete response after two cycles of enfortumab vedotin in a patient with metastatic bladder cancer: A case report**
Ali Kaan Güren, Murat Sari, Osman Köstek

96 **An unusual case of malignant biliary tract obstruction**
Sakditad Saowapa, Chalothorn Wannaphut, Hector Jose Garcia Pleitez, Andrea Ortiz Maldonado, Miriam Alicia Paz Sierra, Natchaya Polpichai, Pharit Siladech, Meenu Sharma, Lukman Tijani

100 **Challenges and considerations in diagnosing mature teratoma during pregnancy: A case report**
Sumaira Siddiqui

105 **Chemotherapy-induced ileus and gastrointestinal hemorrhage following therapy with BrECADD for Hodgkin lymphoma: A case report**
Karl Mayrhofer, Simon Udovica

LETTER TO EDITOR

110 Redefining the role of radiation oncologists in the AI era
Melek Yakar

ACCSCIENCE PUBLISHING

Tumor Discovery

REVIEW ARTICLE

FBXW7 in leukemia: A critical regulator of oncogenic stability and a potential therapeutic target

Xiuming Li and Bin Liu*

Jiangsu Key Laboratory of Marine Pharmaceutical Compound Screening, College of Pharmacy, Jiangsu Ocean University, Lianyungang, Jiangsu, China

(This article belongs to the *Special Issue: Advances in Tumor Immune Regulation: Mechanisms and Therapeutic Insights*)

Abstract

F-Box and WD repeat domain-containing 7 (FBXW7) is a key tumor suppressor and substrate-recognition component of the Skp1-Cullin-F-box E3 ubiquitin ligase complex, responsible for targeting several crucial oncogenic proteins for proteasomal degradation. It plays a significant role in preventing the accumulation of pro-oncogenic substrates, thereby maintaining cellular homeostasis. Mutations or inactivation of FBXW7 disrupt these processes, leading to the stabilization of oncogenic proteins such as c-Myc, Notch, myeloid cell leukemia 1, and cyclin E, which drive malignant transformation in several cancers, including hematological malignancies such as T-cell and B-cell acute lymphoblastic leukemia. These mutations contribute to resistance to apoptosis, dysregulated proliferation, and poor prognosis, highlighting FBXW7 as a critical factor in leukemia pathogenesis and a promising therapeutic target. Here, we review FBXW7's structure and function, its key substrates in leukemia, and therapeutic strategies that restore its function or target the oncogenic pathways it regulates. Advances in genome-wide CRISPR screenings and proteomics have further illuminated FBXW7's involvement in multidrug resistance, positioning it as a biomarker and therapeutic target for improving leukemia treatment outcomes.

Keywords: F-Box and WD repeat domain-containing 7; Leukemia; Ubiquitin-proteasome pathway; c-Myc; Notch; Myeloid cell leukemia 1; Tumor suppressor; Therapeutic target

***Corresponding author:**
Bin Liu
(liubin@jou.edu.cn)

Citation: Li X, Liu B. FBXW7 in leukemia: A critical regulator of oncogenic stability and a potential therapeutic target. *Tumor Discov*. 2025;4(3):1-15.
doi: 10.36922/TD025150027

Received: April 11, 2025

Revised: May 16, 2025

Accepted: May 20, 2025

Published online: June 6, 2025

1. Introduction

1.1. Overview of leukemia

Leukemia is a highly heterogeneous hematologic malignancy, characterized by the abnormal proliferation of leukemia cells in the hematopoietic system.[1] These cells lose normal regulation of proliferation and differentiation. This condition often arises from clonal genetic mutations in hematopoietic stem or progenitor cells, which cause these cells to transform into leukemia cells under uncontrolled conditions.[2] Genetic mutations, chromosomal aberrations, and epigenetic alterations not only grant leukemia cells abnormal proliferative capacity but also lead to the loss of normal differentiation function.[3] As a result, these cells remain in an undifferentiated or poorly differentiated

state, unable to complete normal differentiation programs, and continue to proliferate in the bone marrow, peripheral blood, and other tissues. This abnormal proliferation is driven by dysregulated cell cycle control, differentiation inhibition, and enhanced self-renewal ability. For example, certain leukemia cells acquire specific mutations that disrupt negative feedback regulation of proliferation, further exacerbating uncontrolled cell division by altering cyclin expression or activating abnormal signaling pathways.[4] In addition, these leukemia cells typically lack the ability to respond to death signals, allowing them to evade apoptosis and enhance their survival within the body.[5] The unchecked proliferation of leukemia cells breaks through normal regulatory mechanisms, leading to the accumulation of large numbers of leukemia cells in the blood, disrupting hematopoiesis, and triggering a series of clinical symptoms, including anemia, thrombocytopenia, and neutropenia, which manifest as fatigue, bleeding tendencies, and increased susceptibility to infections.[6] Since normal hematopoietic cells in the bone marrow are replaced by leukemia cells, the patient's immune function is severely compromised, making them highly susceptible to bacterial, viral, and other infections, further exacerbating the condition.[7] Therefore, the treatment of leukemia requires not only controlling the proliferation of leukemia cells but also restoring the normal function of the hematopoietic system, alleviating the patient's clinical symptoms, and improving their quality of life and survival rate.

Leukemia is broadly classified based on the lineage of the affected hematopoietic cells (myeloid or lymphoid) and the degree of cellular maturity (acute or chronic).[8] The most common types of leukemia include (Figure 1):

(i) Acute myeloid leukemia (AML)[9]: Characterized by the rapid accumulation of immature myeloid blasts in the bone marrow.[10]
(ii) Acute lymphoblastic leukemia (ALL)[11]: Involves immature lymphoblasts and is more common in children.[12] ALL can be further subdivided into T-cell ALL (T-ALL)[13] and B-cell ALL (B-ALL).[14]
(iii) Chronic myeloid leukemia (CML)[15]: Typically progresses from a chronic phase with more mature myeloid cells to a more aggressive blast crisis.[16]
(iv) Chronic lymphocytic leukemia (CLL)[17]: A slow-growing leukemia of more mature lymphocytes, commonly affecting older adults.

The clinical manifestations of leukemia include fatigue, recurrent infections, easy bruising, and bleeding,[18] caused by the impaired production of normal blood cells.[19] Advances in molecular diagnostics have revealed a wide array of genetic mutations driving the various leukemia subtypes.[20] Key oncogenes and tumor suppressors, such as NOTCH1 in T-ALL[21] and Breakpoint Cluster Region–Abelson (BCR–ABL)[22] in CML, are implicated in the development and progression of these malignancies. Understanding the molecular landscape of leukemia has enabled more precise diagnostic tools and targeted therapies.

1.2. Leukemia in China: Incidence and risk factors

In China, leukemia remains a major public health issue, particularly affecting children and young adults.[23,24] The high incidence of leukemia, along with challenges in early diagnosis and treatment, poses complex health threats to this population. Due to the incomplete development of the immune system in children and young people, coupled with susceptibility to environmental pollution, genetic factors, and other influences, the incidence of leukemia is especially prominent in this group.[25] Recent epidemiological data indicate that the annual incidence of leukemia is approximately 3 – 4 cases per 100,000 people,[26] with ALL being the most common cancer among children,[27] peaking between the ages of 2 and 5.[28] In adults, the incidence of AML and CLL is relatively higher.[29] Leukemia has become one of the leading causes of cancer-related deaths among children and young adults in China. This phenomenon highlights the urgent need for improvements in early diagnosis, effective prevention, and treatment strategies for leukemia, to reduce the disease burden and improve patient survival rates.

Multiple factors are associated with the etiology of leukemia, including genetic susceptibility, environmental exposures (e.g., radiation, benzene, and pesticides), and viral infections. For instance, exposure to ionizing radiation or chemical carcinogens has been linked to increase leukemia risk.[30] Genetic predisposition also plays a role, with certain inherited disorders, such as Li–Fraumeni syndrome[31] and Fanconi anemia,[32] predisposing individuals to leukemia. In addition, viral infections such as Epstein-Barr virus[33] and human T-cell lymphotropic virus type 1[34] have been implicated in the development of leukemia.

1.3. Molecular pathogenesis of leukemia

Leukemia arises from the accumulation of genetic mutations[35] and chromosomal abnormalities[36] that disrupt normal cell signaling pathways, cell cycle checkpoints, and apoptosis. These genetic lesions often involve oncogenes, tumor suppressor genes, and epigenetic regulators, which collectively drive the clonal expansion of leukemic cells.

For example, BCR-ABL, generated by the t(9;22) chromosomal translocation, is a characteristic marker of CML.[37] The BCR-ABL fusion protein possesses

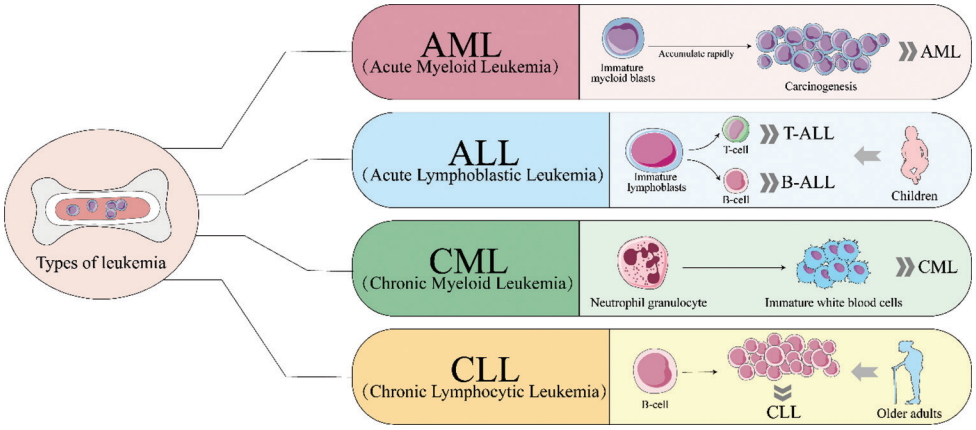

Figure 1. The most common types of leukemia
Abbreviations: B-ALL; B-cell acute lymphoblastic leukemia; T-ALL: T-cell acute lymphoblastic leukemia.

constitutively active tyrosine kinase activity,[38] which drives uncontrolled cell proliferation by activating downstream signaling pathways such as RAS/MAPK,[39] PI3K/AKT,[40] and STAT5,[41] thereby promoting leukemia development. Similarly, in AML, mutations in genes such as *FLT3*,[42] *NPM1*,[43] and *CEBPA*[44] are also common. These mutations lead to abnormal proliferation of myeloid precursor cells and inhibit their differentiation process. In T-ALL, mutations in the *NOTCH1* gene are frequently observed, resulting in continuous activation of the Notch signaling pathway, which promotes T-cell proliferation and leukemia progression.[45] Typical symptoms of T-ALL include persistent fever, lymphadenopathy, hepatosplenomegaly, anemia, bleeding tendencies (such as petechiae or epistaxis), and increased susceptibility to infections.[46] In addition, mutations in tumor suppressor genes such as F-box and WD repeat domain-containing 7 (*FBXW7*) are also common genetic alterations in T-ALL and other types of leukemia.[47] As an important regulatory factor, FBXW7 is responsible for the degradation of key oncogenic proteins. When FBXW7 function is lost, the stability of its oncogenic substrates, such as c-Myc and Notch, increases, further promoting leukemia progression and potentially leading to treatment resistance.[48] Therefore, understanding these genetic alterations is of critical importance for the diagnosis, prognostic assessment, and development of targeted therapeutic strategies for leukemia.

Treatment approaches for leukemia have evolved considerably in recent decades, with the advent of chemotherapy, targeted therapies, immunotherapy, and hematopoietic stem cell transplantation.[48] However, many patients develop resistance to therapy, relapse, or experience significant toxicity, underscoring the need for novel therapeutic approaches that target the underlying molecular mechanisms of leukemia.

2. Structure and function of FBXW7

2.1. Structural insights into FBXW7

FBXW7 (also known as hCDC4 or SEL-10)[49] is one of the best-characterized members of the F-box protein family. As part of the Skp1-Cullin-F-box (SCF) E3 ubiquitin ligase complex, FBXW7 serves as the substrate recognition subunit,[50] targeting specific proteins for ubiquitin-mediated degradation through the proteasome. The degradation of these substrates is essential for regulating critical cellular processes such as cell cycle progression, apoptosis, differentiation, and signal transduction.

Substrate specificity of FBXW7 is dictated by its WD40 repeat domain,[51] a β-propeller structure that recognizes phosphorylated degron motifs on its target proteins.[52] This interaction is dependent on the phosphorylation status of the substrate, often mediated by upstream kinases like glycogen synthase kinase 3.[53] Once a substrate is phosphorylated at specific serine or threonine residues, FBXW7 binds to the phosphorylated degron, marking the protein for ubiquitination.[54]

The F-box domain, located at the N-terminal region of FBXW7, binds to Skp1,[55] anchoring FBXW7 to the larger SCF complex. Together with Cullin1 (Cul1)[56] and Rbx1 (Roc1),[57] the SCF complex facilitates the transfer of ubiquitin from an E2-conjugating enzyme to the substrate, tagging it for proteasomal degradation. This modular structure allows FBXW7 to play a crucial role in maintaining protein homeostasis by regulating the timely turnover of key regulatory proteins involved in oncogenesis (Figure 2).

2.2. The role of FBXW7 in cellular homeostasis and tumor suppression

FBXW7 is integral to the regulation of several key cellular processes, including cell cycle progression, apoptosis,

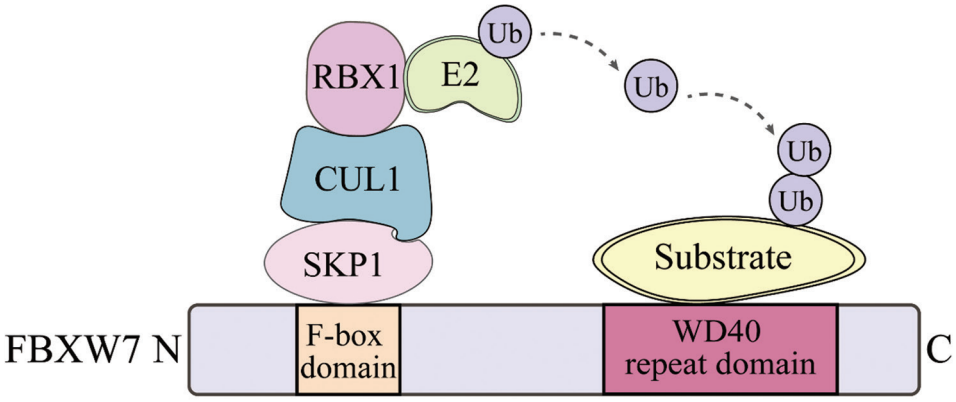

Figure 2. Structure and function of FBXW7
Abbreviations: CUL1: Cullin 1; E2: Ubiquitin-conjugating enzyme E2; FBXW7: F-box and WD repeat domain-containing 7; RBX1: RING-box protein 1; SKP1: S-phase kinase-associated protein 1; Ub: Ubiquitin.

and differentiation.[58] By targeting oncogenic proteins for degradation, FBXW7 prevents their accumulation and ensures that cells progress through the cell cycle in a controlled manner, undergo apoptosis when necessary, and maintain proper differentiation. Some of the major processes regulated by FBXW7 include (Figure 3):

(i) Cell cycle regulation: FBXW7 controls the progression of the cell cycle by degrading cyclin E,[59] a key regulator of the G1-to-S phase transition.[60] In the absence of FBXW7, cyclin E levels become dysregulated, leading to unchecked entry into S phase, excessive DNA replication stress, and genomic instability.[61]

(ii) Apoptosis: FBXW7 also regulates apoptosis by targeting the anti-apoptotic protein Myeloid cell leukemia 1 (MCL-1) for degradation.[62] By maintaining the appropriate levels of MCL-1, FBXW7 ensures that cells with significant DNA damage or other stressors undergo apoptosis. Dysregulation of MCL-1 degradation due to FBXW7 loss contributes to apoptosis resistance[63] and tumor survival.[64]

(iii) Signal transduction: FBXW7 regulates several oncogenic signaling pathways, most notably the Notch signaling pathway. The Notch intracellular domain (NICD)[65] is a transcription factor that drives the expression of genes critical for T-cell development and proliferation.[40,66] FBXW7 targets NICD for degradation, thus preventing prolonged Notch signaling that could otherwise promote leukemogenesis.

(iv) Differentiation and metabolism: FBXW7 also controls the degradation of other key proteins involved in cellular differentiation and metabolism,[67] including transcription factors like KLF5[68] and metabolic regulators like HIF1α.[69] By regulating these processes, FBXW7 helps maintain cellular quiescence and differentiation under physiological conditions.

Mutations in *FBXW7* disrupt its ability to bind and degrade these substrates, leading to their accumulation and the promotion of oncogenic signaling pathways. This loss of function is particularly significant in cancers like leukemia, where *FBXW7* mutations lead to the stabilization of proteins that drive uncontrolled proliferation, apoptosis evasion, and resistance to chemotherapy.

3. FBXW7 as a tumor suppressor in leukemia

3.1. Key substrates of FBXW7 in leukemia

FBXW7 acts as a tumor suppressor by controlling the degradation of several key oncogenic proteins. In leukemia, the loss or mutation of *FBXW7* leads to the accumulation of these substrates, promoting leukemogenesis and resistance to therapy.[70] The most critical FBXW7 substrates implicated in leukemia include (Figure 4):

(i) c-Myc: c-Myc is a master regulator of cell growth, metabolism, and proliferation. It is a transcription factor that drives the expression of genes involved in ribosome biogenesis,[71] nucleotide metabolism,[72] and cell cycle progression.[73] In normal cells, FBXW7 tightly regulates c-Myc levels by targeting it for ubiquitin-mediated degradation.[74] Mutations in *FBXW7* that prevent the degradation of c-Myc lead to its accumulation, driving oncogenic transcriptional programs that promote uncontrolled cell proliferation and metabolic reprogramming in leukemia cells.[75]

(ii) Notch: The Notch signaling pathway is crucial for normal T-cell development, but in T-ALL, mutations in *FBXW7* or in *NOTCH1* result in the stabilization of the NICD.[76] This sustained activation of Notch signaling drives the proliferation of leukemic cells and impairs their differentiation, contributing to disease progression.[77]

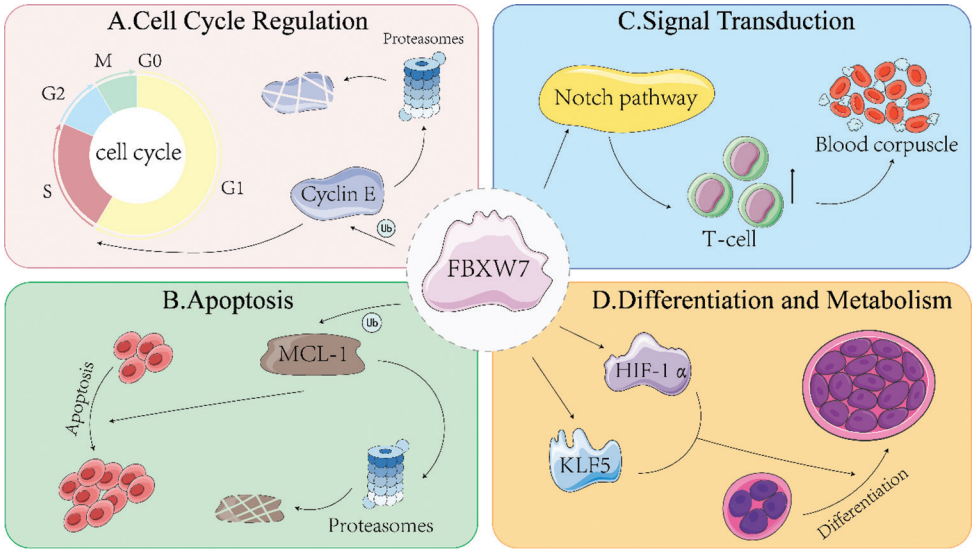

Figure 3. Major biological processes regulated by FBXW7. (A) Cell cycle regulation; (B) apoptosis; (C) signal transduction; and (D) differentiation and metabolism.

Abbreviations: Cyclin E: Cyclin E protein involved in cell cycle regulation; FBXW7: F-box and WD repeat domain-containing 7; HIF-1 α: Hypoxia-inducible factor 1 alpha; MCL-1: Myeloid cell leukemia 1; T-cell: T lymphocyte, a type of immune cell.

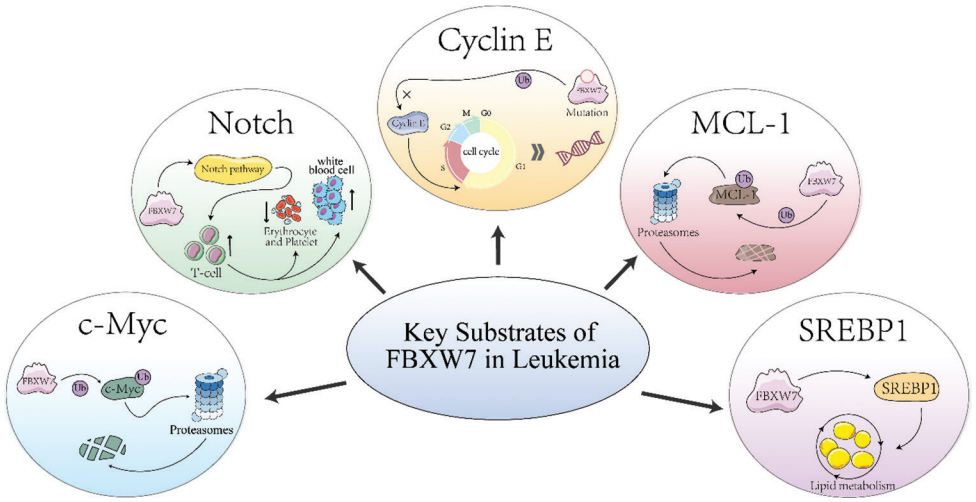

Figure 4. Key substrates of FBXW7 in leukemia

Abbreviations: c-Myc: Cellular myelocytomatosis oncogene; Cyclin E: Cyclin E protein involved in cell cycle regulation; MCL-1: Myeloid cell leukemia 1; Notch: Notch receptor protein involved in cell signaling; SREBP1: Sterol regulatory element-binding protein 1.

(iii) Cyclin E: Cyclin E is a regulator of the G1-to-S phase transition in the cell cycle, and its degradation is necessary to maintain normal cell cycle progression.[78] In FBXW7-mutant leukemia cells, cyclin E is stabilized, resulting in enhanced entry into S phase, leading to excessive DNA replication stress and genomic instability, both of which drive leukemogenesis.[79]

(iv) MCL-1: MCL-1 is a member of the BCL-2 family of anti-apoptotic proteins, and its overexpression is frequently observed in chemotherapy-resistant leukemia.[80] FBXW7 targets MCL-1 for degradation, and the loss of FBXW7 function in leukemia leads to the stabilization of MCL-1, allowing leukemic cells to evade apoptosis and survive under chemotherapeutic pressure.[50]

(v) SREBP1: Recent studies have identified SREBP1, a key regulator of lipid metabolism, as another substrate of FBXW7.[81] SREBP1 plays a role in metabolic reprogramming in cancer cells, and its stabilization in FBXW7-mutant leukemias may contribute to the altered metabolism that supports rapid cell growth and survival under stress conditions.[82]

In addition, FBXW7 also regulates the degradation of other key proteins, such as the cell cycle regulator and negative modulator p27. Stabilization of p27 leads to cell cycle arrest and may promote tumor cell proliferation.[83] Similarly, c-Jun, a transcription factor involved in cellular stress responses and proliferation regulation, is also controlled by FBXW7.[84] When *FBXW7* undergoes mutation or loss of function, the stability of these substrates increases, further driving tumor cell proliferation, survival, and resistance to treatment. Notably, the accumulation of oncogenic proteins such as c-Myc, Notch, cyclin E, and MCL-1, due to impaired FBXW7 activity, becomes a central factor in the pathogenesis of leukemia. This stabilization of key oncogenic proteins not only drives the progression of leukemia but also contributes to resistance to conventional therapies, highlighting FBXW7 as a critical target for therapeutic intervention.

4. Therapeutic targeting of FBXW7 in leukemia

The role of FBXW7 in regulating oncogenic proteins makes it an attractive therapeutic target for treating leukemia, particularly in cases where its loss contributes to resistance to therapy. Therapeutic strategies are being developed to either restore FBXW7 function or target the oncogenic proteins stabilized by *FBXW7* mutations (Figure 5).

4.1. Targeting FBXW7 substrates

Given that the loss of FBXW7 leads to the accumulation of specific oncogenic proteins,[85] therapeutic strategies aimed at these substrates represent promising approaches for overcoming FBXW7-related oncogenesis. Current strategies include:

(i) c-Myc inhibition: The accumulation of c-Myc in FBXW7-deficient leukemias suggests that inhibiting c-Myc could be a promising therapeutic approach. BET-bromodomain inhibitors, such as JQ1,[86] reduce c-Myc transcription by preventing BET proteins from binding to acetylated histones at c-Myc target gene promoters.[87] Preclinical studies have shown that BET inhibitors can reduce c-Myc-driven transcription, leading to decrease leukemia cell proliferation and enhanced apoptosis.[88]

(ii) Notch inhibition: In T-ALL, aberrant Notch signaling is a key driver of disease progression.[89] Gamma-secretase inhibitors (GSIs), which block the cleavage of Notch receptors and prevent the release of NICD, have shown promise in preclinical models of T-ALL.[90] However, the use of GSIs has been limited by gastrointestinal toxicity, highlighting the need for more selective Notch inhibitors or combination therapies that reduce off-target effects.[91]

(iii) MCL-1 inhibition: The stabilization of MCL-1 in FBXW7-deficient leukemia contributes to apoptosis resistance and chemotherapy failure.[92] Small molecule inhibitors of MCL-1, such as S63845, have shown potent activity in preclinical models of leukemia.[93] These inhibitors work by disrupting the interaction between MCL-1 and pro-apoptotic proteins, restoring apoptotic sensitivity and overcoming drug resistance.

4.2. Restoring FBXW7 function

Restoring the function of FBXW7 represents a promising therapeutic strategy, particularly for leukemia cases driven by *FBXW7* mutations. These mutations frequently occur in the WD40 substrate recognition domain, a critical region responsible for the specific binding between FBXW7 and its target proteins.[94] Such mutations impair FBXW7's ability to bind its substrates, thereby hindering the ubiquitination and subsequent degradation of multiple oncogenic proteins, leading to their abnormal accumulation within cells. As a key tumor suppressor, FBXW7 is responsible for the degradation of several pivotal oncogenic proteins, including c-Myc, Notch, and cyclin E. Loss of FBXW7 function disrupts cellular homeostasis, induces uncontrolled cell cycle progression, impairs differentiation, and promotes tumor development.[95] In leukemia, the loss or mutation of *FBXW7* results in the sustained stabilization of these oncogenic substrates, which continuously drive leukemic cell proliferation, accelerate disease progression, and contribute to treatment resistance. Therefore, restoring or substituting FBXW7 function may reinstate proper degradation of these oncogenic proteins, suppress leukemic cell growth, and enhance treatment responsiveness, offering a novel and hopeful direction for targeted leukemia therapy. Several strategies are being explored, including:

(i) Gene therapy: Advances in *CRISPR-Cas9* gene-editing technology have made it possible to correct loss-of-function mutations in *FBXW7*,[96] potentially restoring its tumor-suppressive function.[97] By introducing functional copies of the *FBXW7* gene into leukemia cells, it may be possible to re-establish the degradation of oncogenic proteins, thereby suppressing tumor growth.

(ii) Small molecule stabilizers: Another approach involves the development of small molecules that stabilize FBXW7 or enhance its activity. By promoting the interaction between FBXW7 and its substrates, these molecules could restore the tumor-suppressive function of FBXW7, even in cells with partial loss-of-function mutations.

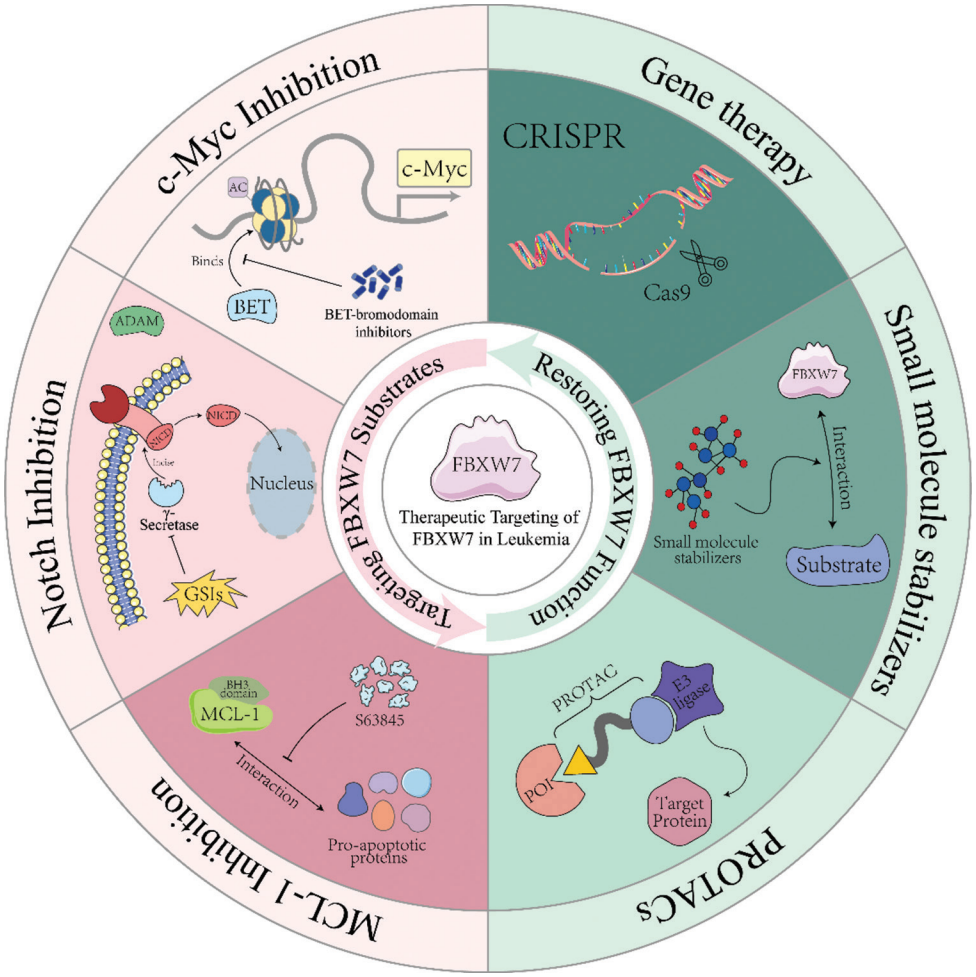

Figure 5. Therapeutic targeting of FBXW7 in leukemia
Abbreviations: AC: Activator complex; ADAM: A disintegrin and metalloproteinase; BET: Bromodomain and extraterminal domain proteins; c-Myc: Cellular Myelocytomatosis oncogene; FBXW7: F-box and WD repeat domain-containing 7; GSIs: Gamma-secretase inhibitors; MCL-1: Myeloid cell leukemia 1; NICD: Notch intracellular domain; POI: Protein of interest.

(iii) Proteolysis-targeting chimeras (PROTACs): PROTACs are an emerging class of therapeutics designed to target specific proteins for ubiquitin-mediated degradation.[98] By harnessing the cell's natural degradation machinery, PROTACs can selectively degrade proteins that are otherwise considered "undruggable."[99] Developing PROTACs that target key FBXW7 substrates, such as c-Myc, could provide a novel therapeutic strategy for FBXW7-deficient leukemias.

5. Challenges and future directions

5.1. Challenges in FBXW7 research

Despite the growing understanding of FBXW7's role in leukemia, several challenges remain:

(i) Mutation heterogeneity: *FBXW7* mutations exhibit significant heterogeneity,[100] typically occurring in various regions of the WD40 domain, which affects substrate recognition.[101] This mutational heterogeneity complicates the development of therapeutic strategies, as different *FBXW7* mutations may lead to dysregulated degradation of distinct substrates, thereby influencing the proliferation, metabolism, and survival pathways of leukemia cells. For example, c-Myc and Notch are primarily involved in cell cycle regulation[102] and differentiation inhibition,[103] while MCL-1 and cyclin E are associated with the regulation of apoptosis and DNA replication stress.[104,105] As a result, different *FBXW7* mutations may lead to the accumulation of specific oncogenic substrates, altering the biological characteristics and therapeutic response of leukemia cells. Some mutations may only affect the degradation of c-Myc, while others may stabilize multiple substrates, thus enhancing the resistance of leukemia cells to treatment.[106] The diversity of these mutations makes

a one-size-fits-all treatment approach ineffective, necessitating the development of personalized therapeutic strategies based on the specific mutation type and substrate stabilization pattern. This approach requires therapeutic strategies targeting the specific degradation dysregulation of substrates to improve the precision and efficacy of treatment.

(ii) Redundancy in degradation pathways: Other E3 ligases, such as β-TrCP, may compensate for the loss of FBXW7 in certain contexts, reducing the efficacy of therapies aimed at restoring FBXW7 function.[107] Understanding the redundancy within the ubiquitin-proteasome system and identifying the contexts in which FBXW7 is indispensable will be key to developing more effective targeted therapies.

(iii) Therapeutic resistance: Leukemia cells with FBXW7 mutations often develop resistance to standard chemotherapies and targeted therapies. This resistance is driven by the stabilization of oncogenic substrates such as MCL-1 and c-Myc, which promote cell survival even in the presence of cytotoxic agents.[108] Overcoming this resistance will require the development of more effective therapies that target these stabilized proteins or their downstream signaling pathways.

(iv) "Undruggable" substrates: Many key FBXW7 substrates, such as c-Myc and MCL-1, have long been considered "undruggable" due to the lack of well-defined small molecule binding pockets.[109] However, recent advancements in drug discovery, particularly the development of PROTAC technology, have opened new possibilities for targeting these proteins. PROTACs overcome the limitation of traditional small molecule inhibitors, which cannot directly bind to their targets, by inducing the degradation of target proteins.[110] This approach provides a novel pathway for treating these challenging targets. Nevertheless, there remain several technical challenges that must be addressed for clinical success. First, the target selectivity of PROTACs needs to be further improved to ensure specific degradation of the target protein without triggering off-target effects.[111] Second, the bioavailability and pharmacokinetic properties of PROTACs require optimization, particularly in terms of stability *in vivo* and the ability to penetrate cell membranes.[112] In addition, the efficacy of PROTACs in different types of tumors or other diseases is not yet fully understood, and enhancing their effectiveness in heterogeneous diseases remains a significant challenge. Only by overcoming these technical obstacles can PROTACs achieve true clinical translation and drive the advancement of targeted therapies for "undruggable" substrates.

5.2. Future directions

To overcome these challenges, several key areas of research should be prioritized:

(i) Advanced preclinical models: Developing genetically engineered mouse models[113] and patient-derived xenografts[114] that accurately recapitulate the spectrum of *FBXW7* mutations found in human leukemia will be essential for studying the biological consequences of FBXW7 loss and testing novel therapeutic strategies. These models will also help to delineate the contexts in which FBXW7 plays a critical role in tumor suppression.

(ii) Identification of novel substrates: Although several key substrates of FBXW7 have been identified, it is likely that additional oncogenic proteins are regulated by FBXW7. High-throughput proteomic approaches, such as mass spectrometry-based interactome studies,[115] could be used to identify new substrates and expand the repertoire of therapeutic targets.

(iii) Combination therapies: Given the complexity of FBXW7's role in regulating multiple oncogenic pathways, combination therapies that target both FBXW7 substrates and compensatory mechanisms are likely to be more effective than monotherapies.[116] Rationally designed combination therapies that include c-Myc or MCL-1 inhibitors, in conjunction with standard chemotherapy or immune checkpoint inhibitors, could enhance treatment efficacy and overcome resistance.

(iv) Restoring FBXW7 function: Gene therapy and small molecule stabilizers offer promising avenues for restoring FBXW7 function in leukemia cells.[117] Continued research into the mechanisms that regulate FBXW7 stability and activity will be crucial for developing these therapies. In addition, small molecules that enhance the interaction between FBXW7 and its substrates may provide an alternative approach to restoring its tumor-suppressive function.

(v) Biomarker development for personalized medicine: As our understanding of the molecular consequences of *FBXW7* mutations deepens, incorporating FBXW7 status as a biomarker of therapeutic response into clinical practice becomes essential for personalized treatment. Biomarkers of therapeutic response are molecular or genetic features that predict how a patient will respond to specific treatments. In cancers such as leukemia, these biomarkers reflect tumor cell sensitivity or resistance to particular therapies. For instance, the status of FBXW7, whether through mutations or functional loss, serves as a key indicator of how tumor cells will respond to targeted therapies or conventional chemotherapy.[118] FBXW7

regulates the degradation of several oncogenic proteins, including c-Myc, Notch, and cyclin E, and mutations in *FBXW7* can lead to the accumulation of these substrates, which, in turn, alters the tumor cell's response to various treatments. For example, the accumulation of c-Myc may increase tumor cell sensitivity to certain chemotherapy drugs,[119] while the stabilization of MCL-1 could enable leukemia cells to evade apoptosis and develop chemotherapy resistance.[120] By monitoring *FBXW7* mutations and the accumulation of its substrates, clinicians can better predict how patients will respond to specific treatment regimens, enabling the development of more targeted therapeutic strategies. Biomarkers based on the *FBXW7* mutation spectrum or substrate accumulation can help identify patients most likely to benefit from particular treatments, including targeted inhibitors or combination therapies. Moreover, the advancement of liquid biopsy techniques, such as circulating tumor DNA analysis,[121] offers the ability to monitor *FBXW7* mutations in real-time, further facilitating personalized treatment approaches. This technology allows for the dynamic tracking of tumor genomic changes during treatment, providing crucial information for optimizing therapeutic plans, adjusting drug dosages, and monitoring recurrence.

6. Conclusion

FBXW7 plays a pivotal role in regulating cell cycle progression, apoptosis, and signal transduction by targeting key oncogenic proteins involved in these processes for ubiquitin-mediated proteasomal degradation. In leukemia, loss or mutation of *FBXW7* leads to the accumulation of substrates such as c-Myc, Notch, and MCL-1, which not only drive leukemogenesis but also contribute to therapeutic resistance. Although directly targeting FBXW7 or restoring its function remains technically challenging, alternative therapeutic strategies aimed at inhibiting its downstream effectors or compensating for its loss have shown promising potential. For instance, synthetic lethality approaches offer novel therapeutic avenues for FBXW7-deficient malignancies. Following FBXW7 inactivation, leukemia cells often become reliant on compensatory survival pathways – such as the mTOR signaling axis – making them selectively vulnerable to mTOR inhibitors without affecting normal cells. Furthermore, advances in gene therapy and gene editing technologies, particularly CRISPR-Cas9, provide a theoretical and technical framework for correcting *FBXW7* mutations. This holds the potential to restore its ubiquitination function, thereby re-establishing the balance of cell proliferation and differentiation. In addition, the growing implementation of precision medicine has enabled the development of individualized therapeutic strategies based on a patient's specific FBXW7 mutational landscape or functional status. By integrating molecular diagnostic data, clinicians can select more targeted drug regimens, thereby enhancing treatment efficacy while minimizing off-target toxicity. Concurrently, the development of therapeutics targeting FBXW7-associated signaling networks is actively progressing, with several candidate compounds already in preclinical or early clinical stages. Looking ahead, the integration of these emerging therapeutic modalities with patient-specific genomic profiling is expected to substantially improve the precision and effectiveness of leukemia treatment, ultimately contributing to enhanced long-term survival and clinical outcomes.

Acknowledgments

None.

Funding

This work was supported by the National Natural Science Foundation of China (82273167), Jiangsu Province Basic Research Program Natural Science Foundation (Outstanding Youth Fund Project, BK20220063), and the Key Program of Basic Science (Natural Science) of Jiangsu Province (22KJA350001).

Conflict of interest

The authors declare no conflicts of interest.

Author contributions

Conceptualization: All authors
Visualization: Xiuming Li
Writing–original draft: All authors
Writing–review & editing: Bin Liu

Ethics approval and consent to participate

Not applicable.

Consent for publication

Not applicable.

Availability of data

Not applicable.

References

1. Zhang A, Liu W, Qiu S. Mitochondrial genetic variations in leukemia: A comprehensive overview. *Blood Sci*. 2024;6(4):e00205.

doi: 10.1097/BS9.0000000000000205

2. Choi HS, Kim BS, Yoon S, Oh SO, Lee D. Leukemic stem cells and hematological malignancies. *Int J Mol Sci*. 2024;25(12):6639.

doi: 10.3390/ijms25126639

3. Iyer P, Jasdanwala SS, Wang Y, Bhatia K, Bhatt S. Decoding acute myeloid leukemia: A clinician's guide to functional profiling. *Diagnostics (Basel)*. 2024;14(22):2560.

doi: 10.3390/diagnostics14222560

4. Hosseini A, Dhall A, Ikonen N, *et al.* Perturbing LSD1 and WNT rewires transcription to synergistically induce AML differentiation. *Nature*. 2025.

doi: 10.1038/s41586-025-08915-1

5. Wiese W, Galita G, Siwecka N, Rozpedek-Kaminska W, Slupianek A, Majsterek I. Endoplasmic reticulum stress in acute myeloid leukemia: Pathogenesis, prognostic implications, and therapeutic strategies. *Int J Mol Sci*. 2025;26(7):3092.

doi: 10.3390/ijms26073092

6. Snaith O, Poveda-Rogers C, Laczko D, Yang G, Morrissette JJ. Cytogenetics and genomics of acute myeloid leukemia. *Best Pract Res Clin Haematol*. 2024;37(1):101533.

doi: 10.1016/j.beha.2023.101533

7. Longhitano AP, Slavin MA, Harrison SJ, Teh BW. Bispecific antibody therapy, its use and risks for infection: Bridging the knowledge gap. *Blood Rev*. 2021;49:100810.

doi: 10.1016/j.blre.2021.100810

8. Xiao W, Nardi V, Stein E, Hasserjian RP. A practical approach on the classifications of myeloid neoplasms and acute leukemia: WHO and ICC. *J Hematol Oncol*. 2024;17(1):56.

doi: 10.1186/s13045-024-01571-4

9. Chen L, Zeng P, Tang H, *et al.* Routes and molecular mechanisms of central nervous system involvement in acute myeloid leukemia (Review). *Oncol Rep.* 2024;52(5):146.

doi: 10.3892/or.2024.8805

10. Demir D. Insights into the new molecular updates in acute myeloid leukemia pathogenesis. *Genes (Basel)*. 2023;14(7):1424.

doi: 10.3390/genes14071424

11. Pagliaro L, Chen SJ, Herranz D, *et al.* Acute lymphoblastic leukaemia. *Nat Rev Dis Primers*. 2024;10(1):41.

doi: 10.1038/s41572-024-00525-x

12. Cerqueira P, Pereira S, Costa R, *et al.* Cutaneous manifestation of acute lymphoblastic leukemia. *Cureus* 2024;16(11): e74022

doi: 10.7759/cureus.74022

13. Chen JJ, Tokumori FC, Del Guzzo C, Kim J, Ruan J. Update on T-cell lymphoma epidemiology. *Curr Hematol Malig Rep.* 2024;19(3):93-103.

doi: 10.1007/s11899-024-00727-w

14. Fallati A, Di Marzo N, D'Amico G, Dander E. Mesenchymal stromal cells (MSCs): An ally of B-cell acute lymphoblastic leukemia (B-ALL) cells in disease maintenance and progression within the bone marrow hematopoietic niche. *Cancers* (*Basel*). 2022;14(14):3303.

doi: 10.3390/cancers14143303

15. Jabbour E, Kantarjian H. Chronic myeloid leukemia: 2025 update on diagnosis, therapy, and monitoring. *Am J Hematol*. 2024;99(11):2191-2212.

doi: 10.1002/ajh.27443

16. Kaehler M, von Bubnoff N, Cascorbi I, Gorantla SP. Molecular biomarkers of leukemia: Convergence-based drug resistance mechanisms in chronic myeloid leukemia and myeloproliferative neoplasms. *Front Pharmacol*. 2024;15:1422565.

doi: 10.3389/fphar.2024.1422565

17. Chen D, Wang MY, Tian C. Research progress of targeted therapy for chronic lymphocytic leukemia/small lymphocytic lymphoma --review. *Zhongguo Shi Yan Xue Ye Xue Za Zhi*. 2024;32(2):643-646.

doi: 10.19746/j.cnki.issn.1009-2137.2024.02.049

18. Gueuning C, Lazaro E, Dupuy H, *et al*. Characteristics of large granular lymphocyte leukemia associated with variable common immunodeficiency disorders: A study of 12 cases. *Eur J Haematol*. 2024;113(4):550-557.

doi: 10.1111/ejh.14265

19. Boucher A, Murray J, Rao S. Cohesin mutations in acute myeloid leukemia. *Leukemia*. 2024;38:2318-2328.

doi: 10.1038/s41375-024-02406-4

20. Walter W, Iacobucci I, Meggendorfer M. Diagnosis of acute lymphoblastic leukaemia: An overview of the current genomic classification, diagnostic approaches, and future directions. *Histopathology*. 2024.

doi: 10.1111/his.15338

21. Tosello V, Di Martino L, Piovan E. Targeted metabolomics of tissue and plasma identifies biomarkers in mice with NOTCH1-dependent T-cell acute lymphoblastic leukemia. *Int J Mol Sci*. 2024;25(12):6543.

doi: 10.3390/ijms25126543

22. Yang F, Zhou H, Luo P, *et al.* Celastrol induces DNA damage and cell death in BCR-ABL T315I-mutant CML by targeting YY1 and HMCES. *Phytomedicine*. 2024;134:155937.

doi: 10.1016/j.phymed.2024.155937

23. Cortes-Lopez PN, Guzman-Montijo E, Fuentes-Venado CE, *et al.* Cutaneous fusarium disease and leukaemias: A systematic review. *Mycoses*. 2024;67(7):e13759.

doi: 10.1111/myc.13759

24. Cuglievan B, Kantarjian H, Rubnitz JE, *et al*. Menin inhibitors in pediatric acute leukemia: A comprehensive review and recommendations to accelerate progress in collaboration with adult leukemia and the international community. *Leukemia*. 2024;38(10):2073-2084.

doi: 10.1038/s41375-024-02368-7

25. Cobaleda C, Godley LA, Nichols KE, Wlodarski MW, Sanchez-Garcia I. Insights into the molecular mechanisms of genetic predisposition to hematopoietic malignancies: The importance of gene-environment interactions. *Cancer Discov*. 2024;14(3):396-405.

doi: 10.1158/2159-8290.CD-23-1091

26. He H, Li J, Li W, *et al.* Clinical features and long-term outcomes of pediatric patients with de novo acute myeloid leukemia in China with or without specific gene abnormalities: A cohort study of patients treated with BCH-AML 2005. *Hematology*. 2024;29(1):2406596.

doi: 10.1080/16078454.2024.2406596

27. Bastos Silveira B, Di Carvalho Melo L, Amorim Dos Santos J, *et al*. Oral manifestations in pediatric patients with leukemia: A systematic review and meta-analysis. *J Am Dent Assoc*. 2024;155(10):858-870.e30.

doi: 10.1016/j.adaj.2024.07.014

28. Cobaleda C, Vicente-Duenas C, Nichols KE, Sanchez-Garcia I. Childhood B cell leukemia: Intercepting the paths to progression. *Bioessays*. 2024;46(9):e2400033.

doi: 10.1002/bies.202400033

29. Robak T, Pula A, Braun M, Robak E. Extramedullary and extranodal manifestations in chronic lymphocytic leukemia - an update. *Ann Hematol*. 2024;103(9):3369-3383.

doi: 10.1007/s00277-024-05854-1

30. Sumbly V, Landry I, Sneed C, *et al.* Leukemic stem cells and advances in hematopoietic stem cell transplantation for acute myeloid leukemia: A narrative review of clinical trials. *Stem Cell Investig*. 2022;9:10.

doi: 10.21037/sci-2022-044

31. Schneider K, Zelley K, Nichols KE, Schwartz Levine A, Garber J. Li-Fraumeni syndrome. In: Adam MP, Feldman J, Mirzaa GM, Pagon RA, Wallace SE, Amemiya A, editors. *GeneReviews (R)*. Seattle (WA): University of Washington; 1993.

32. Bhandari J, Thada PK, Killeen RB, Puckett Y. Fanconi anemia. In: *StatPearls*. Treasure Island, FL: StatPearls Publishing; 2024.

33. Barone PD, Tam W, Geyer JT, Leonard JP, Phillips A, Ouseph MM. Nodal T-cell lymphoma transdifferentiated from mantle cell lymphoma with Epstein-Barr virus infection. *Pathobiology*. 2024;92:1-16.

doi: 10.1159/000541974

34. Ionete A, Bardas A, Varady Z, Vasilica M, Szegedi O, Coriu D. modified prophylactic donor lymphocyte infusion (DLI) in an adult T cell lymphoma/leukemia (ATLL) patient-modality of relapse prevention. *Diseases*. 2024;12(9):210.

doi: 10.3390/diseases12090210

35. Shih AJ, Jun T, Skol AD, *et al.* Inherited cancer predisposing mutations in patients with therapy-related myeloid neoplasms. *Br J Haematol*. 2023;200(4):489-493.

doi: 10.1111/bjh.18543

36. Oiwa K, Lee S, Fujita K, Ueda T, Yamauchi T. Clinical features of clonal cytogenetic abnormalities in Philadelphia-negative cells developed during tyrosine kinase inhibitor treatment. *Intern Med*. 2024;63(5):729-732.

doi: 10.2169/internalmedicine.2182-23

37. Park SE, Lee JK, Kang HJ, Hong YJ, Oh AC, Kim H. A rare case of X-linked four-way Philadelphia chromosome translocation with therapeutic challenges and clonal evolution. *Clin Lab*. 2024;70(9).

doi: 10.7754/Clin.Lab.2024.240323

38. Yang K, Fu K, Zhang H, *et al*. PBA2, a novel inhibitor of the beta-catenin/CBP pathway, eradicates chronic myeloid leukemia including BCR-ABL T315I mutation. *Mol Cancer*. 2024;23(1):209.

doi: 10.1186/s12943-024-02129-1

39. Liu Y, Jang H, Zhang M, Tsai CJ, Maloney R, Nussinov R. The structural basis of BCR-ABL recruitment of GRB2 in chronic myelogenous leukemia. *Biophys J*. 2022;121(12):2251-2265.

doi: 10.1016/j.bpj.2022.05.030

40. Al-Rawashde FA, Al-Wajeeh AS, Vishkaei MN, *et al*. Thymoquinone inhibits JAK/STAT and PI3K/Akt/mTOR signaling pathways in MV4-11 and K562 myeloid leukemia cells. *Pharmaceuticals (Basel)*. 2022;15(9):1123.

doi: 10.3390/ph15091123

41. Shires KL, Rust AJ, Harryparsad R, Coburn JA, Gopie RE. JAK2/STAT5 pathway mutation frequencies in South African BCR/ABL negative MPN patients. *Hematol Oncol Stem Cell Ther*. 2023;16(3):291-302.

doi: 10.56875/2589-0646.1064

42. Hegde PS, Andrew G, Gui G, *et al*. Measurable residual FLT3 tyrosine kinase domain mutations before allogeneic transplant for acute myeloid leukemia. *Bone Marrow Transplant*. 2025;60(2):175-177.

doi: 10.1038/s41409-024-02444-7

43. Gener-Ricos G, Bataller A, Rodriguez-Sevilla JJ, *et al*. NPM1-mutated myeloid neoplasms are a unique entity not defined by bone marrow blast percentage. *Cancer*. 2024;130(20):3452-3462.

doi: 10.1002/cncr.35433

44. Zhao Y, Huang Y, Jiang L, *et al*. Impact of different CEBPA mutations on therapeutic outcome in acute myeloid leukemia. *Ann Hematol*. 2024;103(9):3595-3604.

doi: 10.1007/s00277-024-05884-9

45. Lin ZK, Zhang R, Ge Z, *et al*. Characteristics of NOTCH1 mutation in adult T-cell acute lymphoblastic leukemia. *Zhongguo Shi Yan Xue Ye Xue Za Zhi*. 2013;21(6):1403-1408.

doi: 10.7534/j.issn.1009-2137.2013.06.008

46. Takahashi T, Tsukuda H, Itoh H, Kimura H, Yoshimoto M, Tsujisaki M. Primary and isolated adult T-cell leukemia/lymphoma of the bone marrow. *Intern Med*. 2011;50(20):2393-2396.

doi: 10.2169/internalmedicine.50.5857

47. Kraszewska MD, Dawidowska M, Kosmalska M, *et al*. BCL11B, FLT3, NOTCH1 and FBXW7 mutation status in T-cell acute lymphoblastic leukemia patients. *Blood Cells Mol Dis*. 2013;50(1):33-38.

doi: 10.1016/j.bcmd.2012.09.001

48. Wu X, Wang F, Yang X, *et al*. Advances in drug delivery systems for the treatment of acute myeloid leukemia. *Small*. 2024;20(42):e2403409.

doi: 10.1002/smll.202403409

49. Di Fiore R, Suleiman S, Drago-Ferrante R, *et al*. The role of FBXW7 in gynecologic malignancies. *Cells*. 2023;12(10):1415.

doi: 10.3390/cells12101415

50. Zhu Q, Hu L, Guo Y, Xiao Z, Xu Q, Tong X. FBW7 in hematological tumors. *Oncol Lett*. 2020;19(3):1657-1664.

doi: 10.3892/ol.2020.11264

51. Takeishi S, Nakayama KI. Role of Fbxw7 in the maintenance of normal stem cells and cancer-initiating cells. *Br J Cancer*. 2014;111(6):1054-1059.

doi: 10.1038/bjc.2014.259

52. Hu Y, Bruinstroop E, Hollenberg AN, Fliers E, Boelen A. The role of WD40 repeat-containing proteins in endocrine (dys) function. *J Mol Endocrinol*. 2023;71(1):e220217.

doi: 10.1530/JME-22-0217

53. Liang J, Yu M, Li Y, Zhao L, Wei Q. Glycogen synthase kinase-3: A potential immunotherapeutic target in tumor microenvironment. *Biomed Pharmacother*. 2024;173:116377.

doi: 10.1016/j.biopha.2024.116377

54. Cheng Y, Li G. Role of the ubiquitin ligase Fbw7 in cancer progression. *Cancer Metastasis Rev*. 2012;31(1-2):75-87.

doi: 10.1007/s10555-011-9330-z

55. Zeng J, Chen Z, He Y, *et al*. A patent review of SCF E3 ligases inhibitors for cancer: Structural design, pharmacological activities and structure-activity relationship. *Eur J Med Chem*. 2024;278:116821.

doi: 10.1016/j.ejmech.2024.116821

56. Yang Y, Xie Q, Hu C, *et al*. F-box proteins and gastric cancer: an update from functional and regulatory mechanism to therapeutic clinical prospects. *Int J Med Sci*. 2024;21(8):1575-1588.

doi: 10.7150/ijms.91584

57. Bao E, Zhou Y, He S, *et al*. RING box protein-1(RBX1), a key component of SCF E3 ligase, induced multiple myeloma cell drug-resistance though suppressing p27. *Cancer Biol Ther*. 2023;24(1):2231670.

doi: 10.1080/15384047.2023.2231670

58. Fan J, Bellon M, Ju M, *et al*. Clinical significance of FBXW7 loss of function in human cancers. *Mol Cancer*. 2022;21(1):87.

doi: 10.1186/s12943-022-01548-2

59. Bivik Stadler C, Arefin B, Ekman H, Thor S. PIP degron-stabilized Dacapo/p21(Cip1) and mutations in ago act in an anti- versus pro-proliferative manner, yet both trigger an increase in Cyclin E levels. *Development*. 2019;146(13):dev175927.

doi: 10.1242/dev.175927

60. Knudsen ES, Witkiewicz AK, Rubin SM. Cancer takes many paths through G1/S. *Trends Cell Biol*. 2024;34(8):636-645.

doi: 10.1016/j.tcb.2023.10.007

61. Fagundes R, Teixeira LK. Cyclin E/CDK2: DNA replication, replication stress and genomic instability. *Front Cell Dev Biol*. 2021;9:774845.

doi: 10.3389/fcell.2021.774845

62. Ruan F, Ruan Y, Gu H, Sun J, Chen Q. Clitocine enhances the drug sensitivity of colon cancer cells by promoting FBXW7-mediated MCL-1 degradation via inhibiting the A2B/cAMP/ERK axis. *Am J Physiol Cell Physiol*. 2024;327(4):C884-C900.

doi: 10.1152/ajpcell.00310.2024

63. Song X, Shen L, Tong J, *et al*. Mcl-1 inhibition overcomes intrinsic and acquired regorafenib resistance in colorectal cancer. *Theranostics*. 2020;10(18):8098-8110.

doi: 10.7150/thno.45363

64. Fowler-Shorten DJ, Hellmich C, Markham M, Bowles KM, Rushworth SA. BCL-2 inhibition in haematological malignancies: Clinical application and complications. *Blood Rev*. 2024;65:101195.

doi: 10.1016/j.blre.2024.101195

65. Vazquez-Ulloa E, Lin KL, Lizano M, Sahlgren C. Reversible and bidirectional signaling of notch ligands. *Crit Rev Biochem Mol Biol*. 2022;57(4):377-398.

doi: 10.1080/10409238.2022.2113029

66. Chiplunkar SV, Gogoi D. The multifaceted role of Notch signal in regulating T cell fate. *Immunol Lett*. 2019;206:59-64.

doi: 10.1016/j.imlet.2019.01.004

67. Song C, Guo Y, Chen F, Liu W. IRF-1-inhibited lncRNA XIST regulated the osteogenic differentiation via miR-450b/FBXW7 axis. *Apoptosis*. 2023;28(3-4):669-680.

doi: 10.1007/s10495-023-01820-w

68. Liu Z, Liu X, Liu S, Cao Q. Cholesterol promotes the migration and invasion of renal carcinoma cells by regulating the KLF5/miR-27a/FBXW7 pathway. *Biochem Biophys Res Commun*. 2018;502(1):69-75.

doi: 10.1016/j.bbrc.2018.05.122

69. Sun L. F-box and WD repeat domain-containing 7 (FBXW7) mediates the hypoxia inducible factor-1alpha (HIF-1alpha)/vascular endothelial growth factor (VEGF) signaling pathway to affect hypoxic-ischemic brain damage in neonatal rats. *Bioengineered*. 2022;13(1):560-572.

doi: 10.1080/21655979.2021.2011635

70. Yumimoto K, Nakayama KI. Recent insight into the role of FBXW7 as a tumor suppressor. *Semin Cancer Biol*. 2020;67(Pt 2):1-15.

doi: 10.1016/j.semcancer.2020.02.017

71. Elbahoty MH, Papineni B, Samant RS. Multiple myeloma: clinical characteristics, current therapies and emerging innovative treatments targeting ribosome biogenesis dynamics. *Clin Exp Metastasis*. 2024;41:829-842.

doi: 10.1007/s10585-024-10305-2

72. Liang JH, Ren YM, Du KX, *et al.* MYC-induced cytidine metabolism regulates survival and drug resistance via cGas-STING pathway in mantle cell lymphoma. *Br J Haematol*. 2023;202(3):550-565.

doi: 10.1111/bjh.18878

73. McSweeney K, Hoover P, Ramirez-Solano M, Liu Q, Schwartz JR. Overexpression of human SAMD9 inhibits protein translation and alters MYC signaling resulting in cell cycle arrest. *Exp Hematol*. 2024;137:104249.

doi: 10.1016/j.exphem.2024.104249

74. Hu Z, Wu Y, Sun X, Tong Y, Qiu H, Zhuo E. ARMCX1 inhibits lung adenocarcinoma progression by recruiting FBXW7 for c-Myc degradation. *Biol Direct*. 2024;19(1):82.

doi: 10.1186/s13062-024-00532-8

75. Freie B, Carroll PA, Varnum-Finney BJ, *et al.* A germline point mutation in the MYC-FBW7 phosphodegron initiates hematopoietic malignancies. *Genes Dev*. 2024;38(5-6):253-272.

doi: 10.1101/gad.351292.123

76. Pozzo F, Bittolo T, Tissino E, *et al*. Multiple mechanisms of NOTCH1 activation in chronic lymphocytic leukemia: NOTCH1 mutations and beyond. *Cancers (Basel)*. 2022;14(12):2997.

doi: 10.3390/cancers14122997

77. Luo F, Zhang C, Shi Z, Mao T, Jin LH. Notch signaling promotes differentiation, cell death and autophagy in *Drosophila* hematopoietic system. *Insect Biochem Mol Biol*. 2024;173:104176.

doi: 10.1016/j.ibmb.2024.104176

78. Ohtsubo M, Theodoras AM, Schumacher J, Roberts JM, Pagano M. Human cyclin E, a nuclear protein essential for the G1-to-S phase transition. *Mol Cell Biol*. 1995;15(5):2612-2624.

doi: 10.1128/MCB.15.5.2612

79. Guo X, Zhang R, Ge Z, *et al*. Mutations of FBXW7 in adult T-cell acute lymphocytic leukemia. *Zhongguo Shi Yan Xue Ye Xue Za Zhi*. 2015;23(3):612-618.

doi: 10.7534/j.issn.1009-2137.2015.03.002

80. Bincoletto C, Saad ST, da Silva ES, Queiroz ML. Haematopoietic response and bcl-2 expression in patients with acute myeloid leukaemia. *Eur J Haematol*. 1999;62(1):38-42.

doi: 10.1111/j.1600-0609.1999.tb01112.x

81. Yang Z, Hu N, Wang W, *et al*. Loss of FBXW7 correlates with increased IDH1 expression in glioma and enhances IDH1-mutant cancer cell sensitivity to radiation. *Cancer Res*. 2022;82(3):497-509.

doi: 10.1158/0008-5472.CAN-21-0384

82. He Y, Qi S, Chen L, *et al.* The roles and mechanisms of SREBP1 in cancer development and drug response. *Genes Dis*. 2024;11(4):100987.

doi: 10.1016/j.gendis.2023.04.022

83. Zhang W, Ren Z, Jia L, Li X, Jia X, Han Y. Fbxw7 and Skp2 regulate stem cell switch between quiescence and mitotic division in lung adenocarcinoma. *Biomed Res Int*. 2019;2019:9648269.

doi: 10.1155/2019/9648269

84. Lin H, Ma N, Zhao L, Yang G, Cao B. KDM5c promotes colon cancer cell proliferation through the FBXW7-c-Jun regulatory axis. *Front Oncol*. 2020;10:535449.

doi: 10.3389/fonc.2020.535449

85. Meyer AE, Furumo Q, Stelloh C, Minella AC, Rao S. Loss of Fbxw7 triggers mammary tumorigenesis associated with E2F/c-Myc activation and Trp53 mutation. *Neoplasia*. 2020;22(11):644-658.

doi: 10.1016/j.neo.2020.07.001

86. Chen XY, Yan X, Song BY, Sun J, Mu LJ, Li WP. Effects of BET bromodomain inhibitor JQ1 on double-expressor lymphoma cell lines and its mechanism. *Zhongguo Shi Yan Xue Ye Xue Za Zhi*. 2022;30(4):1094-1100.

doi: 10.19746/j.cnki.issn.1009-2137.2022.04.018

87. Veneziani I, Fruci D, Compagnone M, Pistoia V, Rossi P, Cifaldi L. The BET-bromodomain inhibitor JQ1 renders neuroblastoma cells more resistant to NK cell-mediated recognition and killing by downregulating ligands for NKG2D and DNAM-1 receptors. *Oncotarget*. 2019;10(22):2151-2160.

doi: 10.18632/oncotarget.26736

88. Fiskus W, Piel J, Collins M, *et al*. BRG1/BRM inhibitor targets AML stem cells and exerts superior preclinical efficacy combined with BET or menin inhibitor. *Blood*. 2024;143(20):2059-2072.

doi: 10.1182/blood.2023022832

89. Cao L, Ruiz Buendia GA, Fournier N, *et al.* Resistance mechanism to Notch inhibition and combination therapy in human T-cell acute lymphoblastic leukemia. *Blood Adv*. 2023;7(20):6240-6252.

doi: 10.1182/bloodadvances.2023010380

90. Chang YS, Gills JJ, Kawabata S, *et al.* Inhibition of the NOTCH and mTOR pathways by nelfinavir as a novel treatment for T cell acute lymphoblastic leukemia. *Int J Oncol*. 2023;63(5):128.

doi: 10.3892/ijo.2023.5576

91. Sabol HM, Ferrari AJ, Adhikari M, *et al.* Targeting notch inhibitors to the myeloma bone marrow niche decreases tumor growth and bone destruction without gut toxicity. *Cancer Res*. 2021;81(19):5102-5114.

doi: 10.1158/0008-5472.CAN-21-0524

92. Inuzuka H, Fukushima H, Shaik S, Liu P, Lau AW, Wei W. Mcl-1 ubiquitination and destruction. *Oncotarget*. 2011;2(3):239-244.

doi: 10.18632/oncotarget.242

93. Sneyers F, Kerkhofs M, Speelman-Rooms F, *et al.* Intracellular BAPTA directly inhibits PFKFB3, thereby impeding mTORC1-driven Mcl-1 translation and killing MCL-1-addicted cancer cells. *Cell Death Dis*. 2023;14(9):600.

doi: 10.1038/s41419-023-06120-4

94. Pan Y, Liu J, Gao Y, *et al.* FBXW7 loss of function promotes esophageal squamous cell carcinoma progression via elevating MAP4 and ERK phosphorylation. *J Exp Clin Cancer Res*. 2023;42(1):75.

doi: 10.1186/s13046-023-02630-3

95. Xia H, Dufour CR, Medkour Y, *et al.* Hepatocyte FBXW7-dependent activity of nutrient-sensing nuclear receptors controls systemic energy homeostasis and NASH progression in male mice. *Nat Commun*. 2023;14(1):6982.

doi: 10.1038/s41467-023-42785-3

96. Chan DKH, Mandal A, Hester S, *et al.* Biallelic FBXW7 knockout induces AKAP8-mediated DNA damage in neighbouring wildtype cells. *Cell Death Discov*. 2023;9(1):200.

doi: 10.1038/s41420-023-01494-y

97. Zanganeh S, Zahedi AM, Sattarzadeh Bardsiri M, *et al*. Recent advances and applications of the CRISPR-Cas system in the gene therapy of blood disorders. *Gene*. 2024;931:148865.

doi: 10.1016/j.gene.2024.148865

98. Hesham HM, Dokla EME, Elrazaz EZ, Lasheen DS, Abou El Ella DA. FLT3-PROTACs for combating AML resistance: Analytical overview on chimeric agents developed, challenges, and future perspectives. *Eur J Med Chem*. 2024;277:116717.

doi: 10.1016/j.ejmech.2024.116717

99. Wu M, Zhao Y, Zhang C, Pu K. Advancing proteolysis targeting chimera (PROTAC) nanotechnology in protein homeostasis reprograming for disease treatment. *ACS Nano.* 2024;18(42):28502-28530.

doi: 10.1021/acsnano.4c09800

100. Stephenson SEM, Costain G, Blok LER, *et al.* Germline variants in tumor suppressor FBXW7 lead to impaired ubiquitination and a neurodevelopmental syndrome. *Am J Hum Genet*. 2022;109(4):601-617.

doi: 10.1016/j.ajhg.2022.03.002

101. Zhang Q, Mady ASA, Ma Y, *et al.* The WD40 domain of FBXW7 is a poly(ADP-ribose)-binding domain that mediates the early DNA damage response. *Nucleic Acids Res*. 2019;47(8):4039-4053.

doi: 10.1093/nar/gkz058

102. Duan Y, Liu Z, Wang Q, *et al.* Targeting MYC: Multidimensional regulation and therapeutic strategies in oncology. *Genes Dis*. 2025;12(4):101435.

doi: 10.1016/j.gendis.2024.101435

103. Zhang X, Bian H, Wei W, *et al*. DLX5 promotes osteosarcoma progression via activation of the NOTCH signaling pathway. *Am J Cancer Res*. 2021;11(6):3354-3374.

104. Yao W, Bai L, Wang S, Zhai Y, Sun SY. Mcl-1 levels critically impact the sensitivities of human colorectal cancer cells to APG-1252-M1, a novel Bcl-2/Bcl-X(L) dual inhibitor that induces Bax-dependent apoptosis. *Neoplasia*. 2022;29:100798.

doi: 10.1016/j.neo.2022.100798

105. Yu S, Stappenbelt C, Chen M, *et al.* Cyclin E1 overexpression triggers interferon signaling and is associated with antitumor immunity in breast cancer. *J Immunother Cancer*. 2025;13(3):e009239.

doi: 10.1136/jitc-2024-009239

106. Welcker M, Orian A, Jin J, *et al.* The Fbw7 tumor suppressor regulates glycogen synthase kinase 3 phosphorylation-dependent c-Myc protein degradation. *Proc Natl Acad Sci U S A*. 2004;101(24):9085-9090.

doi: 10.1073/pnas.0402770101

107. Dye KN, Welcker M, Clurman BE, Roman A, Galloway DA. Merkel cell polyomavirus Tumor antigens expressed in Merkel cell carcinoma function independently of the ubiquitin ligases Fbw7 and beta-TrCP. *PLoS Pathog*. 2019;15(1):e1007543.

doi: 10.1371/journal.ppat.1007543

108. Jain N, Croner LJ, Allan JN, *et al*. Absence of BTK, BCL2, and PLCG2 mutations in chronic lymphocytic leukemia relapsing after first-line treatment with fixed-duration ibrutinib plus venetoclax. *Clin Cancer Res*. 2024;30(3):498-505.

doi: 10.1158/1078-0432.CCR-22-3934

109. Tong J, Tan S, Nikolovska-Coleska Z, Yu J, Zou F, Zhang L. FBW7-Dependent Mcl-1 degradation mediates the anticancer effect of Hsp90 inhibitors. *Mol Cancer Ther*. 2017;16(9):1979-1988.

doi: 10.1158/1535-7163.MCT-17-0032

110. Zhou C, Yang S, Wang J, *et al.* Recent advances in PROTAC-based antiviral and antibacterial therapeutics. *Bioorg Chem*. 2025;160:108437.

doi: 10.1016/j.bioorg.2025.108437

111. Cornu M, Lemaitre T, Kieffer C, Voisin-Chiret AS. PROTAC 2.0: Expanding the frontiers of targeted protein degradation. *Drug Discov Today*. 2025;30:104376.

doi: 10.1016/j.drudis.2025.104376

112. Wang Y, Deng S, Xu J. Proteasomal and lysosomal degradation for specific and durable suppression of immunotherapeutic targets. *Cancer Biol Med*. 2020;17(3):583-598.

doi: 10.20892/j.issn.2095-3941.2020.0066

113. Li L, Wazir J, Huang Z, Wang Y, Wang H. A comprehensive review of animal models for cancer cachexia: Implications for translational research. *Genes Dis*. 2024;11(6):101080.

doi: 10.1016/j.gendis.2023.101080

114. Janitri V, ArulJothi KN, Ravi Mythili VM, *et al*. The roles of patient-derived xenograft models and artificial intelligence toward precision medicine. *MedComm (2020)*. 2024;5(10):e745.

doi: 10.1002/mco2.745

115. Burton AJ, Hamza GM, Zhang AX, Muir TW. Chemical biology approaches to study histone interactors. *Biochem Soc Trans*. 2021;49(5):2431-2441.

doi: 10.1042/BST20210772

116. Ihara H, Aoki Y, Aoki T, Toyoda M. Binding of bilirubin to serum albumin in Crigler-Najjar syndrome, type I. *Rinsho Byori*. 1986;34(9):1075-1078.

117. King B, Trimarchi T, Reavie L, *et al*. The ubiquitin ligase FBXW7 modulates leukemia-initiating cell activity by regulating MYC stability. *Cell*. 2013;153(7):1552-1566.

doi: 10.1016/j.cell.2013.05.041

118. Niu M, Wang N, Yang D, *et al.* Multi-omics integration reveals immune hallmarks and biomarkers associated with FLT3 inhibitor sensitivity in FLT3-mutated AML. *Blood Sci*. 2025;7(2):e00227.

doi: 10.1097/BS9.0000000000000227

119. Ayyadevara V, Wertheim G, Gaur S, *et al.* DYRK1A inhibition results in MYC and ERK activation rendering KMT2A-R acute lymphoblastic leukemia cells sensitive to BCL2 inhibition. *Leukemia*. 2025;39(5):1078-1089.

doi: 10.1038/s41375-025-02575-w

120. Tantawy SI, Timofeeva N, Sarkar A, Gandhi V. Targeting MCL-1 protein to treat cancer: opportunities and challenges. *Front Oncol*. 2023;13:1226289.

doi: 10.3389/fonc.2023.1226289

121. Li JY, Zuo LP, Xu J, Sun CY. Clinical applications of circulating tumor DNA in hematological malignancies: From past to the future. *Blood Rev*. 2024;68:101237.

doi: 10.1016/j.blre.2024.101237

ACCSCIENCE PUBLISHING

Tumor Discovery

REVIEW ARTICLE

Emerging immunomodulatory effects of CDK4/6 inhibitors in breast cancer therapy: A comprehensive review

Yuling Zhang[1], Bingfeng Chen[2], Siyue Lin[3], Rendong Zhang[2], Jundong Wu[2,4]*, and Chunfa Chen[2,4]*

[1]Department of Medical Quality Management, Cancer Hospital of Shantou University Medical College, Shantou, Guangdong, China

[2]The Breast Center, Cancer Hospital of Shantou University Medical College, Shantou, Guangdong, China

[3]First Clinical Medical College of Guangdong Medical University, Zhanjiang, Guangdong, China

[4]The Research Laboratory for Breast Cancer Diagnosis and Treatment, Cancer Hospital of Shantou University Medical College, Shantou, Guangdong, China

(This article belongs to the *Special Issue: Advances in Tumor Immune Regulation: Mechanisms and Therapeutic Insights*)

Abstract

Cyclin-dependent kinase 4 and 6 (CDK4/6) inhibitors, initially developed to regulate cell cycle progression, have recently been recognized as potent immunomodulatory agents in cancer therapy. Accumulating evidence indicates that these inhibitors can modulate key immune cells, including T cells, natural killer cells, and macrophages, thereby enhancing their antitumor functions. By arresting cell cycle progression in both tumor and immune cells, CDK4/6 inhibitors create an immune-permissive microenvironment that facilitates more effective immune-mediated tumor eradication. In addition, these inhibitors may help overcome immune resistance mechanisms, providing a strong rationale for their combination with immune checkpoint inhibitors to amplify antitumor responses. Despite these promising findings, the specific mechanisms through which CDK4/6 inhibitors enhance immune responses, as well as their potential applications in breast cancer, remain areas of active investigation. A deeper understanding of their immunomodulatory effects is essential for developing novel combination therapies that could significantly improve the efficacy of cancer immunotherapy. This review synthesizes the latest evidence on the immunomodulatory effects of CDK4/6 inhibitors, highlighting their potential to augment antitumor immunity and exploring future directions for their clinical application.

Keywords: CDK4/6 inhibitors; Immunomodulation; Antitumor immunity; Combination therapy; Cancer treatment

***Corresponding authors:**
Jundong Wu
(wujun-dong@163.com)
Chunfa Chen
(chenchunfa@stu.edu.cn)

Citation: Zhang Y, Chen B, Lin S, Zhang R, Wu W, Chen C. Emerging immunomodulatory effects of CDK4/6 inhibitors in breast cancer therapy: A comprehensive review. *Tumor Discov*. 2025;4(3):16-31. doi: 10.36922/TD025190037

Received: May 8, 2025

Revised: June 28, 2025

Accepted: July 2, 2025

Published online: August 7, 2025

1. Introduction

The field of cancer therapy has undergone remarkable advancements, transitioning from conventional cytotoxic chemotherapy to more precise strategies targeting specific

molecular vulnerabilities within cancer cells. A pivotal breakthrough in this evolution has been the development of cyclin-dependent kinase 4 and 6 (CDK4/6) inhibitors, which have revolutionized the treatment of hormone receptor-positive (HR^+), human epidermal growth factor receptor 2-negative ($HER2^-$) metastatic breast cancer (MBC).[1] These agents exert their therapeutic effects by inducing cell cycle arrest, thereby inhibiting tumor cell proliferation.[2] CDK4/6 inhibitors, including palbociclib, ribociclib, and abemaciclib, have demonstrated impressive efficacy in combination with endocrine therapy, significantly prolonging progression-free survival (PFS) and, in some cases, overall survival (OS).[1,3] Emerging evidence, however, suggests that the biological impact of these inhibitors extends beyond their canonical role in cell cycle regulation, revealing complex and multifaceted effects on tumor biology. Notably, these inhibitors exhibit immunomodulatory properties that are capable of reprogramming the tumor microenvironment (TME).

Immune checkpoint inhibitors (ICIs) have also revolutionized cancer therapy by targeting regulatory proteins on immune cells, such as T cells, which normally act as natural "brakes" to limit immune responses. By releasing these immune "brakes," ICIs enhance the body's ability to recognize and eliminate cancer cells.[4] Key immune checkpoint proteins targeted by ICIs include programmed cell death protein 1 (PD-1) and its ligand, programmed death-ligand 1 (PD-L1), as well as cytotoxic T-lymphocyte-associated protein 4 (CTLA-4).[5] While ICIs have demonstrated remarkable success in treating various cancer, including melanoma, lung cancer, and Hodgkin lymphoma, their efficacy as monotherapy in $HR^+/HER2^-$ breast cancer remains limited.[6] This reduced activity may stem from the relatively low tumor-infiltrating lymphocyte (TIL) density and low tumor mutational burden characteristic of this breast cancer subtype, suggesting a less immunogenic TME. The modest success of ICIs as single agents in $HR^+/HER2^-$ breast cancer underscores the need to explore combination strategies that may enhance tumor immunogenicity and improve immune response efficacy.

Emerging evidence supports the therapeutic rationale for combining CDK4/6 inhibitors with immunotherapy in $HR^+/HER2^-$ breast cancer. These inhibitors exhibit distinct immunomodulatory properties, including enhanced tumor antigen presentation and reduced immunosuppressive regulatory T cells (Tregs), which may potentiate the efficacy of immune-based therapies.[7] The intersection of cell cycle regulation and immune response represents an exciting and evolving area of oncological research, challenging traditional paradigms of cancer treatment.[8]

Given these intriguing and evolving mechanisms, a thorough investigation into combining CDK4/6 inhibitors with ICIs is warranted to elucidate their biological interactions and therapeutic potential. This review examines the promise of such combination strategies, examining the scientific rationale, present clinical evidence, and challenges associated with this approach.

2. The effects of CDK4/6 inhibitors

2.1. Primary mechanisms of CDK4/6 inhibitors

In HR^+ breast cancer, estrogen signaling upregulates cyclin D expression, activating CDK4/6 to drive cell cycle progression.[9] The subsequent molecular cascade is highly coordinated across distinct cell cycle phases: G1 (growth), S (DNA synthesis), G2 (pre-mitotic expansion), and M (mitosis).[10] CDKs are key orchestrators, with cyclin D-CDK4/6 complexes serving as master regulators of the G1/S checkpoint.[1] These complexes initiate retinoblastoma (Rb) protein phosphorylation, inactivating this tumor suppressor and liberating E2F transcription factors to activate genes required for S-phase progression.[11] The estrogen-CDK4/6 signaling axis, therefore, represents a unique therapeutic vulnerability in HR^+ breast cancers, explaining their exceptional sensitivity to CDK4/6 inhibitors, particularly when combined with endocrine therapy.

Building upon this molecular framework, CDK4/6 inhibitors exert their therapeutic effects by blocking Rb phosphorylation, thereby maintaining its growth-suppressive hypophosphorylated state. This inhibition prevents E2F-mediated transcriptional activation of S-phase genes, resulting in potent G1 cell cycle arrest.[12,13] While sharing this core mechanism, CDK4/6 inhibitors display distinct pharmacological characteristics. For instance, abemaciclib demonstrates greater selectivity for CDK4 over CDK6 and exhibits enhanced blood–brain barrier penetration, potentially offering advantages in specific clinical scenarios.[14] It also exhibits off-target effects by inhibiting additional cyclin-dependent kinases, such as CDK2/Cyclin A/E and CDK1/Cyclin B complexes.[15] These differential properties translate to varied biological outcomes, including G2 phase arrest, cell death in Rb phosphorylation-deficient cells, and characteristic transcriptional signatures observed across experimental systems.

2.2. Modulating other cellular processes

Beyond their well-characterized roles in cell cycle control, CDK4/6 inhibitors exert profound impacts on diverse cellular processes through intricate molecular interactions. Depending on specific cellular microenvironments, these inhibitors can induce either cellular quiescence or trigger senescence. This dual regulatory capability provides a

refined strategy for managing cellular behavior.[12] For instance, the induction of quiescence in normal tissue cells preserves cellular function and prevents aberrant proliferation, while the promotion of senescence in cancer cells effectively suppresses their growth and division.

CDK4/6 inhibitors regulate autophagy in a manner dependent on cell type and pathophysiological context, thereby introducing cellular response intricacies and profoundly impacting survival and functionality.[12] Notably, their suppression of autophagy in specific cancer models may enhance the efficacy of chemotherapy or radiotherapy.

A particularly notable impact of these inhibitors is their capacity to reprogram tumor cell metabolism by disrupting the balance between anabolism and catabolism. This alteration modifies the synthesis and utilization of key metabolites, potentially impairing energy supply mechanisms and survival strategies in cancer cells.[12] Consequently, malignant cells may become more responsive to other anticancer therapies.

2. Mechanism of ICIs

The immune system maintains self-tolerance and prevents excessive immune responses through a sophisticated regulatory network known as immune checkpoints.[16] These checkpoints involve interactions between specific proteins expressed on immune cells, such as T cells, and their corresponding ligands on other cells, including tumor cells. PD-1 is an inhibitory receptor expressed on activated T-cells, while its ligand, PD-L1, is frequently overexpressed on tumor cells and antigen-presenting cells. Upon PD-1/PD-L1 binding, inhibitory signals are transmitted to T-cells, leading to T-cell exhaustion and diminished antitumor activity.[17] CTLA-4 is another critical inhibitory receptor on T cells. CTLA-4 primarily functions during early T-cell activation by outcompeting the costimulatory receptor CD28 for binding to B7 proteins on antigen-presenting cells, thereby suppressing T-cell responses.[18] ICIs, typically monoclonal antibodies, are designed to disrupt these protein-ligand interactions.[5] For example, anti-PD-1 antibodies, such as nivolumab and pembrolizumab, block PD-1 on T-cells, preventing PD-L1 engagement and restoring T-cell cytotoxic activity. Anti-PD-L1 antibodies, such as atezolizumab and durvalumab, achieve similar effects by directly targeting PD-L1 on tumor cells. Anti-CTLA-4 antibodies, such as ipilimumab, enhance early T-cell activation by inhibiting CTLA-4-mediated suppression.[19]

3. Research on the immunomodulatory effects of CDK4/6 inhibitors

Recent studies have illuminated the multifaceted immunomodulatory effects of CDK4/6 inhibitors both *in vitro* and *in vivo* (Table 1). *In vitro* research has demonstrated that CDK4/6 inhibition can significantly enhance antitumor immunity through various mechanisms. For instance, it promotes T-cell activation and triggers antitumor responses by inducing the expression of endogenous retroviral elements in tumor cells, thereby increasing antigen presentation and inhibiting the proliferation of Tregs.[8,20] In addition, CDK4/6 inhibition has been shown to inhibit p73 phosphorylation and activate death receptor 5 (DR5), potentially enhancing the efficacy of chemotherapy and immune checkpoint blockade, while also promoting immunogenic cell death in cancer cells.[21] Notably, the CDK4/6 inhibitor abemaciclib, when combined with low-dose radiotherapy, creates an inflammatory TME in Rb-deficient small cell lung cancer, thereby enhancing antitumor immune responses to PD-1 blockade.[22] Other findings have highlighted alterations in TBK1 phosphorylation that inhibit the stimulator of interferon (IFN) genes (STING) signaling pathway in prostate cancer,[23] the use of mesoporous polydopamine for targeted delivery of CDK4/6 inhibitors to improve synergistic immunotherapy in breast cancer,[24] and the promotion of chemokine-mediated T-cell recruitment to breast tumors through metabolic regulation.[25] Furthermore, single-cell profiling has been highlighted as a tool to guide combination immunotherapy for CDK4/6 inhibitor-resistant $HER2^{+}$ breast cancer, overcoming resistance and enhancing treatment efficacy.[26]

Furthermore, CDK4/6 inhibitors have been found to induce T-cell-inflamed TME, enhancing the efficacy of PD-L1 checkpoint blockade and leading to delayed tumor growth and complete regression when combined with anti-PD-L1.[27] These inhibitors also boost the efficacy of oncolytic viruses by increasing tumor-selective cell killing and T-cell activation in refractory glioblastoma, significantly inhibiting tumor growth and prolonging survival.[28] Pharmacological inhibition of CDK4/6 and mitogen-activated protein kinase/extracellular signal-regulated kinase kinase (MEK) has been shown to induce robust cell cycle arrest and interferon (IFN)-related genes, leading to separable cell cycle arrest and immune responses in RAS-mutant disease models.[29] Innovative approaches, such as the use of self-assembled natural triterpenoid compounds for delivering CDK4/6 inhibitors, have also been explored to improve cancer chemotherapeutic immunotherapy.[30]

In vivo studies in animal models have further corroborated the antitumor potential of CDK4/6 inhibition. These studies have shown that CDK4/6 inhibition promotes antitumor immunity by inducing T-cell memory, thereby

Table 1. Summary of research on CDK4/6 inhibition and antitumor immunity

Author	Type	Year	*In vivo/In vitro*	Key finding	Ref.
Deng *et al.*	Article	2018	*In vitro*	CDK4/6 inhibition enhances antitumor immunity by promoting T cell activation.	20
Goel *et al.*	Article	2017	*In vitro*	CDK4/6 inhibition triggers antitumor immunity by activating endogenous retroviral elements in tumor cells, enhancing antigen presentation, and suppressing regulatory T cell proliferation.	8
Tong *et al.*	Article	2022	*In vitro*	CDK4/6 inhibition suppresses p73 phosphorylation and activates DR5, potentially enhancing the efficacy of chemotherapy and immune checkpoint blockade by promoting immunogenic cell death in cancer cells.	21
Wang *et al.*	Article	2024	*In vitro*	The CDK4/6 inhibitor abemaciclib synergizes with low-dose radiotherapy to enhance anti-PD-1 immune responses by remodeling the inflammatory TME in Rb-deficient small cell lung cancer.	22
Li *et al.*	Article	2024	*In vitro*	CDK4/6 inhibitors stimulate the STING pathway and enhance the antitumor effect of STING agonists in prostate cancer, potentially overcoming immunosuppression.	23
Zhou *et al.*	Article	2024	*In vitro*	Mesoporous polydopamine enables targeted delivery of CDK4/6 inhibitors to enhance combinatorial immunotherapy in breast cancer, eliciting robust systemic antitumor immunity.	24
Uzhachenko *et al.*	Article	2021	*In vitro*	Metabolic modulation by CDK4/6 inhibitors promotes chemokine-mediated T cell recruitment into breast tumors, associated with metabolic stress.	25
Wang *et al.*	Article	2019	*In vitro*	Single-cell profiling guides combinatorial immunotherapy for rapidly evolving CDK4/6 inhibitor-resistant HER2+breast cancer to overcome drug resistance.	26
Schaer *et al.*	Article	2018	*In vitro*	The CDK4/6 inhibitor abemaciclib induces a T-cell-inflamed TME and enhances the efficacy of PD-L1 checkpoint blockade, resulting in delayed tumor growth. Combination with anti-PD-L1 leads to complete regression.	27
Xiao *et al.*	Article	2022	*In vitro*	CDK4/6 inhibition enhances oncolytic virotherapy efficacy in refractory glioblastoma by augmenting tumor-selective cytotoxicity and T-cell activation, significantly suppressing tumor growth and prolonging survival.	28
Wu *et al.*	Article	2024	*In vitro*	Pharmacological CDK4/6 and MEK co-inhibition induces dissociable cell cycle arrest and immune responses in RAS-mutant disease models, driving potent cytostatic and IFN-associated genes.	29
Zhang *et al.*	Article	2025	*In vitro*	Self-assembling natural triterpenoids enable targeted delivery of CDK4/6 inhibitors to enhance cancer chemoimmunotherapy.	30
Lelliott *et al.*	Article	2021	*In vivo*	CDK4/6 inhibition promotes antitumor immunity by inducing T cell memory, thereby fostering long-term endogenous antitumor T cell immunity.	31
Yang *et al.*	Article	2024	*In vivo*	CDK4/6 inhibitors and radiotherapy demonstrate synergistic potential with anti-PD-L1 immunotherapy in triple-negative breast cancer, warranting exploration of combination strategies.	32
Zhang *et al.*	Article	2020	*In vivo*	CDK4/6 inhibition promotes immune infiltration in ovarian cancer and synergizes with PD-1 blockade in a B cell-dependent manner, enhancing immunocyte recruitment and inducing pro-inflammatory responses, ultimately generating synergistic antitumor effects when combined with PD-1 inhibitors.	33

Abbreviations: CDK4/6: Cyclin-dependent kinase 4 and 6; DR5: Death receptor 5; HER2: Human epidermal growth factor receptor 2; IFN: Interferon; MEK: Mitogen-activated protein kinase/extracellular signal-regulated kinase kinase; PD-1: Programmed cell death protein 1; PD-L1: Programmed death-ligand 1; STING: Stimulator of interferon genes; Rb: Retinoblastoma; TME: Tumor microenvironment.

facilitating long-term endogenous antitumor T-cell immunity.[31] Combination therapies involving CDK4/6 inhibitors, radiotherapy, and anti-PD-L1 immunotherapy have demonstrated synergistic potential in triple-negative breast cancer, highlighting the importance of exploring such strategies.[32] In addition, CDK4/6 inhibition has been found to promote immune infiltration in ovarian cancer and synergize with PD-1 blockers in a B cell-dependent manner, enhancing immune infiltration, inducing pro-inflammatory immune responses, and producing synergistic antitumor effects when combined with PD-1 blockers.[33] These findings collectively underscore the diverse and potent immunomodulatory roles of CDK4/6 inhibitors, positioning them as promising candidates for advancing cancer immunotherapy.

5. Mechanisms of immunomodulatory effects of CDK4/6 inhibitors

5.1. Enhancement of immune cell responses

5.1.1. T-cell responses

CDK4/6 inhibitors potentiate T-cell activation and function by counteracting immunosuppressive signals, such as PD-1. This effect primarily stems from their ability to relieve suppression of the nuclear factor of activated T cells (NFAT) protein family and its downstream targets, which are critical regulators of T-cell functionality.[20] As shown in Figure 1, by inhibiting NFAT phosphorylation, these inhibitors promote the nuclear translocation of non-phosphorylated NFAT, thereby activating the transcription of effector genes. This cascade upregulates the mRNA expression of interleukins (ILs), such as IL-2, IL-3, and granulocyte-macrophage colony-stimulating factor (GM-CSF), and enhances IL-2 secretion, as demonstrated in PD-1-expressing Jurkat cells and primary human $CD4^+$ T cells.[34,35]

Notably, CDK4/6 inhibitors further amplify antitumor responses by elevating interferon-gamma (IFN-γ) production in T-cells.[34,35] Preclinical and clinical studies reveal that these inhibitors foster memory T-cell differentiation through upregulation of max dimerization protein 4 (MXD4), a negative regulator of myelocytomatosis viral oncogene homolog (MYC) in $CD8^+$ T cells, thereby sustaining durable antitumor immunity.[31,34] In breast cancer patients, palbociclib or abemaciclib treatment increases the proportion of $CD8^+$ T memory precursor cells while suppressing MYC target gene expression.[34] *In vivo* analyses of patient-derived organotypic tumor spheroids demonstrate enhanced infiltration of $CD4^+$ and $CD8^+$ T cells, accompanied by elevated Th1-type cytokines, such as C-X-C motif chemokine ligand (CXCL) 9, CXCL10, and IFN-γ.[20]

Further investigations show that tumor-specific $CD8^+$ T cells pretreated with CDK4/6 inhibitors exhibit superior persistence *in vivo*, markedly improving antitumor immunity.[34] Short-term CDK4/6 inhibition before chimeric antigen receptor T cell therapy further augments cellular longevity and therapeutic efficacy.[31] These synergistic effects not only optimize T-cell performance but also provide a rationale for combining CDK4/6 inhibitors with immunotherapies.

5.1.2. Natural killer (NK) cell interactions

The interaction between CDK4/6 inhibitors and NK cells represents an emerging area of investigation. While

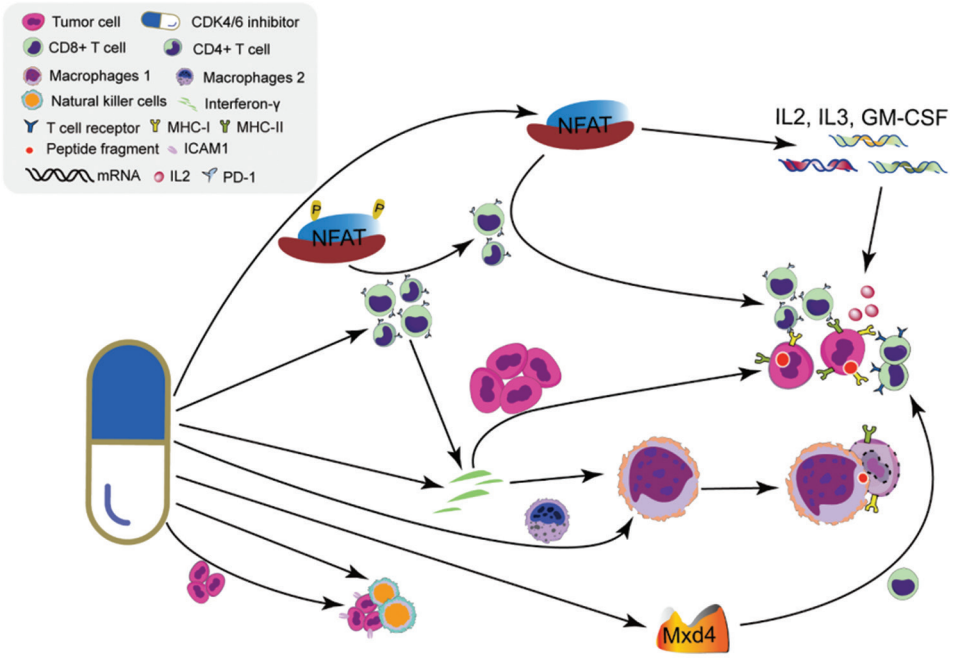

Figure 1. CDK4/6 inhibitors enhance immune cells response. CDK4/6 inhibitors potentiate adaptive immunity by enhancing T-cell activation and augment natural killer cells cytotoxicity. They also reprogram tumor-associated macrophages, shifting their phenotype from the immunosuppressive M2 state to the pro-inflammatory, tumoricidal M1 state. Image created by the authors.

Abbreviations: CDK4/6: Cyclin-dependent kinase 4 and 6; GM-CSF: Granulocyte-macrophage colony-stimulating factor; ICAM1: Intercellular adhesion molecule 1; IL: Interleukin; MHC: Major histocompatibility complex; MXD4: Max dimerization protein 4; NFAT: Nuclear factor of activated T cells; PD-1: Programmed cell death protein 1.

the exact mechanisms are not fully elucidated, available data suggest that these inhibitors can enhance NK cell activation and increase their cytotoxic capabilities (Figure 1). For instance, CDK4/6 inhibitors have been shown to elevate the expression of intercellular adhesion molecule 1, which facilitates the recognition of tumor cells by NK cells.[36] There is a growing consensus that the combination of CDK4/6 inhibitors with other agents, such as MEK inhibitors, may enhance NK cell-mediated tumor elimination through senescence-associated secretory phenotype (SASP) factors.[37] In addition, these inhibitors might influence the formation of the immune synapse between NK cells and tumor cells, potentially amplifying NK cell-mediated cytotoxicity against tumor cells.[38,39]

5.1.3. Modulation of macrophage polarization

CDK4/6 inhibitors have been shown to influence macrophage polarization within the TME. Recent findings suggest that these inhibitors can induce a transition in macrophage phenotype from the immunosuppressive macrophage M2 state to the tumoricidal macrophage M1 phenotype (Figure 1).[40] Specifically, treatment with abemaciclib has been associated with elevated levels of CSF-2, a cytokine that is pivotal for fostering macrophage M1 polarization and enhancing major histocompatibility complex (MHC) II expression in dendritic cells.[41] In addition, ribociclib has been observed to decrease the expression of immunosuppressive chemokines, including C-C motif chemokine ligand (CCL)2, CCL7, and CCL22, which play a role in the chemotaxis and differentiation of immunosuppressive cells, such as macrophage M2.[41] This modulation of macrophage polarization is believed to enhance antitumor immune responses. However, the specific molecular pathways through which CDK4/6 inhibitors reprogram macrophages are not yet fully understood.[42]

5.2. Enhancing tumor cell immunogenicity

CDK4/6 inhibitors enhance the visibility of tumor cells to the immune system by modulating immunogenic signaling pathways (Figure 2). They activate the IFN response, promote the secretion of IFN-γ, and enhance the activity of IFN-stimulated genes, thereby improving the immune system's ability to recognize cancer cells.[43] CDK4/6 inhibition induces the production of IFN-I in tumor cells, which in turn stimulates the secretion of T-cell chemokines, facilitating the recruitment of T-cells to the tumor site and strengthening antitumor immunity.[44,45] Furthermore, CDK4/6 inhibitors trigger epigenetic remodeling by suppressing DNA methyltransferases, leading to the upregulation of endogenous retroviruses. This cascade increases the production of IFN-III and

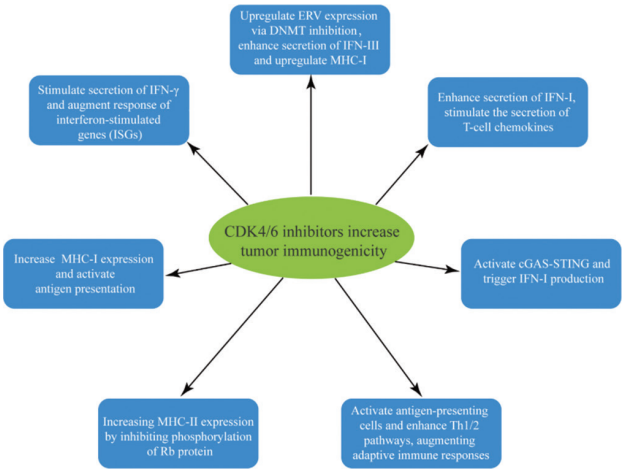

Figure 2. The specific roles of CDK4/6 inhibitors in augmenting tumor cell immunogenicity. Image created by the authors.
Abbreviations: CDK4/6: Cyclin-dependent kinase 4 and 6; cGAS-STING: Cyclic GMP-AMP synthase-stimulator of interferon genes; DNMT: DNA methyltransferase; ERV: Endogenous retroviruses; IFN: Interferon; MHC: Major histocompatibility complex; Rb: Retinoblastoma.

enhances the presentation of MHC-I molecules, making tumors more immunogenic.[46] In addition, these inhibitors activate the cyclic GMP-AMP synthase-STING pathway, driving IFN-I production and amplifying innate immune responses.[47] Finally, CDK4/6 inhibitors prime antigen-presenting cells, such as dendritic cells and macrophages, promoting the activation of Th1/Th2 pathways and playing crucial roles in adaptive immunity.[48]

CDK4/6 inhibitors enhance tumor immunogenicity by upregulating the surface expression of MHC-I molecules, which are essential for antigen presentation to $CD8^+$ T cells that recognize and eliminate tumor cells.[44,49] Research has shown that palbociclib treatment increases MHC-I expression in melanoma cell lines and alters the MHC-I peptide repertoire, thereby enhancing immunogenicity.[50] This effect is mediated through the transcriptional activation of the antigen processing and presentation machinery, including genes encoding proteasomes, transporter-associated antigen processing complexes, and MHC-I subunits. Notably, CDK4/6 inhibitors also increase MHC-II expression in tumor cells.[44,49] Mechanistically, they restore IFN-γ-induced MHC-II transcription by inhibiting the phosphorylation of the Rb protein.[36,41] In breast cancer and lymphoma models, abemaciclib and palbociclib have been shown to increase MHC-II levels, thereby augmenting T-cell activation.[41]

5.3. Remodeling the TME

CDK4/6 inhibitors have emerged as pivotal modulators of the TME, a complex ecosystem comprising immune cells, vasculature, and stromal components. As illustrated

in Figure 3, the inhibition of CDK4/6 diminishes the presence of tumor-infiltrating Tregs,[44,49] thereby reducing immunosuppressive cellular networks and promoting an immuno-permissive TME. However, this therapeutic approach might also deplete dendritic cells within the TME, potentially hindering immune activation. The adoptive transfer of dendritic cells has been demonstrated to circumvent this issue, facilitating effective tumor control when used in conjunction with CDK4/6 inhibitors and immune checkpoint blockade.[51]

Unlike DNA-damaging agents, senescence induced by CDK4/6 inhibitors is marked by minimal expression of pro-tumorigenic factors, such as IL-6 and CXCL8, resulting in a TME with augmented antitumor properties. Numerous studies have shown that CDK4/6 inhibition encourages the infiltration of cytotoxic T-cells into tumors, a critical factor for effective antitumor immunity.[27,49,52] In some cases, CDK4/6 inhibition also alters tumor-associated macrophage populations, potentially steering their polarization toward antitumor phenotypes.[52] These coordinated alterations collectively create an immunologically "hot" TME with diminished immunosuppression, offering a compelling basis for combining CDK4/6 inhibitors with cancer immunotherapy.

Beyond their immunomodulatory effects, emerging evidence suggests that CDK4/6 inhibitors may also impact tumor angiogenesis, the process of new blood vessel formation essential for tumor growth and metastasis. Although CDK6 has been associated with angiogenic regulation, its pharmacological inhibition could simultaneously target both tumor proliferation and vascularization.[53] Given the dual inhibition of CDK4/6, these agents might indirectly influence angiogenesis, even though their mechanisms are less clear compared to their immunological effects. A study on CDK4/vascular endothelial growth factor receptor 2 (VEGFR2) dual-targeting inhibitors showed synergistic suppression of cancer progression and angiogenesis,[54] yet the direct angiogenic effects of standard CDK4/6 inhibitors require further exploration.

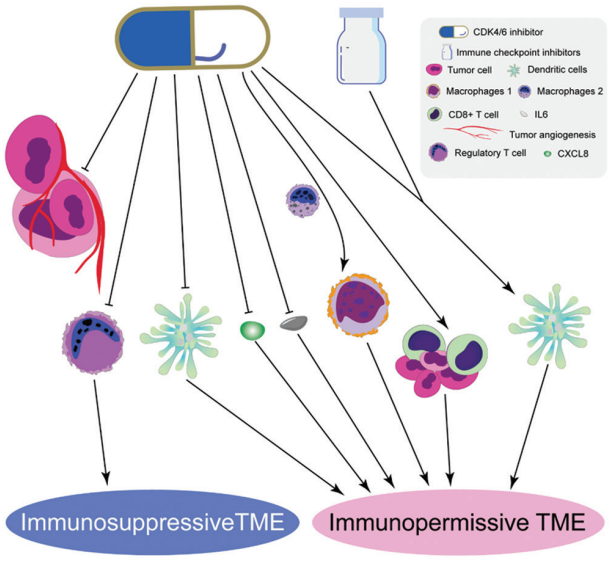

Figure 3. Mechanisms of CDK4/6 inhibitors in TME reprogramming. CDK4/6 inhibitors modulate the TME by acting on a complex ecosystem comprising immune cells, vasculature, and stromal components. Image created by the authors.
Abbreviations: CDK4/6: Cyclin-dependent kinase 4 and 6; CXCL8: C-X-C motif chemokine ligand 8; IL6: Interleukin 6; TME: Tumor microenvironment.

5.4. Regulation of PD-L1 expression

PD-L1, a critical immune checkpoint protein expressed on tumor cell surfaces, suppresses T-cell-mediated immune responses through binding to the PD-1 receptor.[55] This interaction facilitates tumor immune evasion by inhibiting cytotoxic T-cell activity and promoting T-cell exhaustion. To enhance the therapeutic efficacy of combining CDK4/6 inhibitors with ICIs, comprehending the effect of CDK4/6 inhibitors on PD-L1 expression is crucial, as depicted in Figure 4. Studies suggest that CDK4/6 inhibitors can upregulate PD-L1 expression by activating the nuclear factor kappa B signaling pathway.[49] Typically, the CDK4/6-cyclin D complex facilitates the degradation of PD-L1 through the speckle-type POZ protein-cullin 3 (CUL3) ubiquitination pathway. However, CDK4/6 inhibition interferes with this degradation process, leading to the stabilization of PD-L1 protein levels.[56] This stabilization can potentially make tumors more susceptible to

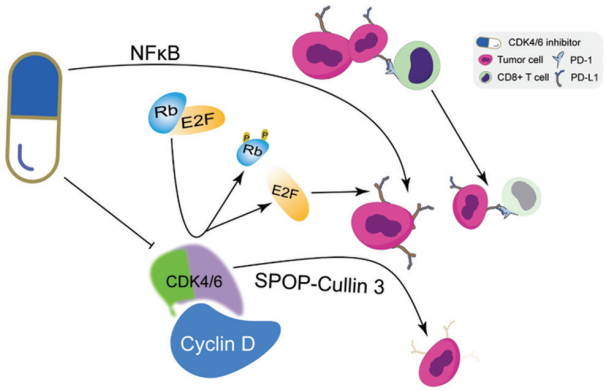

Figure 4. Modulatory effects of CDK4/6 inhibitors on PD-L1 expression. CDK4/6 inhibitors upregulate PD-L1 expression and stabilize PD-L1 protein levels, thereby sensitizing tumors to PD-1/PD-L1 blockade therapies. Image created by the authors.
Abbreviations: CDK4/6: Cyclin-dependent kinase 4 and 6; NFκB: Nuclear factor kappa B; PD-1: Programmed cell death protein 1; PD-L1: Programmed death ligand-1; Rb: Retinoblastoma; SPOP: Speckle-type POZ protein.

PD-1/PD-L1 blockade therapies. Conversely, in certain contexts, such as triple-negative breast cancer, CDK4/6 inhibitors may reduce PD-L1 levels through the RB-E2F signaling axis.[57] The overall impact of CDK4/6 inhibition on PD-L1 expression is context-dependent, varying with tumor type and microenvironment, highlighting the complex interaction that must be taken into account when formulating combination treatment strategies.[58]

6. Clinical evidence and trial assessment of CDK4/6 inhibitors in combination with ICIs in HR$^+$/HER2$^-$ breast cancer

Ongoing clinical trials are actively exploring the therapeutic potential of combining CDK4/6 inhibitors with ICIs for patients with HR$^+$/HER2$^-$ breast cancer. As summarized in Table 2, the CheckMate 7A8 trial, which assessed the

Table 2. Summary of the clinical trial assessment of CDK4/6 inhibitors in combination with immunotherapy in HR$^+$/HER2$^-$ breast cancer

Trial name/ Identifier	Phase	Tumor type	CDK4/6 inhibitor	Immunomodulator agent	Key findings	Ref.
CheckMate 7A8 (NCT04075604)	Phase II	HR$^+$/HER2$^-$early breast cancer	Palbociclib	Nivolumab (anti-PD-1)	Objective response rate of 71.4%.	59
ImmunoADAPT (NCT03820063)	Phase II	Early-stage ER$^+$/HER2$^-$ breast cancer	Palbociclib	Avelumab (anti-PD-L1)	The combination of fulvestrant, palbociclib, and avelumab showed a trend toward improved PFS, with a median PFS of 8.1 months. However, this improvement was not statistically significant compared to fulvestrant alone.	62,63
KEYNOTE-146 (NCT02779751)	Phase I/II	HR$^+$/HER2$^-$MBC	Abemaciclib	Pembrolizumab (anti-PD-1)	Overall response rate of 23.1% and disease control rate of 84.6%.	60
NCT02778685	Phase I/II	HR$^+$/HER2$^-$MBC	Palbociclib	Pembrolizumab (anti-PD-1)	Complete response rate of 31% and PFS of 25.2 months.	61
NCT03294694	Phase I	HR$^+$/HER2$^-$MBC or advanced ovarian cancer	Ribociclib	Spartalizumab (anti-PD-1)	Limited added benefit over ribociclib$^+$fulvestrant alone in HR$^+$MBC. Triplet (with fulvestrant): Objective response rates: ~30% in CDK4/6i-naïve patients. Clinical benefit rate: ~50%. Doublet (without fulvestrant): Limited activity, with objective response rates<15%, suggesting endocrine therapy is critical for synergy.	64
WJOG11418B (NEWFLAME) (NCT04075604)	Phase II	HR$^+$/HER2$^-$MBC	Abemaciclib	Nivolumab (anti-PD-1)	Objective response rates of 54.5% and 40% in the fulvestrant and letrozole cohorts, respectively.	65
PACE (NCT03147287)	Phase II	HR$^+$/HER2$^-$MBC	Palbociclib	Avelumab (anti-PD-L1)	No significant improvement in median PFS was observed with the addition of avelumab to fulvestrant plus palbociclib (8.1 months) compared with fulvestrant plus palbociclib (4.6 months) or fulvestrant alone (4.8 months; *P*=NS). Subgroup analysis showed no benefit in PD-L1$^+$or high-TIL tumors.	66

Abbreviations: CDK4/6i: Cyclin-dependent kinase 4 and 6 inhibitor; ER$^+$: Estrogen receptor-positive; HER2$^-$: Human epidermal growth factor receptor 2-negative; HR$^+$: Hormone receptor-positive; MBC: Metastatic breast cancer; NS: Not significant; PD-1: Programmed cell death protein 1; PD-L1: Programmed death-ligand 1; PFS: Progression-free survival; TIL: Tumor-infiltrating lymphocytes.

neoadjuvant regimen of nivolumab in combination with palbociclib and anastrozole, reported an impressive objective response rate of 71.4%.[59] In addition, a phase II study (NCT02779751) that incorporated pembrolizumab with abemaciclib yielded an overall response rate of 23.1% and a disease control rate as high as 84.6%.[60] Furthermore, another trial (NCT02778685) that employed the combination of pembrolizumab, palbociclib, and letrozole achieved a notable 31% complete response rate, with a PFS extending to 25.2 months.[61]

It is important to highlight that a phase I trial evaluating ribociclib in conjunction with spartalizumab (an anti-PD-1 antibody), with or without fulvestrant, in patients with $HR^+/HER2^-$ MBC did not show significant additional benefit over ribociclib combined with fulvestrant alone.[64] Conversely, the phase II WJOG11418B NEWFLAME trial, which investigated the combination of nivolumab with abemaciclib in $HR^+/HER2^-$ MBC, reported objective response rates of 54.5% and 40% in the fulvestrant and letrozole treatment groups, respectively.[65] Collectively, these results suggest that the combination of CDK4/6 inhibitors with immunotherapy holds promise as a viable treatment strategy for individuals with $HR^+/HER2^-$ breast cancer.

The criteria for identifying the most suitable patients for combinations of CDK4/6 inhibitors with immunotherapy are still being explored.[67] Numerous clinical trials are underway to assess this approach, such as the ImmunoADAPT trial, which is investigating the use of palbociclib in conjunction with avelumab for early-stage estrogen receptor-positive breast cancer.[62,63] Preliminary findings from this trial suggest a trend toward better PFS with the combination of fulvestrant, palbociclib, and avelumab, achieving a median PFS of 8.1 months. However, this enhancement did not reach statistical significance when compared to fulvestrant monotherapy (hazard ratio = 0.75, 90% confidence interval: 0.50–1.12, p=0.23). In addition, the phase II PACE study (NCT03147287), which evaluated palbociclib combined with avelumab in $HR^+/HER2^-$ MBC patients who had progressed on prior CDK4/6 inhibitor treatment, concluded that PD-1/PD-L1 inhibitors offer limited efficacy in this context without a more refined patient selection process.[66]

7. Discussion

7.1. Synergistic mechanisms underlying the combination approach

The scientific rationale for combining CDK4/6 inhibitors with ICIs stems from accumulating evidence demonstrating that these drug classes act through complementary and potentially synergistic mechanisms. This combination strategy simultaneously targets multiple hallmarks of cancer, addressing both aberrant cellular proliferation and enhancing antitumor immunity, while also potentially overcoming resistance mechanisms that limit the efficacy of monotherapies.[39,68,69] The interaction between these agents occurs at multiple levels, creating a comprehensive antitumor approach with the potential for broader therapeutic efficacy.

At the cellular level, CDK4/6 inhibition fundamentally alters cancer cell biology, rendering malignant cells more susceptible to immune-mediated killing. The drug-induced G1 cell cycle arrest correlates with increased expression of endogenous retroviral elements, stimulating viral mimicry responses and subsequent IFN-I/III production.[70] This process enhances tumor immunogenicity through multiple mechanisms, including increased neoantigen presentation, upregulation of MHC-I molecules, and chemokine-mediated recruitment of cytotoxic T lymphocytes. Concurrently, CDK4/6 inhibitors suppress the expression of DNA methyltransferase 1, leading to DNA hypomethylation and further activation of immunostimulatory pathways.[71]

Moreover, CDK4/6 inhibitors remodel the TME to promote enhanced immune cell infiltration, particularly $CD8^+$ T cells and B cells. This augmented immune infiltration may potentiate the efficacy of PD-1/PD-L1 blockade therapies.[33] In certain preclinical models, the combination of CDK4/6 inhibitors with PD-L1 blockade induced complete tumor regression in a significant proportion of mice, even in cases where PD-L1 monotherapy showed limited or no efficacy.[27] Notably, mice that achieved complete responses to either combination therapy or CDK4/6 inhibitor monotherapy demonstrated resistance to tumor rechallenge, indicating the establishment of durable immune memory.[27] These findings suggest that combining CDK4/6 inhibitors with ICIs may represent a promising strategy to enhance antitumor immunity and improve therapeutic outcomes.

7.2. CDK4/6 inhibitors with ICIs tackle resistance

The PALOMA, MONALEESA, and MONARCH trial series have firmly established CDK4/6 inhibitors as a fundamental therapeutic for $HR^+/HER2^-$ advanced breast cancer.[72-79] These pivotal studies evaluated three distinct CDK4/6 inhibitors, including palbociclib, ribociclib, and abemaciclib, in combination with endocrine therapy. Across these studies, these agents consistently demonstrated significant improvements in median PFS, ranging from 16 to 28 months in the first-line setting,[72,73,75,77,78] and 5 to 20 months in later line therapies.[74,76,77,79] Despite these advancements, therapeutic resistance typically

develops after 1–2 years of treatment, posing a significant challenge for long-term disease management. ICIs have emerged as a potential strategy to overcome or delay resistance to CDK4/6 inhibitors.[80] Pre-clinical evidence suggests that CDK4/6 inhibition can modulate immune responses, potentially enhancing the efficacy of ICIs.[61] This combination approach offers two potential mechanisms: Either delaying resistance development when used concomitantly or restoring treatment sensitivity when ICIs are introduced after CDK4/6 inhibitor failure. Early clinical trials evaluating palbociclib combined with pembrolizumab and endocrine therapy have shown encouraging response rates and PFS benefits, particularly in treatment-naïve patients and those with stable disease on prior CDK4/6 inhibition.[61] Introducing ICIs after CDK4/6 inhibitor failure may be an effective strategy to restore treatment sensitivity. By reactivating the immune response against tumor cells, ICIs can overcome resistance mechanisms, transforming immunologically "cold" tumors into "hot" ones. In addition, studies have shown that CDK4/6 inhibitors can enhance the immunogenicity of tumor cells by modulating the expression of genes related to antigen presentation, thereby improving the effectiveness of immunotherapy. This combined treatment strategy offers new possibilities for addressing resistance issues in tumor immunotherapy.[42,81] While these preliminary results suggest ICIs may help address resistance mechanisms, further investigation is required to validate these findings and elucidate the underlying biological interactions.

7.3. Challenges and potential limitations

Despite their proven efficacy, the clinical use of CDK4/6 inhibitors, particularly in HR^+ breast cancer, encounters several challenges. First, clinical observations have highlighted potential adverse effects, including hepatitis and pneumonitis, which may be linked to increased secretion of pro-inflammatory cytokines and impaired Treg function.[41] Second, combination therapies often require dose reductions due to overlapping toxicities, resulting in suboptimal drug exposure and potentially compromised efficacy.[82] A significant issue with these combination regimens is the increased toxicity, particularly immune-related adverse events and hematological toxicities,[61] which must be carefully monitored and managed. Determining the optimal sequence and dosage of these drugs is essential. Third, approximately 30% of breast cancer patients exhibit intrinsic resistance to CDK4/6 inhibitors.[83] Notably, while these drugs enhance antitumor immunity, resistance mechanisms frequently involve dysregulated IFN signaling and SASP. For instance, De Angelis *et al.*[84] demonstrated that high IFN-response gene signatures, characterized by upregulation of signal transducer and activator of transcription 1, interferon regulatory factor 9, and SP100, along with suppression of immunostimulatory genes, such as inducible T-cell costimulatory (ICOS) and CD70, are strongly associated with treatment resistance. The precise mechanisms driving resistance to CDK4/6 inhibitor-immunotherapy combinations remain poorly characterized, hindering the clinical optimization of these treatments.

7.4. Future prospective

CDK4/6 inhibitors have shown significant potential in breast cancer immunotherapy, with ongoing research targeting several key areas. In early-stage breast cancer, abemaciclib has demonstrated the capacity to reduce the risk of recurrence.[85] In addition, numerous studies are investigating the synergistic effects of combining CDK4/6 inhibitors with ICIs to enhance immune responses and improve clinical outcomes.[86] Importantly, the therapeutic applications of these agents have expanded to include $HER2^+$ and triple-negative breast cancer subtypes, where they have shown clinical benefits.[87]

While research on CDK4/6 inhibitors has predominantly focused on breast cancer, there is growing interest in their application to other cancer types. In ovarian cancer, both preclinical and clinical studies are exploring the potential of CDK4/6 inhibitors as monotherapy or in combination treatments.[88] Preliminary evidence indicates that, while BRAF and MEK inhibitors have inherent antitumor effects, their combination with CDK4/6 inhibitors could further enhance immune activation.[89] Many clinical trials are currently assessing the safety and efficacy of these combined strategies, aiming to identify predictive biomarkers for treatment response and resistance. This would optimize therapeutic outcomes across various cancers through synergistic CDK4/6 inhibition.[41]

Recent studies have drawn attention to the potential of metal ions, such as selenium, zinc, and copper, as critical immunomodulatory trace elements that may enhance the efficacy of CDK4/6 inhibitors.[90,91] This enhancement is achieved by reprogramming immunometabolic pathways within the TME. Specifically, selenium bolsters T-cell resilience against oxidative stress through nuclear factor erythroid 2-related factor 2-mediated antioxidant responses.[92] Meanwhile, zinc aids T-cell proliferation through zeta-chain of T-cell receptor-associated protein kinase 70 signaling and modulates PD-L1 expression on dendritic cells.[93,94] These mechanisms indicate promising opportunities for synergistic combination therapies that target both cell cycle regulation and immunometabolic checkpoints.

It is crucial to note that present evidence largely stems from early-phase clinical trials and pre-clinical models.

Large-scale, randomized, placebo-controlled phase III trials are necessary to confirm both the efficacy and safety profiles of these treatments. Patients whose tumors develop resistance through immune evasion mechanisms may benefit more from the addition of ICIs. The gut microbiome may also play a role in predicting responses to ICI combination therapies.[95] Further research is needed to identify specific biomarkers that can predict which patients will benefit most from this approach.

8. Conclusion

CDK4/6 inhibitors modulate antitumor immunity through multifaceted mechanisms, including direct regulation of T-cell activity, remodeling of the immunosuppressive TME, and regulation of immune checkpoint expression. These immunomodulatory effects provide a mechanistic rationale for combining CDK4/6 inhibitors with ICIs, which may overcome resistance and amplify therapeutic efficacy in cancer treatment. Future studies should focus on elucidating the differential impacts of CDK4/6 inhibition across diverse immune cell populations, refining combinatorial strategies with immunotherapy, and validating these observations across a broader spectrum of tumor malignancies.

Acknowledgments

None.

Funding

None.

Conflict of interest

The authors declare they have no competing interests.

Author contributions

Conceptualization: Jundong Wu, Chunfa Chen
Visualization: Bingfeng Chen, Chunfa Chen, Siyue Lin
Writing – original draft: Yuling Zhang, Chunfa Chen, Rendong Zhang
Writing – review & editing: Jundong Wu, Chunfa Chen

Ethics approval and consent to participate

Not applicable.

Consent for publication

Not applicable.

Availability of data

Not applicable.

References

1. George MA, Qureshi S, Omene C, Toppmeyer DL, Ganesan S. Clinical and pharmacologic differences of CDK4/6 inhibitors in breast cancer. *Front Oncol*. 2021;11:693104.

   doi: 10.3389/fonc.2021.693104

2. Schettini F, De Santo I, Rea CG, *et al*. CDK 4/6 inhibitors as single agent in advanced solid tumors. *Front Oncol*. 2018;8:608.

   doi: 10.3389/fonc.2018.00608

3. Ye M, Xu H, Ding J, Jiang L. Therapy for hormone receptor-positive, human epidermal growth receptor 2-negative metastatic breast cancer following treatment progression via CDK4/6 inhibitors: A literature review. *Breast Cancer (Dove Med Press)*. 2024;16:181-197.

   doi: 10.2147/BCTT.S438366

4. Iranzo P, Callejo A, Assaf JD, *et al*. Overview of checkpoint inhibitors mechanism of action: Role of immune-related adverse events and their treatment on progression of underlying cancer. *Front Med (Lausanne)*. 2022;9:875974.

   doi: 10.3389/fmed.2022.875974

5. Shiravand Y, Khodadadi F, Kashani SMA, *et al*. Immune checkpoint inhibitors in cancer therapy. *Current Oncol*. 2022;29(5):3044-3060.

   doi: 10.3390/curroncol29050247

6. Nunes Filho P, Albuquerque C, Pilon Capella M, Debiasi M. Immune checkpoint inhibitors in breast cancer: A narrative review. *Oncol Ther*. 2023;11(2):171-183.

   doi: 10.1007/s40487-023-00224-9

7. Scirocchi F, Scagnoli S, Botticelli A, *et al*. Immune effects of CDK4/6 inhibitors in patients with $HR^+/HER2^-$ metastatic breast cancer: Relief from immunosuppression is associated with clinical response. *EBioMedicine*. 2022;79:104010.

   doi: 10.1016/j.ebiom.2022.104010

8. Goel S, DeCristo MJ, Watt AC, *et al*. CDK4/6 inhibition triggers anti-tumour immunity. *Nature*. 2017;548(7668):471-475.

   doi: 10.1038/nature23465

9. Thu KL, Soria-Bretones I, Mak TW, Cescon DW. Targeting the cell cycle in breast cancer: Towards the next phase. *Cell Cycle*. 2018;17(15):1871-1885.

   doi: 10.1080/15384101.2018.1502567

10. Stanciu IM, Parosanu AI, Orlov-Slavu C, *et al*. Mechanisms of resistance to CDK4/6 inhibitors and predictive biomarkers of response in HR^+/HER2-metastatic breast cancer-a review of the literature. *Diagnostics (Basel)*. 2023;13(5):987.

    doi: 10.3390/diagnostics13050987

11. Goel S, DeCristo MJ, McAllister SS, Zhao JJ. CDK4/6

inhibition in cancer: Beyond cell cycle arrest. *Trends Cell Biol*. 2018;28(11):911-925.

doi: 10.1016/j.tcb.2018.07.002

12. Hendrychova D, Jorda R, Krystof V. How selective are clinical CDK4/6 inhibitors? *Med Res Rev*. 2021;41(3):1578-1598.

doi: 10.1002/med.21769

13. Pandey K, An HJ, Kim SK, *et al*. Molecular mechanisms of resistance to CDK4/6 inhibitors in breast cancer: A review. *Int J Cancer*. 2019;145(5):1179-1188.

doi: 10.1002/ijc.32020

14. Mouron S, Bueno MJ, Munoz M, *et al*. p27Kip1 V109G as a biomarker for CDK4/6 inhibitors indication in hormone receptor-positive breast cancer. *JNCI Cancer Spectr*. 2023;7(2):pkad014.

doi: 10.1093/jncics/pkad014

15. Hafner M, Mills CE, Subramanian K, *et al*. Multiomics profiling establishes the polypharmacology of FDA-approved CDK4/6 inhibitors and the potential for differential clinical activity. *Cell Chem Biol*. 2019;26(8):1067-1080.e8.

doi: 10.1016/j.chembiol.2019.05.005

16. Zhang Y, Zheng J. Functions of immune checkpoint molecules beyond immune evasion. *Adv Exp Med Biol*. 2020;1248:201-226.

doi: 10.1007/978-981-15-3266-5_9

17. Han Y, Liu D, Li L. PD-1/PD-L1 pathway: Current researches in cancer. *Am J Cancer Res*. 2020;10(3):727-742.

18. Hossen MM, Ma Y, Yin Z, *et al*. Current understanding of CTLA-4: From mechanism to autoimmune diseases. *Frontiers in Immunol*. 2023;14:1198365.

doi: 10.3389/fimmu.2023.1198365

19. Rosskopf S, Leitner J, Zlabinger GJ, Steinberger P. CTLA-4 antibody ipilimumab negatively affects $CD4^+$ T-cell responses *in vitro*. *Cancer Immunol Immunother*. 2019;68(8):1359-1368.

doi: 10.1007/s00262-019-02369-x

20. Deng J, Wang ES, Jenkins RW, *et al*. CDK4/6 inhibition augments antitumor immunity by enhancing t-cell activation. *Cancer Discov*. 2018;8(2):216-233.

doi: 10.1158/2159-8290.CD-17-0915

21. Tong J, Tan X, Song X, *et al*. CDK4/6 inhibition suppresses p73 phosphorylation and activates DR5 to potentiate chemotherapy and immune checkpoint blockade. *Cancer Res*. 2022;82(7):1340-1352.

doi: 10.1158/0008-5472.CAN-21-3062

22. Wang L, Wu Y, Kang K, *et al*. CDK4/6 inhibitor abemaciclib combined with low-dose radiotherapy enhances the anti-tumor immune response to PD-1 blockade by inflaming the tumor microenvironment in Rb-deficient small cell lung cancer. *Transl Lung Cancer Res*. 2024;13(5):1032-1046.

doi: 10.21037/tlcr-24-33

23. Li W, Guo F, Zeng R, *et al*. CDK4/6 alters TBK1 phosphorylation to inhibit the STING signaling pathway in prostate cancer. *Cancer Res*. 2024;84(16):2588-2606.

doi: 10.1158/0008-5472.CAN-23-3704

24. Zhou C, Zhao S, Zhang Y, Cheng J, Shi J, Du G. Mesoporous polydopamine targeting CDK4/6 inhibitor toward brilliant synergistic immunotherapy of breast cancer. *Small*. 2024;20(30):e2310565.

doi: 10.1002/smll.202310565

25. Uzhachenko RV, Bharti V, Ouyang Z, *et al*. Metabolic modulation by CDK4/6 inhibitor promotes chemokine-mediated recruitment of T cells into mammary tumors. *Cell Rep*. 2021;35(12):109271.

doi: 10.1016/j.celrep.2021.109271

26. Wang Q, Guldner IH, Golomb SM, *et al*. Single-cell profiling guided combinatorial immunotherapy for fast-evolving CDK4/6 inhibitor-resistant HER2-positive breast cancer. *Nature Commun*. 2019;10(1):3817.

doi: 10.1038/s41467-019-11729-1

27. Schaer DA, Beckmann RP, Dempsey JA, *et al*. The CDK4/6 inhibitor abemaciclib induces a T cell inflamed tumor microenvironment and enhances the efficacy of PD-L1 checkpoint blockade. *Cell Rep*. 2018;22(11):2978-2994.

doi: 10.1016/j.celrep.2018.02.053

28. Xiao J, Liang J, Fan J, *et al*. CDK4/6 inhibition enhances oncolytic virus efficacy by potentiating tumor-selective cell killing and T-cell activation in refractory glioblastoma. *Cancer Res*. 2022;82(18):3359-3374.

doi: 10.1158/0008-5472.CAN-21-3656

29. Wu J, Wang J, O'Connor TN, *et al*. Separable cell cycle arrest and immune response elicited through pharmacological CDK4/6 and MEK inhibition in RAsmut disease models. *Mol Cancer Ther*. 2024;23(12):1801-1814.

doi: 10.1158/1535-7163.MCT-24-0369

30. Zhang Y, Lian Y, Zhou C, *et al*. Self-assembled natural triterpenoids for the delivery of cyclin-dependent kinase 4/6 inhibitors to enhance cancer chemoimmunotherapy. *J Control Release*. 2025;378:791-802.

doi: 10.1016/j.jconrel.2024.12.067

31. Lelliott EJ, Kong IY, Zethoven M, *et al*. CDK4/6 inhibition promotes antitumor immunity through the induction of T-cell memory. *Cancer Discov*. 2021;11(10):2582-2601.

doi: 10.1158/2159-8290.CD-20-1554

32. Yang WC, Wei MF, Huang CS, Shen YC, Kuo SH. Synergistic potential of CDK4/6 inhibitors and radiotherapy with Anti-PD-L1 immunotherapy in triple-negative breast cancer. *Int J*

Radiat Oncol Biol Phys. 2024;120(2 Suppl):S46.

doi: 10.1016/j.ijrobp.2024.07.071

33. Zhang QF, Li J, Jiang K, *et al*. CDK4/6 inhibition promotes immune infiltration in ovarian cancer and synergizes with PD-1 blockade in a B cell-dependent manner. *Theranostics*. 2020;10(23):10619-10633.

doi: 10.7150/thno.44871

34. Heckler M, Ali LR, Clancy-Thompson E, *et al*. Inhibition of CDK4/6 promotes CD8 T-cell memory formation. *Cancer Discov*. 2021;11(10):2564-2581.

doi: 10.1158/2159-8290.CD-20-1540

35. Teh JLF, Erkes DA, Cheng PF, *et al*. Activation of $CD8^+$ T cells contributes to antitumor effects of CDK4/6 inhibitors plus MEK inhibitors. *Cancer Immunol Res*. 2020;8(9):1114-1121.

doi: 10.1158/2326-6066.CIR-19-0743

36. Bai X, Guo ZQ, Zhang YP, *et al*. CDK4/6 inhibition triggers ICAM1-driven immune response and sensitizes LKB1 mutant lung cancer to immunotherapy. *Nature Commun*. 2023;14(1):1247.

doi: 10.1038/s41467-023-36892-4

37. Ruscetti M, Leibold J, Bott MJ, *et al*. NK cell-mediated cytotoxicity contributes to tumor control by a cytostatic drug combination. *Science*. 2018;362(6421):1416-1422.

doi: 10.1126/science.aas9090

38. Wu Y, Shrestha P, Heape NM, Yarchoan R. CDK4/6 inhibitors sensitize gammaherpesvirus-infected tumor cells to T-cell killing by enhancing expression of immune surface molecules. *J Transl Med*. 2022;20(1):217.

doi: 10.1186/s12967-022-03400-z

39. Lai AY, Sorrentino JA, Dragnev KH, *et al*. CDK4/6 inhibition enhances antitumor efficacy of chemotherapy and immune checkpoint inhibitor combinations in preclinical models and enhances T-cell activation in patients with SCLC receiving chemotherapy. *J Immunother Cancer*. 2020;8(2):e000847.

doi: 10.1136/jitc-2020-000847

40. Salewski I, Henne J, Engster L, *et al*. CDK4/6 blockade provides an alternative approach for treatment of mismatch-repair deficient tumors. *Oncoimmunology*. 2022;11(1):2094583.

doi: 10.1080/2162402X.2022.2094583

41. Sun M, Dong L, Wang Y, *et al*. The role of targeting CDK4/6 in cancer immunotherapy. *Holist Integr Oncol*. 2024;3(1):32.

doi: 10.1007/s44178-024-00100-0

42. Zhang S, Xu Q, Sun W, Zhou J, Zhou J. Immunomodulatory effects of CDK4/6 inhibitors. *Biochim Biophys Acta Rev Cancer*. 2023;1878(4):188912.

doi: 10.1016/j.bbcan.2023.188912

43. Liu C, Huang Y, Cui Y, *et al*. The immunological role of CDK4/6 and potential mechanism exploration in ovarian cancer. *Front Immunol*. 2021;12:799171.

doi: 10.3389/fimmu.2021.799171

44. Lee DH, Imran M, Choi JH, *et al*. CDK4/6 inhibitors induce breast cancer senescence with enhanced anti-tumor immunogenic properties compared with DNA-damaging agents. *Mol Oncol*. 2024;18(1):216-232.

doi: 10.1002/1878-0261.13541

45. Pandey P, Khan F, Upadhyay TK, Sharangi AB. Deciphering the immunomodulatory role of cyclin-dependent kinase 4/6 inhibitors in the tumor microenvironment. *Int J Mol Sci*. 2023;24(3):2236.

doi: 10.3390/ijms24032236

46. Watt AC, Cejas P, DeCristo MJ, *et al*. CDK4/6 inhibition reprograms the breast cancer enhancer landscape by stimulating AP-1 transcriptional activity. *Nat Cancer*. 2021;2(1):34-48.

doi: 10.1038/s43018-020-00135-y

47. Fan H, Liu W, Zeng Y, *et al*. DNA damage induced by CDK4 and CDK6 blockade triggers anti-tumor immune responses through cGAS-STING pathway. *Commun Biol*. 2023;6(1):1041.

doi: 10.1038/s42003-023-05412-x

48. Charles A, Bourne CM, Korontsvit T, *et al*. Low-dose CDK4/6 inhibitors induce presentation of pathway specific MHC ligands as potential targets for cancer immunotherapy. *Oncoimmunology*. 2021;10(1):1916243.

doi: 10.1080/2162402X.2021.1916243

49. Liu J, Cheng M, Xu J, Liang Y, Yin B, Liang J. Effect of CDK4/6 inhibitors on tumor immune microenvironment. *Immunol Invest*. 2024;53(3):437-449.

doi: 10.1080/08820139.2024.2304565

50. Stopfer LE, Mesfin JM, Joughin BA, Lauffenburger DA, White FM. Multiplexed relative and absolute quantitative immunopeptidomics reveals MHC I repertoire alterations induced by CDK4/6 inhibition. *Nat Commun*. 2020;11(1):2760.

doi: 10.1038/s41467-020-16588-9

51. Kumar A, Ramani V, Bharti V, *et al*. Dendritic cell therapy augments antitumor immunity triggered by CDK4/6 inhibition and immune checkpoint blockade by unleashing systemic CD4 T-cell responses. *J Immunother Cancer*. 2023;11(5):e006019.

doi: 10.1136/jitc-2022-006019

52. Kohlmeyer JL, Lingo JJ, Kaemmer CA, *et al*. CDK4/6-MEK inhibition in MPNSTs causes plasma cell infiltration, sensitization to PD-L1 blockade, and tumor regression. *Clin Cancer Res*. 2023;29(17):3484-3497.

doi: 10.1158/1078-0432.CCR-23-0749

53. Kollmann K, Heller G, Schneckenleithner C, *et al*. A kinase-independent function of CDK6 links the cell cycle to tumor angiogenesis. *Cancer Cell*. 2016;30(2):359-360.

doi: 10.1016/j.ccell.2016.07.003

54. Huang Z, Zhao B, Qin Z, *et al*. Novel dual inhibitors targeting CDK4 and VEGFR2 synergistically suppressed cancer progression and angiogenesis. *Eur J Med Chem*. 2019;181:111541.

doi: 10.1016/j.ejmech.2019.07.044

55. Liu R, Li HF, Li S. PD-1-mediated inhibition of T cell activation: Mechanisms and strategies for cancer combination immunotherapy. *Cell Insight*. 2024;3(2):100146.

doi: 10.1016/j.cellin.2024.100146

56. Zhang J, Bu X, Wang H, *et al*. Cyclin D-CDK4 kinase destabilizes PD-L1 via cullin 3-SPOP to control cancer immune surveillance. *Nature*. 2018;553(7686):91-95.

doi: 10.1038/nature25015

57. Shrestha M, Wang DY, Ben-David Y, Zacksenhaus E. CDK4/6 inhibitors and the pRB-E2F1 axis suppress PVR and PD-L1 expression in triple-negative breast cancer. *Oncogenesis*. 2023;12(1):29.

doi: 10.1038/s41389-023-00475-1

58. Palicelli A, Croci S, Bisagni A, *et al*. What do we have to know about PD-L1 expression in prostate cancer? A systematic literature review. Part 4: Experimental treatments in pre-clinical studies (cell lines and mouse models). *Int J Mol Sci*. 2021;22(22):12297.

doi: 10.3390/ijms222212297

59. Jerusalem G, Prat A, Salgado R, *et al*. Neoadjuvant nivolumab + palbociclib + anastrozole for oestrogen receptor-positive/human epidermal growth factor receptor 2-negative primary breast cancer: Results from checkMate 7A8. *Breast*. 2023;72:103580.

doi: 10.1016/j.breast.2023.103580

60. Rugo HS, Kabos P, Beck JT, *et al*. Abemaciclib in combination with pembrolizumab for HR+, HER2- metastatic breast cancer: Phase 1b study. *NPJ Breast Cancer*. 2022;8(1):118.

doi: 10.1038/s41523-022-00482-2

61. Yuan Y, Lee JS, Yost SE, *et al*. Phase I/II trial of palbociclib, pembrolizumab and letrozole in patients with hormone receptor-positive metastatic breast cancer. *Eur J Cancer*. 2021;154:11-20.

doi: 10.1016/j.ejca.2021.05.035

62. Santa-Maria C, Wang C, Cimino-Mathews A, *et al*. Abstract OT3-02-03: IMMUNe mOdulation in early stage estrogen receptor positive breast cancer treated with neoADjuvant avelumab, palbociclib, and tamoxifen: The immunoADAPT study (NCT03573648). *Cancer Res*. 2019;79(4 Suppl):OT3-02-03.

doi: 10.1158/1538-7445.SABCS18-OT3-02-03

63. Zavras P, Chen R, Qi H, *et al*. Abstract PO1-01-09: Neoadjuvant endocrine therapy and avelumab with or without palbociclib in stage II/III endocrine receptor-positive breast cancer: The immunoADAPT trial. *Cancer Res*. 2024;84(9 Suppl):PO1-01-09.

doi: 10.1158/1538-7445.SABCS23-PO1-01-09

64. Garrido-Castro AC, Graham N, Ali LR, *et al*. Phase I study of ribociclib (CDK4/6 inhibitor) with spartalizumab (PD-1 inhibitor) with and without fulvestrant in metastatic hormone receptor-positive breast cancer or advanced ovarian cancer. *J Immunother Cancer*. 2025;13(2):e010430.

doi: 10.1136/jitc-2024-010430

65. Masuda J, Sakai H, Tsurutani J, *et al*. Efficacy, safety, and biomarker analysis of nivolumab in combination with abemaciclib plus endocrine therapy in patients with HR-positive HER2-negative metastatic breast cancer: A phase II study (WJOG11418B NEWFLAME trial). *J Immunother Cancer*. 2023;11(9):e007126.

doi: 10.1136/jitc-2023-007126

66. Mayer EL, Ren Y, Wagle N, *et al*. PACE: A randomized phase II study of fulvestrant, palbociclib, and avelumab after progression on cyclin-dependent kinase 4/6 inhibitor and aromatase inhibitor for hormone receptor-positive/human epidermal growth factor receptor-negative metastatic breast cancer. *J Clin Oncol*. 2024;42(17):2050-2060.

doi: 10.1200/JCO.23.01940

67. Kearney MR, McGuinness JE, Kalinsky K. Clinical trial data and emerging immunotherapeutic strategies: Hormone receptor-positive, HER2- negative breast cancer. *Breast Cancer Res Treat*. 2021;189(1):1-13.

doi: 10.1007/s10549-021-06291-8

68. Lelliott EJ, Sheppard KE, McArthur GA. Harnessing the immunotherapeutic potential of CDK4/6 inhibitors in melanoma: Is timing everything? *NPJ Precis Oncol*. 2022;6(1):26.

doi: 10.1038/s41698-022-00273-9

69. Xue Y, Zhai J. Strategy of combining CDK4/6 inhibitors with other therapies and mechanisms of resistance. *Int J Clin Exp Pathol*. 2024;17(7):189-207.

doi: 10.62347/HGNI4903

70. Shim SH, Lee JY, Lee YY, *et al*. Major clinical research advances in gynecologic cancer in 2023: A tumultuous year for endometrial cancer. *J Gynecol Oncol*. 2024;35(2):e66.

doi: 10.3802/jgo.2024.35.e66

71. Wang Y, Liu L, Graff SL, Cheng L. Recent advancements in biomarkers and molecular diagnostics in hormonal receptor-

positive breast cancer. *Histopathology*. 2024;87:3-17.

doi: 10.1111/his.15395

72. Finn RS, Boer K, Bondarenko I, *et al*. Overall survival results from the randomized phase 2 study of palbociclib in combination with letrozole versus letrozole alone for first-line treatment of ER+/HER2- advanced breast cancer (PALOMA-1, TRIO-18). *Breast Cancer Res Treat*. 2020;183(2):419-428.

doi: 10.1007/s10549-020-05755-7

73. Im SA, Mukai H, Park IH, *et al*. Palbociclib plus letrozole as first-line therapy in postmenopausal Asian women with metastatic breast cancer: Results from the phase III, randomized PALOMA-2 study. *J Glob Oncol*. 2019;5:1-19.

doi: 10.1200/JGO.18.00173

74. Cristofanilli M, Rugo HS, Im SA, *et al*. Overall survival with palbociclib and fulvestrant in women with HR+/HER2- ABC: Updated exploratory analyses of PALOMA-3, a double-blind, phase III randomized study. *Clin Cancer Res*. 2022;28(16):3433-3442.

doi: 10.1158/1078-0432.CCR-22-0305

75. Jhaveri K, O'Shaughnessy J, Fasching PA, *et al*. Matching-adjusted indirect comparison of PFS and OS comparing ribociclib plus letrozole versus palbociclib plus letrozole as first-line treatment of HR+/HER2- advanced breast cancer. *Ther Adv Med Oncol*. 2023;15:103580.

doi: 10.1177/17588359231216095

76. Slamon DJ, Neven P, Chia S, *et al*. Phase III randomized study of ribociclib and fulvestrant in hormone receptor-positive, human epidermal growth factor receptor 2-negative advanced breast cancer: MONALEESA-3. *J Clin Oncol*. 2018;36(24):2465-2472.

doi: 10.1200/JCO.2018.78.9909

77. Lu YS, Im SA, Colleoni M, *et al*. Updated overall survival of ribociclib plus endocrine therapy versus endocrine therapy alone in pre- and perimenopausal patients with HR+/HER2- advanced breast cancer in MONALEESA-7: A phase III randomized clinical trial. *Clin Cancer Res*. 2022;28(5):851-859.

doi: 10.1158/1078-0432.CCR-21-3032

78. Johnston S, Martin M, Di Leo A, *et al*. MONARCH 3 final PFS: A randomized study of abemaciclib as initial therapy for advanced breast cancer. *NPJ Breast Cancer*. 2019;5:5.

doi: 10.1038/s41523-018-0097-z

79. Sledge GW Jr., Toi M, Neven P, *et al*. MONARCH 2: Abemaciclib in combination with fulvestrant in women with HR+/HER2- advanced breast cancer who had progressed while receiving endocrine therapy. *J Clin Oncol*. 2017;35(25):2875-2884.

doi: 10.1200/JCO.2017.73.7585

80. Wu S, Xu J, Ma Y, Liang G, Wang J, Sun T. Advances in the mechanism of CDK4/6 inhibitor resistance in HR+/HER2- breast cancer. *Ther Adv Med Oncol*. 2024;16:17588359241282499.

doi: 10.1177/17588359241282499

81. Morrison L, Loibl S, Turner NC. The CDK4/6 inhibitor revolution - a game-changing era for breast cancer treatment. *Nat Rev Clin Oncol*. 2024;21(2):89-105.

doi: 10.1038/s41571-023-00840-4

82. Klein ME, Kovatcheva M, Davis LE, Tap WD, Koff A. CDK4/6 inhibitors: The mechanism of action may not be as simple as once thought. *Cancer Cell*. 2018;34(1):9-20.

doi: 10.1016/j.ccell.2018.03.023

83. Teh JLF, Aplin AE. Arrested developments: CDK4/6 Inhibitor resistance and alterations in the tumor immune microenvironment. *Clin Cancer Res*. 2019;25(3):921-927.

doi: 10.1158/1078-0432.CCR-18-1967

84. De Angelis C, Fu X, Cataldo ML, *et al*. Activation of the IFN signaling pathway is associated with resistance to CDK4/6 inhibitors and immune checkpoint activation in ER-positive breast cancer. *Clin Cancer Res*. 2021;27(17):4870-4882.

doi: 10.1158/1078-0432.CCR-19-4191

85. Sammons S, Moore H, Cushman J, Hamilton E. Efficacy, safety and toxicity management of adjuvant abemaciclib in early stage HR+/HER2- high-risk breast cancer. *Expert Rev Anticancer Ther*. 2022;22(8):805-814.

doi: 10.1080/14737140.2022.2093719

86. Nabieva N, Fasching PA. CDK4/6 inhibitors-overcoming endocrine resistance is the standard in patients with hormone receptor-positive breast cancer. *Cancers(Basel)*. 2023;15(6):1763.

doi: 10.3390/cancers15061763

87. Zhao S, Zhang H, Yang N, Yang J. A narrative review about CDK4/6 inhibitors in the setting of drug resistance: Updates on biomarkers and therapeutic strategies in breast cancer. *Transl Cancer Res*. 2023;12(6):1617-1634.

doi: 10.21037/tcr-22-2807

88. Dall'Acqua A, Bartoletti M, Masoudi-Khoram N, *et al*. Inhibition of CDK4/6 as therapeutic approach for ovarian cancer patients: Current evidences and future perspectives. *Cancers (Basel)*. 2021;13(12):3035.

doi: 10.3390/cancers13123035

89. Lelliott EJ, McArthur GA, Oliaro J, Sheppard KE. Immunomodulatory effects of BRAF, MEK, and CDK4/6 inhibitors: Implications for combining targeted therapy and immune checkpoint blockade for the treatment of melanoma. *Front Immunol*. 2021;12:661737.

doi: 10.3389/fimmu.2021.661737

90. Himoto T, Masaki T. Current trends on the involvement of zinc, copper, and selenium in the process of hepatocarcinogenesis. *Nutrients*. 2024;16(4):472.

doi: 10.3390/nu16040472

91. Lubinski J, Lener MR, Marciniak W, *et al*. Serum essential elements and survival after cancer diagnosis. *Nutrients*. 2023;15(11):2611.

doi: 10.3390/nu15112611

92. Ohl K, Tenbrock K. Oxidative stress in SLE T cells, is NRF2 really the target to treat? *Front Immunol*. 2021;12:633845.

doi: 10.3389/fimmu.2021.633845

93. Kim B, Kim HY, Lee WW. Zap70 regulates TCR-mediated zip6 activation at the immunological synapse. *Front Immunol*. 2021;12:687367.

doi: 10.3389/fimmu.2021.687367

94. George MM, Subramanian Vignesh K, Landero Figueroa JA, Caruso JA, Deepe GS Jr. Zinc induces dendritic cell tolerogenic phenotype and skews regulatory T cell-Th17 balance. *J Immunol*. 2016;197(5):1864-1876.

doi: 10.4049/jimmunol.1600410

95. LeVee AA, Egelston CA, Yost SE, *et al*. A phase I/II trial of palbociclib, pembrolizumab, and endocrine therapy for patients with HR+/HER2- locally advanced or metastatic breast cancer (MBC): Clinical outcomes and stool microbial profiling. *J Clin Oncol*. 2024;42(16 Suppl):1038-1038.

doi: 10.1200/JCO.2024.42.16_suppl.1038

ACCSCIENCE PUBLISHING

Tumor Discovery

ORIGINAL RESEARCH ARTICLE

Genomic alterations of homologous recombination deficiency in Chinese NSCLC patients

Shuang Xiang[1†], Changqiong Shen[2†], Chun Huang[3], Ya-ting Yang[1], Jing Guo[4], Yi Liu[5], Mingzhu Yin[1*], and Song Duan[1*]

[1]Department of Pathology, Chongqing University Three Gorges Hospital, Chongqing, China

[2]Department of Radiology, People's Hospital Affiliated to Chongqing Three Gorges Medical College, Chongqing, China

[3]Department of Respiratory Medicine, Chongqing University Three Gorges Hospital, Chongqing, China

[4]Department of Oncology, Chongqing University Three Gorges Hospital, Chongqing, China

[5]Department of Thoracic Surgery, Chongqing University Three Gorges Hospital, Chongqing, China

(This article belongs to the *Special Issue: New Developments in Lung Cancer Research, Diagnosis, Treatment, and Prognosis*)

Abstract

Homologous recombination deficiency (HRD) affects genomic stability and has potential as a biomarker for the effectiveness of poly (ADP-ribose) polymerase (PARP) inhibitors and immune checkpoint inhibitors. However, the clinical and molecular profile of HRD in non-small cell lung cancer (NSCLC), particularly in the Chinese population, remains poorly characterized. Based on the next-generation sequencing data of 158 Chinese NSCLC patients, we analyzed the HRD scores of mutations in homologous recombination repair (*HRR*) genes and dissected the correlation between HRD state and programmed death-ligand 1 (PD-L1) expression. Alterations in *HRR* genes were observed in 8.9% of the patients, with *ATM* and *BRCA2* being the most commonly affected genes. HRD-high (HRD-H) status was significantly associated with advanced disease stage (≥III) and lung squamous cell carcinoma (LUSC). Transcriptomic analysis revealed distinct gene expression profiles between HRD-H and HRD-low (HRD-L) subgroups, with HRD-H tumors exhibiting predominantly downregulated genes. While *EGFR* mutations occurred at similar frequencies across HRD status, *TP53* mutations were significantly enriched in HRD-H cases. HRD-H status correlated with higher PD-L1 positivity in NSCLC overall, but not within the lung adenocarcinoma (LUAD) subgroup in our cohort. The Cancer genome atlas analysis showed higher PD-L1 protein expression in HRD-H LUAD, but not in LUSC. Kyoto Encyclopedia of Genes and Genomes analysis identified enrichment of complement and coagulation cascades, ABC transporters, and bile secretion pathways in HRD-H tumors, suggesting links to immune evasion and drug resistance. This study elucidates the genomic landscape of HRD in Chinese NSCLC patients and provides insights into its potential clinical utility for therapeutic targeting. Our findings suggest that integrated HRD scoring may guide the application of PARP inhibitors and immunotherapy in specific NSCLC patient subgroups. Further prospective clinical studies are needed to validate the predictive value of HRD scoring in NSCLC treatment and to optimize patient selection strategies.

Keywords: Homologous recombination deficiency; Immunotherapy biomarkers; Next-generation sequencing; Non-small cell lung cancer; Programmed death-ligand 1

†These authors contributed equally to this work.

***Corresponding authors:**
Mingzhu Yin
(yinmingzhu2008@126.com)
Song Duan
(duansong2024@163.com)

Citation: Xiang S, Shen C, Huang C, *et al*. Genomic alterations of homologous recombination de iciency in Chinese NSCLC patients. *TumorDiscov*. 2025;4(3):32-45.
doi: 10.36922/TD025180032

Received: April 30, 2025

Revised: May 20, 2025

Accepted: May 21, 2025

Published online: June 6, 2025

1. Introduction

Lung cancer is the most common type of cancer (accounting for 11.6% of all cancer cases) and the leading cause of cancer death worldwide (accounting for 18.4% of all cancer deaths). Lung cancer is one of the leading causes of cancer-related death in China, and its 5-year survival rate is only 19.8%.[1] Roughly 80 – 85% of lung cancers are categorized as non-small cell lung cancer (NSCLC), with lung adenocarcinoma (LUAD) and lung squamous cell carcinoma (LUSC) being the predominant subtypes of NSCLC.[2] Recent innovations in NSCLC management involve the use of targeted therapies, immunotherapies, and the synergistic pairing of chemotherapy and immunotherapy.[3] Nevertheless, around one-third of individuals diagnosed with LUAD and most patients with LUSC lack oncogenic driver mutations that can be targeted for treatment.[4-6] NSCLC patients without identifiable oncogenic driver alterations can undergo chemotherapy or chemo-immunotherapy, depending on the cancer subtype and the expression of the programmed death ligand-1 gene (*PD-L1*).[7] However, only a small percentage (<20%) of unselected NSCLC patients respond to immunotherapy, and some of these patients experience severe immunotoxicity.[8] Hence, there exists an unmet need to explore potential novel and effective treatment modalities to improve the therapeutic outcomes for NSCLC.

Homologous recombination is pivotal for maintaining genome stability through the repair of DNA double-strand breaks (DSBs) and stalled DNA replication forks.[9] Tumors exhibiting deficiencies in homologous recombination still require intact mechanisms for the repair of DNA lesions that are critical for cell viability, and thus shift their reliance to other functional DNA repair pathways.[10] Targeting these dependent pathways in DNA damage response (DDR)-deficient cancer cells induce a synthetic lethality effect, thereby inhibiting cancer cell proliferation.[11] Poly (ADP-ribose) polymerase (PARP) inhibitors selectively eradicate cells with homologous recombination repair (HRR) deficiencies through synthetic lethality interactions.[12] This synthetic lethality has been extensively applied in breast, ovarian, and prostate cancers with *BRCA1* and *BRCA2* mutations.[13] Therefore, *BRCA* mutations and the status of homologous recombination deficiency (HRD) serve as biomarkers for predicting the efficacy of PARP inhibitors.[14] Alterations in genes of the homologous recombination pathway have been extensively studied, leading to the development of HRD scoring algorithms utilizing various assays to quantify the extent of genomic instability. These algorithms rely on metrics associated with loss of heterozygosity, telomeric allelic imbalance, and large-scale state transitions.[15] The breast cancer susceptibility genes *BRCA1* and *BRCA2* are the most well-known genes associated with HRD.[16] Other genes, such as ataxia telangiectasia mutated (*ATM*), *BRCA1* associated RING domain 1 (*BARD1*), and *BRCA1* interacting protein C-terminal helicase 1 (*BRIP1*), have been identified as participants in homologous recombination and related pathways.[17] Numerous studies have demonstrated the presence of HRD in lung cancer.[18-20] However, the expansion of PARP inhibitors into the field of lung cancer through experimental and clinical studies is still limited, and considerable efforts are needed before their application in lung cancer.

Deficiency of homologous recombination, or HRD, arises from defects in DNA repair pathways, particularly the HRR system responsible for repairing DSBs. Abnormalities in HRR can be attributed to germline or somatic mutations of some genes including *BRCA1*, *BRCA2*, *ATM*, *RAD51*, and *BARD1*. These genetic alterations result in genomic instability, a hallmark of cancer development.[20,21] The specific HRD features include large-scale state transitions, loss of heterozygosity, and telomeric allelic imbalances. These genomic characteristics have been used to predict response to PARP inhibitors in ovarian and breast cancers, and have been associated with improved overall survival in patients with *BRCA* mutations, ovarian and breast cancers, and high HRD scores.[22] However, HRD could also be both hereditary and secondary; some tumors become HRD even without *BRCA* mutations, but this makes it useful for more cancer types.

Beyond conferring sensitivity to PARP inhibitors, HRD is also linked to increased tumor immunogenicity. Several investigations have shown that the mutation rate in HRD-positive tumors is higher and that these mutations may give rise to neoantigens and increased infiltration of tumor tissue by immune cells.[23] HRD is associated with increased expression of immune checkpoint proteins such as PD-L1 and activation of interferon signaling pathways, suggesting a potential interaction between HRD and immunotherapy.[24] For example, in microsatellite stable cancers, it has been demonstrated that the utilization of HRD increases the effectiveness of immune checkpoint inhibitors (ICI), including anti-PD-1 and anti-PD-L1 agents.[25] The combination of PARP inhibitors and ICIs is based on pre-clinical evidence that PARP inhibition releases intracellular DNA to activate the cGAS-STING pathway, enhancing immunity against the tumor. That is why today there are many clinical trials of such combinations for various malignancies. For example, the MEDIOLA trial exposed a relatively favorable outcome of combining olaparib and durvalumab in *BRCA*-mutant metastatic breast cancer with a high response rate and disease control.[26]

Despite these advances, studies specifically addressing the clinical and molecular landscape of HRD in NSCLC, particularly in East Asian populations, remain scarce. Most large-scale HRD studies have focused on breast, ovarian, and prostate cancers, where HRD is more prevalent and its prognostic and predictive value is well established.[27] In NSCLC, the prevalence, clinical significance, and biomarker potential of HRD, especially the commonly mutated genes such as *EGFR*, *TP53*, and ALK are not well characterized, and evidence from Chinese populations is particularly limited. At present, the mainstream HRD score is based on the Food and Drug Administration-approved Myriad HRD assay, which uses a threshold of 42.[28] In this study, the HRD threshold was set at 43, determined according to the genomic database of the Chinese population. This threshold better reflects the practical value of our research in Asian NSCLC patients.

In addition, evidence has shown that cancers with HRD exhibit enhanced immunogenicity, and checkpoint inhibitors demonstrate potential efficacy.[29] Numerous oncological studies have illustrated the potential of HRD as a biomarker for immunotherapy.[30,31] One previous study observed the disparities in PD-L1 expression status, genetic backgrounds, and exposure to the environment between Asia and the United States.[32] Thus, there is a need for region-specific research on the applicability and predictive/prognostic values of HRD. Further investigation into HRD could be crucial for identifying new therapeutic targets in NSCLC.

In this study, we aim to describe the correlation between HRD scores and clinical characteristics in Chinese patients with NSCLC, as well as the mutation status in HRD-related genes. Furthermore, we attempted to analyze the relationship between HRD scores and PD-L1 expression, providing foundational data for selecting biomarkers in future clinical targeted therapies for NSCLC.

2. Materials and methods

2.1. Patient cohort and sample collection

This study is a retrospective study conducted on 158 pathologically proven NSCLC patients treated at the Chongqing University Three Gorges Hospital. The cohort included 148 patients with LUAD and 10 patients with LUSC, which are the two most common subtypes of NSCLC.

Patients were enrolled consecutively according to the order of their thoracic surgery admissions over a 6-month period, from August 2023 to January 2024. The inclusion criteria are as follows: (i) age between 18 and 75 years; (ii) histologically confirmed diagnosis of NSCLC (LUAD or LUSC); (iii) availability of sufficient formalin-fixed paraffin-embedded (FFPE) tumor tissue for DNA extraction, with tumor cellularity >30%; (iv) availability of matched germline peripheral blood samples; (v) ability to provide written informed consent; and (vi) complete clinicopathological and demographic data.

The exclusion criteria are as follows: (i) prior neoadjuvant chemotherapy, radiotherapy, or targeted therapy before tissue sampling, to avoid treatment-induced genomic alterations; (ii) insufficient tumor cellularity (<30%) in FFPE samples; (iii) poor DNA quality or quantity after extraction; (iv) diagnosis of small cell lung cancer or other rare NSCLC subtypes; and (v) presence of medical or psychiatric conditions that precluded the possibility of obtaining informed consent.

These criteria were established to ensure high-quality genomic data and accurate HRD assessment and to reduce confounding factors that could artificially alter the observed HRD-related mutation frequency. By excluding patients with prior systemic therapy, inadequate tissue or DNA, or inability to provide informed consent, we aimed to capture the true prevalence of HRD-related mutations in treatment-naïve, representative Chinese NSCLC patients. Informed consent was obtained from all patients, and the study protocol was approved by the institutional ethical review committee.

2.2. DNA extraction and quality control

Total genomic DNA from FFPE tumor tissues was isolated using the Paraffin-Embedded Tissue DNA Extraction Kit (centrifugal column method) from Novogene Biotechnology, Tianjin, China; it is a modified protocol of a standard DNA extraction kit that provides high yield and quality of purified DNA from the fragmented genomic DNA from FFPE samples. For germline DNA, leukocyte from the peripheral blood sample was used, and the DNA was extracted using the Tienken Blood DNA kit of Tiangen Biotech, Beijing, China. DNA yield and quality were determined by using a Qubit Fluorometer (Thermo Fisher Scientific, Waltham, USA) and Agilent 2,100 Bioanalyzer (Agilent Technologies, Santa Clara, USA).

2.3. Gene panel design and sequencing

Targeted next-generation sequencing (NGS) was done on a DNAseq custom hybrid capture panel consisting of 188 cancer genes and 37,000 genome-wide single nucleotide polymorphism (SNP) markers. This panel was selectively used to detect somatic and germline mutations in the genes related to HRR and to assess the HRD score based on genomic instability. The panel includes comprehensive coverage of *EGFR* mutation hotspots and other driver

alterations that occur at significantly higher frequencies in East Asian NSCLC patients compared to Western populations. The selected genes include some known oncogenes and DDR-associated genes that are involved in tumor development and therapy response. Sequencing libraries were prepared with 0.5 μg of good-quality DNA per sample. DNA was sheared to 180 – 280 bp using a Covaris M220 ultrasonicator (Massachusetts, USA). End-repair was then performed, followed by A-tailing and adapter ligation, and the samples were finally subjected to polymerase chain reaction enrichment using index primes. DNA samples were purified using AMPure XP beads (Beckman Coulter, USA) and all the libraries were then quantified using a high-sensitivity DNA assay kit from Agilent. DNA sequencing was done in the Illumina NovaSeq 6,000 where the tool used was 2 × 150 bp paired-end. With a significance level at $p<0.05$ and power of 0.90, a minimum average coverage depth was set for targeted genes and SNPs loci at ×1,000 and ×200, respectively, to ensure an adequate HRD scoring and mutation detection.

2.4. Bioinformatics pipeline and variant calling

The raw sequencing data were then filtered using FASTP version 0 (HaploX Biotechnology, China) with adapters trimming and removing low-quality reads. The clean reads were then mapped to the target human genomic reference sequence, specifically the hg19 or the NCBI Build 37. Sambamba was used in the process of sorting the BAM files and Samblaster in identifying the duplicate reads. Somatic and germline single nucleotide variants, as well as small insertion-deletions were called from the tumor and normal samples using VarScan2 (Washington University, USA). All variants were filtered with an in-house pipeline and were then validated using Integrative Genomics Viewer (Broad Institute, USA) to ensure that these were accurate.

2.5. Calculation of HRD score and classification

For the evaluation of HRD, we utilized the scarHRD R package (https://github.com/sztup/scarHRD) to calculate HRD scores based on three genomic instability metrics: loss of heterozygosity, telomeric allelic imbalance, and large-scale state transitions. The use of 37,000 genome-wide SNP markers provided high-resolution detection of these events, tailored to the genetic background of Chinese patients. The patients were further divided into two subgroups according to their scores of the HRD as follows:

- HRD-High (HRD-H): Score ≥43
- HRD-Low (HRD-L): Score <43.

This threshold has been taken from other previously validated works[24] and is a biologically significant cut-off to signify patients with high genomic instability and therefore possible responders to therapeutics.

2.6. Biomarker and clinical feature integration

Expression of PD-L1 was assessed using immunohistochemistry, and mutation status for key oncogenes was determined from sequencing data. This comprehensive biomarker assessment allows for an analysis of HRD's clinical significance in the Chinese context.

2.7. Statistical analysis

In this study, we performed the statistical analysis and visualization using the R package map tools. Landscape analyses, statistical tests, and other pertinent studies were made easier by this package.[1] For comparisons between two categorical and continuous variables, Fisher's exact test and the Mann–Whitney *U* tests were used. In addition, the software used for differential analysis of the cancer genome atlas (TCGA) transcriptomic data was limma, and the software used for differential analysis of HRD-RNAseq data was DESeq2. The criteria for selecting differentially expressed genes (DEGs) were $|\log2FC| > 1$ and adjusted $p<0.05$, and all other tests were also performed at the statistically significance level <0.05.

3. Results

3.1. Mutational landscape of *HRR* genes in Chinese NSCLC patients

To study the association between HRD score and NSCLC clinicopathological and genetic features, we employed an NGS test covering 188 cancer-related genes and more than 37,000 SNPs distributed across the human genome. Among 158 NSCLC patients, 8.9% (14/158) harbored somatic genomic alterations in *HRR* genes. Within these 14 patients, we identified 17 mutations in *HRR* genes, with the majority (88.2%) being missense mutations. In addition, 24.7% (39/158) of patients exhibited germline genomic alterations in the *HRR* genes. Among these 39 patients, we identified 49 mutations in the *HRR* genes, with 18.4% being classified as pathogenic mutations (Figure 1A). In our cohort of Chinese NSCLC patients, *ATM* emerged as the most frequently somatically mutated *HRR* gene, occurring in 4.4% of cases. The most common germline mutated gene among the *HRR* genes was *BRCA2,* present in 7.0% of cases, followed by *ATM* at 3.2%, *BRIP1* at 3.2%, and *BARD1* at 2.5% (Figure 1A). Our analysis revealed that *EGFR* alterations were mutually exclusive with many other genetic alterations, suggesting that *EGFR* mutations represent the most potent driver events in NSCLC. Conversely, we observed that changes in multiple

[1] Accessible at http://bioconductor.org/packages/release/bioc/vignettes/maftools/inst/doc/maftools.html

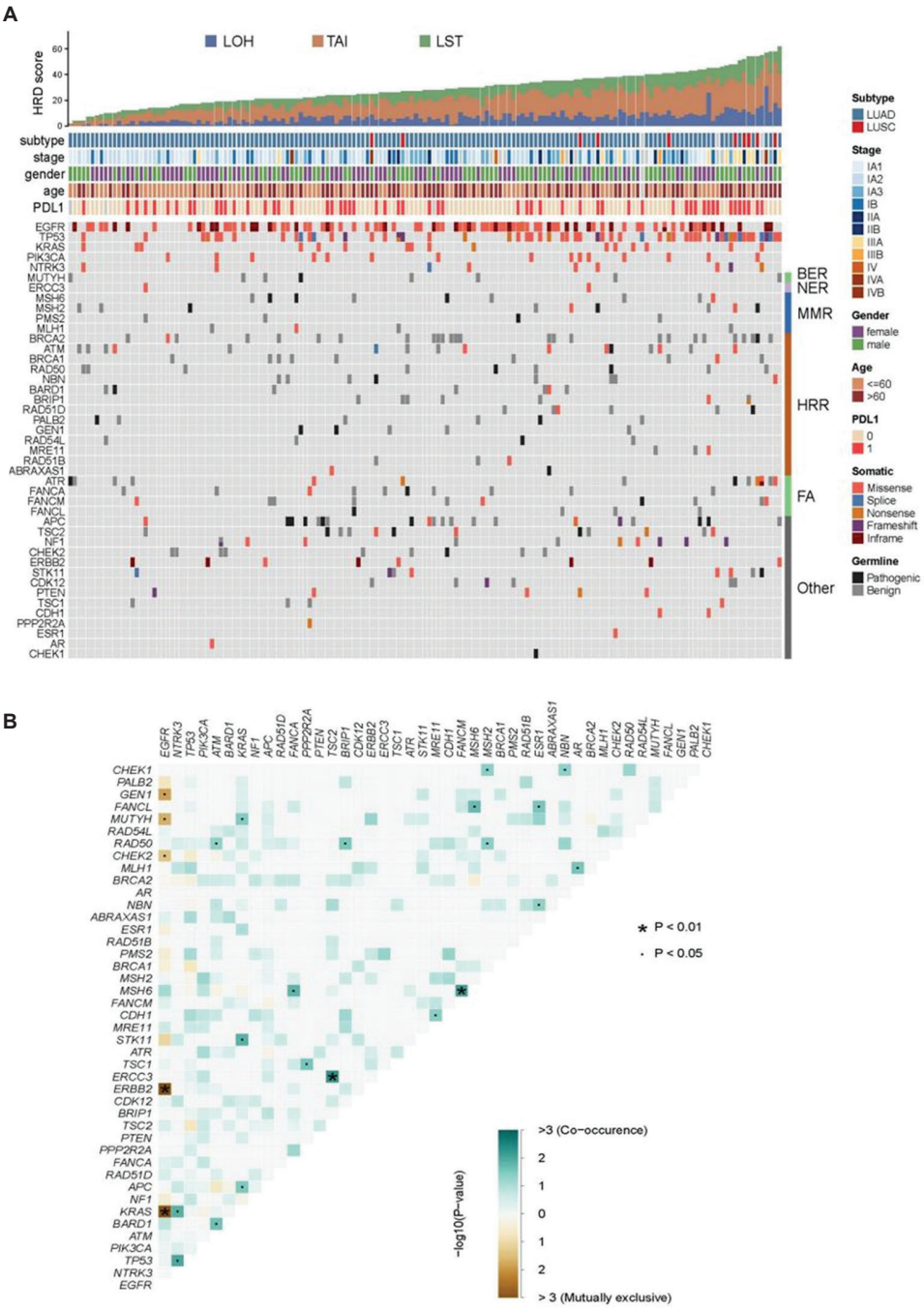

Figure 1. Genomic HRD score and mutation landscape in Chinese non-small cell lung cancer (NSCLC) patients. (A) Landscape of *HRR* genes and clinical characteristics in 158 Chinese NSCLC patients sorted by HRD score. In this cohort, 8.9% (14/158) exhibited somatic genomic alterations in *HRR* genes, identifying 17 mutations predominantly of the missense type (88.2%). Germline genomic alterations were observed in 24.7% (39/158) of the cohort with 49 mutations identified, and 18.4% were categorized as pathogenic. *ATM* was the most frequently mutated somatic *HRR* gene (4.4%), while *BRCA2* was the most commonly mutated germline *HRR* gene (7.0%), followed by *ATM* (3.2%), *BRIP1* (3.2%), and *BARD1* (2.5%). (B) Co-occurring and mutually exclusive somatic mutations in the cohort are illustrated. *EGFR* alterations showed mutual exclusivity with many other genetic alterations, underscoring its potential as a major driver event in NSCLC. Significant co-occurrences of mutations were found particularly between *ERCC3* and *TSC2*, and between *MSH6* and *FANCM* (p<0.01).

Note: p-values were calculated using Fisher's exact test: *p<0.01, p<0.05.

Abbreviations: BER: Base-Excision Repair; FA: Fanconi Anemia; HRD: Homologous recombination deficiency; HRR: Homologous recombination repair; LOH: Loss of heterozygosity; LST: Large-scale state transition; LUAD: Lung adenocarcinoma; LUSC: Lung squamous cell carcinoma; MMR: Mismatch Repair; NER: Nucleotide Excision Repair; NSCLC: Non-small cell lung cancer; TAI: Telomeric allelic imbalance.

genes often occur simultaneously, suggesting potential synergistic effects among these genes. Particularly, the concurrent mutations in the *ERCC3* and *TSC2* genes, as well as the co-mutations in the *MSH6* and *FANCM* genes, demonstrated significant statistical importance ($p<0.01$) (Figure 1B).

3.2. The relationship between clinicopathological characters and the HRD score in NSCLC

To further illustrate the clinical value of HRD score in NSCLC, we analyzed the relationship between clinicopathological characteristics and HRD score (Figure 1A). Patients with advanced-stage (stage III and above) NSCLC are more likely to have high HRD scores compared to those with early-stage (stage I and II) disease (Table 1), but not in the TCGA cohort. Furthermore, individuals with LUSC have a higher incidence of HRD than patients with LUAD, which was consistent with the TCGA cohort. No significant differences in clinical characteristics, including age, smoking history, and gender, were observed between HRD-H and HRD-L patients (Table 1).

To further analyze the transcriptomic differences between HRD-H and HRD-L subgroups, RNA sequencing (RNA-seq) data from both the TCGA dataset and our NSCLC cohort were analyzed. Volcano plots (Figure 2A and C) revealed a higher number of DEGs in HRD-H compared to HRD-L, with a predominance of downregulated genes. This suggests that HRD-H may suppress certain transcriptional programs, potentially linked to genomic instability caused by homologous recombination defects. Heatmaps (Figure 2B and D) validated these findings, demonstrating consistent expression patterns of DEGs across distinct samples. These results highlight systematic transcriptomic disparities between HRD-H and HRD-L subgroups, underscoring their potential as biomarkers for NSCLC stratification.

Table 1. Clinical characteristics of HRD-H and HRD-L patients

Characteristics	HRD-H (n=19)	HRD-L (n=139)	p-value
Age (%)			0.3354
Young (≤60 years)	8 (42.11)	76 (54.68)	
Old (>60 years)	11 (57.89)	63 (45.32)	
Gender (%)			0.9999
Female	9 (47.37)	70 (50.36)	
Male	10 (52.63)	69 (49.64)	
Stage (%)			***<0.0001
Early (<III)	10 (55.56)	122 (93.13)	
Late (≥III)	8 (44.44)	9 (6.87)	
Histology (%)			**0.0032
LUAD	14 (73.68)	126 (96.18)	
LUSC	5 (26.32)	5 (3.82)	
Smoking (%)			0.3075
Yes	9 (47.37)	47 (33.81)	
No	10 (52.63)	92 (66.19)	

Notes: **$p<0.01$, ***$p<0.001$.
Abbreviations: HRD-H: Homologous recombination deficiency-high; HRD-L: Homologous recombination deficiency-low; LUAD: Lung adenocarcinoma; LUSC: Lung squamous cell carcinoma.

3.3. Genetic alterations between HRD-H and HRD-L patients in LUAD

To gain deeper insights into the genomic alteration spectrum associated with the HRD phenotype in LUAD patients, we assessed and contrasted the frequencies of gene mutations between individuals classified within HRD-H and HRD-L groups. *EGFR* and *TP53* were the most commonly mutated genes in both the HRD-H and HRD-L groups (Figure 3A). In the HRD-H group, 10 out of 14 cases exhibited mutations in the *EGFR* gene. *TP53* gene was more frequently mutated in HRD-H than in HRD-L patients (Figure 3B and Figure A1 in the Appendix).

3.4. Association between HRD status and PD-L1 expression

In our study, we assessed the PD-L1 expression status in 154 patients. Out of these patients, 36.4% (56/154) tested positive for PD-L1 expression. We found that the positive rate of PD-L1 expression was significantly higher in the HRD-H group compared to the HRD-L group in NSCLC (Figure 4A and Figure A2 in the Appendix). Nevertheless, there was no correlation of HRD phenotype with PD-L1 expression in either the HRD-H or the HRD-L group in LUAD (Figure 4B). In addition, we analyzed the PD-L1 expression in the TCGA database. The TCGA PD-L1 expression data of LUSC and LUAD datasets were directly pulled down from the UCSC Xena RPPA TCGA hub.[2] These data include 352 LUAD patients and 321 LUSC patients. Since the PD-L1 status in the TCGA database cannot be classified as positive or negative, we examined its relationship with HRD status by comparing numerical values. Our analysis revealed that in TCGA-LUAD, the mean protein expression of PD-L1 was significantly higher in the HRD-H group compared to the HRD-L group (Figure 4C). However, in TCGA-LUSC, there was no significant difference observed (Figure 4D).

3.5. Kyoto Encyclopedia of Genes and Genomes (KEGG) pathway enrichment analysis in TCGA and study cohorts

KEGG pathway enrichment analysis of HRD-H and HRD-L

[2] https://xenabrowser##net/datapages/

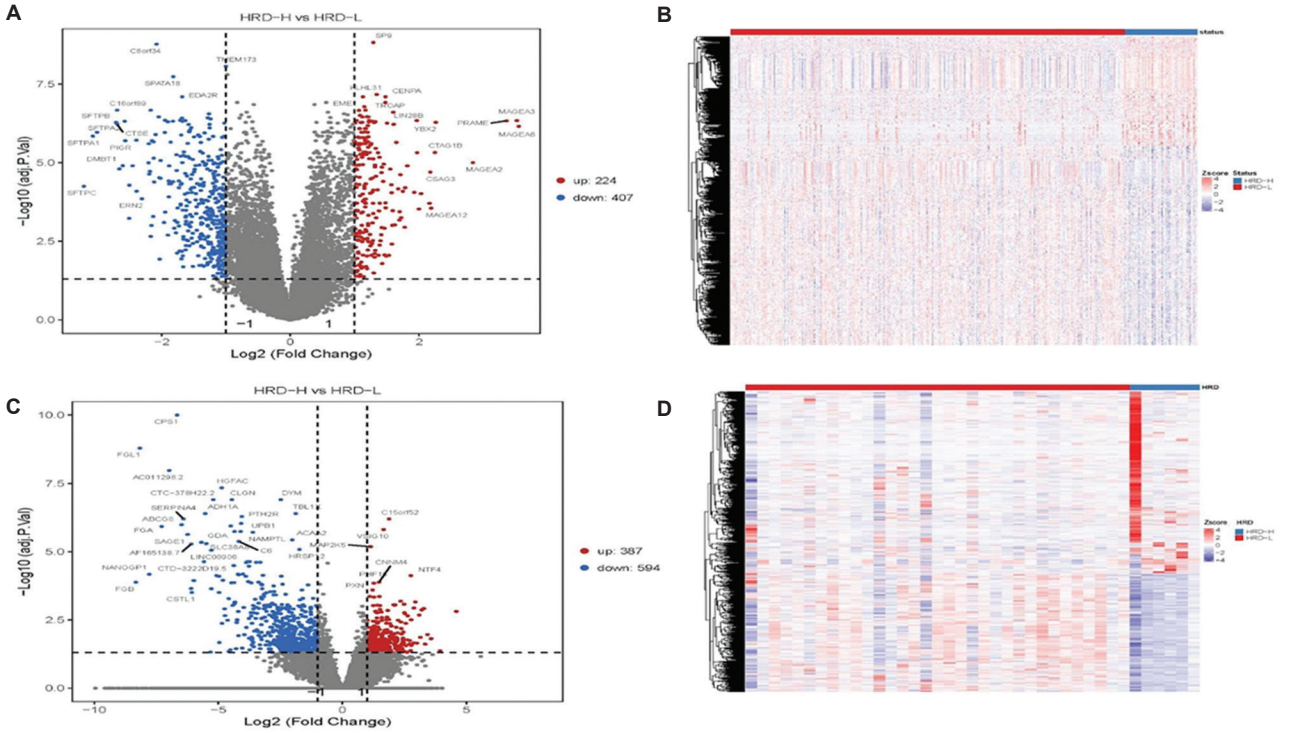

Figure 2. Differentially expressed genes between HRD-H and HRD-L RNA-seq. (A) Volcano plot depicting DEGs between HRD-H and HRD-L subgroups in the TCGA database. A greater number of DEGs are observed in HRD-H compared to HRD-L, with predominance of downregulated genes, indicative of potentially suppressed transcriptional programs linked to homologous recombination defects. Genes with significant differential expression (upregulated, red; downregulated, blue) are highlighted. (B) Heat map illustrating the expression patterns of DEGs between HRD-H and HRD-L groups in the TCGA dataset. Consistent expression patterns are noted across samples, validating the differential expression observed in the volcano plot. (C) Volcano plot of DEGs between HRD-H and HRD-L in RNA-seq data from 40 NSCLC cases in China. Similar to the TCGA analysis, HRD-H samples exhibit more DEGs, with a significant number of downregulated genes highlighted (blue) compared to upregulated genes (red). (D) Heat map showing consistent expression patterns of DEGs in HRD-H and HRD-L groups in the cohort of 40 Chinese NSCLC patients, reinforcing the observed transcriptomic disparities between the HRD subgroups.

Abbreviations: DEGs: Differentially expressed genes; HRD-H: Homologous recombination deficiency-high; HRD-L: Homologous recombination deficiency-low; NSCLC: Non-small cell lung cancer; RNA-seq: RNA sequencing; TCGA: The Cancer Genome Atlas.

subgroups in both the TCGA cohort and our study cohort (Figure 5A-D) revealed distinct metabolic, immune, and drug-response signatures in HRD-H tumors. In the TCGA cohort (Figure 5A and B), HRD-H tumors exhibited significant downregulation of the protein digestion and absorption pathway ($P_{adjust} \approx 0.10$) and pancreatic secretion pathway, suggesting impaired nutrient metabolism that may exacerbate genomic instability. Concurrently, the complement and coagulation cascades pathway (Rich factor >10) was markedly enriched in HRD-H tumors (Figure 5B), indicating complement-dependent immune evasion. In our cohort (Figure 5C and D), recurrent enrichment of the complement and coagulation cascades pathway ($P_{adjust} < 0.05$) further validated the immunosuppressive phenotype of HRD-H. Strikingly, upregulation of the ABC transporters pathway (Rich factor >15) and bile secretion pathway (Figure 5D) highlighted enhanced drug efflux as a potential resistance mechanism in HRD-H tumors. These pathway-level insights underscore the potential value of HRD as a biomarker for guiding precision therapy in NSCLC.

4. Discussion

In this study, we investigated the epidemiologic characteristics of HRD in Chinese NSCLC patients and discussed the rationale for using HRD as a biomarker in treatment strategies. The results showed that 8.9% of NSCLC patients had somatic variants in *HRR* genes, of which *ATM* and *BRCA2* were most affected. This observation is clinically significant, as patients with HRD, particularly those harboring *BRCA1/2* or *ATM* mutations may be candidates for PARP inhibitor therapy. PARP inhibitors have been known to be effective in patients with HR-positive breast and ovarian cancers and its applicability to NSCLC patient has been explored and found effective in patients who meet genomic instability criteria.

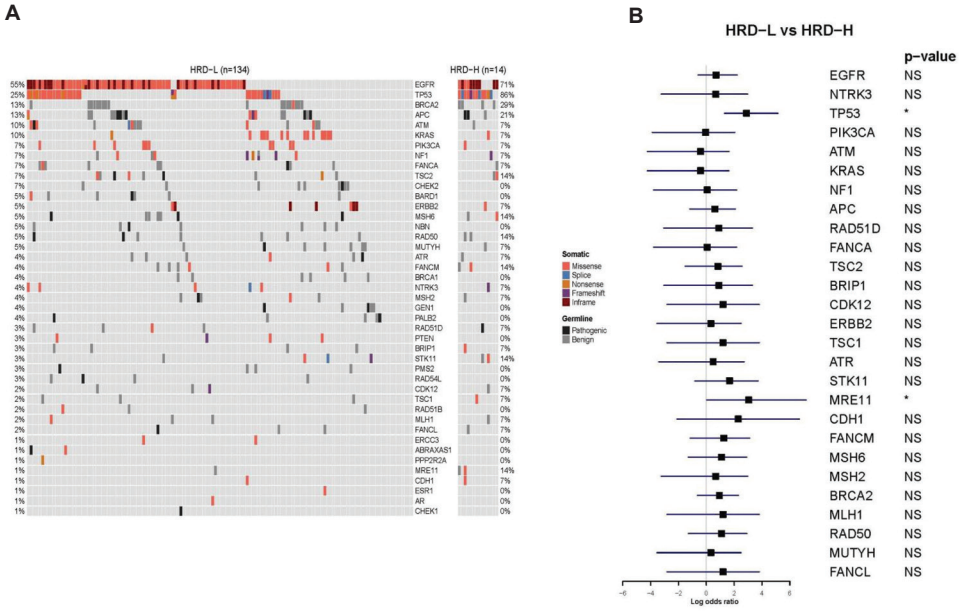

Figure 3. Comparison of genomic alterations between the HRD-L and HRD-H groups of Chinese NSCLC patients. (A) Mutational landscapes of HRD-L (n = 134) and HRD-H (n = 14) groups highlighting the frequencies of gene mutations. *EGFR* and *TP53* genes were the most frequently mutated in both HRD-H and HRD-L groups. Notably, 71% of HRD-H cases harbored mutations in the *EGFR* gene, and *TP53* was more frequently mutated in HRD-H (86%) than in HRD-L patients (26%). (B) Forest plot depicting the enrichment of gene mutations in HRD-L and HRD-H groups, measured by logarithmic odds ratio (*p<0.05). The x-axis shows the log odds ratio. Despite the higher mutation rates of *EGFR* and *TP53* in the HRD-H group, these did not reach statistical significance in the comparative analysis. Other genes, including *PIK3CA*, *ATM*, *KRAS*, and *MSH6*, also showed variations in mutation frequency between the two groups, without statistically significant differences.
Note: NS denotes not significant.
Abbreviations: HRD-H: Homologous recombination deficiency-high; HRD-L: Homologous recombination deficiency-low; NSCLC: Non-small cell lung cancer.

Furthermore, this study provides valuable insights into the genetic and clinical differences between HRD-H and HRD-L patients. Notably, HRD-H patients were more frequently diagnosed at advanced stages and exhibited a higher prevalence of *TP53* mutations, further supporting the association between HRD and genomic instability.[33] The co-occurrence of HRD-H status and *TP53* mutations is particularly noteworthy, as both features are individually associated with aggressive tumor biology and poor prognosis in NSCLC.[32] *TP53* mutations can compromise cell cycle control and apoptosis,[34] while HRD leads to defective DNA repair and increased genomic instability.[23] The combination of these alterations may synergistically promote tumor progression, resulting in more advanced disease at diagnosis and potentially poorer clinical outcomes. This synergistic effect is evident in our cohort, where patients with HRD-H status exhibited significantly higher rates of advanced disease (stage IIIB-IV) compared to HRD-L patients (approximately 60% vs. 40%). This association likely reflects the aggressive phenotype driven by extreme genomic instability when both alterations are present.

From a therapeutic perspective, this co-occurrence may have complex implications. On the one hand, tumors harboring both HRD-H and *TP53* mutations might be more sensitive to DNA-damaging agents, such as platinum-based chemotherapy and PARP inhibitors,[35] due to their impaired ability to repair DNA damage. On the other hand, the presence of *TP53* mutations has been associated in some studies with resistance to certain therapies and with a more immunosuppressive tumor microenvironment, which could influence response to ICIs.[36] Therefore, the dual presence of HRD-H and *TP53* mutations may define a subset of patients with both high therapeutic vulnerability and high risk, showing the need for tailored treatment strategies and close clinical monitoring. Further research is warranted to clarify the prognostic and predictive value of this co-occurrence and to optimize therapeutic approaches for these patients.

Apart from the management of PARP inhibitors, HRD may have applicability in identifying the patients who would benefit from the use of ICIs. In contrast to the TCGA-LUAD set, *a priori*-defined HRD was not associated with PD-L1 expression in our LUAD cohort, although previous reports also indicated that the latter had higher immunogenicity in cancers with HRD.[37] Molecularly, HRD results in DNA damage that can activate the cGAS-STING

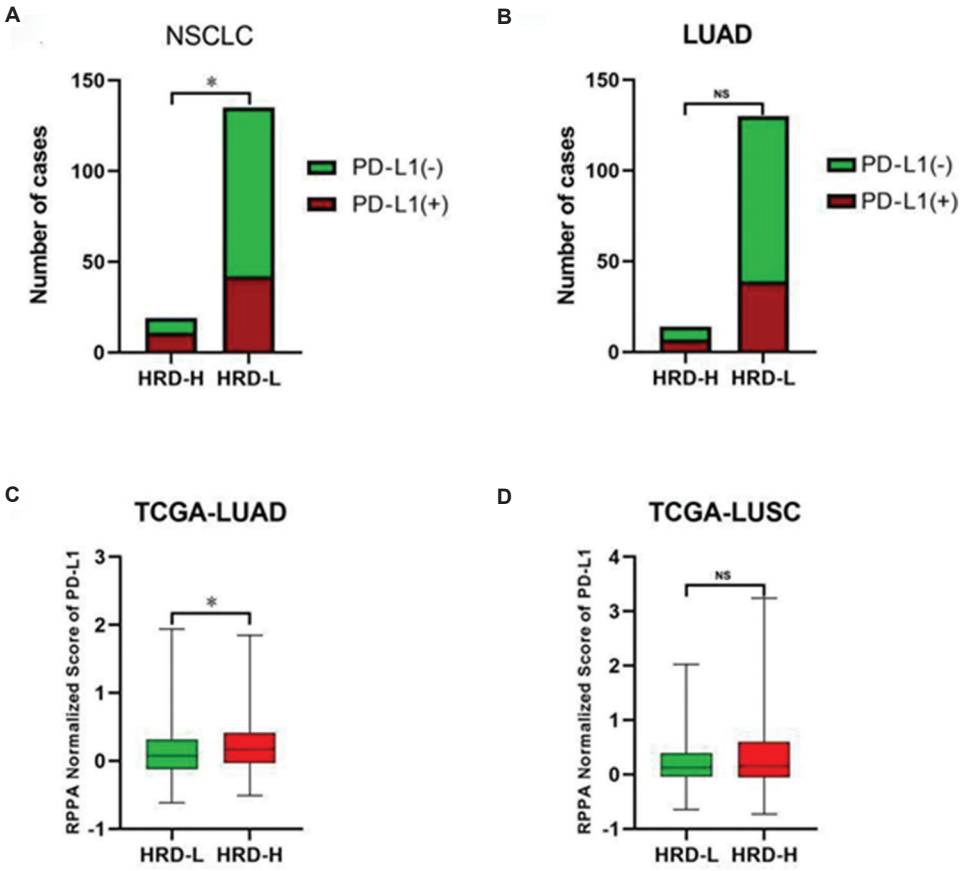

Figure 4. The association of HRD status with PD-L1 expression in this cohort and TCGA cohort. (A) Comparison of the number of PD-L1 positive and negative cases between the HRD-H (n = 14) and HRD-L (n = 140) groups in NSCLC. The HRD-H group exhibited a significantly higher rate of PD-L1 positive expression compared to the HRD-L group. (B) Comparison of the number of PD-L1 positive and negative cases between the HRD-H and HRD-L groups in LUAD. No significant correlation was observed between HRD phenotype and PD-L1 expression in LUAD. (C) Comparison of normalized scores of PD-L1 expression between the HRD-L (n=321) and HRD-H (n = 31) groups in the TCGA-LUAD dataset. The mean PD-L1 protein expression was significantly higher in the HRD-H group compared to the HRD-L group. (D) Comparison of normalized scores of PD-L1 expression between the HRD-L (n = 317) and HRD-H (n = 31) groups in the TCGA-LUSC dataset. No significant difference in PD-L1 expression was observed between the HRD-L and HRD-H groups in the TCGA-LUSC dataset.
Note: *p<0.05, NS denotes not significant.
Abbreviations: HRD-H: Homologous recombination deficiency-high; HRD-L: Homologous recombination deficiency-low; LUAD: Lung adenocarcinoma; LUSC: Lung squamous cell carcinoma; NSCLC: Non-small cell lung cancer; PD-L1: Programmed death-ligand 1; RPPA: Reverse phase protein array; TCGA: The Cancer Genome Atlas.

pathway and release type I interferons, thus increasing immune cell infiltration.[38] This process may upregulate immune checkpoint molecules, including PD-L1, thereby increasing tumor immunogenicity. Clinically, this suggests that HRD-positive tumors could be more responsive to ICIs. Recent clinical evidence strongly supports this dual biomarker approach. In the CheckMate-9LA study, patients with both HRD positivity and PD-L1 ≥1% who received nivolumab plus ipilimumab combined with chemotherapy achieved a remarkable 3-year overall survival rate of 38%, significantly outperforming patients positive for only one biomarker.[39] Therefore, HRD status, in combination with PD-L1 expression, could serve as a composite biomarker to identify patients most likely to benefit from immunotherapy or combination regimens.

Although in our LUAD cohort, pre-defined HRD was not significantly associated with PD-L1 expression, this does not rule out the potential for synergy between PARP inhibitors and ICIs in NSCLC. Previous studies in other solid tumors have demonstrated that combining PARP inhibitors with ICIs can enhance anti-tumor immune responses, as seen in the MEDIOLA and TOPACIO trials.[40] Therefore, integrating HRD status and PD-L1 expression into clinical decision-making could help stratify patients: Those with both high HRD scores and elevated PD-L1 expression may be prioritized for combination therapies, while those with only one or neither biomarker may be directed toward alternative strategies. This approach could optimize therapeutic outcomes and minimize unnecessary toxicity.

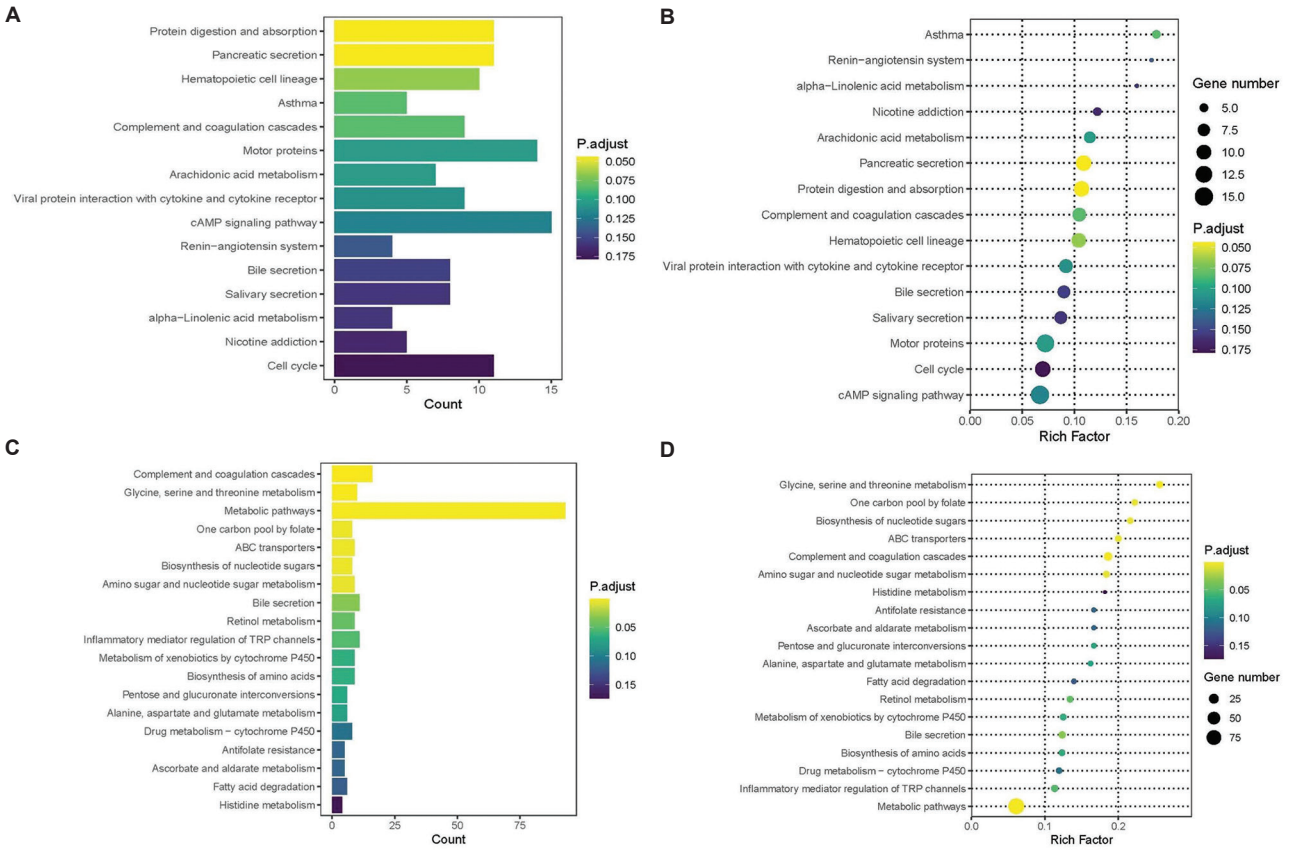

Figure 5. KEGG pathway analysis. (A and B) KEGG pathway analysis for TCGA databases. (C and D) KEGG pathway analysis for our study participant's RNA-seq data. (A and C) Bar plots display the number of genes involved in significantly enriched KEGG pathways for HRD-H tumors compared to HRD-L tumors. The bar color gradient indicates the adjusted *p*-value significance, from yellow (less significant) to purple (more significant). (B and D) Bubble plots summarizing KEGG pathway enrichment, with the y-axis listing pathways and the x-axis showing the Rich factor, a measure of pathway enrichment. Abbreviations: HRD-H: Homologous recombination deficiency-high; HRD-L: Homologous recombination deficiency-low; KEGG: Kyoto Encyclopedia of Genes and Genomes; RNA-seq: RNA sequencing; TCGA: The Cancer Genome Atlas.

However, there are several limitations in this study. First, the sample size was relatively small for certain subgroups, such as HRD-H and LUSC, limiting the statistical power to detect additional associations. Second, this is a retrospective study. Without prospective data collection, we were unable to systematically capture important clinical outcomes such as survival data and treatment response rates. The retrospective design also precluded the assessment of the HRD score as a direct predictor of treatment efficacy or as a prognostic factor under specific therapeutic regimens. Moreover, the discrepancy between our cohort's data and the TCGA-LUAD data on PD-L1 mainly implies that genetic factors such as ancestry, tumor microenvironment, and immune system might affect the association between HRD and immunogenicity on a population level. These limitations underscore the necessity for larger, prospective, population-specific studies to fully elucidate the clinical utility of HRD as a biomarker in NSCLC and to validate our preliminary findings. Despite these constraints, our study provides valuable insights into the genomic landscape of HRD in Chinese NSCLC patients and lays important groundwork for future investigations into targeted therapeutic approaches.

5. Conclusion

The present study provides preliminary evidence supporting the implementation of HRD status to subclassify NSCLC and to guide precision therapy strategies. HRD may serve not only as a biomarker for selecting patients likely to benefit from PARP inhibitors but also as a potential predictor of immunotherapy efficacy. Future large-scale, prospective studies that integrate comprehensive clinical data and evaluate combination treatment regimens are warranted to further validate the prognostic and therapeutic value of HRD in NSCLC.

Acknowledgments

None.

Funding

This study was jointly funded by the Wanzhou District Science and Technology Bureau of Chongqing (Grant No.: wzstc-kw2022029) and the Wanzhou District Health Commission of Chongqing (Grant No. wzstc-kw2022029).

Conflict of interest

Mingzhu Yin is an Editor-in-Chief of this journal but was not in any way involved in the editorial and peer-review process conducted for this paper, directly or indirectly. Separately, other authors declared that they have no known competing financial interests or personal relationships that could have influenced the work reported in this paper.

Author contributions

Conceptualization: Shuang Xiang, Song Duan, Mingzhu Yin
Formal analysis: Yi Liu
Investigation: Chun Huang, Ya-ting Yang
Methodology: Jing Guo
Writing – original draft: Shuang Xiang, Changqiong Shen
Writing – review & editing: Song Duan, Mingzhu Yin

Ethics approval and consent to participate

The study was approved by the Research Ethics Committee of the Chongqing University Three Gorges Hospital (Institutional Review Board approval number: 2022-Scientific Research No. 145). Written informed consent was obtained from the patients before their participation.

Consent for publication

Patients consented on the publication of their data.

Availability of data

The sequencing data were obtained from the public datasets of TCGA and affiliated research centers.

References

1. Zhao Z, Du L, Wang L, Wang Y, Yang Y, Dong H. Preferred lung cancer screening modalities in China: A discrete choice experiment. *Cancers (Basel)*. 2021;13(23):6110.

   doi: 10.3390/cancers13236110

2. Yang J, Hao R, Zhang Y, Deng H, Teng W, Wang Z. Construction of circRNA-miRNA-mRNA network and identification of novel potential biomarkers for non-small cell lung cancer. *Cancer Cell Int*. 2021;21(1):611.

   doi: 10.1186/s12935-021-02278-z

3. Moreno-Rubio J, Ponce S, Álvarez R, *et al*. Clinical-pathological and molecular characterization of long-term survivors with advanced non-small cell lung cancer. *Cancer Biol Med*. 2020;17(2):444-457.

   doi: 10.20892/j.issn.2095-3941.2019.0363

4. Khaddour K, Felipe Fernandez M, Khabibov M, *et al*. The prognostic and therapeutic potential of DNA damage repair pathway alterations and homologous recombination deficiency in lung cancer. *Cancers (Basel)*. 2022;14(21):5305.

   doi: 10.3390/cancers14215305

5. Li Z, Su W, Bai B, *et al*. Single-cell sequencing for lung cancer research: Progress and prospects. *Eur J Med Oncol*. 2025:6883.

   doi: 10.36922/ejmo.6883

6. Karacin C, Eren T, Imamoglu GI, *et al*. The relationship between primary tumor localization and driver mutation in lung cancer. *Eur J Med Oncol*. 2020;4(3):215-218.

   doi: 10.14744/ejmo.2020.13543

7. Bittoni M, Yang JC, Shih JY, *et al*. Real-world insights into patients with advanced NSCLC and MET alterations. *Lung Cancer*. 2021;159:96-106.

   doi: 10.1016/j.lungcan.2021.06.015

8. Huang Q, Li F, Hu H, *et a*l. Loss of TSC1/TSC2 sensitizes immune checkpoint blockade in non-small cell lung cancer. *Sci Adv*. 2022;8(5):eabi9533.

   doi: 10.1126/sciadv.abi9533

9. Matsuzaki K, Kondo S, Ishikawa T, Shinohara A. Human RAD51 paralogue SWSAP1 fosters RAD51 filament by regulating the anti-recombinase FIGNL1 AAA+ ATPase. *Nat Commun*. 2019;10(1):1407.

   doi: 10.1038/s41467-019-09190-1

10. Bukhari AB, Lewis CW, Pearce JJ, Luong D, Chan GK, Gamper AM. Inhibiting Wee1 and ATR kinases produces tumor-selective synthetic lethality and suppresses metastasis. *J Clin Invest*. 2019;129(3):1329-1344.

    doi: 10.1172/JCI122622

11. Turdo A, Gaggianesi M, Di Franco S, *et al*. Effective targeting of breast cancer stem cells by combined inhibition of Sam68 and Rad51. *Oncogene*. 2022;41(15):2196-2209.

    doi: 10.1038/s41388-022-02239-4

12. Peng G, Chun-Jen Lin C, Mo W, *et al*. Genome-wide transcriptome profiling of homologous recombination DNA repair. *Nat Commun*. 2014;5:3361.

    doi: 10.1038/ncomms4361

13. Pratz KW, Rudek MA, Gojo I, *et al*. A phase I study of topotecan, carboplatin and the PARP inhibitor veliparib in acute leukemias, aggressive myeloproliferative neoplasms, and chronic myelomonocytic leukemia. *Clin Cancer Res*. 2017;23(4):899-907.

    doi: 10.1158/1078-0432.CCR-16-1274

14. Conrad LB, Lin KY, Nandu T, Gibson BA, Lea JS, Kraus WL. ADP-ribosylation levels and patterns correlate with gene expression and clinical outcomes in ovarian cancers. *Mol Cancer Ther*. 2020;19(1):282-291.

doi: 10.1158/1535-7163.MCT-19-0569

15. Jia Z, Liu Y, Qu S, *et al*. Evaluative methodology for HRD testing: Development of standard tools for consistency assessment. *Genomics Proteomics Bioinform*. 2025.

doi: 10.1093/gpbjnl/qzaf017

16. Makvandi M, Pantel A, Schwartz L, *et al*. A PET imaging agent for evaluating PARP-1 expression in ovarian cancer. *J Clin Invest*. 2018;128(5):2116-2126.

doi: 10.1172/JCI97992

17. Hahnen E, Lederer B, Hauke J, *et al*. Germline mutation status, pathological complete response, and disease-free survival in triple-negative breast cancer: Secondary analysis of the geparsixto randomized clinical trial. *JAMA Oncol*. 2017;3(10):1378-1385.

doi: 10.1001/jamaoncol.2017.1007

18. Shang X, Qi K, Liu X, *et al*. Signatures associated with homologous recombination deficiency and immune regulation to improve clinical outcomes in patients with lung adenocarcinoma. *Front Oncol*. 2022;12:854999.

doi: 10.3389/fonc.2022.854999

19. Su R, Liu Y, Wu X, Xiang J, Xi X. Dynamically accumulating homologous recombination deficiency score served as an important prognosis factor in high-grade serous ovarian cancer. *Front Mol Biosci*. 2021;8:762741.

doi: 10.3389/fmolb.2021.762741

20. Qing T, Wang X, Jun T, Ding L, Pusztai L, Huang KL. Genomic determinants of homologous recombination deficiency across human cancers. *Cancers (Basel)*. 2021;13(18):4572.

doi: 10.3390/cancers13184572

21. Bever KM, Le DT. DNA repair defects and implications for immunotherapy. *J Clin Invest*. 2018;128(10):4236-4242.

doi: 10.1172/JCI122010

22. Ray-Coquard I, Leary A, Pignata S, *et al*. Olaparib plus bevacizumab first-line maintenance in ovarian cancer: Final overall survival results from the PAOLA-1/ENGOT-ov25 trial. *Ann Oncol*. 2023;34(8):681-692.

doi: 10.1016/j.annonc.2023.05.005

23. Yang C, Zhang Z, Tang X, *et al.* Pan-cancer analysis reveals homologous recombination deficiency score as a predictive marker for immunotherapy responders. *Hum Cell*. 2022;35(1):199-213.

doi: 10.1007/s13577-021-00630-z

24. Cosgrove N, Varešlija D, Keelan S, *et al*. Mapping molecular subtype specific alterations in breast cancer brain metastases identifies clinically relevant vulnerabilities. *Nat Commun*. 2022;13(1):514.

doi: 10.1038/s41467-022-27987-5

25. Marquard AM, Eklund AC, Joshi T, *et al*. Pan-cancer analysis of genomic scar signatures associated with homologous recombination deficiency suggests novel indications for existing cancer drugs. *Biomark Res*. 2015;3:9.

doi: 10.1186/s40364-015-0033-4

26. Rempel E, Kluck K, Beck S, *et al*. Pan-cancer analysis of genomic scar patterns caused by homologous repair deficiency (HRD). *NPJ Precis Oncol*. 2022;6(1):36.

doi: 10.1038/s41698-022-00276-6

27. Takamatsu S, Brown JB, Yamaguchi K, *et al*. Utility of homologous recombination deficiency biomarkers across cancer types. *JCO Precis Oncol*. 2022;6:e2200085.

doi: 10.1200/PO.22.00085

28. Hodgson D, Lai Z, Dearden S, *et al*. Analysis of mutation status and homologous recombination deficiency in tumors of patients with germline BRCA1 or BRCA2 mutations and metastatic breast cancer: OlympiAD. *Ann Oncol*. 2021;32(12):1582-1589.

doi: 10.1016/j.annonc.2021.08.2154

29. Zhou Z, Ding Z, Yuan J, *et al*. Homologous recombination deficiency (HRD) can predict the therapeutic outcomes of immuno-neoadjuvant therapy in NSCLC patients. *J Hematol Oncol*. 2022;15(1):62.

doi: 10.1186/s13045-022-01283-7

30. González-Martín A, Pothuri B, Vergote I, *et al*. Niraparib in patients with newly diagnosed advanced ovarian cancer. *N Engl J Med*. 2019;381(25):2391-2402.

doi: 10.1056/NEJMoa1910962

31. Telli ML, Timms KM, Reid J, *et al*. Homologous recombination deficiency (HRD) score predicts response to platinum-containing neoadjuvant chemotherapy in patients with triple-negative breast cancer. *Clin Cancer Res*. 2016;22(15):3764-3773.

doi: 10.1158/1078-0432.CCR-15-2477

32. Feng J, Lan Y, Liu F, *et al*. Combination of genomic instability score and TP53 status for prognosis prediction in lung adenocarcinoma. *NPJ Precis Oncol*. 2023;7(1):110.

doi: 10.1038/s41698-023-00465-x

33. Moretto R, Elliott A, Zhang J, *et al*. Homologous recombination deficiency alterations in colorectal cancer: Clinical, molecular, and prognostic implications. *J Natl Cancer Inst*. 2022;114(2):271-279.

doi: 10.1093/jnci/djab169

34. Khan R, Pari B, Puszynski K. Comprehensive bioinformatic investigation of TP53 dysregulation in diverse cancer

landscapes. *Genes (Basel)*. 2024;15(5):577.

doi: 10.3390/genes15050577

35. Tsilingiri K, Chalari A, Christopoulou G, *et al*. Genomic scarring score predicts the response to PARP inhibitors in non-small cell lung cancer. *NPJ Precis Oncol*. 2024;8(1):291.

doi: 10.1038/s41698-024-00777-6

36. Wang Y, Ma Y, He L, *et al*. Clinical and molecular significance of homologous recombination deficiency positive non-small cell lung cancer in Chinese population: An integrated genomic and transcriptional analysis. *Chin J Cancer Res*. 2024;36(3):282-297.

doi: 10.21147/j.issn.1000-9604.2024.03.05

37. Bie F, Tian H, Sun N, *et al*. Comprehensive analysis of PD-L1 expression, tumor-infiltrating lymphocytes, and tumor microenvironment in LUAD: Differences between Asians and Caucasians. *Clin Epigenetics*. 2021;13(1):229.

doi: 10.1186/s13148-021-01221-3

38. Wang S, Qin L, Liu F, Zhang Z. Unveiling the crossroads of STING signaling pathway and metabolic reprogramming: The multifaceted role of the STING in the TME and new prospects in cancer therapies. *Cell Commun Signal*. 2025;23(1):171.

doi: 10.1186/s12964-025-02169-0

39. Paz-Ares L, Ciuleanu TE, Cobo M, *et al*. First-line nivolumab plus ipilimumab combined with two cycles of chemotherapy in patients with non-small-cell lung cancer (CheckMate 9LA): An international, randomised, open-label, phase 3 trial [published correction appears in Lancet Oncol. 2021;22(3):e92.

doi: 10.1016/S1470-2045(21)00082-6.]. *Lancet Oncol*. 2021;22(2):198-211.

doi: 10.1016/S1470-2045(20)30641-0

40. Domchek SM, Postel-Vinay S, Im SA, *et al*. Olaparib and durvalumab in patients with germline BRCA-mutated metastatic breast cancer (MEDIOLA): An open-label, multicentre, phase 1/2, basket study. *Lancet Oncol*. 2020;21(9):1155-1164.

doi: 10.1016/S1470-2045(20)30324-7

Appendices

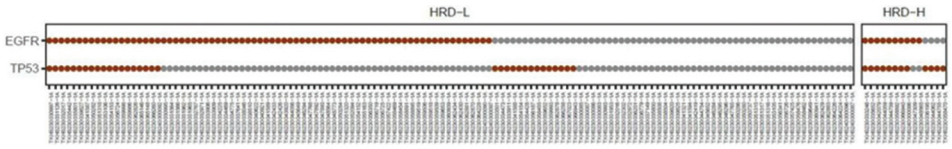

Figure A1. Distribution of gene mutations in the HRD-H and HRD-L groups, showing the distribution of mutation status (mutated/unmutated) of different genes in patients. X-axis: Group (HRD-H, HRD-L). Y-axis: Gene name (*EGFR*, *TP53*). Each point represents a patient, with mutation/unmutated marked by color.
Abbreviations: HRD-H: Homologous recombination deficiency-high; HRD-L: Homologous recombination deficiency-low.

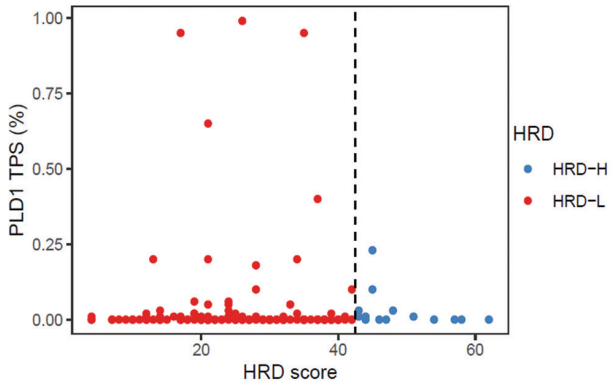

Figure A2. The difference in PD-L1 expression distribution between the HRD-H and HRD-L groups, visually presenting the PD-L1 expression status of each data point (patient). X-axis: Group (HRD-H, HRD-L). Y-axis: PD-L1 expression level (percentage). Each point represents a patient.
Abbreviations: HRD-H: Homologous recombination deficiency-high; HRD-L: Homologous recombination deficiency-low; PD-L1: Programmed death-ligand 1; TPS: Tumor proportion score.

ACCSCIENCE PUBLISHING

Tumor Discovery

ORIGINAL RESEARCH ARTICLE

Prognostication in palliative cancer care: Both probabilities and uncertainties must be taken into account

Erik Torbjørn Løhre[1,2,3*], Ragnhild Hansdatter Habberstad[1], Tora Skeidsvoll Solheim[1,2], Pål Klepstad[4,5], Gunnhild Jakobsen[1,6], and Morten Thronæs[1,2,3]

[1]Cancer Clinic, St. Olavs Hospital, Trondheim University Hospital, Trondheim, Norway

[2]Department of Clinical and Molecular Medicine, Faculty of Medicine and Health Sciences, NTNU–Norwegian University of Science and Technology, Trondheim, Norway

[3]Centre for Crisis Psychology, Faculty of Psychology, University of Bergen, Bergen, Norway

[4]Clinic of Anesthesiology and Intensive Care Medicine, St. Olavs Hospital, Trondheim University Hospital, Trondheim, Norway

[5]Department of Circulation and Medical Imaging, Faculty of Medicine and Health Sciences, NTNU–Norwegian University of Science and Technology, Trondheim, Norway

[6]Department of Public Health and Nursing, Faculty of Medicine and Health Sciences, NTNU–Norwegian University of Science and Technology, Trondheim, Norway

Abstract

Prognosticating survival in palliative cancer patients has been a longstanding challenge. While different tools and approaches may ease prognostication, biological variability limits their accuracy. Assessment of physical status is important for prognostication, along with evaluating the degree of systemic inflammation and patient-reported symptom burden. The distribution of survival was examined among palliative cancer patients with different functional status (Eastern Cooperative Oncology Group Performance Status), inflammation-related markers (modified Glasgow prognostic score [mGPS]), and self-reported symptom intensities (the eleven-point numeric rating scale [0 – 10]). Physical status and biomarkers of systemic inflammatory responses yielded important prognostic information in patients with advanced cancer. Among 147 hospitalized patients, median survival was longer for those continuing anti-cancer treatment, those with better functional status, and those with normal levels of C-reactive protein and/or albumin. Regarding the functional status categories, patients with PS 2 exhibited the widest range of survival. All categories, except PS 4, included patients with actual survival of almost 1 year or more. In terms of inflammatory markers, the widest survival range was observed among patients with mGPS 0. All categories included patients with actual survival of more than half a year, and mGPS 0 and 1 included patients with survival of more than one and a half years. No statistically significant differences in survival were identified between patients with mild and higher intensities of the symptoms under investigation. A wide range of survival outcomes at the group level makes prognostication for individual patients particularly challenging.

Keywords: Prognostication; Palliative cancer care; Probabilities and uncertainties

***Corresponding author:**
Erik Torbjørn Løhre
(erik.t.lohre@ntnu.no)

Citation: Løhre ET, Habberstad RH, Solheim TS, Klepstad P, Jakobsen G, Thronæs M. Prognostication in palliative cancer care: Both probabilities and uncertainties must be taken into account. *Tumor Discov*. 2025;4(3):46-57. doi: 10.36922/td.8576

Received: January 17, 2025

Revised: May 1, 2025

Accepted: May 14, 2025

Published online: July 2, 2025

1. Introduction

More than 50 years ago, a highly ranked medical journal stated that the survival of cancer patients not receiving active treatment is difficult to predict and that lifespan estimates should be interpreted with great caution.[1] However, prognostication is considered a core clinical skill important for robust decision-making.[2] To address both challenges and requirements, many different procedures have been developed to improve forecasting accuracy.[3] Prognoses may be communicated by a variety of techniques and can be expressed as, for instance, anticipated remaining lifespan, possibility of death, or probability of survival within a defined time frame.[3] In addition, survival prediction is a continuous process, as prognostic factors may change throughout the disease trajectory.[4] The most common prognostic approach is clinician prediction of survival (CPS).[3] Clinical prediction of survival represents a complex process that, based on expertise and experience, attempts to estimate the patients' expected lifespan.[4,5] As prognostic accuracy varies by the patient population under consideration, setting, and time frame, CPS may be supplemented by designated and appropriate instruments.[3,6] Many specific prognostic tools include objective observations, but also subjective symptom scores may be relevant in prognostication, as cancer patients experience a higher intensity of certain symptoms towards the end of life.[4,7-9]

The European Society for Medical Oncology (ESMO) has published a clinical practice guideline for prognostic evaluation in patients with advanced cancer.[6] This guideline emphasizes the importance of CPS and promotes clinical predictions with varying degrees of supplementary information from prognostic factors and multivariable models. For patients receiving disease-modifying treatment (DMT), additional assessments of physical function and inflammation are recommended, whereas the use of multivariable prognostic models is considered optional. For patients no longer receiving DMT and being closer to death, CPS remains important, along with relevant measures of prognostic factors and clinical signs of impending death.[6] In everyday clinical practice, the traditional diagnostic work-up consists of patient-reported information, physical examination, and laboratory findings.[10] Consequently, information on performance status (PS), biomarkers of systemic inflammatory responses, and PROMs may also be routinely available for prognostication purposes.

Formal assessments of physical function, such as the Karnofsky Performance Scale Index and the Eastern Cooperative Oncology Group PS (ECOG PS), were originally developed to evaluate chemotherapy tolerability and responses.[11,12] Although calibrated differently, both systems share the fundamental idea of evaluating patients' ability to carry out normal activities and their dependence on nursing care. For years, these scales have been found relevant and applicable in the prognostication process.[13-15] PS independently predicts survival, and some authors have been described it as a cornerstone of prognosis in advanced cancer.[14] A frequently cited paper, based on data from more than 1,600 participants, reported that patients with advanced cancer and ECOG PS 1 had a median survival of just under 200 days; those with PS 2, approximately 100 days; those with PS 3, approximately 50 days; and patients with end-stage cancer and PS 4, a median remaining lifespan of approximately 25 days.[13]

Inflammation represents another cornerstone of prognosis in advanced cancer.[14] While PS assessments include elements of subjective judgment and clinical evaluation, biomarkers of systemic inflammatory responses are strictly objective measures.[14,16,17] The presence of a systemic inflammatory response may be due to increased disease activity and cancer progression, and research has shown that combined assessment of C-reactive protein (CRP) and serum albumin has independent prognostic value.[18] This combination was named as the Glasgow prognostic score (GPS).[19] Both the GPS and the modified GPS (mGPS) utilize CRP and albumin levels to score patients into three different categories, and the system has been extensively validated for different cancer diagnoses.[14,18,20-22] Higher scores correspond to a more dismal prognosis, and the mGPS is recommended by the ESMO for prognostic evaluation in patients with advanced cancer receiving DMT.[6]

The presence of certain clinical signs and symptoms, such as some of the anorexia-cachexia syndrome, dyspnea, and delirium or cognitive failure, has been demonstrated to carry prognostic significance in patients with advanced cancer.[23] Accordingly, the existence of particular clinical signs and symptoms are incorporated to varying extents into prognostic tools for this group of patients.[7,24] A study of more than 10,000 cancer patients followed over the last 6 months of their lives showed that the PROMs for tiredness, loss of appetite, reduced well-being, and drowsiness increased dramatically towards the end of life.[8] In fact, most of the patients described the intensities of these four symptoms as moderate to severe during the last weeks of life.[8] Additionally, dyspnea tends to intensity as death approaches and is used in several prognostic tools for patients with advanced cancer.[7,8,25] The optimal thresholds for classifying symptom intensity as mild or moderate on the eleven-point numeric rating scale (NRS 0 – 10) are debated.[26,27] For the Edmonton Symptom Assessment

Scale (ESAS), optimal thresholds may even differ by symptom.[26] Personalized NRS 0 – 10 symptom goals for patients with advanced cancer have been investigated, and it is demonstrated that NRS 3 represents a symptom goal for many patients.[28] Additionally, a symptom intensity of NRS 4 or higher has been recommended as a trigger for further measures.[26] This threshold may thus be relevant for distinguishing between mild and more severe symptom intensities.

Despite clinical skills and access to both laboratory results and PROMs, prognostication of the remaining lifespan is encumbered with inaccuracy, as the exact timing of death cannot be predicted with certainty.[4] The introduction of novel treatments, such as targeted anticancer therapy and immunotherapy, has further complicated prognostication.[29] Patients receiving such interventions may experience either major temporary improvements or sustained long-term responses.[29] Furthermore, when prognosticating median survival, defined as the midpoint in an organized dataset, approximately half of the patients will live shorter and half longer than the anticipated time frame.[4] Therefore, clear measures of variability may provide information equally important as measures of central tendency, both in terms of fostering hopes and establishing realistic expectations for the individual patient.[30] Hence, information on expected survival may be challenging to formulate and even more difficult to apprehend.[31] In addition, various prognostic assessments may be considered as tests with defined sensitivities, specificities, and positive and negative predictive values.[32] For practitioners, this implies that results must be interpreted from a clinical perspective and delivered both with caution and careful consideration. Awareness of the potential for contradictory information to arise can further promote sound clinical practice.

By using our previously published data, we aimed to study the inherent uncertainties of commonly used prognostic methods in patients with advanced cancer.[33] Survival was examined across different ECOG PS categories, separate mGPS groups, and among patients with mild or higher intensities of self-reported symptoms known to increase towards the end of life. Additionally, characteristics of patients with both short and longer survival durations were further described.

2. Methods

2.1. Design

The current paper is based on data from a study published by the research group in 2021.[33] The primary study reported on interventions conducted and symptom relief achieved in patients with advanced cancer admitted to an acute palliative care unit (APCU) at a tertiary cancer clinic. The palliative care unit at the cancer clinic, St. Olavs Hospital, Trondheim University Hospital, Norway, comprises 12 beds and receives approximately 450 admissions each year. The clinic has for years been a certified ESMO-designated center of integrated oncology and palliative care. In the primary study, all patients admitted to the APCU between January 15, 2019, and January 15, 2020, were assessed. This paper presents secondary and supplementary analyses of the data collected.

2.2. Patients

The patients referred to the APCU are adult persons with advanced cancer, and for whom palliative care interventions are considered relevant and beneficial. Ongoing anti-cancer treatment does not preclude referral to the APCU, but patients with hematological, gynecological, and pulmonary malignancies are treated at their respective university hospital departments. These patients are only referred to the APCU for follow-up on neuraxial pain management. The present analysis included all patients with available ECOG PS registrations, relevant biomarkers of systemic inflammatory responses, and intensities of self-reported symptoms. Readmissions of previously included patients were excluded from the analysis.

2.3. Assessments

For the current research, data registered at the time of admission were used. ECOG PS registrations, the serum biomarkers CRP and albumin, and patient-reported symptom intensities for tiredness, loss of appetite, reduced well-being, drowsiness, and dyspnea (NRS 0 – 10) were retrieved. The assessment period for PROMs covered the past 24 h. In addition, information was collected on patient demographics, cancer diagnosis, metastatic status, care trajectory (ongoing anti-cancer treatment along with palliative care versus palliative care alone), and survival from admission.

2.4. Analyses

Descriptive statistics were used for demographics and to report survival (in days) for the entire cohort, across different care trajectories, and among different PS groups. Similarly, survival was calculated in patients classified into mGPS categories 0, 1, and 2, respectively.[6] Patients with CRP ≤ 10 mg/L scored 0, patients with CRP > 10 mg/L and albumin ≥ 35 g/L scored 1, and patients with CRP > 10 and albumin <35 g/L scored 2.[18] PROMs for tiredness, loss of appetite, reduced well-being, drowsiness, and dyspnea

were each dichotomized into scores of ≤3 (mild symptom intensities) and scores of ≥4 (higher symptom intensities), and survival was computed accordingly for patients with mild and higher symptom intensities.[8,26,28]

In accordance with ESMO guidance, patients were categorized based on survival time after admission into days (0 – 13 days), weeks (14 – 55 days), or months (≥56 days), with respect to care trajectories, ECOG PS categories, mGPS classes, and symptom intensity levels assessed for the study.[6] Patients with ECOG PS 3 surviving months or longer, and patients with PS 2 surviving only weeks, were further studied with respect to biomarkers of systemic inflammatory responses.

Due to the non-normal distribution of data, non-parametric tests were used for group survival comparisons. Medians were used as the measure of central tendency, and range as the measure of dispersion. The Mann–Whitney U test was used for comparisons between two independent groups, while the Kruskal–Wallis test was used for comparisons involving more than two groups. To investigate which pairs that were different, the Dunn procedure was performed. $p \leq 0.05$ were considered statistically significant.

All calculations were conducted using STATA v17 (Stata Corporation LP; College Station, TX, USA).

2.5. Ethics

The Regional Committee for Medical Research Ethics, Health Region Central Norway (REK) (2018/925/REK midt and 2021/212312/REK midt) defined the primary study and secondary analyses as healthcare improvement activities. In accordance with Norwegian health care legislation, explicit informed consent was not needed.

3. Results

3.1. Demographics

Altogether, 195 readmissions among 451 hospitalizations were excluded from the study. Of the 256 unique patients, 147 had recorded registrations of ECOG PS, CRP, albumin, and self-reported symptom registrations for tiredness, appetite, well-being, drowsiness, and dyspnea at admission. These 147 patients were included in the current analysis and their characteristics are presented in Table 1. The median age was 73 years, 67.3% were males, gastrointestinal and urological cancers were the most common diagnoses, 89.1% had metastatic disease, and 38.8% received anti-cancer treatment. Median overall survival was 52 days (range 3 – 708 days), with significantly longer median survival observed in those receiving anti-cancer treatment (Tables 1 and 2, Figure 1).

Table 1. Demographic and clinical characteristics

Characteristic	Sample	%
Age (median, range)	73 (29 – 92)	
Gender		
Male	99	67.3
Female	48	32.7
Cancer diagnosis		
Gastrointestinal	66	44.9
Breast	10	6.8
Prostate	22	15.0
Other urological	15	10.2
Other	34	23.1
Metastases		
Yes	131	89.1
No	16	10.9
Survival in days (median, range)	52 (3 – 708)	
Care trajectory		
Ongoing anti-cancer treatment	57	38.8
Palliative care alone	89	60.5
Missing	1	0.7
ECOG PS		
1	15	10.2
2	55	37.4
3	69	46.9
4	8	5.4
mGPS		
0	24	16.3
1	75	51.0
2	48	32.7

Abbreviations: ECOG PS: Eastern cooperative oncology group performance status; mGPS: Modified glasgow prognostic score.

3.2. PS and survival

At admission, 15 patients (10.2%) were categorized as ECOG PS 1, 55 (37.4%) as PS 2, 69 (46.9%) as PS 3, and 8 (5.4%) as PS 4. Survival after admission for patients in each category is described in Table 2 and illustrated in Figure 2. Median survival varied across groups, with no statistically significant difference observed between patients with ECOG PS 1 and PS 2. The range for survival also varied and was largest for patients with PS 2. Except for those with PS 4, all categories included patients who survived almost 1 year or more. All categories also included patients who survived <1 month.

3.3. Biomarkers and survival

At admission, 24 patients (16.3%) were scored as mGPS 0, 75 (51.0%) as mGPS 1, and 48 (32.7%) as mGPS 2. Survival

Table 2. Care trajectory, performance status, biomarkers, symptom intensities, and days of survival

	n	Median	Range	*p*-value*
Care trajectory				
Ongoing anti-cancer treatment	57	82	3 – 629	<0.01
Palliative care alone	89	40	6 – 708	
Missing	1			
ECOG PS[2]				
1	15	122	19 – 368	ref. category
2	55	79	10 – 708	0.23
3	69	42	3 – 320	<0.01
4	8	19	6 – 33	<0.01
mGPS[3]				
0	24	68	13 – 708	ref. category
1	75	68	6 – 629	0.44
2	48	30	3 – 273	<0.01
Tiredness				
Mild symptom intensity	28	81	3 – 629	0.08
Higher symptom intensity	119	44	6 – 708	
Loss of appetite				
Mild symptom intensity	56	60	6 – 708	0.09
Higher symptom intensity	91	45	3 – 368	
Reduced well-being				
Mild symptom intensity	55	52	6 – 361	0.74
Higher symptom intensity	92	52	3 – 708	
Drowsiness				
Mild symptom intensity	40	75	3 –629	0.16
Higher symptom intensity	107	45	6 – 708	
Dyspnea				
Mild symptom intensity	84	64	6 – 708	0.13
Higher symptom intensity	63	42	3 – 439	

Note: *Variables with two categories were compared with the Mann–Whitney *U* test, and variables with more than two categories with the Kruskal–Wallis test and the Dunn procedure.
Abbreviations: ECOG PS: Eastern cooperative oncology group performance status; mGPS: Modified glasgow prognostic score.

after admission for patients with the respective scores is delineated in Table 2 and illustrated in Figure 2. Median

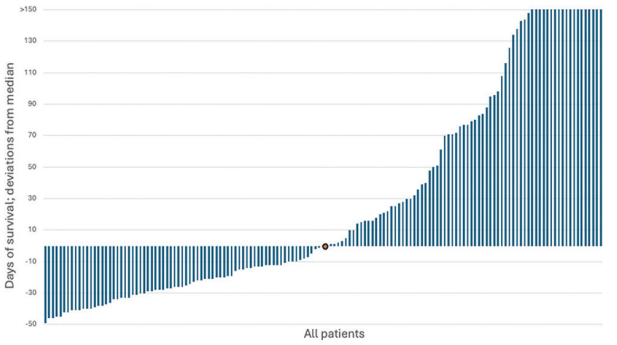

Figure 1. Survival variability in the study population. Zero on the y-axis represents median survival for the entire study population. The vertical bars represent negative and positive deviations from the median survival (in days) for each patient.

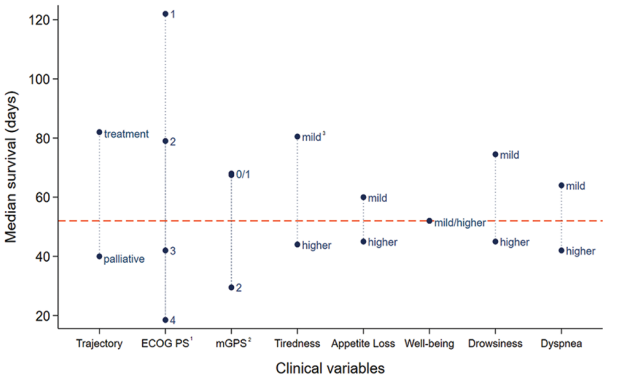

Figure 2. Selected patient characteristics and median survival for the respective groups
Notes: [a]Eastern cooperative oncology group performance status (ECOG PS); [b]Modified glasgow prognostic score (mGPS); [c]Mild and higher symptom intensities; [d]The dotted horizontal line represents the median survival for the entire study population; [e]Median survival was similar for patients with mGPS 0 and 1, as well as for those with mild and higher symptom intensities related to reduced well-being.

survival was similar for patients with mGPS 0 and 1, but significantly different in patients with mGPS 2. The range for survival varied and was largest for patients with mGPS 0. All categories included patients who survived more than half a year, whereas those with mGPS 0 and 1 included patients who survived over one and a half years. All categories also included patients who survived <1 month.

3.4. Symptom intensity and survival

Details on dichotomized symptom intensities for tiredness, loss of appetite, reduced well-being, drowsiness, and dyspnea related to survival are depicted in Table 2 and illustrated in Figure 2. No statistically significant differences in survival were observed between patients with mild and higher intensities of these symptoms. Except for well-being, there was a non-significant trend

towards decreased survival for those with higher symptom intensity scores. All categories included patients who survived approximately a year or more, as well as patients who survived <1 week.

3.5. Characteristics of patients who survived days, weeks, and months

Fourteen patients (9.5%) survived 0 – 13 days, 65 patients (44.2%) survived 14 – 55 days, and 68 patients (46.3%) survived 56 days or more after admission. The distribution of the respective care trajectories, ECOG PS categories, mGPS classes, and symptom intensity levels assessed for the study purpose is shown in Table 3. Patients with longer actual survival had better functional status and less systemic inflammation, and anti-cancer treatment was withdrawn in most patients who survived only days. No patients with ECOG PS 4 lived for months, and no patients with PS 1 survived only days. However, 25 patients with ECOG PS 3 lived for months or longer, and 22 patients with PS 2 survived only weeks. Further analyses (not shown in the tables) demonstrated that the percentage of patients with mGPS 2 was similar (7/25 [28.0%] vs. 6/22 [27.3%], respectively) in these two groups and that almost one third (6/22 [27.3%]) of patients with PS 2 and only weeks of survival had mGPS 0.

Table 3. Characteristics of patients who survived days, weeks, and months

	Days (*n*=14)		Weeks (*n*=65)		Months (*n*=68)	
	n	%	*n*	%	*n*	%
Care trajectory						
Ongoing anti-cancer treatment	2	14.3	20	30.8	35	51.5
Palliative care alone	12	85.7	44	67.7	33	48.5
Missing			1	1.5		
ECOG PS						
1	0	0	4	6.2	11	16.2
2	1	7.1	22	33.8	32	47.1
3	10	71.4	34	52.3	25	36.8
4	3	21.4	5	7.7	0	0
mGPS						
0	1	7.1	11	16.9	12	17.6
1	3	21.4	29	44.6	43	63.2
2	10	71.4	25	38.5	13	19.1
Tiredness						
Mild symptom intensity	2	14.3	10	15.4	16	23.5
Higher symptom intensity	12	85.7	55	84.6	52	76.5
Loss of appetite						
Mild symptom intensity	3	21.4	25	38.5	28	41.2
Higher symptom intensity	11	78.6	40	61.5	40	58.8
Well-being						
Mild symptom intensity	5	35.7	24	36.9	26	38.2
Higher symptom intensity	9	64.3	41	63.1	42	61.8
Drowsiness						
Mild symptom intensity	3	21.4	16	24.6	21	30.9
Higher symptom intensity	11	78.6	49	75.4	47	69.1
Dyspnea						
Mild symptom intensity	6	42.9	34	52.3	44	64.7
Higher symptom intensity	8	57.1	31	47.7	24	35.3

Abbreviations: ECOG PS: Eastern cooperative oncology group performance status; mGPS: Modified glasgow prognostic score.

4. Discussion

4.1. Statement of principal findings

As demonstrated in previously published research, ECOG PS status and biomarkers of systemic inflammatory responses yielded important information for prognostication in patients with advanced cancer. Notably for the clinician, some patients with reduced functional status and systemic inflammation lived for months or longer, and some with better function or little inflammation survived only days. Although no patients with ECOG PS 4 lived for months and no one with PS 1 survived only days, the studied factors could not accurately predict the timing of death for the individual patient. In this single-center study with a limited number of patients included, statistically significant survival differences for patients with mild and higher intensities of the symptoms under investigation were not demonstrated.

4.2. Appraisal of methods

As evidence-based practice is an important basis for palliative cancer care, appreciating the study design employed to answer a particular research question is critical.[34] Retrospective analyses exhibit important design limitations that should be considered.[34] However, they have a place in research, earn their utility, and contributed to important discoveries, such as the association between smoking and lung cancer.[34,35] However, retrospective studies are subjected to biases and are unable to display causal relationships.[34] The results should be interpreted with caution but may provide hypotheses for future prospective studies.[34] The current paper presents secondary analyses of data collected with the intent to describe interventions and symptom relief in an APCU.[33] Consequently, the data were gathered for purposes other than to address the study objectives.[36] In addition, this study did not investigate the recommended use of combinations of techniques to improve prognostication accuracy.[6] Furthermore, the

small sample size and study context, with a single-center design and a highly selected patient population, represent other factors affecting the risk of false results, incorrect associations, and limited external validity.[37,38] Moreover, the current study included patients from two different care trajectories with significantly different prognoses, and both sample size and survival variability affect statistical power.[39]

4.3. Comparison with previous work

Prognostic information is important at several levels for patients, their families, and health care providers.[6] For patients and their next of kin, it may guide and facilitate realistic future planning when time is limited, addressing both opportunities and limitations. For health care providers, prognostic information may represent a valuable tool for optimizing resource utilization and ensuring quality of care.[6] Therefore, previous research conducted to improve the accuracy and precision of prognostication methods and to describe associations with quality of life is highly relevant.[23,40-43]

Clinicians should use their clinical experience to predict the survival of patients with advanced cancer, and it is suggested that they supplement their judgment with input from multiple professionals.[6] In addition, over the years, it has become increasingly evident that combining several factors improves prognostication accuracy.[6,23,40,44] The ESMO Clinical Practice Guideline on prognostic evaluation in patients with advanced cancer in the last months of life also endorses this practice.[6] After the development of the Palliative Performance Scale, which is a modified Karnofsky Performance scale, more complex scoring systems and predictor models have been developed.[45-49] To varying degrees, comprehensive tools such as the palliative prognostic index, the palliative prognostic score, the Feliu prognostic nomogram, and the prognosis in palliative care study incorporate knowledge based on patient-reported information, laboratory findings, as well as physical examination and evaluations.[7,48] The goal was neither to validate established approaches nor to suggest new ones; the focus was solely to underline that prognostication implies dealing with uncertainties that must be considered from a clinical point of view.[1,31,50,51]Properly addressing these uncertainties includes gauging the patients' baseline understanding of their prognosis and gathering knowledge about the type of information they would like to discuss.[6]

Patients with advanced cancer may suffer from sudden and unexpected worsening and clinical crises, often regarded as oncological emergencies.[52] In the dataset on which the current study is based, 302 out of 451 admissions (67%) were due to emergencies, and during 57 hospitalizations (13%) the patient died.[33] With emerging therapies, more oncology patients are expected to live longer but also face the risk of undergoing a rapid and unpredicted decline.[29,53] This emphasizes the importance of available contextual information in the prognostication process.

Functional performance typically dwindles as cancer patients are approaching death, and ECOG PS is strongly associated with survival in patients with late-stage disease.[8,54] PS is incorporated into existing tools and evaluated for its prognostic capacity across different clinical settings.[6,7,14,40,55-58] The ESMO clinical practice guideline on prognostic evaluation in patients with advanced cancer during the last months of life also recommends the use of PS for prognostication purposes.[6] However, variability in individual survival within each ECOG PS group has been demonstrated in populations with both shorter and longer median survival than reported in the current study.[13,54] These findings, combined with the current results, underscore the challenges of using group data to treat or prognosticate individuals.[59] Nevertheless, communicating prognosis based on declined functional performance may represent an easily understandable starting point for both shared decision-making and advance care planning.[6]

Inflammation and tumor progression are closely linked, and from a prognostic perspective, CRP and albumin have been studied in thousands of patients.[18,60] These two measures constitute the components of the mGPS, with increased CRP levels recognized as a reliable negative prognostic factor, particularly when accompanied by decreased albumin levels.[6,18,40] The ESMO clinical practice guideline on prognostic evaluation in patients with advanced cancer during the last months of life also advises the inclusion of systemic inflammation markers in the prognostic assessment.[6] Nevertheless, as observed for ECOG PS categories, a large individual variability in survival exists within each mGPS group. Furthermore, median survival values for groups do not allow precise predictions for individual patients. Additionally, palliative cancer patients face a high risk of serious infections, and alternative explanations for the presence of systemic inflammatory biomarkers should also be considered.[61]

Patients with advanced cancer may experience a multitude of symptoms.[62] Many of these symptoms are clustered, with four common groupings identified: Anxiety-depression, nausea-vomiting, nausea-appetite loss, and fatigue-dyspnea-drowsiness-pain.[62] Both the presence and severity of certain symptoms, as well as overall symptom intensity scores, have been shown to negatively correlate to survival.[58,63] However, when interpreting results on symptom burden and survival, it is important to consider

that even the mere exposure of NRS 0 – 10 assessments may be positively associated with survival.[64] Nonetheless, higher symptom scores are associated with an increased risk of death, and many patients report increased tiredness and drowsiness, decreased appetite and well-being, and dyspnea towards the end of life.[8,9] Based on the limited number of patients with a wide range in survival times, statistically significant differences between low and higher symptom intensities could not be demonstrated for symptoms previously demonstrated to increase near the end of life.[8,39] With a large sample size and a different patient population, the results may have been different.

The remaining lifespan of palliative care patients varies, and although predictions are often inaccurate, survival may be expressed and presented as median days, weeks, or months.[6,49,61,65] To fully convey prognostic information, it is essential to present not only measures of central tendency but also interpretable and understandable measures of biological variability.[66] In this context, the range provides information into both the minimum and maximum expected survival times.[66] Effectively communicating the uncertainty, limitations, and unreliability of prognostic information is an important clinical skill.[2,6] To illustrate the intrinsic restrictions of established methods of prognostication, this study examined functional status, systemic inflammation, and self-reported symptoms in patients who survived for days, weeks, or months after admission to an APCU. Although functional status and degree of systemic inflammation provide important prognostic information, outliers complicate the clinical interpretation and reduce the predictive value of parameters registered at a single time point when estimating the remaining lifespan for individual patients.

4.4. Future work

Directions for future research on prognostication in advanced cancer have been published.[3] These include ten important themes with the potential to advance prognostication science. Emphasis is placed on improving prognostication accuracy while acknowledging inherent uncertainty and considering how prognostic information can be used in everyday clinical practice.[3] For tools to be relevant to palliative care physicians, they must be simple enough for practicality and complex enough to be effective.[67,68] This study illustrated the limitations and pitfalls of using variables recorded at a single time point to prognosticate the dynamics trajectory of palliative cancer care.[8] For instance, dynamic changes in systemic inflammatory markers may provide important information regarding cancer aggressiveness.[69] Employing information from repeated assessments is considered as good clinical practice in palliative cancer care and may be widely utilized in prognostication research.[70] Such an approach would also be more robust in accounting for intercurrent events that can affect functional status, laboratory findings, and symptom presentation.

5. Conclusion

Commonly used prognostic markers have demonstrated utility at the population level. However, for individual patients, statistical measures of central tendency may have limited clinical value. Palliative cancer care patients who present with favorable prognostic factors may live shorter than expected, whereas others with disadvantageous markers may outlive the expectancy. Prognostic communication should acknowledge and incorporate this inherent uncertainty.

Acknowledgments

The authors would like to express their deep gratitude both to the Cancer Clinic, St. Olavs Hospital, Trondheim University Hospital, and the Department of Clinical and Molecular Medicine, Faculty of Medicine and Health Sciences, NTNU–Norwegian University of Science and Technology, for their support in enabling the preparation of this manuscript. We also would like to thank all the patients who contributed to the study. Finally, the authors acknowledge the dedicated and sustained efforts of all the physicians and nurses at the Palliative Care Unit, Cancer Clinic, St. Olavs Hospital, Trondheim University Hospital, without whom this study would not have been possible.

Funding

None.

Conflict of interest

The authors declare that they have no competing interest.

Author contributions

Conceptualization: All authors
Formal analysis: All authors
Investigation: All authors
Methodology: Erik Torbjørn Løhre, Ragnhild Hansdatter Habberstad, Pål Klepstad, Gunnhild Jakobsen, Morten Thronæs
Writing – original draft: All authors
Writing – review & editing: All authors

Ethics approval and consent to participate

This investigation containing both primary study and secondary analyses was approved by The Regional Committee for Medical Research Ethics, Health Region Central Norway (REK) (2018/925/REK midt

and 2021/212312/REK midt). In accordance with the Norwegian health care legislation, explicit informed consent was not needed.

Consent for publication

On specific request, The Regional Committee for Medical Research Ethics, Health Region Central Norway (REK) stated that addressing patients or relatives of deceased patients for consent for publication would constitute a burden without benefit, as the presented data are completely anonymized and by no means suitable for identifying individual patients. Thus, a request of consent for publication was not recommended or needed.

Availability of data

All the primary data and all the analyzes are stored at an institutional server and can be obtained from the corresponding author at reasonable request.

References

1. Parkes CM. Accuracy of predictions of survival in later stages of cancer. *Br Med J*. 1972;2(5804):29-31.

   doi: 10.1136/bmj.2.5804.29

2. Glare PA, Sinclair CT. Palliative medicine review: Prognostication. *J Palliat Med*. 2008;11(1):84-103.

   doi: 10.1089/jpm.2008.9992

3. Hui D, Paiva CE, Del Fabbro EG, *et al*. Prognostication in advanced cancer: Update and directions for future research. *Support Care Cancer*. 2019;27(6):1973-1984.

   doi: 10.1007/s00520-019-04727-y

4. Hui D. Prognostication of survival in patients with advanced cancer: Predicting the unpredictable? *Cancer Control*. 2015;22(4):489-497.

   doi: 10.1177/107327481502200415

5. Cheon S, Agarwal A, Popovic M, *et al*. The accuracy of clinicians' predictions of survival in advanced cancer: A review. *Ann Palliat Med*. 2016;5(1):22-29.

   doi: 10.3978/j.issn.2224-5820.2015.08.04

6. Stone P, Buckle P, Dolan R, *et al*. Prognostic evaluation in patients with advanced cancer in the last months of life: ESMO clinical practice guideline. *ESMO Open*. 2023;8(2):101195.

   doi: 10.1016/j.esmoop.2023.101195

7. Simmons CPL, McMillan DC, McWilliams K, *et al*. Prognostic tools in patients with advanced cancer: A systematic review. *J Pain Symptom Manage*. 2017;53(5):962-970.e10.

   doi: 10.1016/j.jpainsymman.2016.12.330

8. Seow H, Barbera L, Sutradhar R, *et al*. Trajectory of performance status and symptom scores for patients with cancer during the last six months of life. *J Clin Oncol*. 2011;29(9):1151-1158.

   doi: 10.1200/JCO.2010.30.7173

9. Haupt EC, Sharma I, Nguyen HQ. Symptom burden and survival in patients receiving outpatient and home-based palliative care. *J Palliat Med*. 2023;26(6):843-848.

   doi: 10.1089/jpm.2022.0267

10. Løhre ET, Klepstad P, Bennett MI, *et al*. From "breakthrough" to "episodic" cancer pain? A European association for palliative care research network expert Delphi survey toward a common terminology and classification of transient cancer pain exacerbations. *J Pain Symptom Manage*. 2016;51(6):1013-1019.

    doi: 10.1016/j.jpainsymman.2015.12.329

11. Karnofsky DA, Abelmann WH, Craver LF, Burchenal JH. The use of the nitrogen mustards in the palliative treatment of carcinoma - with particular reference to bronchogenic carcinoma. *Cancer*. 1948;1(4):634-656.

    doi: 10.1002/1097-0142(194811)1:4<634:AID-CNCR2820010410>3.0.CO;2-L

12. Oken MM, Creech RH, Tormey DC, *et al*. Toxicity and response criteria of the Eastern cooperative oncology group. *Am J Clin Oncol*. 1982;5(6):649-655.

13. Jang RW, Caraiscos VB, Swami N, *et al*. Simple prognostic model for patients with advanced cancer based on performance status. *J Oncol Pract*. 2014;10(5):e335-e341.

    doi: 10.1200/JOP.2014.001457

14. Rocha BMM, Dolan RD, Paiva CE, *et al*. Inflammation and performance status: The cornerstones of prognosis in advanced cancer. *J Pain Symptom Manage*. 2023;65(4):348-357.

    doi: 10.1016/j.jpainsymman.2022.11.021

15. Evans C, McCarthy M. Prognostic uncertainty in terminal care: Can the Karnofsky index help? *Lancet*. 1985;1(8439):1204-1206.

    doi: 10.1016/s0140-6736(85)92876-4

16. Kim YJ, Hui D, Zhang Y, *et al*. Differences in performance status assessment among palliative care specialists, nurses, and medical oncologists. *J Pain Symptom Manage*. 2015;49(6):1050-1058.e2.

    doi: 10.1016/j.jpainsymman.2014.10.015

17. Sorensen JB, Klee M, Palshof T, Hansen HH. Performance status assessment in cancer patients. An inter-observer variability study. *Br J Cancer*. 1993;67(4):773-775.

    doi: 10.1038/bjc.1993.140

18. McMillan DC. The systemic inflammation-based Glasgow prognostic score: A decade of experience in patients with

cancer. *Cancer Treat Rev*. 2013;39(5):534-540.

doi: 10.1016/j.ctrv.2012.08.003

19. Forrest LM, McMillan DC, McArdle CS, Angerson WJ, Dunlop DJ. Comparison of an inflammation-based prognostic score (GPS) with performance status (ECOG) in patients receiving platinum-based chemotherapy for inoperable non-small-cell lung cancer. *Br J Cancer*. 2004;90(9):1704-1706.

doi: 10.1038/sj.bjc.6601789

20. Nozoe T, Iguchi T, Egashira A, Adachi E, Matsukuma A, Ezaki T. Significance of modified Glasgow prognostic score as a useful indicator for prognosis of patients with gastric carcinoma. *Am J Surg*. 2011;201(2):186-191.

doi: 10.1016/j.amjsurg.2010.01.03

21. Hu X, Wang Y, Yang WX, Dou WC, Shao YX, Li X. Modified Glasgow prognostic score as a prognostic factor for renal cell carcinomas: A systematic review and meta-analysis. *Cancer Manag Res*. 2019;11:6163-6173.

doi: 10.2147/CMAR.S208839

22. Shimada A, Matsuda T, Sawada R, *et al*. The modified Glasgow prognostic score is a reliable predictor of oncological outcomes in patients with rectal cancer undergoing neoadjuvant chemoradiotherapy. *Sci Rep.* 2023;13(1):17111.

doi: 10.1038/s41598-023-44431-w

23. Maltoni M, Caraceni A, Brunelli C, *et al*. Prognostic factors in advanced cancer patients: Evidence-based clinical recommendations--a study by the steering committee of the European association for palliative care. *J Clin Oncol*. 2005;23(25):6240-6248.

doi: 10.1200/JCO.2005.06.866

24. Stone P, Vickerstaff V, Kalpakidou A, *et al*. Prognostic tools or clinical predictions: Which are better in palliative care? *PLoS One*. 2021;16(4):e0249763.

doi: 10.1371/journal.pone.0249763

25. Mori M, Morita T, Bruera E, Hui D. Prognostication of the last days of life. *Cancer Res Treat*. 2022;54(3):631-643.

doi: 10.4143/crt.2021.1573

26. Oldenmenger WH, De Raaf PJ, De Klerk C, Van Der Rijt CC. Cut points on 0-10 numeric rating scales for symptoms included in the Edmonton symptom assessment scale in cancer patients: A systematic review. *J Pain Symptom Manage*. 2013;45(6):1083-1093.

doi: 10.1016/j.jpainsymman.2012.06.007

27. Serlin RC, Mendoza TR, Nakamura Y, Edwards KR, Cleeland CS. When is cancer pain mild, moderate or severe? Grading pain severity by its interference with function. *Pain*. 1995;61(2):277-284.

doi: 10.1016/0304-3959(94)00178-H

28. Hui D, Park M, Shamieh O, *et al*. Personalized symptom goals and response in patients with advanced cancer. *Cancer*. 2016;122(11):1774-1781.

doi: 10.1002/cncr.29970

29. Geijteman ECT, Kuip EJM, Oskam J, Lees D, Bruera E. Illness trajectories of incurable solid cancers. *BMJ*. 2024;384:e076625.

doi: 10.1136/bmj-2023-076625

30. Casarett D. The median is not the (only) message. *Ann Intern Med*. 2006;145(9):700-701.

doi: 10.7326/0003-4819-145-9-200611070-00014

31. Hemingway H, Croft P, Perel P, *et al*. Prognosis research strategy (PROGRESS) 1: A framework for researching clinical outcomes. *BMJ*. 2013;346:e5595.

doi: 10.1136/bmj.e5595

32. Trevethan R. Sensitivity, specificity, and predictive values: Foundations, pliabilities, and pitfalls in research and practice. *Front Public Health*. 2017;5:307.

doi: 10.3389/fpubh.2017.00307

33. Thronaes M, Lohre ET, Kvikstad A, *et al*. Interventions and symptom relief in hospital palliative cancer care: Results from a prospective longitudinal study. *Support Care Cancer*. 2021;29(11):6595-6603.

doi: 10.1007/s00520-021-06248-z

34. Talari K, Goyal M. Retrospective studies - utility and caveats. *J R Coll Physicians Edinb*. 2020;50(4):398-402.

doi: 10.4997/JRCPE.2020.409

35. Doll R, Hill AB. Smoking and carcinoma of the lung; Preliminary report. *Br Med J*. 1950;2(4682):739-748.

doi: 10.1136/bmj.2.4682.739

36. Cheng HG, Phillips MR. Secondary analysis of existing data: Opportunities and implementation. *Shanghai Arch Psychiatry*. 2014;26(6):371-375.

doi: 10.11919/j.issn.1002-0829.214171

37. Hackshaw A. Small studies: Strengths and limitations. *Eur Respir J*. 2008;32(5):1141-1143.

doi: 10.1183/09031936.00136408

38. Ross PT, Bibler Zaidi NL. Limited by our limitations. *Perspect Med Educ*. 2019;8(4):261-264.

doi: 10.1007/s40037-019-00530-x

39. Norton BJ, Strube MJ. Understanding statistical power. *J Orthop Sports Phys Ther*. 2001;31(6):307-315.

doi: 10.2519/jospt.2001.31.6.307

40. Laird BJ, Kaasa S, McMillan DC, *et al*. Prognostic factors in patients with advanced cancer: A comparison of clinicopathological factors and the development of an

inflammation-based prognostic system. *Clin Cancer Res*. 2013;19(19):5456-5464.

doi: 10.1158/1078-0432.CCR-13-1066

41. Laird BJ, Fallon M, Hjermstad MJ, *et al*. Quality of life in patients with advanced cancer: Differential association with performance status and systemic inflammatory response. *J Clin Oncol*. 2016;34(23):2769-2775.

doi: 10.1200/JCO.2015.65.7742

42. Simmons CP, Koinis F, Fallon MT, *et al*. Prognosis in advanced lung cancer--a prospective study examining key clinicopathological factors. *Lung Cancer*. 2015;88(3):304-309.

doi: 10.1016/j.lungcan.2015.03.020

43. Hui D, Ross J, Park M, *et al*. Predicting survival in patients with advanced cancer in the last weeks of life: How accurate are prognostic models compared to clinicians' estimates? *Palliat Med*. 2020;34(1):126-133.

doi: 10.1177/0269216319873261

44. Scarpi E, Maltoni M, Miceli R, *et al*. Survival prediction for terminally ill cancer patients: Revision of the palliative prognostic score with incorporation of delirium. *Oncologist*. 2011;16(12):1793-1799.

doi: 10.1634/theoncologist.2011-0130

45. Anderson F, Downing GM, Hill J, Casorso L, Lerch N. Palliative performance scale (PPS): A new tool. *J Palliat Care*. 1996;12(1):5-11.

46. Morita T, Tsunoda J, Inoue S, Chihara S. The palliative prognostic index: A scoring system for survival prediction of terminally ill cancer patients. *Support Care Cancer*. 1999;7(3):128-133.

doi: 10.1007/s005200050242

47. Pirovano M, Maltoni M, Nanni O, *et al*. A new palliative prognostic score: A first step for the staging of terminally ill cancer patients. Italian multicenter and study group on palliative care. *J Pain Symptom Manage*. 1999;17(4):231-239.

doi: 10.1016/s0885-3924(98)00145-6

48. Feliu J, Jimenez-Gordo AM, Madero R, *et al*. Development and validation of a prognostic nomogram for terminally ill cancer patients. *J Natl Cancer Inst*. 2011;103(21):1613-1620.

doi: 10.1093/jnci/djr388

49. Gwilliam B, Keeley V, Todd C, *et al*. Development of prognosis in palliative care study (PiPS) predictor models to improve prognostication in advanced cancer: Prospective cohort study. *BMJ*. 2011;343:d4920.

doi: 10.1136/bmj.d4920

50. Chu C, White N, Stone P. Prognostication in palliative care. *Clin Med (Lond)*. 2019;19(4):306-310.

doi: 10.7861/clinmedicine.19-4-306

51. Gupta A, Burgess R, Drozd M, Gierula J, Witte K, Straw S. The surprise question and clinician-predicted prognosis: Systematic review and meta-analysis. *BMJ Support Palliat Care*. 2024;15:12-35.

doi: 10.1136/spcare-2024-004879

52. Nauck F, Alt-Epping B. Crises in palliative care--a comprehensive approach. *Lancet Oncol*. 2008;9(11):1086-1091.

doi: 10.1016/S1470-2045(08)70278-X

53. Liu B, Zhou H, Tan L, Siu KTH, Guan XY. Exploring treatment options in cancer: Tumor treatment strategies. *Signal Transduct Target Ther*. 2024;9(1):175.

doi: 10.1038/s41392-024-01856-7

54. Allende-Perez S, Rodriguez-Mayoral O, Pena-Nieves A, Bruera E. Performance status and survival in cancer patients undergoing palliative care: Retrospective study. *BMJ Support Palliat Care*. 2024;14:1256-1262.

doi: 10.1136/spcare-2022-003562

55. Tas F, Sen F, Odabas H, Kilic L, Keskin S, Yildiz I. Performance status of patients is the major prognostic factor at all stages of pancreatic cancer. *Int J Clin Oncol*. 2013;18(5):839-846.

doi: 10.1007/s10147-012-0474-9

56. Carey MS, Bacon M, Tu D, Butler L, Bezjak A, Stuart GC. The prognostic effects of performance status and quality of life scores on progression-free survival and overall survival in advanced ovarian cancer. *Gynecol Oncol*. 2008;108(1):100-105.

doi: 10.1016/j.ygyno.2007.08.088

57. Hsu CY, Lee YH, Hsia CY, *et al*. Performance status in patients with hepatocellular carcinoma: Determinants, prognostic impact, and ability to improve the Barcelona clinic liver cancer system. *Hepatology*. 2013;57(1):112-119.

doi: 10.1002/hep.25950

58. Jung EH, Hiratsuka Y, Suh SY, *et al*. Clinicians' prediction of survival is most useful for palliative care referral. *Palliat Med Rep.* 2024;5(1):365-372.

doi: 10.1089/pmr.2024.0013

59. Dahabreh IJ, Hayward R, Kent DM. Using group data to treat individuals: Understanding heterogeneous treatment effects in the age of precision medicine and patient-centred evidence. *Int J Epidemiol*. 2016;45(6):2184-2193.

doi: 10.1093/ije/dyw125

60. Coussens LM, Werb Z. Inflammation and cancer. *Nature*. 2002;420(6917):860-867.

doi: 10.1038/nature01322

61. Moen MK, Lohre ET, Jakobsen G, Thronaes M, Klepstad P. Antibiotic therapy in integrated oncology and palliative cancer care: An observational study. *Cancers (Basel)*. 2022;14(7):1602.

doi: 10.3390/cancers14071602

62. Dong ST, Butow PN, Costa DS, Lovell MR, Agar M. Symptom clusters in patients with advanced cancer: A systematic review of observational studies. *J Pain Symptom Manage*. 2014;48(3):411-450.

doi: 10.1016/j.jpainsymman.2013.10.027

63. Ahn GS, Kim HR, Kang B, *et al*. Symptom burden and characteristics of patients who die in the acute palliative care unit of a tertiary cancer center. *Ann Palliat Med*. 2020;9(2):216-223.

doi: 10.21037/apm.2020.02.06

64. Barbera L, Sutradhar R, Seow H, *et al*. The impact of routine Edmonton symptom assessment system (ESAS) use on overall survival in cancer patients: Results of a population-based retrospective matched cohort analysis. *Cancer Med*. 2020;9(19):7107-7115.

doi: 10.1002/cam4.3374

65. White N, Reid F, Harris A, Harries P, Stone P. A systematic review of predictions of survival in palliative care: How accurate are clinicians and who are the experts? *PLoS One*. 2016;11(8):e0161407.

doi: 10.1371/journal.pone.0161407

66. Cardinal LJ. Central tendency and variability in biological systems. *J Community Hosp Intern Med Perspect*. 2015;5(3):27930.

doi: 10.3402/jchimp.v5.27930

67. Brenne AT, Lohre ET, Knudsen AK, *et al*. Standardizing integrated oncology and palliative care across service levels: Challenges in demonstrating effects in a prospective controlled intervention trial. *Oncol Ther*. 2024;12(2):345-362.

doi: 10.1007/s40487-024-00278-3

68. Lohre ET, Thronaes M, Brunelli C, Kaasa S, Klepstad P. An in-hospital clinical care pathway with integrated decision support for cancer pain management reduced pain intensity and needs for hospital stay. *Support Care Cancer*. 2020;28(2):671-682.

doi: 10.1007/s00520-019-04836-8

69. Lin JX, Huang YQ, Wang ZK, *et al*. Prognostic importance of dynamic changes in systemic inflammatory markers for patients with gastric cancer. *J Surg Oncol*. 2021;124(3):282-292.

doi: 10.1002/jso.26498

70. Crawford GB, Dzierzanowski T, Hauser K, *et al*. Care of the adult cancer patient at the end of life: ESMO clinical practice guidelines. *ESMO Open*. 2021;6(4):100225.

doi: 10.1016/j.esmoop.2021.100225

ACCSCIENCE PUBLISHING

Tumor Discovery

ORIGINAL RESEARCH ARTICLE

Highly specific and sensitive gene panels for cancer screening: First application of only-normal and only-tumor genes

Gabriel Gil[1], Claudia Carricarte[2], Julio C. Drake-Pérez[3], Yasser Perera[4,5], and Augusto Gonzalez[1]*

[1]Department of Theoretical Physics, Institute of Cybernetics, Mathematics and Physics, Havana, Cuba

[2]Group of Computation, Faculty of Biology, University of Havana, Cuba

[3]Department of General Physics, Faculty of Physics, University of Havana, Cuba

[4]Biomedical Research Division, Center for Genetic Engineering and Biotechnology, Havana, Cuba

[5]China-Cuba Biotechnology Joint Innovation Center, Yongzhou Zhong Gu Biotechnology Co., Ltd, Yongzhou, Hunan, China

Abstract

The traditional paradigm of gene expression dysregulation emphasizes log-fold differential expression, with differentially expressed genes presumed to play key roles in relevant biological processes. In cancer, where normal tissue and tumors occupy non-overlapping regions in gene expression space, we propose an alternative and broader framework based on differentially expressed only-tumor genes (T-genes) and non-differentially dysregulated only-normal genes (N-genes). N-genes exhibit expression intervals found exclusively in normal samples, while T-genes display intervals exclusive to tumor samples. These N- and T-genes serve as markers that can be combined into small gene panels capable of perfectly discriminating between normal and tumor tissues. In most cases, these panels highlight biologically significant properties, such as altered glutamine metabolism in tumors. We provide an inventory of perfect gene panels for 12 cancer types, with potential applications in diagnostics and immunotherapy. Significance: Highly specific and sensitive combinatorial gene panels for the identification of 12 types of solid tumors in humans were derived from RNA sequencing expression profiles reported by The Cancer Genome Atlas network (https://www.cancer.gov/ccg/research/genome-sequencing/tcga). The corresponding software is available at the GitHub repository https://github.com/gabriel-gil/GenePan. This study revisits the concept of cancer-related gene expression dysregulation by introducing N-genes and T-genes as novel dysregulation patterns that can be leveraged in diagnosis, tumor classification, and therapeutic interventions.

Keywords: Cancer; Combinatorial gene panel; Expression dysregulation; Only-normal genes; Only-tumor genes

***Corresponding author:**
Augusto Gonzalez
(agonzale@icimaf.cu)

Citation: Gil G, Carricarte C, Drake-Pérez JC, Perera Y, Gonzalez A. Highly specific and sensitive gene panels for cancer screening: First application of only-normal and only-tumor genes. *Tumor Discov*. 2025;4(3):58-69. doi: 10.36922/TD025190035

Received: May 7, 2025

Revised: June 6, 2025

Accepted: June 20, 2025

Published online: July 17, 2025

1. Introduction

The Human Genome Project of the 1990s opened the door to many large-scale omics catalogs.[1] In the following decade, the field advanced further with the advent of

high-throughput microarrays and next-generation RNA sequencing (RNA-seq).[2] These technologies enabled the development of increasingly specialized databases with a focus on biomedical applications.[3] A prominent example is The Cancer Genome Atlas (TCGA), which provides potentially crucial information on cancer detection, treatment, and the fundamental biology of oncogenesis.[4,5] TCGA hosts extensive genomic, epigenomic, transcriptomic, and proteomic data on tumor and normal tissue samples for 33 cancer types.[6] All of this data are publicly available for mining and analysis in pursuit of discovering specific genetic markers and targets.[6] As expected, the current analyses of TCGA data reflect the scale and complexity of this experimental feat of collecting such a vast amount of data.[7,8] However, a definitive consensus on the most adequate set of genes for diagnosis and therapy remains elusive.

Gene discovery relevant to carcinogenesis and tumor progression is partially guided by the assessment of gene dysregulation based on both statistical and biological significance.[9] The paradigmatic kind of gene dysregulation is differential expression,[10] whereby a gene is expressed differently in a tumor compared to a normal tissue. Conventionally, differential expression is associated with cancer only when there is a marked deviation from normal expression levels, typically defined in terms of average values across tumor and normal samples. However, as emphasized by several authors,[11-14] framing gene expression dysregulation solely in terms of central tendency can hinder gene discovery in translational cancer research. Indeed, gene expression levels in tumor or normal tissue samples may differ in their variance or distribution, even when mean values remain unchanged. Consequently, the detection of differential dispersion[12,13] and differential distribution[14] provides a broader perspective on human cancer-related genes by addressing the shortcomings of standard differential expression protocols. Despite their important contributions, these alternative techniques often rest on distributional assumptions that may not reflect the regulatory dynamics of many genes, such as those involved in circadian rhythm control.[15] To the best of our knowledge, the field still lacks sufficiently flexible methods to detect diverse patterns of gene expression dysregulation beyond changes in central tendency.

In this context, we identify novel candidate genes for cancer therapy and diagnostics by applying an original non-parametric approach to gene expression profiles from the TCGA database. Rather than relying on uniform characterizations based on averages or specific distributional shapes, we explore gene-dependent definitions of normal and tumor-like expression using intervals that encompass either all normal or all tumor samples. This allowed us to identify genes that serve as classifiers without false positives or false negatives when distinguishing tumor and normal tissue within the training data. We refer to these as T-genes (differentially expressed only-tumor genes) and N-genes (non-differentially dysregulated only-normal genes). These genes are characterized by specific expression intervals that are exclusively populated by tumor and normal tissue samples, respectively. By combining N- or T-genes, we constructed compact gene panels – referred to as "perfect gene panels" – that perfectly discriminate between tumor and normal samples within the training data.

Our core procedure resembles formal concept analysis[16-27] and rough set theory (RST),[28-39] both with a growing number of applications in omics. The main scope of these techniques is to discover patterns (namely, formal concepts or rough sets) in multivariate data, where a set of attributes is made to correspond to a set of objects through a specific relation.[40,41] This is precisely the framework under consideration, with the following mapping: genes take the role of attributes, clinical samples correspond to objects, and gene expression profiles define the relation between them.[18] Our sets of N-genes and T-genes define both formal and attribute-oriented concepts,[40,41] where the extents of these concepts correspond to either tumor or normal samples, depending on the concept type. Moreover, the perfect gene panels align with the notion of a reduct in RST,[42-45] in the sense that none of their gene members can be removed without compromising the panel's ability to perfectly classify samples.

Perfect gene panels appear in various forms, depending on the location of tumor-exclusive or normal-exclusive intervals within the gene expression space. Some of these panels have a clear interpretation within the state-of-the-art taxonomy of driver genes, provided an interventionist proof of their causal power. For instance, certain panels feature a single gene whose over-expression signals a tumor – a behavior akin to oncogenes. Conversely, for other panels, a single non-silenced gene is an indication of a tumor-free sample, which fits our current understanding of tumor suppressor genes. Other panels may include cooperative tumor suppressor genes, oncogenes, and oscillatory genes.

In this paper, we explore 12 solid tumors among the 33 cancer types in TCGA. For each tissue analyzed, we identify perfect gene panels with potential applications in diagnosis and therapy. By design, perfect panels achieve zero false positives or false negatives within the training data. Notably, one T-gene panel for lung adenocarcinoma (LUAD) also demonstrated high sensitivity and specificity in an external dataset.

The remainder of the article is structured as follows. Section 2 (Materials and Methods) provides a detailed and thorough account of our methodology. In Section 3 (Results), we illustrate our workflow for a case in point (namely, LUAD) and summarize our findings for the other selected cancer types. In addition, we provide a validation analysis of our gene panels in different datasets. Section 4 (Discussion) addresses gene dysregulation as conceptualized in this study, highlighting how it enables us to better understand homeostasis and cancer. We further examine potential applications of the proposed gene panels and their role in tumorigenesis. Section 5 (Conclusion) summarizes the key findings and offers an outlook for future translational research based on this framework.

2. Materials and methods

2.1. Data

TCGA is a publicly accessible database of gene expression profiles drawn from cohort studies involving hundreds of normal tissue and solid tumor biopsy samples, classified by histopathological techniques.[6] Expression profiles were obtained through RNA-seq, capturing 60,483 genes per sample. TCGA reports gene expression values using the standard units of fragments per kilobase of transcript per million mapped reads. The size of the dataset varies with the cancer type and is consistently skewed toward tumor samples.

We selected 12 cancer types from TCGA for a systematic analysis (Table 1). These cancers manifest as solid tumors, particularly affecting the liver, breast, colon, head and neck, kidneys, lungs, prostate, stomach, thyroid, and uterus. We included five (out of six) of the most common cancer types (breast, lung, colon, prostate, and stomach), each with an incidence of over a million cases in 2020. Among the selected cancer types, there were also the most common causes of cancer death (lung, colon, liver, stomach, and breast), each accounting for over half a million deaths in 2020 (worldwide statistics reported by the World Health Organization[46]).

Table 1. Cancer types, the cancer genome atlas abbreviations, and the number of samples

Cancer types	Abbreviation	Normal samples	Tumor samples
Breast invasive carcinoma	BRCA	112	1,096
Colon adenocarcinoma	COAD	41	473
Head and neck squamous cell carcinoma	HNSC	44	502
Kidney renal clear cell carcinoma	KIRC	74	539
Kidney renal papillary cell carcinoma	KIRP	32	289
Liver hepatocellular carcinoma	LIHC	50	374
Lung adenocarcinoma	LUAD	59	535
Lung squamous cell carcinoma	LUSC	49	502
Prostate adenocarcinoma	PRAD	52	499
Stomach adenocarcinoma	STAD	32	375
Thyroid carcinoma	THCA	58	510
Uterine corpus endometrial carcinoma	UCEC	23	552

The selection of cancer types for our systematic study was motivated by the number of normal samples available in the data. For the cases under study, TCGA reports more than 20 normal samples per cancer type. Notably, achieving a reliable discrimination between normal and tumor tissues based on gene expression profiles required both normal and tumor samples to be adequately represented in the datasets.

2.2. Pre-processing of data

Gene expression distributions tend to be heavy-tailed, with many low-frequency outliers.[47] RNA-seq is known to be inaccurate at detecting low expression levels and may produce spurious null readings for genes that are nearly silenced.[48] To avoid artifacts associated with the low-expression region, we set all values below 0.1 fragments per kilobase of transcript per million mapped reads to zero. Moreover, we excluded all genes with non-zero expression in fewer than 5% of normal samples and fewer than 10% of tumor samples from the analysis.

2.3. Expression dysregulation patterns

We searched for genes that exhibit specific dysregulation patterns. In our framework, a gene conforms to a "differential expression" pattern if all normal samples express it in a certain manner (specified below), while a significant number of tumor samples exhibit a distinctly different expression. Conversely, a gene conforms to a "non-differential dysregulation" pattern if all tumor samples express it in a certain way, while a substantial number of normal samples express it differently. Non-differential dysregulation can be interpreted as the dual category of differential expression, achieved by swapping the roles of normal and tumor samples. By monitoring the expression values of a differentially expressed or non-differentially dysregulated gene, we can classify samples with no type I errors – i.e., no false positives for tumors in the case of differential expression and no false positives for normal samples in the case of non-differential dysregulation.

For simplicity, this study focuses on four types of gene sets, each named to reflect the classificatory potential of its individual gene members. Let x represent a class of samples,

either normal (N) or tumor (T). Genes that are only expressed above or below a threshold level for class x are referred to as "only x above" or "only x below," respectively. Specifically, we examined the "only-T-above," "only-T-below," "only-N-above," and "only-N-below" gene sets. By combining the "above" and "below" within the same class, we obtained the full sets of T-genes and N-genes. Notably, a single gene may simultaneously belong to both the only-T-above and only-N-below groups.

2.4. Data digitalization

We explicitly defined normal and tumor expression intervals for each gene. In each case, the populated expression space can be segmented into three regions: "N-only," "N-T," and "T-only" subintervals, which were associated with the ternary values −1, 0, and 1, respectively.

Figure 1 shows the distribution of expression values for *PYCR1*, *ALDH18A1*, and *TRIM27* genes in normal lung and LUAD samples. Notably, all three genes contain only-T intervals above the common N-T region. The number of tumor samples in the only-T interval is significant (above 90% of the tumor population). Thus, they may be included in the only-T-above set of genes.

These genes also show N-only intervals below the N-T region. However, the number of samples in the N-only intervals may not be sufficient to be included in the only-N-below class.

2.5. Statistically significant expression dysregulations

The significance of dysregulation patterns within the T-only and N-only sample subsets can be assessed using Fisher's exact test[49] to filter out genes exhibiting such patterns by chance.

Verifications show that with a p=0.01 and the sample sizes in Table 1, a dysregulation pattern is significant when observed in approximately 5% of normal samples (N-only subset) or 10% of tumor samples (T-only subset). We applied these thresholds, respectively, across all cancer types. This threshold justifies the exclusion of certain genes from analysis and explains why some genes identified in the previous subsection do not appear in the only-N-below set.

2.6. Expression dysregulation matrix

Gene expression profiles were encoded into a matrix where each column corresponded to a clinical sample and each row represented a significantly dysregulated gene. The matrix entries, derived from the prior data digitalization step, were assigned values of −1, 1, and 0, indicating

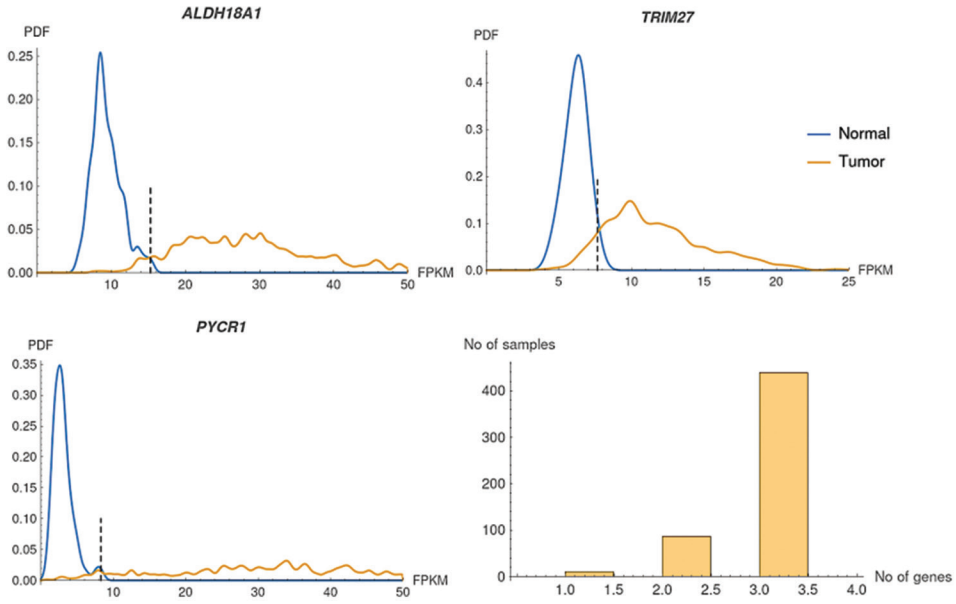

Figure 1. The Cancer Genome Atlas-Lung adenocarcinoma gene expression data for three "only-T-above" genes forming a perfect panel. Smooth probability density functions (PDF) are shown as solid lines, whereas the maximum of the normal set of values (the threshold) is marked by a dashed line. There are intervals for each gene common to both normal and tumor samples (expression values below the threshold), and "T-only" intervals populated only by tumor samples (expression above the threshold). The histogram shows that there is at least one dysregulated gene, i.e., with expression above the threshold, for each tumor sample; thus, the panel correctly classifies all of the normal samples with 0 dysregulated genes and all of the tumors, which show at least one dysregulated gene.
Abbreviation: FPKM: Fragments per kilobase of transcript per million mapped reads.

whether the gene's expression interval was N-exclusive, T-exclusive, or shared by N and T. This matrix structure provided all the necessary information for constructing perfect gene panels.

2.7. Perfect panels

Differentially expressed and non-differentially dysregulated genes often form large pools containing over a thousand members, which are impractical for real-world applications. In genetic-based hereditary risk assessment, diagnostics, and therapy, smaller gene panels (comprising 5 – 50 genes) are often preferred.[50]

Due to the low dimensionality of the gene expression data,[51] it is possible to extract compact panels from these large gene sets. In particular, panels can be designed to perfectly classify all normal and tumor samples collectively, with the additional requirement that removing any member from the panel would compromise this classification accuracy.

These panels can be identified using a concept similar to, but distinct from, reducts in RST,[42,43] which we termed a formal-concept reduct. To the best of our knowledge, this is the first presentation of formal-concept reducts,[44] although more stringent related concepts have been proposed by Zhang.[45]

Our algorithm for constructing perfect panels is based on progressively maximizing sensitivity. At each step, we iteratively add the differentially expressed genes that are most dysregulated in tumor samples not yet identified by the current panel (i.e., those samples where the included genes show no dysregulation), until all tumor samples are discovered.

The equivalent procedure involves iteratively adding the non-differentially dysregulated gene that most frequently exhibits normal regulation in the remaining undiscovered normal samples (i.e., those in which the genes already included are dysregulated) until all normal samples are discovered. If, at any iteration, there is gene selection ambiguity, we prioritize the most redundant candidate – i.e., the gene whose dysregulation pattern overlaps maximally with existing panel members across already classified samples. Further ambiguities are resolved by arbitrarily selecting the first candidate in the list.

Panels constructed this way are minimal: no gene can be removed without compromising perfect classification. However, they are not necessarily the smallest collection of genes achieving such goal nor are they necessarily unique. Modifying ambiguity-resolution criteria may give rise to different and/or smaller gene sets that can achieve perfect discrimination between normal and tumor samples, while remaining irredundant. In practice, these panels comprise 1 – 20 genes, making them suitable for cancer diagnostics.[50]

In the example considered in Section 2.4, the three-gene set constitutes a perfect panel for the only-T-above class. In its expression dysregulation matrix, normal samples show expression values of −1 or 0. Every tumor sample has at least one dysregulated gene (value 1) in the panel, as shown in the histogram of Figure 1. Thus, this panel exhibits no false negatives or false positives.

3. Results

First, we note that, in the average cancer type, only nearly 3% of the genes qualify as N-genes. The observation that more than one-third of the genome, and the vast majority of classifier genes, fall within the T-gene category aligns with cancer's characterization as a high-entropic state of gene regulatory networks[52,53] and is an indication of the abundance of potential genetic triggers for cancer.

Perfect panels constructed according to our procedure are summarized in Table 2. When no perfect panel exists, we reported the size of the minimal gene set that classifies the largest sample subset. Notably, only-T-above and only-T-below panels may include oncogenes and tumor suppressors, respectively. As shown in Table 2, all 12 cancer types exhibit perfect panels of both T-types.

Conversely, perfect panels with only-N-above or only-N-below genes appear irregularly in some tissues (Table 2). Specifically, breast invasive carcinoma (BRCA), head and neck squamous cell carcinoma, kidney renal clear cell carcinoma, kidney renal papillary cell carcinoma, LUAD, prostate adenocarcinoma, and thyroid carcinoma contain only only-N-above, uterine corpus endometrial carcinoma, colon adenocarcinoma (COAD), lung squamous cell carcinoma, and stomach adenocarcinoma contain both N-types, while liver hepatocellular carcinoma contains only only-N-below.

An inventory of perfect gene panels for the 12 types of cancer under study is presented in the Supplementary File. Notably, some cancer types can be perfectly classified using a single gene. This is the case for COAD with *SCARA5*, kidney renal papillary cell carcinoma with *UMOD*, and uterine corpus endometrial carcinoma with either *PLSCR4* or *TBC1D7*.

4. Discussion

4.1. Gene expression dysregulation

Dysregulation in gene expression can promote cancer.[54] Within this phenomenon, differential expression – where genes show altered expression in tumors versus normal tissues – represents the most extensively studied subset.[10]

Table 2. Summary of classifier genes per tissue

Set of genes	LIHC	BRCA	COAD	HNSC	KIRC	KIRP	LUAD	LUSC	PRAD	STAD	THCA	UCEC
Only-T-above	[a]3/23,986	[a]6/15,361	[a]2/17,536	[a]4/13,293	[a]4/22,654	[a]3/11,447	[a]3/20,274	[a]2/19,596	[a]8/8,093	[a]3/13,773	[a]5/5,744	[a]1/7,825
Only-N-above	11/40	[a]10/739	[a]1/876	[a]8/1,903	[a]3/780	[a]1/1,140	[a]5/613	[a]3/1,198	[a]14/1,415	[a]5/1,244	[a]11/794	[a]1/993
Only-T-below	[a]5/3,812	[a]6/6,701	[a]1/8,418	[a]5/2,093	[a]3/9,132	[a]1/10,263	[a]4/8,285	[a]2/9,404	[a]15/3,865	[a]5/1,499	[a]6/5,376	[a]1/7,443
Only-N-below	[a]5/1,246	12/682	[a]2/297	6/1,339	8/191	5/214	8/449	[a]3/985	15/915	[a]5/2,536	17/92	[a]1/506

Note: Each column identifies a cancer type based on The Cancer Genome Atlas terminology. Each row represents a different set of classifier genes (see main text for shorthand notation). Within each cell, we show the minimal number of genes that classify the largest number of samples, together with the total number of genes of the same sort. [a]marks the minimal gene sets that constitute perfect panels.
Abbreviations: BRCA: Breast invasive carcinoma; COAD: Colon adenocarcinoma; HNSC: Head and neck squamous cell carcinoma; KIRC: Kidney renal clear cell carcinoma; KIRP: Kidney renal papillary cell carcinoma; LIHC: Liver hepatocellular carcinoma; LUAD: Lung adenocarcinoma; LUSC: Lung squamous cell carcinoma; N: Normal; PRAD: Prostate adenocarcinoma; STAD: Stomach adenocarcinoma; T: Tumor; THCA: Thyroid carcinoma; UCEC: Uterine corpus endometrial carcinoma.

In cancer research, differential expression is often deemed significant only when the deviation from normal expression is substantial, consistent (i.e., always upregulated or downregulated), and present across most tumors.[55] A common practice is to define the lower and upper bounds of normal gene expression as ×0.5 and ×2 a reference level, respectively.[56] Therefore, a gene can be differentially expressed only if most tumors express either >×2 or <×0.5 the reference value. In turn, any such gene is considered differentially expressed when its expression level crosses the specific threshold above or below which most tumors are expressed.

From the outset, we contend that gene expression dysregulation comprises broader patterns than conventional differential expression. Certain dysregulation forms do not conform to either our definition of differential expression or the conventional one used in the field. As a result, these patterns are often overlooked in the analysis of gene expression data.

For example, consider a gene with bimodal expression distribution under normal conditions, such as those governed by circadian oscillations. If these oscillations are lost in tumor tissue, the gene may fall into the only-T-inside category. While such genes were identified through our data mining, they are not reported in this paper. Other underreported categories, like the only-T-outside genes, were also encountered.

Conversely, what we term as non-differential dysregulation, corresponding to N-genes, is typically overlooked. In our study, we focused on the only-N-above and only-N-below classes, although the only-N-outside and only-N-inside groups may likewise be present in specific tissues.

It is worth emphasizing that in single-cell RNA-seq expression analyses,[3] gene markers are routinely identified for individual cell types under normal conditions. However, to the best of our knowledge, this is the 1st time that markers are introduced specifically for whole normal tissue samples.

4.2. Panel validation

We provided two examples of panel validation using other datasets. The first involves the *SCARA5* gene in COAD. Microarray readings from Khamas *et al.*[57] demonstrate the perfect classification capability of *SCARA5* (data available at NCBI GEO,[58] accession GDS4382). Notably, this gene has also been independently identified as a biomarker for colorectal cancer.[59]

The second case concerns the LUAD dataset from a comprehensive study of a Chinese cohort,[60] which includes RNA-seq profiles from 51 tumor and 49 control samples. We evaluated the performance of our perfect only-T-above panel on this dataset. As shown in Figure S1, the genes *TRIM27*, *PYCR1*, and *ALDH18A1* fall within the only-T-above class, as they exhibit significantly populated T-exclusive intervals above the shared N–T expression range. The histogram in Figure S1 confirms that the panel remains perfect, achieving both maximal sensitivity and specificity in classification. However, within this particular cohort, the *TRIM27* gene proves redundant and can be removed without any loss in classification accuracy.

This finding raises an important question regarding the minimal number of genes required to assemble a perfect panel, and the extent to which that number remains robust to variations in cohort size.

4.3. The minimal number of genes needed to identify a tumor

The LUAD dataset[60] is particularly noteworthy, not only because its cohort differs markedly from that of TCGA but also due to its substantially smaller size, approximately an order of magnitude fewer samples. Specifically, the TCGA LUAD dataset comprises 59 normal and 535 tumor samples. This prompts the question: how does the number

of genes required for a perfect panel depend on the size of the tumor sample set?

The results, summarized in Figure S2, revealed that in the smaller external dataset, a single gene identifies 98% of the tumor samples, and the addition of a second gene completes the panel, achieving maximal sensitivity and specificity without requiring *TRIM27*. In contrast, for the larger TCGA dataset, the first gene alone covers only 95% of tumors, and the two-gene panel still leaves 1% of samples unclassified. In that case, *TRIM27* is necessary to achieve full classification. These observations suggest rare tumor variants emerge only in larger datasets. Their low frequency means that they are often absent in smaller cohorts, where simpler panels may suffice.

For illustration, a hypothetical cohort of 5,000 tumor samples is also considered in Figure S2. In that scenario, the 3-gene panel covers 99.7% of tumors, indicating that a fourth gene would likely be needed to achieve complete coverage. The figure also shows that saturation is reached very quickly: the number of classified tumor samples increases steeply with the addition of genes to the panel. This strongly supports our assertion that a small number of genes can effectively capture the global state of the Gene Regulatory Network, consistent with the effective reduced dimensionality of the tumor manifold.[51]

In summary, the expression distribution functions used to define the panels depend on the sample set size. When the sample size reaches the order of hundreds, the distribution appears "saturated," showing only minor changes when the number of samples is further increased.

This insight allowed us to evaluate how our panels would change with an increased number of normal samples. For instance, assuming that the distribution functions are saturated in BRCA (112 normal samples and 1094 tumor samples), we performed re-sampling to assess the performance of the six-gene only-T-above panel found for BRCA (Supplementary File) under highly imbalanced situations, such as 20 normal samples and 500 tumor samples. The results, shown in Figure S3, indicate that while the panel size tends to decrease in the reduced sets, notably, two genes from the original panel still classify more than 95% of samples in all cases.

Thus, we expect, for example, that the single-gene only-T-above panel found for uterine corpus endometrial carcinoma (23 normal samples) may change as the normal sample size grows, but the original gene will continue to cover at least 85% of the tumor samples.

It is worth noting that Figure S3 can also be interpreted as a form of validation of the six-gene only-T-above panel for BRCA across different experimental conditions.

4.4. Cancer diagnosis, tumor taxonomy, and gene therapy

Our construction of perfect gene panels follows a data-driven approach to gene expression profiles that do not require prior domain knowledge of the biological relevance of individual genes in a given tissue. These panels have an apparent value as candidate combinatorial biomarkers for diagnosis, which could be further enhanced by incorporating information about gene ontology and function into our data mining process.

In addition, the perfect T-gene panels could be leveraged in tumor taxonomy. Typically, tumor classification and the associated therapeutic decisions are made based on the most frequently mutated genes in a given tumor (for example, Ruiz-Cordero *et al.*,[61] for lung cancer). However, the classification is often incomplete, with a subset of tumors assigned to the so-called "wild-type" category, meaning that none of the genes in the reference panel are mutated. In our framework, any perfect T-gene panel enables a complete classification of tumors by providing the list of dysregulated genes in each tumor sample. Moreover, since multiple perfect panels may exist for a given tissue, tumors could be fully classified under different but equally valid criteria.

Consider, for example, the only-T-above panel for LUAD, examined above. Both *ALDH10A1* and *PYCR1* genes, related to glutamine metabolism, are known to play an important role in lung cancer.[62,63] The taxonomy based on this panel indicates that around 98 % of LUAD tumors rely on glutamine metabolism to foster cell proliferation and induce an immune-suppressive tumor microenvironment. In the remaining 2% of tumors, cell proliferation is regulated by *TRIM27* through the SIX homeobox 3-β-catenin signaling pathway.[64] These statements reflect the known role of these genes and their dysregulation frequencies in the tumor subpopulation. Nevertheless, further research is needed to validate these findings and translate them into therapeutic recommendations.

Moreover, N- and T-genes included in the perfect panels may have important applications in gene therapy. Consider, for instance, a gene belonging to both N- and T-groups, such as the *AGER* gene in LUAD. This gene is silenced in tumors and strongly expressed in normal samples. What happens if, through a transfection vector, its expression were shifted from the N-region to the T-region or vice versa? Such an experiment has already been conducted on cellular lines,[65] and the results indicate a significant change in the proliferation rate and invasion capacity of both tumor and normal cells. These astonishing results warrant further investigation.

4.5. Other challenges

Several other challenges remain, such as the role of low-expressed genes, the method's performance in highly heterogeneous tumors, and the possible impact of batch effects. In principle, our gene panels are robust against these concerns. Specifically, our N- and T-genes exhibit distinct expression intervals populated only by a significant fraction of N and T samples, respectively. They are not low-expressed genes. Regarding batch effects, the TCGA data used for panel discovery is largely free from such biases, as all samples were processed using a consistent technological framework and standardized procedures. For each tissue, there is a single batch of normal samples and a single batch of tumor samples. Concerning tumor heterogeneity, because the taxonomy derived from a panel is comprehensive, the panel should be capable of detecting tumors regardless of their mosaic composition or degree of heterogeneity.

5. Conclusion

We have shown that it is possible to construct a combinatorial gene panel that acts as a perfect biomarker for cancer. By monitoring the gene expression profile of the panel members, samples can be accurately classified as either normal or tumorous. In some cases, it is possible to classify a sample as tumorous based on the overexpression of a single gene. However, this represents just one example among various panel types, all of which are highly sensitive and specific.

Our study analyzed 12 cancer types from the TCGA database, encompassing many of the most prevalent cancers in the world. Panels are provided on a per-cancer-type basis, tailored to each specific context. A comprehensive inventory of these panels can be found in the Supplementary Information. Despite the fact that other panels combining classifier genes could be constructed, these are not discussed in the present paper.

While a single gene can have sufficient discriminative power in one tissue, other tissues require panels of up to nine genes to achieve the same level of accuracy. Figure S4 shows the relationship between panel length and the distance between the centers of the normal and tumor sample clusters in gene expression space.[66,67] It is evident that the shorter inter-cluster distances correspond to greater overlap between normal and tumor expression profiles, complicating classification and necessitating larger panels. The figure also suggests that the inter-cluster distance in gene expression space functions as a global tumor classifier, a factor often overlooked in tumor studies.

Our gene discovery framework extends beyond the paradigm of differential expression by introducing the concepts of N-genes and T-genes, characterized by gene expression intervals populated only by normal and tumor samples, respectively. The construction of perfect gene panels represents the first practical application of these concepts, which we anticipate can be translated into flexible and effective diagnostic tools.

In addition, this paper presents arguments supporting the use of perfect panels in tumor taxonomy and highlights their gene members as candidate targets of therapeutic applications. Other potential applications, such as early diagnosis and efficacy monitoring, alongside challenges, like technical standardization and cost considerations in clinical implementation, are particularly important and warrant further attention. Research in this direction is currently in progress.

Acknowledgments

The author, Augusto Gonzalez is grateful to Rolando Perez for a careful reading of the manuscript. The author, Gabriel Gil thanks Laura Azor, Fabiana Fuentes, Jorge Mato, and Karen Alfaro for critical comments and suggestions.

Funding

The research was supported by the Financial and International Projects Office of the Ministry of Sciences, Cuba (project PN692LH007-095).

Conflict of interest

The authors declare that they have no competing interests.

Author contributions

Conceptualization: Gabriel Gil, Augusto Gonzalez
Formal analysis: Gabriel Gil, Julio C. Drake-Pérez
Investigation: All authors
Methodology: Gabriel Gil, Augusto Gonzalez
Writing–original draft: Gabriel Gil, Augusto Gonzalez
Writing–review & editing: All authors

Ethics approval and consent to participate

Not applicable.

Consent for publication

Not applicable.

Availability of data

The data used was taken from TCGA public network (https://portal.gdc.cancer.gov/). Relevant software is available at the GitHub repository https://github.com/gabriel-gil/GenePan.

Further disclosure

Initial versions of the paper have been deposited in the bioRxiv preprint server (doi: 10.1101/2022.07.25.501449, 10.1101/2024.07.25.604730).

References

1. Collins FS, Morgan M, Patrinos A. The human genome project: Lessons from Large-scale biology. *Science.* 2003;300(5617):286-290.

   doi: 10.1126/science.1084564

2. Chu Y, Corey DR. RNA sequencing: Platform selection, experimental design, and data interpretation. *Nucleic Acid Ther.* 2012;22(4):271-274.

   doi: 10.1089/nat.2012.0367

3. Haque A, Engel J, Teichmann SA, Lönnberg T. A practical guide to single-cell RNA-sequencing for biomedical research and clinical applications. *Genome Med.* 2017;9(1):75.

   doi: 10.1186/s13073-017-0467-4

4. The Cancer Genome Atlas Research Network, Weinstein J, Collisson E, *et al.* The cancer genome atlas pan-cancer analysis project. *Nat Gen.* 2013;45(10):1113-1120.

   doi: 10.1038/ng.2764

5. Hutter C, Zenklusen JC. The cancer genome atlas: Creating lasting value beyond its data. *Cell.* 2018;173(2):283-285.

   doi: 10.1016/j.cell.2018.03.042

6. The Cancer Genome Atlas Research Network. *The Cancer Genome Atlas*. 2006. Available from: https://www.cancer.gov/tcga [Last accessed on 2025 Apr 15].

7. Cheng PF, Dummer R, Levesque MP. Data mining the cancer genome atlas in the era of precision cancer medicine. *Swiss Med Wkly.* 2015;145:w14183.

   doi: 10.4414/smw.2015.14183

8. Liñares-Blanco, J, Pazos, A, Fernandez-Lozano, C. Machine learning analysis of TCGA cancer data. *PeerJ Comput Sci.* 2021;7:e584.

   doi: 10.7717/peerj-cs.584

9. Li Q, Dai W, Liu J, Sang Q, Li YX, Li YY. Gene dysregulation analysis builds a mechanistic signature for prognosis and therapeutic benefit in colorectal cancer. *J Mol Cell Biol.* 2020;12(11):881-893.

   doi: 10.1093/jmcb/mjaa041

10. Ali HEA, Lung PY, Sholl AB, *et al.* Dysregulated gene expression predicts tumor aggressiveness in African-American prostate cancer patients. *Sci Rep.* 2018;8(1):16335.

    doi: 10.1038/s41598-018-34637-8

11. Mezlini AM, Das S, Goldenberg A. Finding associations in a heterogeneous setting: Statistical test for aberration enrichment. *Genome Med.* 2021;13(1):68.

    doi: 10.1186/s13073-021-00864-4

12. Le Priol C, Azencott CA, Gidrol X. Detection of genes with differential expression dispersion unravels the role of autophagy in cancer progression. *PLoS Comput Biol.* 2023;19(3):e1010342.

    doi: 10.1371/journal.pcbi.1010342

13. Li H, Khang TF. clrDV: A differential variability test for RNA-Seq data based on the skew-normal distribution. *PeerJ.* 2023;11:e16126.

    doi: 10.7717/peerj.16126

14. Roberts AGK, Catchpoole DR, Kennedy PJ. Identification of differentially distributed gene expression and distinct sets of cancer-related genes identified by changes in mean and variability. *NAR Genom Bioinform.* 2022;4(1):lqab124.

    doi: 10.1093/nargab/lqab124

15. Andreani TS, Itoh TQ, Yildirim E, Hwangbo DS, Allada R. Genetics of circadian rhythms. *Sleep Med Clin.* 2015;10(4):413-421.

    doi: 10.1016/j.jsmc.2015.08.007

16. Gebert J, Motameny S, Faigle U, Forst CV, Schrader R. Identifying genes of gene regulatory networks using formal concept analysis. *J Comput Biol.* 2008;15(2):185-194.

    doi: 10.1089/cmb.2007.0107

17. Choi V, Huang Y, Lam V, Potter D, Laubenbacher R, Duca K. Using formal concept analysis for microarray data comparison. *J Bioinform Comput Biol.* 2008;6(1):65-75.

    doi: 10.1142/s021972000800328x

18. Motameny S, Versmold B, Schmutzler R. Formal Concept Analysis for the Identification of Combinatorial Biomarkers in Breast Cancer. In: Medina R, Obiedkov S, editors. *Formal Concept Analysis. ICFCA 2008. Lecture Notes in Computer Science*. Vol. 4933. Berlin, Heidelberg: Springer; 2008. p 229–240.

    doi: 10.1007/978-3-540-78137-0_17

19. Amin II, Kassim SK, Hassanien A, Hefny HA. Formal Concept Analysis for Mining Hypermethylated Genes in Breast Cancer Tumor Subtypes. In: *12th International Conference on Intelligent Systems Design and Applications (ISDA)*. Kochi, India; 2012. p. 764-769.

    doi: 10.1109/ISDA.2012.6416633

20. Kaytoue-Uberall M, Duplessis S, Napoli A. Using Formal Concept Analysis for the Extraction of Groups of Co-expressed Genes. In: Le Thi HA, Bouvry P, Pham Dinh T, editors. *Modelling, Computation and Optimization in Information Systems and Management Sciences. MCO 2008. Communications in Computer and Information Science*. Vol. 14. Berlin, Heidelberg: Springer; 2008.

    doi: 10.1007/978-3-540-87477-5_47

21. Kaytoue M, Kuznetsov SO, Napoli A, Duplessis S. Mining gene expression data with pattern structures in formal concept analysis. *Inf Sci.* 2011;181(10):1989-2001.

    doi: 10.1016/j.ins.2010.07.007

22. González-Calabozo JM, Valverde-Albacete FJ, Peláez-Moreno C. Interactive knowledge discovery and data mining on genomic expression data with numeric formal concept analysis. *BMC Bioinform.* 2016;17(1):374.

    doi: 10.1186/s12859-016-1234-z

23. Singh PK, Kumar CA, Gani AA. Comprehensive survey on formal concept analysis, its research trends, and applications. *Int J Appl Math Comput Sci.* 2016;26(2):495-516.

    doi: 10.1515/amcs-2016-0035

24. Raza K. Formal concept analysis for knowledge discovery from biological data. *Int J Data Min Bioinform*. 2017;18(4):281.

    doi: 10.1504/IJDMB.2017.088138

25. Ferreira LM, Pinto CLN, Dias SM, Nobre CN, Zárate LE. Extraction of Conservative Rules for Translation Initiation Site Prediction Using Formal Concept Analysis. In: *Proceedings of the 19th International Conference on Enterprise Information Systems (ICEIS).* Vol. 1. SciTePress; 2017. p. 265-271.

    doi: 10.5220/0006326202650271

26. Zhao M, Zhang S, Li W, Chen G. Matching biomedical ontologies based on formal concept analysis. *J Biomed Semantics.* 2018;9(1):11.

    doi: 10.1186/s13326-018-0178-9

27. Roscoe S, Khatri M, Voshall A, Batra S, Kaur S, Deogun J. Formal concept analysis applications in bioinformatics. *ACM Comput Surv.* 2023;55(8):1-40.

    doi: 10.1145/3554728

28. Maji P, Paul S. Rough set based maximum relevance-maximum significance criterion and gene selection from microarray data. *Int J Approx Reason.* 2011;52(3):408-426.

    doi: 10.1016/j.ijar.2010.09.006

29. Midelfart H, Komorowski J, Nørsett K, Yadetie F, Sandovik AK, Lægreid A. Learning rough set classifiers from gene expressions and clinical data. *Fundam Inform.* 2002;53(2):155-183.

    doi: 10.3233/FUN-2002-53204

30. Dai J, Xu Q. Attribute selection based on information gain ratio in fuzzy rough set theory with application to tumor classification. *Appl Soft Comput.* 2013;13(1):211-221.

    doi: 10.1016/j.asoc.2012.07.029

31. Li D, Zhang W. Gene selection using rough set theory. In Wang GY, Peters JF, Skowron A, Yao Y, editors. *Rough Sets and Knowledge Technology. RSKT 2006. Lecture Notes in Computer Science*. Vol. 4062. Berlin, Heidelberg: Springer; 2006. p. 778-785.

    doi: 10.1007/11795131_113

32. Mishra D, Dash R, Rath AK, Acharya M. Feature selection in gene expression data using principal component analysis and rough set theory. In: Arabnia HR, Tran QN, editors. *Software Tools and Algorithms for Biological Systems. Advances in Experimental Medicine and Biology*. Vol. 696. New York: Springer; 2011. p. 91-100.

    doi: 10.1007/978-1-4419-7046-6_10

33. Pati SK, Das AK, Ghosh A. Gene Selection Using Multi-objective Genetic Algorithm Integrating Cellular Automata and Rough Set Theory. In: Panigrahi BK, Suganthan, PN, Das S, Dash SS, editors. *Swarm, Evolutionary, and Memetic Computing. SEMCCO 2013. Lecture Notes in Computer Science*. Vol. 8298. Cham: Springer; 2013. p. 144-155.

    doi: 10.1007/978-3-319-03756-1_13

34. Zhang Q, Xie Q, Wang G. A survey on rough set theory and its applications. *CAAI Trans Intell Technol.* 2016;1(4):323-333.

    doi: 10.1016/j.trit.2016.11.001

35. Chen Y, Zhang Z, Zheng J, Ma Y, Xue Y. Gene selection for tumor classification using neighborhood rough sets and entropy measures. *J Biomed Inform.* 2017;67:59-68.

    doi: 10.1016/j.jbi.2017.02.007

36. Sun L, Zhang X, Xu J, Wang W, Liu R. A Gene selection approach based on the fisher linear discriminant and the neighborhood rough set. *Bioengineered*. 2018;9(1):144-151.

    doi: 10.1080/21655979.2017.1403678

37. Saha S, Roy S, Ghosh A, Dey KN. Gene-Gene Interaction Analysis: Correlation, Relative Entropy and Rough Set Theory Based Approach. In: *Bioinformatics and Biomedical Engineering: 6th International Work-Conference, IWBBIO 2018. Proceedings, Part II*. Granada, Spain: Springer-Verlag; 2018. p. 397-408.

    doi: 10.1007/978-3-319-78759-6_36

38. Patil S, Balmuri KR, Frnda J, Parameshachari BD, Konda S, Nedoma J. Identification of triple-negative breast cancer genes using rough set-based feature selection algorithm and ensemble classifier. *Hum Centric Comput Inf Sci.* 2022;12:54.

    doi: 10.22967/HCIS.2022.12.054

39. Majumder S, Thakran Y, Pal V, Singh K. Fuzzy and rough set theory based computational framework for mining genetic interaction triplets from gene expression profiles for lung adenocarcinoma. *IEEE/ACM Trans Comput Biol Bioinform.* 2022;19(6):3469-3481.

    doi: 10.1109/TCBB.2021.3120844

40. Duntsch N, Gediga G. Modal-style Operators in Qualitative Data Analysis. In: *2002 IEEE International Conference*

on Data Mining Proceedings. Maebashi City, Japan; 2002. p. 155-162.

doi: 10.1109/ICDM.2002.1183898

41. Lai H, Zhang D. Concept lattices of fuzzy contexts: Formal concept analysis vs. rough set theory. *Int J Approx Reason.* 2009;50(5):695-707.

doi: 10.1016/j.ijar.2008.12.002

42. Pawlak, Z. Rough sets. *Int J Comput Inf Sci.* 1982;11(5):341-356.

doi: 10.1007/BF01001956

43. Pawlak Z. *Rough Sets: Theoretical Aspects of Reasoning about Data*. Dordrecht: Springer; 1991.

doi: 10.1007/978-94-011-3534-4

44. Jia X, Shang L, Zhou B, Yao Y. Generalized attribute reduct in rough set theory. *Knowl Based Syst*. 2016;91:204-218.

doi: 10.1016/j.knosys.2015.05.017

45. Zhang W. Attribute reduction theory and approach to concept lattice. *Sci China Ser F Inf Sci.* 2005;48(6):713-726.

doi: 10.1360/122004-104

46. World Health Organization. *Cancer*. Available from: https://www.who.int/news-room/factsheets/detail/cancer [Last accessed on 2025 April 15].

47. Bengtsson M, Ståhlberg A, Rorsman P, Kubista M. Gene expression profiling in single cells from the pancreatic islets of Langerhans reveals lognormal distribution of mRNA levels. *Genome Res.* 2005;15(10):1388-1392.

doi: 10.1101/gr.3820805

48. Sha Y, Phan JH, Wang MD. Effect of Low-expression Gene Filtering on Detection of Differentially Expressed Genes in RNA-seq Data. In: *37th Annual International Conference of the IEEE Engineering in Medicine and Biology Society*. 2015. p. 6461.

doi: 10.1109/EMBC.2015.7319872

49. Fang Z, Martin J, Wang Z. Statistical methods for identifying differentially expressed genes in RNA-Seq experiments. *Cell Biosci.* 2012;2(1):26.

doi: 10.1186/2045-3701-2-26

50. Durães C, Pereira Gomes C, Costa JL, Quagliata L. Demystifying the discussion of sequencing panel size in oncology genetic testing. *Eur Med J.* 2022;7(2):68-77

doi: 10.33590/emj/22C9259

51. Gonzalez A, Leon DA, Perera Y, Perez R. On the gene expression landscape of cancer. *PLoS One*. 2023;18(2):e0277786.

doi: 10.1371/journal.pone.0277786

52. Mesa-Rodríguez A, Gonzalez A, Estevez-Rams E, Valdes-Sosa PA. Cancer segmentation by entropic analysis of ordered gene expression profiles. *Entropy (Basel).* 2022;24(12):1744.

doi: 10.3390/e24121744

53. Gonzalez A, Quintela F, Leon DA, Bringas Vega ML, Valdes-Sosa P. Estimating the number of available states for normal and tumor tissues in gene expression space. *Biophys Rep (NY).* 2022;2(2):100053.

doi: 10.1016/j.bpr.2022.100053

54. Bradner JE, Hnisz D, Young RA. Transcriptional addiction in cancer. *Cell.* 2017;168(4):629-643.

doi: 10.1016/j.cell.2016.12.013

55. Li Q, Dai W, Liu J, Sang Q, Li YX, Li YY. DysRegSig: An R package for identifying gene dysregulations and building mechanistic signatures in cancer. *Bioinformatics.* 2021;37(3):429-430.

doi: 10.1093/bioinformatics/btaa688

56. Dalman MR, Deeter A, Nimishakavi G, Duan ZH. Fold change and p-value cutoffs significantly alter microarray interpretations. *BMC Bioinform.* 2012;13(Suppl 2):S11.

doi: 10.1186/1471-2105-13-S2-S11

57. Khamas A, Ishikawa T, Shimokawa K, *et al.* Screening for epigenetically masked genes in colorectal cancer using 5-Aza-2'-deoxycytidine, microarray and gene expression profile. *Cancer Genomics Proteomics*. 2012;9(2):67-75.

58. Barrett T, Wilhite SE, Ledoux P, *et al.* NCBI GEO: Archive for functional genomics data sets--update. *Nucleic Acids Res.* 2013;41(D1):D991-D995.

doi: 10.1093/nar/gks1193

59. Liu J, Zheng ML, Shi PC, Cao YP, Zhang JL, Xie YP. SCARA5 is a novel biomarker in colorectal cancer by comprehensive analysis. *Clin Lab.* 2020;66(7).

doi: 10.7754/Clin.Lab.2019.191015

60. Xu JY, Zhang C, Wang X, *et al.* Integrative proteomic characterization of human lung adenocarcinoma. *Cell.* 2020;182(1):245-261.e17.

doi: 10.1016/j.cell.2020.05.043

61. Ruiz-Cordero R, Ma J, Khanna A, *et al.* Simplified molecular classification of lung adenocarcinomas based on EGFR, KRAS, and TP53 mutations. *BMC Cancer.* 2020;20(1):83.

doi: 10.1186/s12885-020-6579-z

62. Ren H, Ge DF, Yang ZC, Cheng ZT, Zhao SX, Zhang B. Integrated bioinformatics analysis identifies ALDH18A1 as a prognostic hub gene in glutamine metabolism in lung adenocarcinoma. *Discov Oncol.* 2025;16(1):1.

doi: 10.1007/s12672-024-01698-3

63. Zhang L, Zhao X, Wang E, Yang Y, Hu L, Xu H, Zhang B. PYCR1 promotes the malignant progression of lung cancer through the JAK-$STAT_3$ signaling pathway via PRODH-dependent glutamine synthesize. *Transl Oncol.*

2023;32:101667.

doi: 10.1016/j.tranon.2023.101667

64. Liu S, Tian Y, Zheng Y, Cheng Y, Zhang D, Jiang J, Li S. TRIM27 acts as an oncogene and regulates cell proliferation and metastasis in non-small cell lung cancer through SIX3-β-catenin signaling. *Aging (Albany NY).* 2020;12(24):25564-25580.

doi: 10.18632/aging.104163

65. Wang Q, Zhu W, Xiao G, Ding M, Chang J, Liao H. Effect of AGER on the biological behavior of non-small cell lung cancer H1299 cells. *Mol Med Rep.* 2020;22(2):810-818.

doi: 10.3892/mmr.2020.11176

66. Gonzalez A, Nieves J, Leon DA, Bringas Vega ML, Valdes Sosa P. Gene expression rearrangements denoting changes in the biological state. *Sci Rep.* 2021;11(1):8470.

doi: 10.1038/s41598-021-87764-0

67. Nieves J, Gonzalez A. The geometry of normal tissue and cancer gene expression manifolds. *Acta Biotheor.* 2024;72(3):9.

doi: 10.1007/s10441-024-09483-z

ACCSCIENCE PUBLISHING

Tumor Discovery

ORIGINAL RESEARCH ARTICLE

Magnesium-28: A theorical novel self-theranostic strategy targeting metabolic enzyme disruption and intracellular irradiation

Tran Van Luyen*

KLT Research and Application Center, Saigon Scientific and Technological Development Institute, Ong Lanh bridge Ward, Ho Chi Minh City, Vietnam

Abstract

The limitations of conventional cancer therapies, such as low selectivity and significant side effects, necessitate innovative approaches. This study proposes a pioneering self-theranostic strategy using magnesium-28 (Mg-28) alone, enabling simultaneous diagnosis, therapy, and treatment monitoring. Exploiting the elevated Mg ion demand in cancer cells, Mg-28 selectively targets Mg-dependent enzymes (e.g., DNA/RNA polymerases, hexokinase, telomerase) within intracellular organelles, such as the nucleus and mitochondria, without requiring biochemical carriers or nanoparticles, as in recent methods. A theoretical model based on the Mg-uptake coefficient predicts selective Mg-28 accumulation in tumors following intravenous administration. The Mg-28 decay chain—progressing through Aluminum-28 to stable Silicon-28—delivers highly localized irradiation through beta particles, Auger electrons, and recoil ions to critical intracellular structures, while simultaneously disrupting essential Mg-dependent enzymes. This results in a dual mechanism of radiotherapy and multi-enzyme inactivation. Simulations of linear energy transfer, radiation range, and absorbed dose show that nanogram-scale amounts of Mg-28 can deliver 60–400 Gy to tumors ranging from 0.03 mg to 500 g, suggesting potent cytotoxicity across a broad range of tumor sizes and stages. This potential is grounded in the universal metabolic reliance of cancer cells on Mg. Moreover, gamma emissions from Mg-28 and its daughter isotopes support early tumor detection and real-time treatment monitoring, enhancing therapeutic precision. As the first proposed single-isotope theranostic approach leveraging Mg dependency, this innovative strategy provides a robust foundation for future pre-clinical and clinical investigations aimed at validating its therapeutic efficacy, pharmacokinetics, and biosafety—thereby inaugurating a novel hypothesis for cancer therapy.

Keywords: Magnesium-28; Intracellular irradiation; Multienzyme inactivation; Precision metabolic targeting; Self-theranostics; Magnesium uptake

***Corresponding author:**
Tran Van Luyen
(luyen.tranvan@gmail.com)

Citation: Luyen TV. Magnesium-28: A theorical novel self-theranostic strategy targeting metabolic enzyme disruption and intracellular irradiation. *Tumor Discov*. 2025;4(3):70-80. doi: 10.36922/TD025070010

Received: February 10, 2025

1st revised: April 15, 2025

2nd revised: May 2, 2025

3rd revised: May 19, 2025

Accepted: May 21, 2025

Published online: August 13, 2025

1. Introduction

Cancer remains a paramount global health challenge, responsible for approximately 10 million deaths worldwide in 2020.[1] Despite significant progress in medical oncology, conventional treatment modalities—such as surgery, chemotherapy, radiotherapy, and immunotherapy—are often limited by reduced efficacy in advanced stages, debilitating

systemic side effects, and the persistent issue of tumor relapses due to incomplete eradication of cancer cells.[2]

The advent of targeted therapies, including nanoparticle delivery systems,[3] monoclonal antibodies,[4] peptides,[5] clustered regularly interspaced short palindromic-Cas9,[6] and chimeric antigen receptor-T cells,[7] has improved the precision of cancer cell targeting. However, these approaches predominantly focus on extracellular targets and often require complex delivery mechanisms. A critical gap persists in our ability to effectively target key intracellular processes, particularly the enzymes essential for cancer cell metabolism and replication.

While radioisotopes, such as iodine-131, phosphorus-32, lutetium-177, holmium-166, and yttrium-90 have advanced the field of extracorporeal radiotherapy, including techniques, such as brachytherapy,[2,8] these methods typically rely on carriers to deliver isotopes to the vicinity of tumors and primarily exert their effects extracellularly. As a result, their impact on the intracellular machinery of cancer cells remains limited.[9] For instance, although iodine-131 is effective in treating thyroid cancer, its use carries the risk of inducing secondary malignancies.[10]

A fundamental challenge in current cancer treatment is the failure to comprehensively disrupt the core processes that drive cancer progression, namely, uncontrolled proliferation, limitless replicative potential (immortality), invasion, metastasis, and the sustained energy supply required to support these processes. Intriguingly, all these critical functions are heavily reliant on magnesium ions (Mg^{2+}), which serve as an essential cofactor for numerous Mg-dependent enzymes.[11] Tumor cells characterized by rapid proliferation and heightened metabolic demands, exhibit a significantly elevated requirement for Mg^{2+} compared to normal cells. This metabolic vulnerability presents a unique and underexplored therapeutic opportunity.

Historically, magnesium-28 (Mg-28) has been utilized as a valuable tracer in metabolic studies, particularly in plant biology and in investigations into the pathophysiology of diabetes.[12-14] However, it's potential as a therapeutic agent for cancer remains largely unexplored. This study introduces Mg-28 as a dual-action agent that combines targeted intracellular irradiation with the direct inactivation of Mg-dependent enzymes. A potential concern regarding the use of Mg-28 stems from the fact that Mg^{2+} is a cofactor for over 300 enzymes, raising questions about potential off-target effects in vital organs, such as the lungs, liver, and brain. However, this research demonstrates the contrary: Mg-28 exhibits a strong propensity to selectively concentrate on malignant tumors—the very sites where cell survival, proliferation, invasion, and metastasis require Mg levels far exceeding those of healthy tissues. Following intravenous administration, Mg-28 is hypothesized to selectively accumulate within these tumor cells, competitively replacing stable Mg^{2+} in crucial enzymes. The subsequent decay of Mg-28 emits beta particles, Auger electrons, and recoil ions that directly target intracellular structures, such as the nucleus and mitochondria. This dual mechanism aims to overcome therapeutic resistance, minimize off-target effects, and enable self-theranostic applications by integrating both therapy and diagnostics within a single agent.

The overarching objective of this work is to comprehensively analyze the Mg-28 approach and demonstrate its feasibility as a groundbreaking strategy that combines the precision of targeted intracellular chemotherapy with radiotherapy, while minimizing damage to healthy tissues and enabling early diagnosis and dynamic monitoring of therapeutic progress. This research seeks to unlock the transformative potential of Mg-28 as a next-generation theranostic platform in the ongoing fight against cancer. In fact, this approach may serve as a foundation for pre-clinical and clinical evaluation in the future.

2. Methodology

This theoretical study evaluates the feasibility of Mg-28 as a precision cancer therapy through a comprehensive analysis encompassing five key aspects: (1) The fundamental principles of metalloenzyme inactivation; (2) the mechanism of Mg-dependent multienzyme disruption due to changes in cofactor valence and ionic radius; (3) the calculation of linear energy transfer (LET) and the range of emitted radiation particles, including recoil effects; (4) the quantification of absorbed dose in tumors of varying volumes and the assessment of systemic dose; and (5) the tumor-specific uptake of Mg ions driven by the metabolic demands of cancer cells. This approach builds upon the basic principles of metalloenzyme inactivation detailed in our previous publications.[15,16]

2.1. Principles of metalloenzyme inactivation

The strategy is based on the substitution of stable metal ion cofactors in metalloenzymes with suitable radioisotopes to induce enzyme inactivation. Ideal radioisotopes for this purpose should emit beta particles or Auger electrons and possess a half-life ($T_1/_2$) that is neither excessively long (to minimize prolonged radiation exposure) nor too short (to allow for clinical utility). Furthermore, their decay products should be isotopes of elements that do not function as cofactors at the enzyme's active site. Mg-28 ($T_1/_2 \approx 21$ h) meets these criteria for targeting Mg-dependent enzymes, decaying into Aluminum-28 (Al-28) and subsequently

Silicon-28 (Si-28), with emissions capable of disrupting the function of these critical enzymes in cancer cells.[17]

2.2. Mechanism of Mg-dependent enzyme inactivation

Mg^{2+} typically stabilizes the active sites of Mg-dependent enzymes by forming six-coordinate bonds with oxygen atoms from carboxylate and phosphate groups.[18-21] This coordination is essential for substrate binding and catalytic activity. Upon radioactive decay, Mg-28 transforms into Al^{3+} and then Si^{4+}, both of which possess higher charges and smaller ionic radii (Al^{3+}: 0.50 Å; Si^{4+}: 0.40 Å) compared to Mg^{2+} (0.72 Å).[22,23] This substitution disrupts the electrostatic interactions within the active site, leading to structural stress, distortion, weakened substrate binding, and ultimately, impaired or abolished catalytic efficiency. In addition, the recoil of Al-28 and Si-28 ions during decay (with a displacement of 0.022–1.5 Å) can cause local distortions at the enzyme active site. Given the precise spatial requirements for enzymatic catalysis, such displacements can further impair enzyme functionality. The high-LET particles (beta particles and Auger electrons) emitted during decay also contribute to enzyme inactivation by breaking covalent and non-covalent bonds within the apoenzyme and generating free radicals that denature surrounding proteins.

2.3. LET and radiation range

The LET and the range of beta particles, Auger electrons, and recoil ions emitted during Mg-28 decay were calculated using the NIST ESTAR program[24] and Medical Internal Radiation Dose (MIRD) data.[17,25] For recoil ions (Al-28 and Si-28), recoil energies were derived using Equation I, based on the principle of conservation of momentum following beta particle emission from the parent Mg-28 nucleus.

$$E_{recoil} = \frac{E_{\beta}^2}{2Mc^2} \quad \text{(I)}$$

where E_{recoil} is the recoil energy of the daughter nucleus (Al-28 or Si-28); E^{β} is the energy of the emitted beta particle; M is the mass of the daughter nucleus; and $c^2 = 9 \times 10^{16}\ m^2/s^2$ is the square of the speed of light.

These resulting energy values were then used to model the LET and range of these recoil ions in different tissue types.

2.4. Absorbed dose calculations

Absorbed dose calculations were performed for tumors of different volumes (T_0–T_5) and for the whole body of a 60-kg individual using the MIRD program[26] and publicly available nuclear data.[17,25] Modeled scenarios assumed the administration of Mg-28 in doses ranging from 0.1 to 6.2 ng and included three delivery scenarios: (1) Intravenous injection without tumor-specific uptake, (2) intravenous injection with high tumor-specific uptake (based on the Mg uptake coefficient of tumor cells), and (2) direct injection into the tumor. In addition, absorbed doses were evaluated for different treatment regimens involving 62, 300, and 400 Mg-28 ions/cell. These correspond to different levels of inhibition, with the aim of inactivating approximately 300 Mg-dependent enzymes.

2.5. Tumor-specific Mg uptake

The selective accumulation of Mg^{2+} by cancer cells, compared to their normal counterparts, forms the foundation for employing the radioisotope Mg-28 in targeted cancer therapy. This differential uptake arises primarily from the significantly higher replication rates of cancerous tissues, leading to an increased demand for Mg^{2+}—a crucial cofactor for numerous enzymes involved in DNA replication, protein synthesis, and energy metabolism.[11,20] Although intracellular concentrations of stable Mg^{2+} may be similar in individual normal and cancerous cells, the dynamic process of rapid cell division leads to a significantly greater overall Mg^{2+} uptake at the tissue level in tumors.

To quantify this difference, we model the reproductive capacity of healthy and cancerous tissues over time. The proliferation of healthy and cancerous tissues can be calculated using Equations II and III, respectively, while the growth ratio between the two types of tissues is expressed as in Equation IV.

$$Healthytissue: A = 2^{(n_a)}; \left(n_a = t/T_a \right) \quad \text{(II)}$$

$$Cancer\ tissue: B = 2^{(n_b)}; \left(n_b = t/T_b \right) \quad \text{(III)}$$

$$B/A = 2^{(n_b - n_a)} = 2^{t(1/Tb - 1/Ta)} \quad \text{(IV)}$$

where A and B are the number of healthy cells and cancer cells, respectively; n_a and n_b are the number of doubling periods of healthy tissue and cancerous tissue, respectively; t is the actual copy time; and T_a and T_b are the replication cycle of healthy cells and cancer cells, respectively.

By introducing the doubling time ratio $k = T_a/T_b$, which reflects the differences in cell division dynamics, Equation IV can be transformed to Equation V.

$$B/A = 2^{t/T_b \times (1-1/k)} \quad \text{(V)}$$

where A and B are the number of healthy cells and cancer cells, respectively; t is the actual copy time; T_b is the replication cycle of cancer cells; and k is the doubling time ratio.

Unlike normal cells, cancer cells are not regulated by cyclin-dependent kinases,[27] which ensure genomic integrity, accurate protein synthesis, and complete DNA repair in healthy cells. For this reason, their replication is faster—resulting in k >1.

Rapid replication in cancer cells creates a disproportionately high demand for resources essential for survival and division, including Mg^{2+}. This demand doubles during the M phase of the cell cycle. Therefore, this ratio, when normalized to the initial number of cells, is known as the Mg-28 uptake coefficient. This preferential Mg uptake by cancer cells is the cornerstone of the Mg-28 therapy. The elevated demand for Mg^{2+} in rapidly dividing cancer cells acts as a natural driving force for the selective accumulation of the Mg-28 radioisotope within the tumor microenvironment. This intrinsic targeting mechanism eliminates the need for complex biochemical carriers or nanoparticles, simplifying the treatment process and reducing potential off-target toxicities. The high Mg-uptake coefficient not only enhances the intracellular delivery of Mg-28 for enzyme inactivation and irradiation but also underpins its potential for early diagnosis and real-time monitoring, as even small tumors exhibit a measurable increase in Mg accumulation. This coefficient is also the basis for calculating absorbed doses and enzyme inactivation in intravenous treatment regimens, where energy transfer from Mg-28 decay within the cancer cell microenvironment leads to the disruption of molecular bonds.

3. Results

3.1. Mg-uptake coefficient

The Mg-uptake coefficient (B/A), a key determinant of Mg-28 distribution, was calculated by Equation V with an assumed value of k = 2. The results demonstrate a significant increase in the coefficient with tumor size and the number of replication cycles.

As demonstrated in Table 1, the coefficient increases dramatically with the number of replication cycles (n_b) and the value of k. For instance, even with a modest k value of 2, the Mg-uptake coefficient escalates from 1.8×10^2 at 15 cycles (T_0 tumor) to 7.1×10^5 at 39 cycles (T_5 tumor). This highlights the profound ability of growing tumors to selectively accumulate Mg ions. This trend reflects the elevated Mg demand of rapidly proliferating cancer cells, which enhances the selective targeting of Mg-28 to larger and more metabolically active tumors compared to smaller or less active ones, and significantly more than to normal cells.

3.2. LET and particle range

The LET values and corresponding ranges for the particles emitted during Mg-28 decay are presented in Table 2 and illustrated in Figure 1.

Electron Auger, Beta particles (β), and recoiled ions[26,27]

Electron Auger of Mg-28 is KLL(Mg-28); E = 0.0014 MeV

Electron Auger (1) of Al-28 is (Al-28) KLL; E = 0.00159 MeV

Electron Auger (2) of Al-28 is (Al-28) KLX; E = 0.00170 MeV

Electron Auger (3) of Al-28 is (Al-28) KXY; E = 0.00181 MeV

β1 Mg-28 E = 0.0659 MeV

β 2 Mg-28 E = 0.1559 MeV

β 3 Mg-28 E = 0.3192 MeV

β Al-28 E = 1.124 MeV

Recoiled ion Al-28: from β1 of Mg-28; E = 0.0039 eV

Recoiled ion Al-28: from β2 of Mg -28; E = 0.0109 eV

Recoiled ion Al-28: from β3 of Mg -28; E = 0.0366 eV

Recoiled ion Si-28: from β1 of Al-28; E = 0.*171 eV*

Beta-minus particles exhibit LET values of 0.002–0.09 eV/Å with a range of 0.07–6.11 mm. Auger electrons demonstrate higher LET values, ranging 0.81–1.6 eV/Å, but with a shorter range of 88–224 nm. Recoil ions (Al-28 and Si-28) have LET values between

Table 1. Tissue characteristics and magnesium-28 absorbtion coefficient

Content	Tissue level					
	T_0	T_1	T_2	T_3	T_4	T_5
Mass (g)	3.1E-05	5.0E-03	5.0E-02	5.0E-01	5.0E+00	5.0E+02
Number of cells	3.1E+04	5.0E+06	5.0E+07	5.0E+08	5.0E+09	5.0E+11
Number of cell cycles, n_b	15	22	27	29	32	39
Absorption coefficient	1.8E+02	3.2E+03	7.1E+03	2.2E+04	7.1E+04	7.1E+05

Notes: T_0 was defined using Equation III after n_b=15 cycles, where $B = 2^{n_b}$ and $\left(n_b = t/T_b\right)$. The absorption coefficient is calculated based on the cumulative uptake over successive cell cycles, assuming k=2.

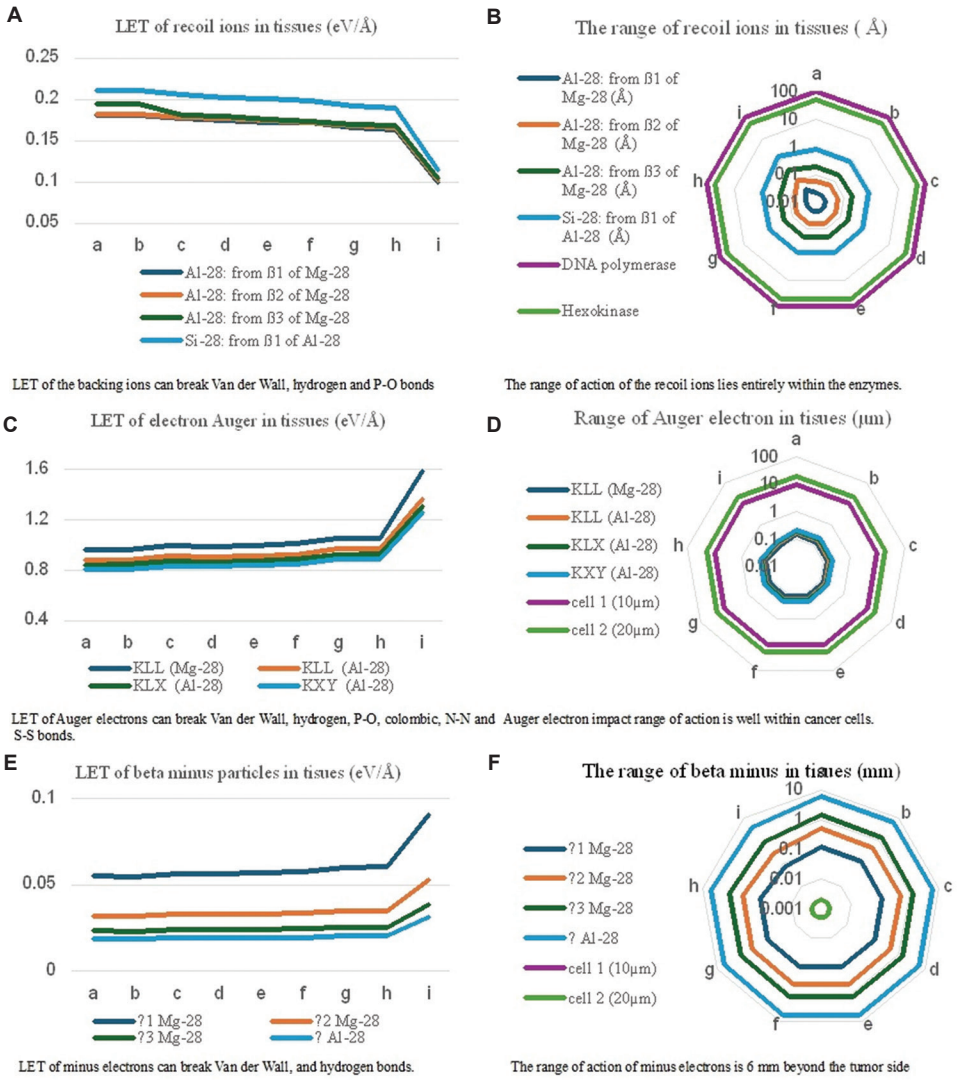

Figure 1. LET and range of different particles in biological tissues, derived from Table 2 and Table 3. (A and B) LET and range of recoil ions from Mg-28 and Al-28 decay. LET of the recoil ions can break Van der Wall, hydrogen, and P-O bonds, and their range of action lies entirely within the enzymes. (C and D) LET and range of Auger electrons from electron shell transitions (KLL, KLX, KXY). LET of Auger electrons can break Van der Wall, hydrogen, P-O, coulombic, N-N, and S-S bonds, and their impact range of action is well within cancer cells. (E and F) LET and range of beta-minus particles from different isotopes of Mg-28 and Al-28. LET of the electrons can break Van der Wall and hydrogen bonds, and their range of action is 6 mm beyond the tumor side. Labels (a-i) indicate different tissue types: (a) Water; (b) Soft tissue (ICRP); (c) brain; (d) Musculoskeletal (ICRP); (e) lung; (f) blood; (g) skin (ICRP); (h) M-E liquid, Sucrose; (i) Cortical bone (ICRP). Abbreviations: Al-28: Aluminium-28; ICRP: International Commission on Radiological Protection; KLL, KLX, KXY: Auger electron transitions between electron shells (K, L, X, Y); LET: Linear energy transfer; M-E: Mass-equivalent; Mg-28: Magnesium-28; P–O: Phosphorus-oxygen; S–S: Sulfur-sulfur.

Table 2. LET and range of Auger electrons, beta-minus particles, and recoil ions

Particle	LET (eV/Å)	Range
Auger electron	0.81–1.6	88–224 nm
Beta minus	0.002–0.09	0.07–6.11 mm
Recoil ion	0.1–0.21	0.022–1.5 Å

Notes: LET is expressed in eV/Å, equivalent to keV/µm using the conversion factor 1 keV/µm=0.1 eV/Å. Conversion constants: 1 keV=10^3 eV; 1 MeV=10^6 eV; 1 µm=10^3 nm=10^4Å.
Abbreviation: LET: Linear energy transfer.

0.1 eV/Å and 0.21 eV/Å and a very short range of 0.022–1.5 Å. The values in Table 3 indicate that Auger electrons possess the highest LET and medium range, enabling them to effectively break a variety of molecular bonds within tumor cells. Examples of such bonds include Van der Waals, hydrophobic, coulombic, P-O (ATP/ADP), N-N, and S-S bonds. Recoil ions, despite their limited range and relatively weaker overall effect, can effectively disrupt enzyme bonds due to their highly localized action at the molecular level, targeting coulombic, hydrophobic, and

Van der Waals bonds. In contrast, beta-minus particles, due to their long range and lowest LET, primarily affect hydrophobic and Van der Waals bonds and produce free radicals along their path. The therapeutic impact can thus be characterized by the focused molecular-level action of recoil ions, the intracellular effect of Auger electrons, and the extended influence of beta-minus particles up to 6mm beyond tumor margins. These distinctions are further illustrated in Figure 1.

3.3. Absorbed dose

Absorbed dose calculations by the MIRD code,[26] with 0.1 ng of Mg-28 administered intravenously over 21 h (Table 4), showed the potential for highly effective tumor cell killing with minimal impact on healthy tissues. Three regimens were modeled: (a) Whole-body cell dose, (b) Mg-uptake coefficient-based cell dose, and (c) direct tumor cell dose. In regimen (a), the doses ranged from

Table 3. Impact of linear energy transfer (LET) from magnesium-28 (Mg-28) decay on the dissociation of biological molecular bonds

Bond type	Length (Å)	Bond energy (kJ/mol)	Beta minus (kJ/mol)	Auger electron (kJ/mol)	Recoiled ions (kJ/mol)
Van der Waals	3.0–4.0	~ 2.4–4	7.08–34.84	311.81–612.41	38.12–81.08
Hydrogen bond	1.5–2.0	~4–40	3.54–17.42	155.91–306.21	19.06–40.54
P–O (in ATP/ADP)[28]*	~1.60	~30.5	2.83–13.94	124.72–244.96	15.25–32.43
Ionic	2.0–4.0	~20–200	7.08–34.84	311.81–612.41	38.12–81.08
N–N	~1.45	~163	2.57–12.63	112.88–222.00	13.82–29.39
S–S	2.05	~250	3.64–17.82	156.31–381.20	19.46–41.54

Notes: (1) *Bond energy released when ATP hydrolyzes to ADP; 1eV=96.485 kJ/mol. (2) Van der Waals interactions (3.0–4.0 Å) are weak but critical for stabilizing protein side chains and stacked DNA bases. Hydrogen bonds (1.5–2.0 Å) maintain DNA base pairing (A=T, G≡C) and play a key role in enzyme-substrate interactions. Ionic (Coulombic) interactions (2.0–4.0 Å) are prominent between oppositely charged side chains of proteins and in ATP–Mg^{2+}coordination complexes. Phosphodiester (P–O) bonds (~1.60 Å) form the DNA/RNA backbone and are targets for strand cleavage during radiation damage. Disulfide bridges (S–S) (~2.05 Å) stabilize the tertiary/quaternary structure of many enzymes, particularly in oxidative environments. Nitrogen–nitrogen (N–N) bonds (~1.45 Å) are present in some nucleotide base pairs and enzyme cofactors (e.g., flavins). The LET values from Mg-28 decay are sufficient to break all the above interactions, directly impairing nucleic acid integrity and enzymatic function essential to cellular integrity, especially in cancer cells.

Table 4. Absorbed dose to tumors across different regimens and the amount of magnesium-28 (Mg-28) required

Content	Regimen	Cancer type					
		T_0	T_1	T_2	T_3	T_4	T_5
Number of cells		3.28E+04	5.00E+06	5.00E+07	5.00E+08	5.00E+09	5.00E+11
Intravenous cell dose, uniformly distributed throughout the body (Gy)	a	1.01E-11	1.55E-09	1.55E-08	1.55E-07	1.55E-06	1.55E-04
Intravenous cell dose with Mg absorption coefficient (Gy)	b	1.83E-09	3.46E-06	1.09E-04	3.46E-03	1.09E-01	1.09E+02
Cell dose injected directly into the tumor (Gy)	c	3.04E+04	2.23E+02	2.23E+01	2.23E+00	2.23E-01	2.23E-02
Tumor dose (Gy)	a	3.31E-07	7.75E-03	7.75E-01	7.75E+01	7.75E+03	7.75E+07
	b	6.00E-05	11.15E+00	11.15E+03	11.15E+05	11.15E+08	11.15E+13
	c	9.97E+08	38.75E+08	38.75E+08	38.75E+08	38.75E+08	38.75E+09
	d	6.01E+01	6.01E+01	6.01E+01	6.01E+01	6.01E+01	6.01E+01
	e	3.12E+02	3.12E+02	3.12E+02	3.12E+02	3.12E+02	3.12E+02
	f	4.15E+02	4.15E+02	4.15E+02	4.15E+02	4.15E+02	4.15E+02
Whole-body absorbed dose (Gy)	d	3.52E-01	2.03E-02	8.91E-03	2.82E-03	8.91E-04	8.91E-05
	e	1.72E+00	9.81E-02	4.42E-02	1.44E-02	4.42E-03	4.42E-04
	f	2.33E+00	1.32E-01	5.92E-02	1.92E-02	5.92E-03	5.92E-04
Amount of Mg-28 required (ng)	d	9.31E-01	5.33E-02	2.42E-02	7.51E-03	2.44E-03	2.44E-04
	e	4.62E+00	2.63E-01	1.22E-01	3.71E-02	1.22E-02	1.22E-03
	f	6.21E+00	3.51E-01	1.63E-01	5.04E-02	1.63E-02	1.63E-03

Note: All absorbed dose calculations are based on a 21-h decay duration. Regimen (d) assumes 62 Mg-28 ions/cell, regimen (e) assumes 300 ions/cell, and regimen (f) assumes 400 ions/cell.

10^{-11} to 10^{-4} Gy for T_0–T_5 tumors (0.03 mg–500 g). For the same tumors, the doses increased from 10^{-9} to 10^{2} Gy in regimen (b) but decreased from 10^{4} to 10^{-2} Gy in regimen (c). These results indicate that applying the Mg-uptake coefficient significantly increases the cell dose compared to a uniform whole-body distribution.

Based on these results, we proposed three additional intravenous regimens: (d) 62, (e) 300, and (f) 400 Mg-28 ions/cell. These regimens were capable of targeting 20%, 100%, and 133% of the total 300 Mg-dependent enzymes, respectively. They achieved absorbed doses ranging from 60 to 415 Gy across T_0–T_5 tumors, with a total Mg-28 quantity of only 6.2 ng. Notably, the highest effective systemic absorbed dose among the regimens remained below 2.4 Gy, indicating a favorable safety profile. These results demonstrate that Mg-28 delivers sufficient absorbed doses to induce significant cytotoxicity in cancer cells across a wide range of tumor sizes, with minimal damage to surrounding healthy tissues and limited overall radioisotope exposure. These results are shown in Figure 2.

4. Discussion

4.1. Tumor growth, replication cycle, and Mg uptake

Cancer cell replication cycles are known to vary depending on tumor type and microenvironmental conditions. Our data, presented in Table 1, indicate a clear relationship between tumor size, the number of replication cycles, and the Mg-uptake coefficient. For instance, a microscopic tumor at stage T_0 (mass ~3.1×10^{-5} g, approximately 3.1×10^{4} cells) after 15 replication cycles exhibits an Mg-uptake coefficient of 1.8×10^{2}. As the tumor progresses through stages T_1–T_5, with increasing mass and number of replication cycles, the Mg-uptake coefficient demonstrates a significant upward trend, reaching 7.1×10^{5} for a large T_5 tumor (mass ~500 g, ~5.0×10^{11} cells) after 39 cycles, assuming a replication cycle ratio (k) of 2 between cancerous and healthy tissue.

This substantial increase in the Mg-uptake coefficient with tumor growth underscores the elevated Mg demand of rapidly proliferating cancer cells. As tumors expand, their metabolic and replicative requirements for Mg—a crucial cofactor for numerous enzymes involved in these processes—escalate. Consequently, Mg-28 is preferentially accumulated in larger and more aggressive tumors, making it an increasingly effective agent for targeted radiotherapy in advanced stages.

Furthermore, the relatively high Mg-uptake coefficient observed even in early-stage T_0 tumors suggests a promising avenue for early cancer detection, which will be discussed further in the subsequent section. The dependence of the Mg-uptake coefficient on the number of replication cycles and the k-factor highlights the importance of considering tumor growth dynamics in optimizing Mg-28-based treatment strategies. Tumors with faster replication rates (higher k values) are expected to exhibit even greater Mg-28 accumulation, potentially enhancing therapeutic efficacy and reducing the required dosage.

4.2. Early diagnosis and real-time monitoring

The exceptionally high Mg-uptake coefficient observed even in early-stage, microscopic tumors (T_0: 1.8×10^{2}, as shown in Table 1) provides a strong foundation for early cancer diagnosis. This preferential accumulation of Mg-28 in nascent tumors allows for robust imaging signals through gamma rays, Bremsstrahlung, and X-rays, enabling detection through positron emission tomography (PET) or single-photon emission computed tomography (SPECT) imaging. The ability to visualize tumors as small as ~3.1×10^{-5} g (approximately 31,000 cells) represents a significant advancement over many current diagnostic

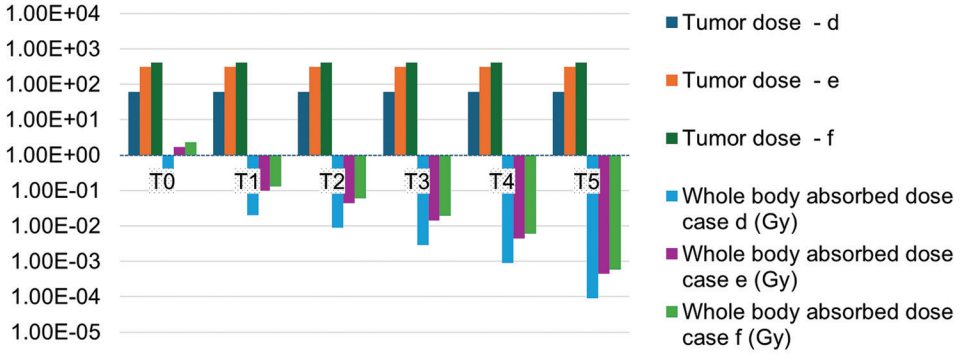

Figure 2. Comparison of absorbed radiation dose delivered to tumors and the whole body across different regimens. The tumor-specific and systemic absorbed dose are computed from Table 4. Regimens d, e, and f correspond to assumptions where 62, 300, and 400 magnesium-28 ions were taken up per cancer cell to inactivate magnesium-dependent enzymes. Tumor doses range between 60 Gy and 415 Gy, while whole-body doses are from 1.0×10^{-4} Gy to 2.4 Gy, indicating high therapeutic selectivity and patient safety.

modalities that may only detect larger tumor masses. Traditional methods usually diagnose cancer at the milligram scale using PET-computed tomography (CT) or SPECT-CT.[2,8,9]

Moreover, the continuous uptake of Mg-28 by tumor cells, sustained throughout the treatment period, facilitates real-time monitoring of therapeutic response. Changes in Mg-28 concentration within the tumor, as visualized through imaging, can provide immediate feedback on treatment efficacy, allowing for timely adjustments to the therapeutic regimen. This dual diagnostic and therapeutic (theranostic) functionality, achieved with a single isotope, simplifies the clinical workflow and eliminates the need for paired diagnostic and therapeutic agents, representing a key advantage of the Mg-28 method. Current methods often use two or more radioactive isotopes for diagnosis and treatment monitoring, such as Tc-99m + Y-90 or Tc-99m + Lu-177 with SPECT-CT, and F-18 + Y-90 or F-18 + Lu-177 with PET-CT.[2,8,9]

4.3. Enzyme inactivation and intracellular irradiation

Data from Table 2 reveal the LET and range of the particles emitted during Mg-28 decay. Auger electrons exhibit the highest LET (0.81–1.6 eV/Å), followed by recoil ions (0.1–0.21 eV/Å), while beta-minus particles have a lower LET (0.002–0.09 eV/Å) but a much longer range (0.07–6.11 mm).

The high LET of Auger electrons and recoil ions is particularly significant for enzyme inactivation and intracellular damage. As shown in Table 3, the energy deposited by these particles per unit length is sufficient to break various critical biological bonds, including the relatively strong covalent bonds, such as S-S (disulfide) and P-O (in ATP/ADP), as well as weaker non-covalent bonds, such as Van der Waals and hydrogen bonds that are crucial for maintaining the three-dimensional structure and function of enzymes and DNA. The recoil of Al-28 and Si-28 ions, although occurring over a very short range (0.022–1.5 Å), can directly disrupt the active sites of enzymes due to the momentum transfer and local structural distortion. These effects, together with the difference in charge and ionic radius from Mg^{2+} to Al^{3+} to Si^{4+}, will certainly inactivate Mg-dependent enzymes once Mg-28 replaces stable Mg in these enzymes. Specifically, the inactivation of DNA/RNA polymerases, helicase, topoisomerase, and DNA repair enzymes disrupts or arrests the S phase of the cell cycle, leading to apoptosis. Targeting telomerase prevents cancer cells from achieving immortality, thus limiting tumor growth and reducing the potential for invasion. Furthermore, the inactivation of matrix metalloproteinases (MMPs) impairs the ability of cancer cells to invade surrounding tissues and metastasize. By disrupting key metabolic enzymes, such as hexokinase, kinases, and ATPases, Mg-28 deprives cancer cells of essential energy, leading to metabolic collapse and necrosis.

Beta-minus particles, despite their lower LET, have a longer range that allows them to traverse larger cellular distances, generating free radicals along their path. These free radicals can indirectly damage DNA, proteins, and other cellular components, contributing to the overall cytotoxic effect of Mg-28. The combined action of direct bond breakage by high-LET particles and indirect damage by free radicals ensures a multifaceted attack on essential cellular machinery.

Targeted irradiation within the nucleus and mitochondria is achieved through the selective uptake of Mg-28, where crucial Mg-dependent enzymes, such as DNA/RNA polymerases, hexokinase, and telomerase reside. The subsequent decay of Mg-28 directly induces localized irradiation through beta particles, Auger electrons, and recoil ions, resulting in a concentrated release of damaging particles close to their molecular targets, thus maximizing enzyme inactivation and cellular destruction. Traditional inhibitors or modern methods[3-7] usually use one inhibitor for one specific enzyme or one biochemical agent for one determined molecular target.

4.4. Precision targeting and safety profile

The distinct ranges of the emitted particles from Mg-28 decay contribute to its precision targeting and favorable safety profile. The very short range of recoil ions (0.022–1.5 Å) ensures that their destructive energy is deposited within nanometer distances, primarily affecting the enzyme molecules in their immediate vicinity. Auger electrons, with a slightly longer range (88–224 nm), also deposit their energy within the subcellular compartments, causing localized damage to organelles, such as the nucleus and mitochondria.

In contrast, the longer range of beta-minus particles (up to 6.11 mm) might suggest the potential for off-target effects. However, the preferential uptake of Mg-28 by cancer cells, as indicated by the high Mg-uptake coefficient, concentrates the source of these beta particles within the tumor tissue. Furthermore, the energy deposition per unit length (LET) of beta-minus particles is lower compared to Auger electrons and recoil ions, meaning that while they can travel further, the density of ionization events along their path is less intense. This localized delivery of radiation, particularly the high-LET emissions within the tumor cells, minimizes the exposure of surrounding healthy tissues to significant radiation doses.

The absence of a need for bulky biochemical carriers or nanoparticles further enhances the precision and safety of Mg-28 therapy. As a naturally recognized ion, Mg-28 is efficiently transported into cancer cells, ensuring direct intracellular irradiation without the complexities and potential drawbacks of exogenous delivery systems. This intrinsic targeting mechanism contributes to the high local dose within the tumor while minimizing systemic toxicity.

4.5. High local dose with minimal systemic toxicity

Simulation results using the MIRD code (Table 4) demonstrate the potential of Mg-28 to deliver a high absorbed dose to tumors while maintaining minimal systemic toxicity. The calculations, performed over 21 h (approximately one half-life of Mg-28), considered different treatment regimens based on the number of Mg-28 ions internalized per cancer cell.

Assuming a regimen of 400 Mg-28 ions/cell (regimen f), a tumor absorbed dose of 415 Gy can be achieved across all tumor stages (T_0–T_5). This dose is significantly above the generally accepted therapeutic threshold of around 50 Gy required for effective tumor control. Notably, the total amount of Mg-28 needed to deliver this high local dose is remarkably small, with a maximum of only 6.2 ng required for even the largest T_5 tumors. This high efficacy at the nanogram scale underscores the potency and economic viability of the Mg-28 approach.

Conversely, the corresponding whole-body absorbed dose for the same regimen (regimen f) remains consistently low, with a maximum of 2.33 Gy observed for the smallest T_0 tumors, decreasing to the mGy range for larger tumors (e.g., 59.2 mGy for T_2 and 5.92 mGy for T_4). This significant disparity between the high local tumor dose and the low systemic exposure highlights the inherent safety advantage of Mg-28 therapy, minimizing potential damage to healthy organs and tissues.

The enhanced Mg uptake by cancer cells, driven by their elevated metabolic and replicative demands, further contributes to this favorable dose distribution. This biological preference ensures that Mg-28 is selectively concentrated within the tumor microenvironment, maximizing the therapeutic effect while sparing normal cells.

The data in Table 4 also illustrate the dose-response relationship with varying numbers of Mg-28 ions/cell (regimens d, e, and f). Even with lower intracellular concentrations of Mg-28 (62 and 300 ions/cell), therapeutically relevant tumor doses (60.1 Gy and 312 Gy, respectively) can be achieved with correspondingly lower systemic exposure and amounts of Mg-28 required. This flexibility in dosing regimens allows for tailored treatment strategies based on tumor characteristics and patient-specific factors.

4.6. Summary of key advantages

The Mg-28 therapy presents a transformative and biologically intelligent approach to cancer treatment, offering several key advantages that distinguish it from conventional modalities.

4.6.1. Dual mechanism of action for enhanced efficacy

By simultaneously targeting multiple critical Mg-dependent enzymes essential for cancer cell survival and proliferation (DNA/RNA polymerases, hexokinase, telomerase, and MMPs) and delivering highly localized intracellular irradiation through its decay products (beta particles, Auger electrons, and recoil ions), Mg-28 offers a synergistic therapeutic effect. This can overcome drug resistance and achieve comprehensive tumor control—a key advantage over single-target traditional inhibitors.

4.6.2. Intrinsic and highly selective tumor targeting

The therapy leverages the inherent metabolic vulnerability of cancer cells, characterized by their rapid proliferation and elevated demand for Mg. The quantified Mg-uptake coefficient demonstrates a significant preferential accumulation of Mg-28 within tumor tissues, eliminating the need for complex and potentially toxic biochemical carriers or nanoparticles. This natural targeting mechanism ensures a high concentration of the therapeutic agent directly within the tumor microenvironment.

4.6.3. Integrated self-theranostic capability

Mg-28 uniquely combines diagnostic and therapeutic functionalities within a single radioisotope, embodying a self-theranostic approach. Its gamma emissions allow for early tumor detection using PET or SPECT imaging—even at microscopic stages—while its continuous uptake facilitates real-time monitoring of treatment response, enabling personalized and adaptive therapeutic strategies without the need for additional agents.

4.6.4. Maximized local efficacy with minimized systemic toxicity

Simulation data indicate that Mg-28 can deliver cytotoxic radiation doses directly to tumor cells at the nanogram scale, while the absorbed dose to surrounding healthy tissues remains remarkably low. This favorable therapeutic index is attributed to the selective tumor uptake and the short-range, high-LET emissions of its decay products, which concentrate the destructive energy within the tumor volume.

4.6.5. Broad applicability and potential for expanded therapeutic horizons

The fundamental principle of exploiting the increased metabolic demands of rapidly dividing cells suggests that Mg-28 therapy holds promise across a wide spectrum of cancer types and stages. In addition, the concept of targeting host cell enzymes essential for pathogen replication opens avenues for exploring its utility in treating other diseases, such as viral infections—including coronaviruses that rely on host cell RNA polymerase for replication. Furthermore, this approach may be extended to other cofactors, such as copper, iron, manganese, zinc, and selenium.

5. Conclusion and future directions

The Mg-28 method represents a revolutionary and multifaceted approach to cancer therapy, characterized by its dual mechanism of action: The targeted inactivation of crucial Mg-dependent enzymes and highly localized intracellular irradiation.

The intrinsic selectivity of this approach is biologically elegant, driven by the elevated Mg demand of rapidly proliferating cancer cells. This phenomenon, quantified by the Mg-uptake coefficient, allows for natural tumor targeting without the need for complex biochemical carriers or nanoparticles—thereby enhancing both treatment precision and safety.

Preliminary analytical modeling and LET-dose simulations support the foundational hypothesis, demonstrating that nanogram-scale doses of Mg-28 can achieve therapeutic cytotoxic thresholds. Importantly, the behavior of Mg-28 within the tumor microenvironment embodies a form of natural biological targeting, where cancer cells, fueled by their metabolic and replicative demands, act as selective attractors for Mg^{2+}. This pathway allows Mg-28 to efficiently infiltrate intracellular compartments, particularly the nucleus and mitochondria, where it disrupts the enzymatic machinery critical for cancer progression.

Furthermore, the inherent gamma emissions of Mg-28 confer an integrated self-theranostic capability, enabling early tumor detection and real-time monitoring of treatment response, thus offering unparalleled precision in cancer management. Significantly, this approach holds promise for application across all cancer types and stages, a distinct advantage over many existing therapies. Beyond oncology, the principle of targeting host cell enzymes extends to infectious diseases. For instance, Mg-28 may disrupt the replication cycle of viruses—such as coronaviruses—by inactivating host RNA polymerase, thus offering a novel antiviral strategy. This innovative approach sets a strong foundation for future research and deserves in-depth exploration through pre-clinical (*in vitro* and *in vivo*) and clinical studies to evaluate its efficacy, pharmacokinetics, and biosafety. Ultimately, Mg-28 therapy could inform the development of a new paradigm in cancer and infectious disease treatment.

Despite its promising potential, several challenges must be addressed to translate Mg-28 therapy from theory to practice. The clinical safety and therapeutic efficacy require extensive, rigorous validation. In addition, Mg-28 production is costly and technically complex, and the clinical trials and regulatory approval processes demand significant logistical and financial investments. The short half-life of Mg-28 necessitates extremely rapid and efficient transportation and administration systems to ensure effective delivery.

To overcome these challenges and pave the way for clinical translation, the following strategic actions are recommended on duct: (1) Conduct *in vitro* and *in vivo* studies to validate the model; (2) establish cancer treatment centers near nuclear facilities; (3) invest in research and development of on-site Mg-28 production systems; and (4) design and implement prioritized transportation networks for timely delivery of Mg-28 to treatment centers.

Acknowledgments

The authors thank Dr. Vu Thien Y (Pharmaceutical Faculty, Ton Duc Thang University, Vietnam) for the valuable feedback provided during manuscript preparation.

Funding

None.

Conflict of Interest

The author declares no competing interests.

Author contributions

This is a single-authored article.

Ethics approval and consent to participate

Not applicable.

Consent for publication

Not applicable.

Availability of data

Data are available from the corresponding author upon reasonable request.

References

1. International Agency for Research on Cancer. *Latest Global Cancer Data: Cancer Burden Rises to 19.3 Million New Cases*

and 10.0 Million Deaths in 2020. Available from: https://www.iarc.who.int/news-events/latest-global-cancer-data-cancer-burden-rises-to-19-3-million-new-cases-and-10-0-million-cancer-deaths-in-2020 [Last accessed on 2025 May 21].

2. Baskar R, Lee KA, Yeo R, Yeoh KW. Cancer and radiation therapy: Current advances and future directions. *Int J Med Sci*. 2012;9:193-199.

   doi: 10.7150/ijms.3635

3. Fan D, Cao Y, Cao M, Wang Y, Cao Y, Gong T. Nanomedicine in cancer therapy. *Sig Transduct Target Ther*. 2023;8:293.

   doi: 10.1038/s41392-023-01536-y

4. Zahavi D, Weiner L. Monoclonal antibodies in cancer therapy. *Antibodies (Basel)*. 2020;9:34.

   doi: 10.3390/antib9030034

5. Kalmouni M, Al-Hosani S, Magzoub M. Cancer targeting peptides. *Cell Mol Life Sci*. 2019;76:2171-2183.

   doi: 10.1007/s00018-019-03061-0

6. Ratan ZA, Son YJ, Haidere MF, *et al*. CRISPR-Cas9: A promising genetic engineering approach in cancer research. *Ther Adv Med Oncol*. 2018;10.

   doi: 10.1177/1758834018755089

7. Sterner RC, Sterner RM. CAR-T cell therapy: Current limitations and potential strategies. *Blood Cancer J*. 2021;11:69.

   doi: 10.1038/s41408-021-00459-7

8. Lee S, Kim J. Advances in radioisotope applications for cancer diagnosis and treatment. *J Nucl Med*. 2019;60:345-357.

9. Krishnamurthy GT, Blahd WH. Radioiodine I-31 therapy in the management of thyroid cancer. A prospective study. *Cancer*. 1977;40:195-202.

   doi: 10.1002/1097-0142(197707)40:1<195::AID-CNCR2820400131>3.0.CO;2-C

10. Tran TVT, Rubino C, Allodji R, *et al*. Breast cancer risk among thyroid cancer survivors and the role of I-131 treatment. *Br J Cancer*. 2022;127:2118-2124.

    doi: 10.1038/s41416-022-01982-5

11. Castiglioni S, Farruggia G, Cappadone C. *Magnesium in Human Health and Disease*. MDPI Books; 2021. Available from: https://www.mdpi.com/books/pdfview/book/4389 [Last accessed on 2025 May 21].

12. Smith A, Jones B, Williams C. Utilization of magnesium-28 as a tracer in metabolic studies. *J Metab Res*. 2012;45:233-245.

13. Brown R, Green P, Taylor M. Tracking magnesium uptake and distribution using Mg-28. *BioMetals*. 2016;29:163-178.

14. Johnson L, Thompson D. Magnesium-28 in cellular metabolism: Insights and applications. *Metab J*. 2014;48:456-467.

15. Tran VL, Hoang T. Nuclear transformation in metalloenzyme: A novel and high potential cancer treatment research. *BioRxiv*. 2023.

    doi: 10.1101/2023.08.10.552823

16. Luyen VT. A proposal for a cancer treatment study involving radioactive metal co-factor enzymes. In: *Highlights on Medicine and Medical Science*. Vol. 15. West Bengal: BPI; 2021. p. 1-5.

    doi: 10.9734/bpi/hmms/v15/9276D

17. National Nuclear Data Center. *Mg-28 Beta Decay Data*. Available from: https://www.nndc.bnl.gov/ensnds/28/Mg/beta_decay.pdf [Last accessed on 2025 May 21].

18. Cowan JA. Structural and catalytic chemistry of magnesium-dependent enzymes. *Biometals*. 2002;15:225-235.

    doi: 10.1023/A:1016091118583

19. Hubscher U, Maga G, Villani G, Spadari S. *DNA Polymerases: Discovery, Characterization and Functions in Cellular DNA Transactions*. Singapore: World Scientific Publishing; 2010.

20. De Baaij JHF, Hoenderop JGJ, Bindels RJM. Magnesium in man: Implications for health and disease. *Physiol Rev*. 2015;95:1-46.

    doi: 10.1152/physrev.00012.2014

21. Rahm M, Hoffmann R, Ashcroft NW. Atomic and ionic radii of elements 1-96. *Chemistry*. 2016;22:14625-14632.

    doi: 10.1002/chem.201602949

22. Greenwood NN, Earnshaw A. *Chemistry of the Elements*. 2nd ed. Oxford: Butterworth-Heinemann; 1997.

23. Fenton E. *Silicon Biochemistry*. Hoboken, New Jersey: Wiley-Interscience; 2001.

24. National Institute of Standards and Technology. *E-STAR Program: Electron Stopping Power Data*. Available from: https://physics.nist.gov/PhysRefData/Star/Text/ESTAR.html [Last accessed on 2025 May 21].

25. National Nuclear Data Center. *Al-28 Beta Decay Data*. Available from: https://www.nndc.bnl.gov/ensnds/28/Al/beta_decay.pdf [Last accessed on 2025 May 21].

26. National Nuclear Data Center. *MIRD Program*. Available from: https://www.nndc.bnl.gov/nudat3/mird/ [Last accessed on 2025 May 21].

27. Sherr CJ. Cancer cell cycles. *Science*. 1996;274:1672-1677.

    doi: 10.1126/science.274.5293.1672

28. Nelson DL, Cox MM. *Lehninger Principles of Biochemistry*. 6th ed. United States: W. H. Freeman and Company.

ACCSCIENCE PUBLISHING

Tumor Discovery

SHORT COMMUNICATION

Sorafenib generates microvesicle particles in non-small cell lung cancer

Yevgeniy Gladkiy[1], Anita Thyagarajan[2]*, Morgann Hendrixson[1], and Ravi P. Sahu[1]*

[1]Boonshoft School of Medicine, Wright State University, Dayton, Ohio, United States of America

[2]Department of Pharmacology and Toxicology, Boonshoft School of Medicine, Wright State University, Dayton, Ohio, United States of America

(This article belongs to the *Special Issue: New Developments in Lung Cancer Research, Diagnosis, Treatment, and Prognosis*)

Abstract

Despite the improved clinical outcomes resulting from the use of sorafenib, the development of resistance mechanisms continues to undermine its treatment efficacy. Recent studies have implicated the role of a phospholipid mediator, platelet-activating factor receptor (PAFR) pathway, and extracellular vesicles known as microvesicle particles (MVP) in influencing cellular behavior and the efficacy of therapeutic agents. In this study, we determined the impact of the PAFR pathway and the acid sphingomyelinase (aSMase), which is required for the biogenesis of MVP, on sorafenib-induced effects on lung cancer growth and MVP release. Using A549 and H1299 non-small cell lung cancer (NSCLC) cell lines, we showed that sorafenib treatment reduced cell viability in a dose and time-dependent manner. Notably, sorafenib also enhanced MVP formation in both NSCLC cell lines. This MVP release was significantly attenuated by pharmacologic inhibition of the PAFR pathway through the WEB2086 compound and the aSMase inhibitor, imipramine, indicating the involvement of the PAFR and aSMase in sorafenib-induced MVP biogenesis. Moreover, co-treatment with imipramine enhanced the cytotoxic effects of sorafenib, suggesting that targeting MVP-associated pathways may improve sorafenib response. Collectively, these findings offer mechanistic insight into how sorafenib modulates MVP release and supports the therapeutic potential of combining tyrosine kinase inhibitors with agents that disrupt MVP biogenesis in NSCLC.

Keywords: Non-small cell lung cancer; Tyrosine kinase inhibitors; Sorafenib; Platelet-activating factor-receptor; Acid sphingomyelinase; Microvesicle particles

***Corresponding authors:**
Anita Thyagarajan (anita.thyagarajan@wright.edu)
Ravi P. Sahu (ravi.sahu@wright.edu)

Citation: Gladkiy Y, Thyagarajan A, Hendrixson M, Sahu RP. Sorafenib generates microvesicle particles in non-small cell lung cancer. *Tumor Discov*. 2025;4(3):81-91. doi: 10.36922/TD025110019

Received: March 11, 2025

Revised: April 30, 2025

Accepted: May 7, 2025

Published online: June 19, 2025

1. Introduction

Lung cancer is the leading cause of cancer-related mortality in the United States and worldwide.[1] It is estimated that 234,580 new cases and 125,070 deaths (~20% of all cancer-related deaths) are attributed to lung cancer.[2] Of the two subtypes, non-small cell lung cancer (NSCLC) accounts for about 80 – 85% of all lung cancer cases.[2] The management of NSCLC includes chemotherapy, immunotherapy, and targeted treatments

that have enhanced survival outcomes, particularly in patients with early-stage or resectable disease.[3] Notably, advances in immune checkpoint inhibitors and targeted therapies have provided tailored options based on tumor characteristics such as programmed cell death ligand 1 (PD-L1) expression and specific genetic mutations (*i.e.*, epidermal growth factor receptor [EGFR] and anaplastic lymphoma kinase) leading to better disease control and prolonged survival.[3] Despite these advances, emergence of resistance mechanisms remains a significant challenge, which includes on-target mutations, bypass pathways, and histological transformation.[3]

Among targeted therapies, tyrosine kinase inhibitors (TKIs), including sorafenib, have been used to treat NSCLC.[3,4] Sorafenib, a multikinase inhibitor, has emerged as a promising agent targeting multiple pathways involved in tumor progression, angiogenesis, and resistance mechanisms.[4] Notably, reactive oxygen species (ROS) generation is one of the key mechanisms through which TKIs induce cytotoxic effects; however, elevated ROS levels activate resistance mechanisms enabling the tumor to evade therapy and continue to grow.[5] For example, oxidative modifications of EGFR and associated downstream signaling pathways enhance tumor progression and resistance to EGFR TKIs.[6] These findings highlight the paradoxical nature of ROS in NSCLC therapy. While ROS generation is critical for the effectiveness of TKIs, the adaptive responses of NSCLC cells to oxidative stress underscore the need for combination strategies that both amplify ROS cytotoxicity and inhibit resistance pathways to improve therapeutic outcomes. Among these signaling pathways, ROS non-enzymatically cleaves lipid membranes to produce oxidized glycerophosphocholines (Ox-GPCs) that exhibit platelet-activating factor (PAF) agonistic properties, which mediate angiogenesis, tumor growth, metastasis, and immune modulation.[7-10] In addition, PAF-like molecules are often upregulated in response to radiation and chemotherapy, exacerbating immune suppression and therapy resistance.[10-13] Our group has shown that in NSCLC models, both tumor and its environment are modulated by PAF and platelet-activating factor-receptor (PAFR) signaling.[9,14,15] Moreover, PAFR plays a significant role in vesicular formation and is dependent on pathways such as mitogen-activated protein kinase (MAPK), nuclear factor kappa B (NF-κB), and acid sphingomyelinase (aSMase).[16-19] Notably, formed vesicles have been shown to contain PAF-like agonists and serve as bioactive molecules.[18-22]

Mounting evidence points to these large extracellular vesicles, also referred to as microvesicle particles (MVP), as critical mediators of treatment resistance, including NSCLC.[23-26] By sequestering and exporting oncogenic proteins, nucleic acids, and even chemotherapeutic agents, MVP can diminish drug accumulations in tumor cells and modulate the surrounding microenvironment to favor cancer progression.[23,24] It has been demonstrated that PAF and related lipid mediators can be packaged within MVP, enabling inflammatory and immune-modulating responses that further compromise treatment efficacy.[18,20-22] These findings underscore that in addition to targeting primary oncogenic pathways, strategies that disrupt MVP release may aid in overcoming drug resistance.

Imipramine, a tricyclic antidepressant, has garnered attention as an effective aSMase inhibitor that disrupts ceramide biosynthesis, a key lipid mediator in MVP formation and NSCLC pathophysiology.[27-32] By reducing ceramide production, imipramine decreases the budding of vesicles, thus curtailing MVP release.[27,33] Therefore, imipramine and other sphingolipid-targeted drugs have been of interest as adjunct therapies.[27,34-37] For example, studies by Irep *et al.*,[32] have demonstrated enhanced inhibitory effects on cisplatin/etoposide by targeting small extracellular vesicles (also referred to as exosomes) synthesis and trafficking in a small cell lung cancer model. In NSCLC, sorafenib's efficacy has also been shown to significantly improve with dual-therapy approaches.[4,38-40] However, no approach to aSMase inhibition, such as with imipramine, has been investigated.

2. Materials and methods

2.1. Reagents

Culture media was obtained from GE Healthcare Biosciences (Marlborough, MA, USA), with fetal bovine serum (FBS) from Corning (Corning, NY, USA). Penicillin-streptomycin was acquired from Hyclone (Logan, UT, USA) and antibiotic-antimycotic solution was purchased from Gibco (Gaithersburg, MD, USA). The PAFR agonist carbamoyl-PAF (CPAF), the antagonist WEB2086, and the aSMase inhibitor imipramine were all obtained from Cayman Chemicals Co. (Ann Arbor, MI, USA). Sorafenib tosylate was procured from Millipore Sigma (St. Louis, MO, USA). All other reagents were purchased from Sigma-Aldrich (St. Louis, MO, USA).

2.2. Cell lines

Human NSCLC lines, A549 and H1299, were used for all experiments as both express PAFR at similar levels.[14] These cell lines were a kind gift from Dr. Weiwen Long (Department of Biochemistry and Molecular Biology at Wright State University). A549 cells were maintained in F-12K medium supplemented with 10% FBS, 2.5 mL penicillin-streptomycin, 2.5 mL antibiotic-antimycotic,

and 15 μL of 2 M magnesium chloride. H1299 cells were grown in RPMI-1640 medium containing 10% FBS, 2.5 mL penicillin-streptomycin, 2.5 mL antibiotic-antimycotic, 2.25 mL of 40% glucose, and 5 mL of 100 mM sodium pyruvate. All cell cultures were maintained at 37°C with 95% humidity and 5% CO_2.

2.3. Cell survival assay

As per our previous reports, sulforhodamine-B (SRB) assay was used to assess cell survival.[14,15] H1299 and A549 cells were plated into 96-well plates at a seeding density of 5×10^3 cells per well and treated with 0.1% dimethyl sulfoxide (DMSO) as control, or with sorafenib at concentrations ranging from 1 to 16 μM. In separate experiments, sorafenib was used at a concentration of 4 μM, imipramine at 20 μM, and their co-treatment at given concentrations. After 24, 48, and 72 h, cells were fixed with 100 μL of 10% trichloroacetic acid followed by incubation at 4°C for 1 h. Fixed cells were gently rinsed with distilled water three times and stained using 100 μL 0.4% (w/v) SRB (prepared in 1% acetic acid), followed by 15-min incubation at room temperature in the dark. Excess dye was removed by triple rinsing with distilled water containing 1% glacial acetic acid and then allowed to air dry. Bound SRB dye was solubilized using 150 μL of 10 mM Tris base (tris(hydroxymethyl) aminomethane) while placing the plates on a shaker for 10 min. Absorbance was measured at 570 nm using a Synergy H1Mf plate reader. Cell viability for each group was normalized to its respective vehicle-treated control (0.1% DMSO).

2.4. MVP isolation and quantification

Isolation and quantification of MVP were performed using methods previously described by our group.[14,18,19] Briefly, A549 and H1299 cells were grown to approximately 80–90% confluency, after which cultures were rinsed three times with serum-free Hanks' Balanced Salt Solution (HBSS, Cytiva, USA). Cells were then incubated with 0.1% DMSO for negative control, or 100 nM CPAF and phorbol myristate acetate (PMA) for positive controls, and sorafenib at various concentrations (4, 8, and 16 μM) in HBSS containing 1% free fatty acid. Similarly, combination experiments used pre-treatments with the PAFR antagonist, WEB2086 (10 μM), and imipramine (20 μM) for 1 h, followed by treatment with or without sorafenib (8 μM). After 4 h of incubation, the conditioned medium was centrifuged at 2,000 ×*g* for 20 min at 4°C to remove residual cells and debris. The clarified supernatant was centrifuged at 20,000 ×*g* for 70 min at 4°C to pellet MVP. Pellets were then resuspended with 100 μL of sterile-filtered phosphate-buffered saline (PBS) to prepare for nanoparticle tracking analysis. MVP concentration was assessed using the NanoSight NS300 instrument (Malvern Instruments, UK). MVP counts were normalized with the cell number as per previous reports.[14,18,19]

2.5. Statistical analysis

All statistical analyses were conducted using GraphPad Prism software version 10 (GraphPad Software, San Diego, CA, USA). Each *in vitro* experiment was performed independently at least three times using biological replicates. Data were analyzed by unpaired Student's *t*-test or one-way analysis of variance (ANOVA) with *post hoc* Dunnet's multiple comparison tests. The $p<0.05$ was considered statistically significant.

3. Results

3.1. Sorafenib inhibits the survival of NSCLC cell lines in a time- and dose-dependent manner

Our first studies tested the dose- and time-response effects of sorafenib treatment on the survival of A549 and H1299 NSCLC cell lines through the SRB assay. These cell lines have been widely used as NSCLC models to determine the mechanisms and cellular responses of sorafenib alone or its combination with other agents.[39,41-44] It was observed that the survival of A549 and H1299 cell lines was inhibited by sorafenib in a dose- and time-dependent manner (Figure 1A and B).

Interestingly, despite both A549 and H1299 cells lacking EGFR mutations and being inherently resistant to EGFR-TKIs,[45] A549 cells demonstrated greater sensitivity to sorafenib compared to H1299 cells. This observation is consistent with previous report showing that A549 cells, which harbor a *KRAS* G12S mutation, are more susceptible to sorafenib's effects, likely due to its inhibition of RAF-dependent signaling.[46] Given that sorafenib also targets vascular endothelial growth factor receptor (VEGFR) and platelet-derived growth factor receptor (PDGFR), its anti-proliferative effect on A549 cells may also involve angiogenic signaling pathways.[47]

Despite being p53-null and KRAS wild-type, H1299 cells also exhibited a significant reduction in cell viability with sorafenib treatment. However, the degree of inhibition was lower than in A549 cells at comparable doses. This suggests that sorafenib's mechanism of action may be more effective in KRAS-mutant NSCLC models, aligning with findings from previous studies utilizing A549 and PC-9 cells.[38]

3.2. PAFR and aSMase pathways mediate sorafenib-induced MVP release

Given that exposure to EGFR-TKIs induces MVP release,[14] which have been shown to carry PAF agonists and serve

as mediator of PAFR-induced effect,[18,19] our next studies evaluated if sorafenib treatment can induce MVP release. Furthermore, as MVP release is an earlier event, which significantly peaks at 4 – 8 h time points,[14] and could impact tumor cell behavior in responses to therapeutic agents, we tested three different doses (4, 8, and 16 μM) of sorafenib from the cell viability assay shown in Figure 1A and 1B, that resulted in differential cytotoxic response. To that end, A549 and H1299 cell lines were separately treated with vehicle (0.1% DMSO) as a negative control, CPAF (a known PAFR agonist, 100 nM) and PMA (PAFR-independent agonist, 100 nM) as positive controls, and various doses of sorafenib. After 4 h, we extracted and analyzed MVP as per our published reports.[14,18,19] The data demonstrated that sorafenib induces MVP release from both cell lines in a dose-dependent manner as compared to vehicle control (Figure 2A and B). In addition, we found that sorafenib-mediated MVP release was comparable to CPAF and PMA treatments (Figure 2A and B).

As PAFR activation mediates MVP release, and the aSMase is a key mediator of MVP biogenesis,[14] our next studies determined the underlying mechanisms, particularly, the roles of the PAFR signaling and an aSMase using the optimal dose (8 μM) of sorafenib. To that end, A549 and H1299 cell lines were pre-treated with a well-known PAFR antagonist, WEB2086 (10 μM),[14] or an aSMase inhibitor, imipramine (20 μM),[14] followed by the treatments with or without CPAF, PMA, or sorafenib. After 4 h, we extracted and analyzed MVP. Our studies demonstrated that the WEB2086 compound

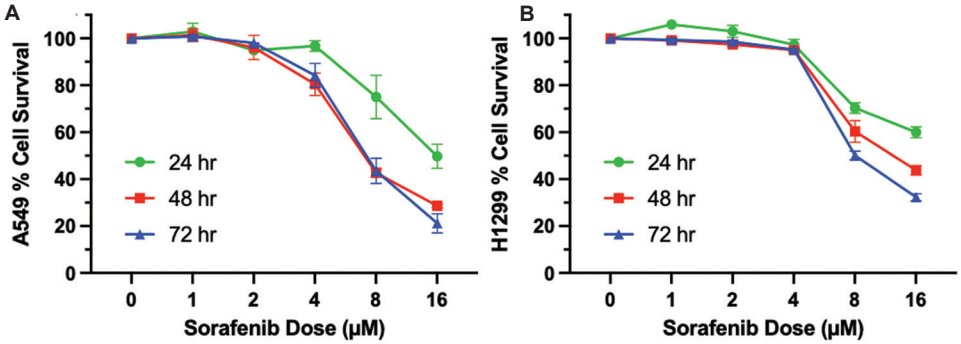

Figure 1. Effects of sorafenib on cell survival. (A) Dose response curve of sorafenib effect on A549 cells. (B) Dose response curve of sorafenib effect on H1299 cell lines. Data are presented as mean ± scanning electron microscope of four independent biological replicates.

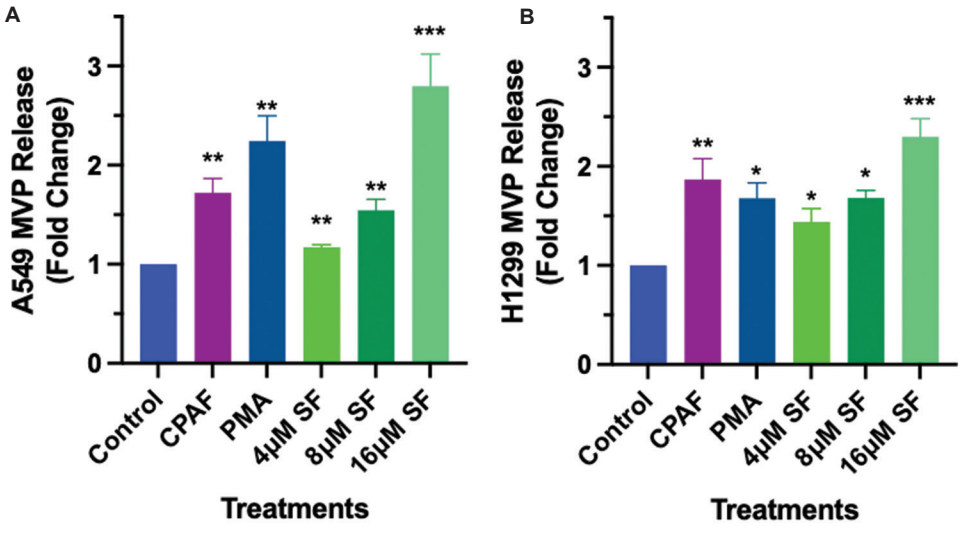

Figure 2. Dose-response effect of sorafenib treatment on MVP release. A549 (A) and H1299 (B) cell lines were treated with vehicle (0.1% DMSO), CPAF (100 nM), PMA (100 nM), and various doses of sorafenib. After 4 h of incubation, MVP extraction and analyses were performed. Data are presented as mean ± scanning electron microscope of three independent biological replicates, normalized per 1×10^6 cells. Statistically significant differences were observed between control and other groups.

Notes: *p<0.05, **p<0.01, ***p<0.001.

Abbreviations: CPAF: Carbamoyl-platelet-activating factor; MVP: Microvesicle particle; PMA: Phorbol myristate acetate; SF: Sorafenib.

significantly blocked CPAF and sorafenib-induced, but not PMA-induced MVP release in both the cell lines (Figure 3A and B), indicating the involvement of the PAFR signaling in MVP release. On the other hand, imipramine significantly blocked CPAF-, PMA-, and sorafenib-induced MVP release, indicating that involvement of an aSMase in MVP release (Figure 3A and B). These data also indicate that regardless of the nature of the stimuli used, inhibiting aSMase blocks MVP release. These data are consistent with our previous findings,[14,18,19] demonstrating that other ROS-generating stimuli induce MVP release in a PAFR and aSMase-dependent manner.

3.3. Imipramine enhances the antiproliferative effect of sorafenib

Given that aSMase inhibitors block MVP release and have been evaluated in cancer patients,[34,48] the next studies tested if blocking aSMase could increase the efficacy of sorafenib. To evaluate the synergy of an aSMase inhibitor on sorafenib-mediated growth inhibition in NSCLC cells, A549 and H1299 cells were pre-treated with imipramine (20 μM for 1 h),[14] followed by treatment with or without sorafenib at a lower concentration (4 μM), consistent with prior studies utilizing lower micromolar concentrations of sorafenib in combination strategies.[41,49] The cell survival was assessed using the SRB assay at 24- and 48-h time points. As shown in Figure 4A-D, imipramine enhanced the cytotoxic effect of sorafenib resulting in a significant reduction in cell viability compared to sorafenib monotherapy. We also noticed a modest but significant inhibition of cell viability by imipramine alone at the 48-h time point (Figure 4B and D), indicating a chemopreventive ability of this repurposed drug, providing a rationale for it to be explored in combination with other therapeutic agents.

Taken together, these results suggest that imipramine enhances the antiproliferative effects of sorafenib, through its ability to inhibit aSMase-mediated pathways, thereby reducing ceramide production and MVP release, as shown in Figure 5. These findings highlight the potential implication of imipramine to enhance the efficacy of sorafenib in NSCLC.

4. Discussion

As NSCLC continues to pose challenges,[1-3] sorafenib, a multikinase inhibitor, has demonstrated variable antitumor effects in NSCLC models by targeting multiple signaling pathways, including those associated with angiogenesis and ROS generation.[3,4] Although ROS can mediate cytotoxicity in tumors, elevated levels of ROS may paradoxically enhance survival and promote resistance through compensatory pathways.[5,6] Consequently, combination approaches that both exploit sorafenib's cytotoxic potential and suppress parallel pro-survival pathway have garnered significant attention in efforts to improve NSCLC outcomes.[26]

A growing body of evidence implicates MVP as a mediator of therapy resistance, tumor progression, and immune evasion in multiple cancer models, including NSCLC.[23,25] By encapsulating pro-survival factors,

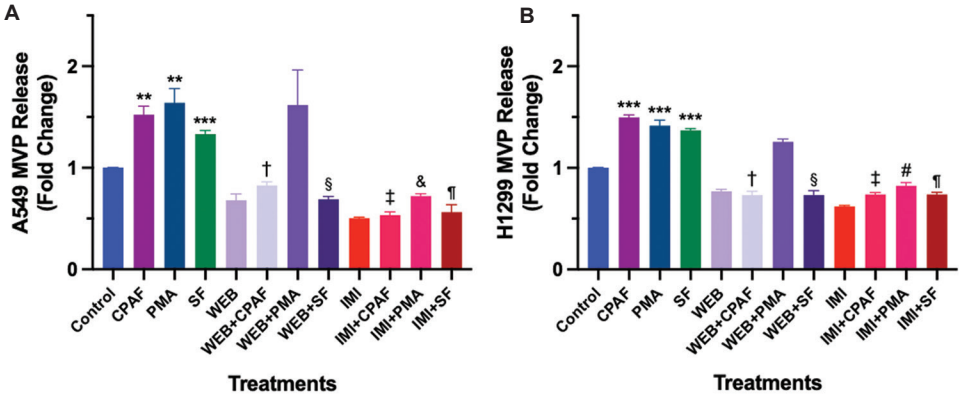

Figure 3. Effects of PAFR antagonist and aSMase inhibitor on sorafenib-induced MVP release. A549 (A) and H1299 (B) cells were pre-treated with WEB2086 (a PAFR antagonist, 10 μM, 1 h) or imipramine (an aSMase inhibitor, 20 μM, 1 h) followed by the treatments with or without CPAF (100 nM), PMA (100 nM), or sorafenib (8 μM). These cell lines were also treated with vehicle (0.1% DMSO), WEB2086 (10 μM) and imipramine (20 μM) alone. After 4 h of incubation, MVP were isolated and analyzed. Data are presented as mean ± scanning electron microscope of three independent biological replicates, normalized per 1×10^6 cells. The statistically significant differences were observed between control and CPAF, PMA, and sorafenib alone groups; CPAF and WEB+CPAF; SF and WEB+SF; CPAF and IMI+CPAF; PMA and IMI + PMA; and SF and IMI + SF.
Notes: $^{**}p<0.01$, $^{***}p<0.001$ compared with control; $^{\dagger}p<0.001$ compared with CPAF; $^{\S}p<0.001$ compared with SF; $^{\ddagger}p<0.001$ compared with CPAF; $^{\&}p<0.05$ compared with PMA; $^{\#}p<0.001$ compared with PMA; $^{\P}p<0.001$ compared with SF.
Abbreviations: aSMase: Acid sphingomyelinase; CPAF: Carbamoyl-platelet-activating factor; IMI: Imipramine; MVP: Microvesicle particles; PAFR: Platelet-activating factor-receptor; PMA: Phorbol myristate acetate; SF: Sorafenib; WEB: WEB2086.

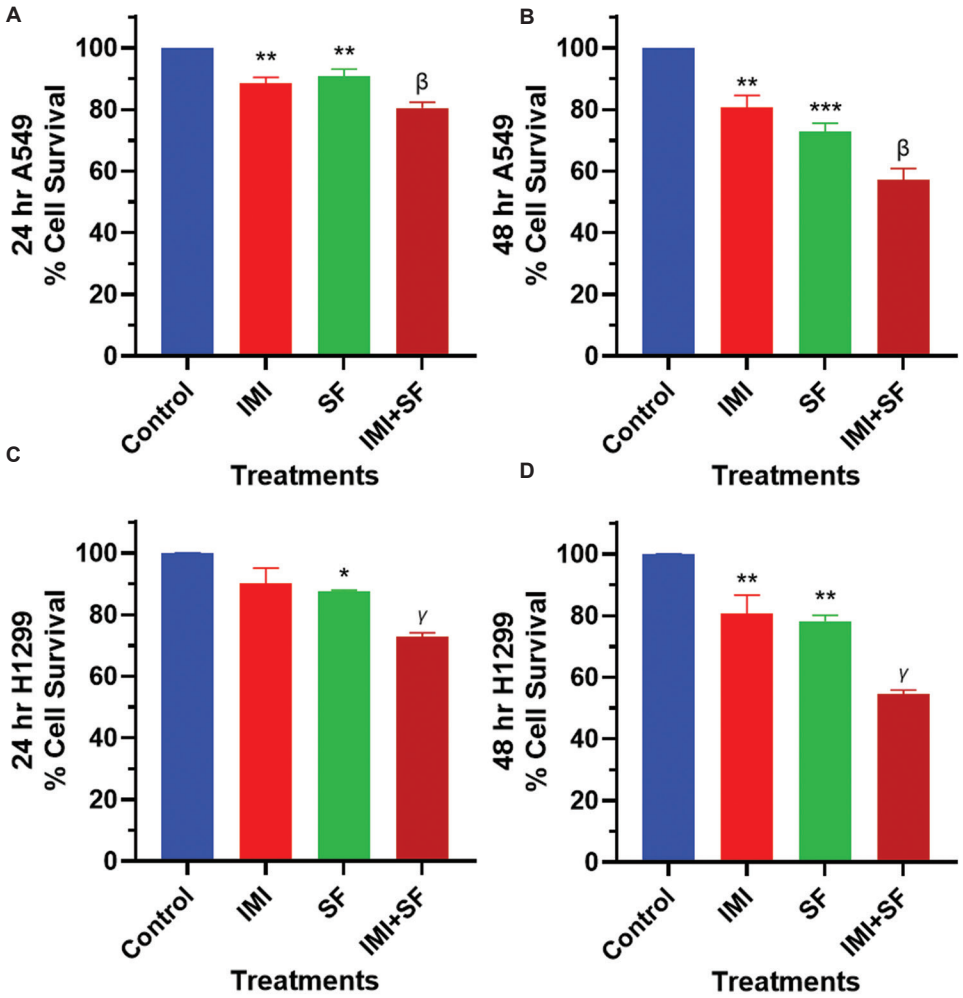

Figure 4. Effect of an aSMase inhibitor on sorafenib cytotoxicity. A549 cells (A, B) and H1299 cells (C, D) were pre-treated with imipramine (an aSMase inhibitor, 20 μM for 1 h) followed by treatment with or without sorafenib (4 μM). After 24 and 48 h, cell viability was assessed through sulforhodamine-B assay. Data are presented as mean ± scanning electron microscope of three independent biological replicates. Statistically significant differences were observed between control and imipramine or sorafenib alone, as well as sorafenib and sorafenib with imipramine co-treatment.
Notes: $^{**}p<0.01$, $^{***}p<0.001$ compared with control; $^{\beta}p<0.05$ compared with SF; $^{\gamma}p<0.001$ compared with SF.
Abbreviations: aSMase: Acid sphingomyelinase; IMI: Imipramine; SF: Sorafenib.

oncogenic proteins, or even chemotherapeutic agents, MVP can attenuate the intracellular accumulation of drugs and facilitate communications within the tumor microenvironment that favor cancer cell survival.[23,24] Our findings indicate that sorafenib treatment increases MVP release in NSCLC cell lines, aligning with prior work demonstrating that other anticancer agents also elevate MVP shedding.[14,19] This phenomenon may represent an adaptive mechanism by which cancer cells reduce intracellular drug toxicity and exchange signals conducive to tumor growth.

Notably, PAFR signaling and aSMase activity both emerged as critical players in mediating MVP generation. In line with previous reports, PAFR activation appears to drive MVP release across various cancers, including NSCLC.[9,14,18] Similarly, aSMase catalyzes the hydrolysis of sphingomyelin to ceramide, a lipid known to promote membrane budding and MVP formation.[27,28,33] Our data confirm that pharmacological blockade of PAFR (via WEB2086) or inhibition of aSMase (via imipramine) substantially diminishes sorafenib-induced MVP release in NSCLC cell lines. These results underscore a therapeutic opportunity, indicating that targeting the MVP production pathways may enhance the efficacy of established anticancer drugs by reducing the vesicular export of survival signals and other resistance factors.

Importantly, imipramine, a tricyclic antidepressant, has garnered attention for its potent aSMase-inhibiting

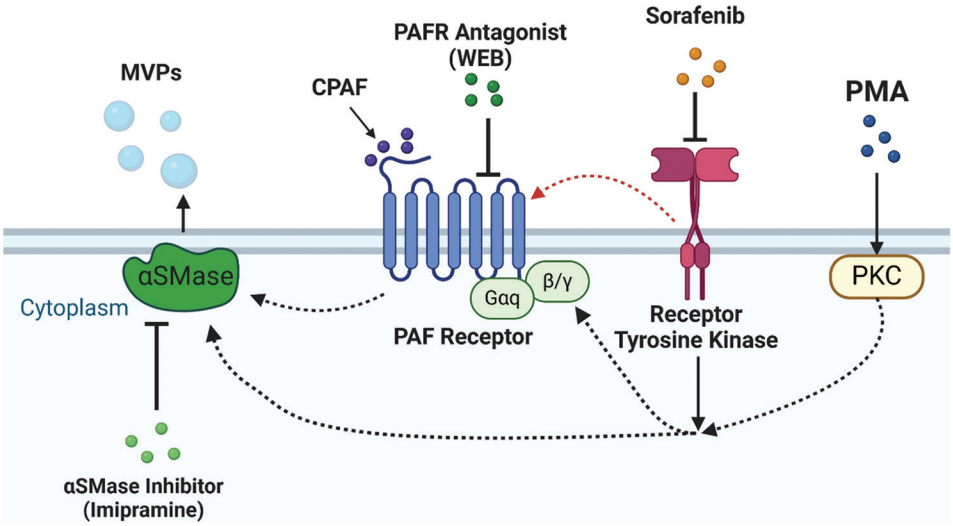

Figure 5. Schematic representation of PAFR and aSMase-dependent MVP release. Created in BioRender. Gladkiy, Y. (2025) https://BioRender.com/a16u165.
Abbreviations: aSMase: Acid sphingomyelinase; CPAF: Carbamoyl-platelet-activating factor; MVP: Microvesicle particles; PAFR: Platelet-activating factor-receptor; PKC: Protein kinase C; PMA: Phorbol myristate acetate; WEB: WEB2086.

properties, restricting ceramide-dependent MVP biogenesis.[27] In our experiments, co-treatment with imipramine significantly attenuated MVP generation triggered by sorafenib, reinforcing the concept that MVP blockade might resensitize tumor cells to therapy. As PAFR-mediated MVP release is dependent on pathways, such as MAPK and NF-κB, which crosstalk with aSMase, and sorafenib targets MAPK and NF-κB pathways,[16-19,50] we anticipate that these downstream signaling cascades could be involved in mediating sorafenib-induced MVP release. Notably, imipramine also enhanced the antiproliferative effect of sorafenib on both A549 and H1299 cell lines, echoing prior studies in other lung cancer models where combined extracellular vesicle inhibition and chemotherapy improved therapeutic outcomes.[32] Given that MVPs contain PAF-like agonists and serve as bioactive molecules,[18-22] these findings point to a potential synergy wherein sorafenib disrupts key oncogenic pathways, while imipramine obstructs MVP-mediated drug efflux and paracrine signaling. Such a combination strategy may thus counteract adaptive resistance more effectively than either agent alone.

Sorafenib has previously been shown to exhibit synergistic or additive effects when combined with other agents, including gemcitabine, pemetrexed, and erlotinib.[38-40,51,52] In each case, multi-target inhibition or blockade of complementary pathways amplified the overall antitumor response. Our data on the sorafenib–imipramine partnership extend this notion by focusing on MVP-mediated resistance, highlighting a novel mechanism that can be exploited to improve therapeutic outcomes (Figure 5). Although further *in vivo* investigation is warranted, these findings contribute to the broader literature advocating for rationally designed combination regimens in NSCLC.

Despite these promising insights, several limitations must be addressed. First, our work is primarily based on *in vitro* models using A549 and H1299 cell lines, which do not fully represent the complexities of human tumors. Second, the specific downstream signaling events by which sorafenib-induced MVP promotes resistance remain to be fully characterized. Third, while imipramine has demonstrated its efficacy as an aSMase inhibitor, its clinical repurposing requires careful consideration of known dose-dependent toxicities, including anticholinergic side effects.[27,53] Further research may benefit from evaluating more selective aSMase inhibitors and novel drug delivery systems to improve safety profiles and efficacy.[34] Finally, the optimal dosing, timing, and safety profile for combining imipramine with sorafenib have yet to be delineated, highlighting the need for rigorous *in vivo* studies and ultimately, clinical trials. Identifying patients most likely to benefit from such a combination – potentially through biomarkers such as high basal MVP release or elevated aSMase expression – also represents an important area for future research.[54,55]

5. Conclusion

Overall, our findings underscore the importance of targeting MVP production to overcome adaptive resistance

in NSCLC. By combining sorafenib with imipramine, our studies demonstrated successfully reduced MVP release and enhanced sorafenib's cytotoxic activity in NSCLC cells. These observations build on accumulating evidence that MVP-focused interventions can potentiate the efficacy of conventional and targeted therapies. Going forward, additional *in vivo* validation and clinical exploration are warranted to determine whether this dual-targeting strategy can translate into improved outcomes for patients with NSCLC.

Acknowledgments

None.

Funding

The financial support from the BSOM Medical Student Research Grant (Y.G. and M.H. with A.T. and R.P.S. as mentors) and the NIH R21 grant ES033806 (R.P.S.) are greatly appreciated.

Conflict of interest

Ravi P. Sahu is an Editorial Board Member of this journal, but was not in any way involved in the editorial and peer-review process conducted for this paper, directly or indirectly. Separately, other authors declared that they have no known competing financial interests or personal relationships that could have influenced the work reported in this paper.

Author contributions

Conceptualization: Anita Thyagarajan, Ravi P. Sahu
Data curation: Yevgeniy Gladkiy, Anita Thyagarajan
Formal analysis: Yevgeniy Gladkiy
Investigation: Yevgeniy Gladkiy, Anita Thyagarajan
Methodology: Yevgeniy Gladkiy, Anita Thyagarajan, Ravi P. Sahu
Supervision: Anita Thyagarajan, Ravi P. Sahu
Writing – original draft: Yevgeniy Gladkiy
Writing – review & editing: All authors

Ethics approval and consent to participate

Not applicable.

Consent for publication

Not applicable.

Availability of data

All datasets generated for this study are available from the corresponding authors on reasonable request.

Further disclosure

Part of the findings have been presented in the Ohio Valley Chapter of the Society of Toxicology Annual Meeting, West Lafayette, Indiana, USA (2023); Annual Boonshoft School of Medicine Research Symposium, Dayton, Ohio, USA (2023); and 16th Annual Meeting of the Korean Society of Medical Oncology, Seoul, Korea (2023).

References

1. Bray F, Laversanne M, Sung H, *et al.* Global cancer statistics 2022: GLOBOCAN estimates of incidence and mortality worldwide for 36 cancers in 185 countries. *CA Cancer J Clin.* 2024;74(3):229-263.
   doi: 10.3322/caac.21834
2. Society AC. *Lung Cancer; 2024.* Available from: https://www.cancer.org/cancer/types/lung-cancer.html [Last accessed on 2024 Dec 18].
3. Hendriks LEL, Remon J, Faivre-Finn C, *et al.* Non-small-cell lung cancer. *Nat Rev Dis Primers.* 2024;10(1):71.
   doi: 10.1038/s41572-024-00551-9
4. Hendrixson M, Gladkiy Y, Thyagarajan A, Sahu RP. Efficacy of sorafenib-based therapies for non-small cell lung cancer. *Med Sci (Basel).* 2024;12(2):20.
   doi: 10.3390/medsci12020020
5. Lin W, Wang X, Diao M, *et al.* Promoting reactive oxygen species accumulation to overcome tyrosine kinase inhibitor resistance in cancer. *Cancer Cell Int.* 2024;24(1):239.
   doi: 10.1186/s12935-024-03418-x
6. Weng MS, Chang JH, Hung WY, Yang YC, Chien MH. The interplay of reactive oxygen species and the epidermal growth factor receptor in tumor progression and drug resistance. *J Exp Clin Cancer Res.* 2018;37(1):61.
   doi: 10.1186/s13046-018-0728-0
7. Tsoupras A, Adamantidi T, Finos MA, *et al.* Re-assessing the role of platelet activating factor and its inflammatory signaling and inhibitors in cancer and anti-cancer strategies. *Front Biosci (Landmark Ed).* 2024;29(10):345.
   doi: 10.31083/j.fbl2910345
8. Haak VM, Huang S, Panigrahy D. Debris-stimulated tumor growth: A pandora's box? *Cancer Metastasis Rev.* 2021;40(3):791-801.
   doi: 10.1007/s10555-021-09998-8
9. Hackler PC, Reuss S, Konger RL, Travers JB, Sahu RP. Systemic platelet-activating factor receptor activation augments experimental lung tumor growth and metastasis. *Cancer Growth Metastasis.* 2014;7:27-32.
   doi: 10.4137/cgm.S14501

10. Sahu RP, Konger RL, Travers JB. Platelet-activating factor-receptor and tumor immunity. *JSM Cell Dev Biol.* 2014;2(1):1008.

doi: 10.47739/2379-061X/1008

11. Sahu RP, Harrison KA, Weyerbacher J, *et al.* Radiation therapy generates platelet-activating factor agonists. *Oncotarget.* 2016;7(15):20788-20800.

doi: 10.18632/oncotarget.7878

12. Sahu RP, Turner MJ, DaSilva SC, *et al.* The environmental stressor ultraviolet B radiation inhibits murine antitumor immunity through its ability to generate platelet-activating factor agonists. *Carcinogenesis.* 2012;33(7):1360-1367.

doi: 10.1093/carcin/bgs152

13. Sahu RP, Ocana JA, Harrison KA, *et al.* Chemotherapeutic agents subvert tumor immunity by generating agonists of platelet-activating factor. *Cancer Res.* 2014;74(23):7069-7078.

doi: 10.1158/0008-5472.Can-14-2043

14. Chauhan SJ, Thyagarajan A, Chen Y, Travers JB, Sahu RP. Platelet-activating factor-receptor signaling mediates targeted therapies-induced microvesicle particles release in lung cancer cells. *Int J Mol Sci.* 2020;21(22):8517.

doi: 10.3390/ijms21228517

15. Chauhan SJ, Thyagarajan A, Sahu RP. Effects of miRNA-149-5p and platelet-activating factor-receptor signaling on the growth and targeted therapy response on lung cancer cells. *Int J Mol Sci.* 2022;23(12):6772.

doi: 10.3390/ijms23126772

16. Travers JB, Rohan JG, Sahu RP. New insights into the pathologic roles of the platelet-activating factor system. *Front Endocrinol (Lausanne).* 2021;12:624132.

doi: 10.3389/fendo.2021.624132

17. Bihl JC, Rapp CM, Chen Y, Travers JB. UVB generates microvesicle particle release in part due to platelet-activating factor signaling. *Photochem Photobiol.* 2016;92(3):503-506.

doi: 10.1111/php.12577

18. Liu L, Awoyemi AA, Fahy KE, *et al.* Keratinocyte-derived microvesicle particles mediate ultraviolet B radiation-induced systemic immunosuppression. *J Clin Invest.* 2021;131(10):e144963.

doi: 10.1172/jci144963

19. Thyagarajan A, Kadam SM, Liu L, *et al.* Gemcitabine induces microvesicle particle release in a platelet-activating factor-receptor-dependent manner via modulation of the MAPK pathway in pancreatic cancer cells. *Int J Mol Sci.* 2018;20(1):32.

doi: 10.3390/ijms20010032

20. Patel KD, Zimmerman GA, Prescott SM, McIntyre TM. Novel leukocyte agonists are released by endothelial cells exposed to peroxide. *J Biol Chem.* 1992;267(21):15168-15175.

doi: 10.1016/S0021-9258(18)42161-8

21. Smiley PL, Patel KD, Stremler KE, Zimmerman GA, Prescott SM, McIntyre TM. Novel neutrophil agonists: Oxidatively-fragmented phosphatidylcholines. In: Bailey JM, editor. *Prostaglandins, Leukotrienes, Lipoxins, and PAF: Mechanism of Action, Molecular Biology, and Clinical Applications*. Boston, MA: Springer US; 1991. p. 269-279.

22. Fahy K, Liu L, Rapp CM, *et al.* UVB-generated microvesicle particles: A novel pathway by which a skin-specific stimulus could exert systemic effects. *Photochem Photobiol.* 2017;93(4):937-942.

doi: 10.1111/php.12703

23. Maacha S, Bhat AA, Jimenez L, *et al.* Extracellular vesicles-mediated intercellular communication: Roles in the tumor microenvironment and anti-cancer drug resistance. *Mol Cancer.* 2019;18(1):55.

doi: 10.1186/s12943-019-0965-7

24. Muralidharan-Chari V, Kohan HG, Asimakopoulos AG, *et al.* Microvesicle removal of anticancer drugs contributes to drug resistance in human pancreatic cancer cells. *Oncotarget.* 2016;7(31):50365-50379.

doi: 10.18632/oncotarget.10395

25. Yang Q, Xu J, Gu J, *et al.* Extracellular vesicles in cancer drug resistance: Roles, mechanisms, and implications. *Adv Sci.* 2022;9(34):2201609.

doi: 10.1002/advs.202201609

26. Yang Y, Li S, Wang Y, Zhao Y, Li Q. Protein tyrosine kinase inhibitor resistance in malignant tumors: Molecular mechanisms and future perspective. *Signal Transduct Target Ther.* 2022;7(1):329.

doi: 10.1038/s41392-022-01168-8

27. Catalano M, O'Driscoll L. Inhibiting extracellular vesicles formation and release: A review of EV inhibitors. *J Extracell Vesicles.* 2020;9(1):1703244.

doi: 10.1080/20013078.2019.1703244

28. Bianco F, Perrotta C, Novellino L, *et al.* Acid sphingomyelinase activity triggers microparticle release from glial cells. *EMBO J.* 2009;28(8):1043-1054.

doi: 10.1038/emboj.2009.45

29. Deng L, Peng Y, Jiang Y, *et al.* Imipramine protects against bone loss by inhibition of osteoblast-derived microvesicles. *Int J Mol Sci.* 2017;18(5):1013.

doi: 10.3390/ijms18051013

30. Kosgodage US, Trindade RP, Thompson PR, Inal JM, Lange S. Chloramidine/bisindolylmaleimide-i-mediated inhibition of exosome and microvesicle release and enhanced efficacy of cancer chemotherapy. *Int J Mol Sci.*

2017;18(5):1007.

doi: 10.3390/ijms18051007

31. Goldkorn T, Chung S, Filosto S. Lung cancer and lung injury: The dual role of ceramide. *Handb Exp Pharmacol.* 2013;216:93-113.

doi: 10.1007/978-3-7091-1511-4-5

32. Irep N, Inci K, Tokgun PE, Tokgun O. Exosome inhibition improves response to first-line therapy in small cell lung cancer. *J Cell Mol Med.* 2024;28(4):e18138.

doi: 10.1111/jcmm.18138

33. Xiang H, Jin S, Tan F, Xu Y, Lu Y, Wu T. Physiological functions and therapeutic applications of neutral sphingomyelinase and acid sphingomyelinase. *Biomed Pharmacother.* 2021;139:111610.

doi: 10.1016/j.biopha.2021.111610

34. Companioni O, Mir C, Garcia-Mayea Y, LLeonart ME. Targeting sphingolipids for cancer therapy. *Front Oncol.* 2021;11:745092.

doi: 10.3389/fonc.2021.745092

35. Hoshi A, Kanzawa F, Kuretani K. Enhancement of antitumor activity of cyclophosphamide with imipramine. *Chem Pharm Bull (Tokyo).* 1969;17(8):1694-1697.

doi: 10.1248/cpb.17.1694

36. Wang Y, Wang X, Wang X, *et al.* Imipramine impedes glioma progression by inhibiting YAP as a hippo pathway independent manner and synergizes with temozolomide. *J Cell Mol Med.* 2021;25(19):9350-9363.

doi: 10.1111/jcmm.16874

37. Chryplewicz A, Scotton J, Tichet M, *et al.* Cancer cell autophagy, reprogrammed macrophages, and remodeled vasculature in glioblastoma triggers tumor immunity. *Cancer Cell.* 2022;40(10):1111-1127.e9.

doi: 10.1016/j.ccell.2022.08.014

38. Li J, Pan YY, Zhang Y. Synergistic interaction between sorafenib and gemcitabine in EGFR-TKI-sensitive and EGFR-TKI-resistant human lung cancer cell lines. *Oncol Lett.* 2013;5(2):440-446.

doi: 10.3892/ol.2012.1017

39. Martinelli E, Troiani T, Morgillo F, *et al.* Synergistic antitumor activity of sorafenib in combination with epidermal growth factor receptor inhibitors in colorectal and lung cancer cells. *Clin Cancer Res.* 2010;16(20):4990-5001.

doi: 10.1158/1078-0432.Ccr-10-0923

40. Wang J, Ma S, Chen X, Zhang S, Wang Z, Mei Q. The novel PI3K inhibitor S1 synergizes with sorafenib in non-small cell lung cancer cells involving the Akt-S6 signaling. *Invest New Drugs.* 2019;37(5):828-836.

doi: 10.1007/s10637-018-0698-2

41. Kim YS, Jin HO, Seo SK, *et al.* Sorafenib induces apoptotic cell death in human non-small cell lung cancer cells by down-regulating mammalian target of rapamycin (mTOR)-dependent survivin expression. *Biochem Pharmacol.* 2011;82(3):216-226.

doi: 10.1016/j.bcp.2011.04.011

42. Li Y, Yan H, Xu X, Liu H, Wu C, Zhao L. Erastin/sorafenib induces cisplatin-resistant non-small cell lung cancer cell ferroptosis through inhibition of the Nrf2/xCT pathway. *Oncol Lett.* 2020;19(1):323-333.

doi: 10.3892/ol.2019.11066

43. Lei C, Liu D, Zhou Q, Ma S, Qian H. RETRACTED: Engineering of dopamine conjugated with bovine serum albumin and zeolite imidazole framework: A promising drug delivery nanocarrier on lung cancer cells. *Heliyon.* 2024;10(17):e36580.

doi: 10.1016/j.heliyon.2024.e36580

44. Bow YD, Ko CC, Chang WT, *et al.* A novel quinoline derivative, DFIQ, sensitizes NSCLC cells to ferroptosis by promoting oxidative stress accompanied by autophagic dysfunction and mitochondrial damage. *Cancer Cell Int.* 2023;23(1):171.

doi: 10.1186/s12935-023-02984-w

45. Sharma SV, Bell DW, Settleman J, Haber DA. Epidermal growth factor receptor mutations in lung cancer. *Nat Rev Cancer.* 2007;7(3):169-181.

doi: 10.1038/nrc2088

46. Wilhelm SM, Carter C, Tang L, *et al.* BAY 43-9006 exhibits broad spectrum oral antitumor activity and targets the RAF/MEK/ERK pathway and receptor tyrosine kinases involved in tumor progression and angiogenesis. *Cancer Res.* 2004;64(19):7099-7109.

doi: 10.1158/0008-5472.Can-04-1443

47. Escudier B, Eisen T, Stadler WM, *et al.* Sorafenib in advanced clear-cell renal-cell carcinoma. *N Engl J Med.* 2007;356(2):125-134.

doi: 10.1056/NEJMoa060655

48. Zingone A, Brown D, Bowman ED, *et al.* Relationship between anti-depressant use and lung cancer survival. *Cancer Treat Res Commun.* 2017;10:33-39.

doi: 10.1016/j.ctarc.2017.01.001

49. Chen C, Ju R, Shi J, *et al.* Carboxyamidotriazole synergizes with sorafenib to combat non-small cell lung cancer through inhibition of NANOG and aggravation of apoptosis. *J Pharmacol Exp Ther.* 2017;362(2):219-229.

doi: 10.1124/jpet.117.240986

50. Chen JC, Chuang HY, Hsu FT, Chen YC, Chien YC, Hwang JJ. Sorafenib pretreatment enhances radiotherapy through targeting MEK/ERK/NF-κB pathway in human

hepatocellular carcinoma-bearing mouse model. *Oncotarget.* 2016;7(51):85450-85463.

doi: 10.18632/oncotarget.13398

51. Giovannetti E, Labots M, Dekker H, *et al.* Molecular mechanisms and modulation of key pathways underlying the synergistic interaction of sorafenib with erlotinib in non-small-cell-lung cancer (NSCLC) cells. *Curr Pharm Des.* 2013;19(5):927-939.

doi: 10.2174/1381612811306050927

52. Li J, Wang S, Su ZF, Yuan Y. Synergistic effects of sorafenib in combination with gemcitabine or pemetrexed in lung cancer cell lines with K-ras mutations. *Contemp Oncol (Pozn).* 2016;20(1):33-38.

doi: 10.5114/wo.2016.58499

53. Riess JW, Jahchan NS, Das M, *et al.* A phase iia study repositioning desipramine in small cell lung cancer and other high-grade neuroendocrine tumors. *Cancer Treat Res Commun.* 2020;23:100174.

doi: 10.1016/j.ctarc.2020.100174

54. Kachler K, Bailer M, Heim L, *et al.* Enhanced acid sphingomyelinase activity drives immune evasion and tumor growth in non-small cell lung carcinoma. *Cancer Res.* 2017;77(21):5963-5976.

doi: 10.1158/0008-5472.Can-16-3313

55. Hasan H, Sohal IS, Soto-Vargas Z, *et al.* Extracellular vesicles released by non-small cell lung cancer cells drive invasion and permeability in non-tumorigenic lung epithelial cells. *Sci Rep.* 2022;12(1):972.

doi: 10.1038/s41598-022-04940-6

ACCSCIENCE PUBLISHING

Tumor Discovery

CASE REPORT

Complete response after two cycles of enfortumab vedotin in a patient with metastatic bladder cancer: A case report

Ali Kaan Güren*, Murat Sari, and Osman Köstek

Department of Internal Medicine, Division of Medical Oncology, Marmara University School of Medicine, Istanbul, Turkey

Abstract

Metastatic urothelial carcinoma, the most common subtype of advanced bladder cancer, remains associated with poor outcomes and limited treatment options despite systemic therapies. Enfortumab vedotin (EV), an antibody-drug conjugate targeting Nectin-4, has shown significant improvements in progression-free and overall survival in platinum- and immunotherapy-pretreated patients, as demonstrated in the EV-201 and EV-301 trials. In this report, we present a case of a patient who had previously received platinum-based neoadjuvant chemotherapy and experienced disease progression under nivolumab maintenance therapy but subsequently achieved a complete response in a short period with EV treatment. EV has emerged as a valuable treatment alternative in this aggressive disease, where survival expectations are generally poor. However, questions remain regarding which patients benefit most from the treatment and whether the response is correlated with nectin-4 expression levels.

Keywords: Metastatic urothelial carcinoma; Enfortumab vedotin; Complete response

***Corresponding author:**
Ali Kaan Güren
(ali.guren@marmara.edu.tr)

Citation: Güren AK, Sari M, Köstek O. Complete response after two cycles of enfortumab vedotin in a patient with metastatic bladder cancer: A case report. *Tumor Discov*. 2025;4(3):92-95. doi: 10.36922/TD025150026

Received: April 07, 2024

Revised: May 19, 2025

Accepted: May 22, 2025

Published online: June 5, 2025

1. Background

Non-muscle invasive bladder cancer accounts for approximately 75% of all bladder cancer cases, while muscle-invasive bladder cancer (MIBC) accounts for the remaining 25%. Although the rate of metastatic disease is around 5% at the time of diagnosis, distant metastases can develop in up to 50% of patients during follow-up despite receiving radical treatments, especially in patients diagnosed with MIBC.[1]

Metastatic urothelial carcinoma (mUC) is the most common histological subtype of advanced bladder cancer.[2] Despite systemic treatment approaches, mUC remains associated with poor survival outcomes and limited therapeutic options. Platinum-based chemotherapy protocols have long been accepted as the standard approach for the first-line treatment of metastatic disease; however, many patients develop non-response or relapse. While the use of immunotherapy in mUC has expanded in recent years, effective targeted therapies are still lacking for those who develop resistance or do not derive sufficient clinical benefit from these agents.[3,4]

Enfortumab vedotin (EV) is an antibody-drug conjugate targeting Nectin-4, a protein highly expressed in urothelial carcinoma cells. Upon binding to nectin-4 on the tumor

cell surface, EV is internalized and releases the cytotoxic agent monomethyl auristatin E, disrupting microtubule formation and leading to tumor cell death by apoptosis.[5] Phase II EV-201 and Phase III EV-301 clinical trials have shown significant benefits on progression-free survival (PFS) and overall survival (OS) among patients with locally advanced or mUC who had previously received platinum-based chemotherapy and programmed cell death protein 1/programmed death-ligand 1 (PD-1/PD-L1) inhibitor therapy.[6,7] Given the significance of the findings from these studies, EV has emerged as an important treatment option for treatment-resistant mUC. In this context, we present a case of metastatic bladder cancer treated with EV.

2. Case presentation

A 66-year-old male patient with a known history of arterial hypertension, managed with amlodipine 10 mg daily, and a 40-pack-year smoking history, presented to our institution with a 3-month history of painless hematuria, which had gradually increased in frequency. Ultrasonography revealed a malignant lesion on the left side wall of the bladder with increased thickness extending into the bladder lumen. The patient subsequently underwent transurethral resection of the bladder tumor. Histopathological analysis of the transurethral resection of the bladder tumor specimen revealed high-grade urothelial carcinoma with a pathological stage of at least T2. Staging with positron emission tomography/computed tomography (PET/CT) revealed abnormal bladder wall thickening and multiple lymph nodes in the perivesical, internal, and external iliac regions suspicious for malignancy; however, no distant metastases were detected. Based on the diagnosis of locally advanced bladder cancer, the patient received neoadjuvant chemotherapy consisting of gemcitabine (1,000 mg/m^2 on days 1 and 8) and cisplatin (70 mg/m^2 on day 1) in a 21-day cycle for a total of four cycles. The patient subsequently underwent radical cystectomy with pelvic lymph node dissection, followed by orthotopic neobladder reconstruction. Final pathology revealed ypT3N2, indicating post-neoadjuvant therapy pathological staging with tumor invasion into perivesical tissue (T3) with involvement of multiple regional lymph nodes (N2), consistent with high-grade urothelial carcinoma. Due to the presence of residual tumor, adjuvant treatment with nivolumab was initiated at a dose of 240 mg every 2 weeks.

At the 9th month of treatment, a follow-up PET/CT scan revealed increased 18 F-fluorodeoxyglucose (FDG) uptake in several regions. A 12 × 16 mm lymph node located in the right lateral aspect of the mesorectum adjacent to the rectum demonstrated a maximum standardized uptake value (SUVmax) of 7.8. Additional FDG-avid soft tissue foci were observed adjacent to the left external iliac vascular structures (SUVmax: 6.5) and in the right mesorectal fascia (SUVmax: 4.9). A soft tissue mass measuring 18 × 34 × 30 mm extending from the right side of the mesorectum to the right mesorectal fascia at the level of the coccyx showed intense FDG uptake (SUVmax: 13.6). Furthermore, increased pathological FDG uptake was noted in the soft tissue adjacent to the posterior aspect of the symphysis pubis (SUVmax: 5.5). PET/CT images are presented in Figure 1.

Following these findings, the patient was initiated on EV at a dose of 1.25 mg/kg administered on days 1, 8, and 15 of a 28-day cycle. After two cycles, follow-up PET/CT imaging demonstrated near-complete to complete morphological and complete metabolic regression of previously identified metastatic lesions. Specifically, resolution was noted in lymphadenopathy located in the right common iliac area, right mesorectal fascia and its vicinity, and the posterior aspect of the symphysis pubis, compared to the prior scan. PET/CT images are shown in Figure 2. During treatment, the patient experienced grade 1 peripheral neuropathy and grade 1 cutaneous reactions. These adverse events were mild and did not necessitate any dose modifications. As of the 9th month of treatment, the patient remains on EV, with no radiologically detectable lesions, and maintains a complete response.

3. Discussion

EV has emerged as a valuable treatment option for patients with mUC who have previously received platinum-based chemotherapy and PD-1/PD-L1 inhibitor therapy, demonstrating significant response rates and survival

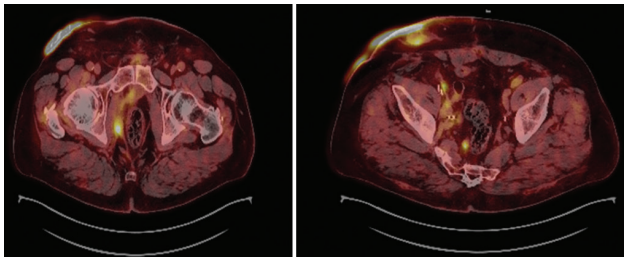

Figure 1. Positron emission tomography-computed tomography images obtained prior to the initiation of enfortumab vedotin therapy

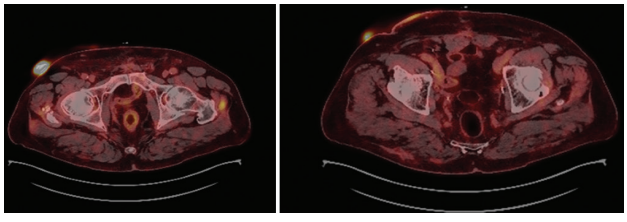

Figure 2. Positron emission tomography-computed tomography images obtained after two cycles of enfortumab vedotin therapy

benefit. As an antibody-drug conjugate targeting nectin-4, it offers high tumor selectivity and, as observed in our case, can induce a rapid therapeutic response, making it an effective targeted approach in heavily pretreated patients. To the best of our knowledge, our case represents one of the most rapid complete responses to EV reported in the literature for mUC. This case may serve as a valuable reference, particularly in symptomatic patients or those requiring a prompt therapeutic response.

EV was first evaluated in the single-arm phase 2 trial EV-201, where it demonstrated promising outcomes in mUC patients previously treated with platinum-based chemotherapy and immune checkpoint inhibitors. The study reported a median PFS of 5.8 months and a median OS of 11.7 months.[6] Subsequently, the phase 3 EV-301 trial compared EV with standard chemotherapy options in a similar patient population. EV achieved a median OS of 12.88 months versus 8.97 months with chemotherapy and a median PFS of 5.55 months versus 3.71 months, respectively. In addition, the complete response rate in the EV arm was 4.9%, with a disease control rate of 71.9%.[7] In our case, the patient had previously received platinum-based neoadjuvant chemotherapy and experienced disease progression under maintenance of nivolumab. Notably, a complete response was achieved following treatment with EV.

The median time to response for EV was reported as 1.8 months in the EV-201 trial and 1.41 months in the EV-301 trial.[6,7] These findings suggest that EV provides a rapid and effective tumor response in patients with mUC. However, neither study specified the exact time at which a complete response was achieved among responders.[6,7] In our case, a complete response was observed after two cycles (approximately 2 months) of treatment.

Immunotherapeutic agents have gained a significant role in the treatment algorithm of mUC by markedly improving OS, particularly through the use of PD-1 and PD-L1 inhibitors. For cisplatin-ineligible patients with mUC, first-line immunotherapy options include atezolizumab, as demonstrated in the IMvigor210 trial,[8] and pembrolizumab, as shown in the KEYNOTE-052 trial.[9] Pembrolizumab has shown an OS benefit in patients with disease progression after platinum-based chemotherapy, as demonstrated in the KEYNOTE-045 trial.[10] Similarly, nivolumab demonstrated efficacy as a second-line treatment in the CheckMate 275 trial.[11] In addition, avelumab provided a survival advantage as a maintenance therapy in patients who responded to platinum-based chemotherapy, according to the findings of the JAVELIN Bladder 100 trial.[12] The CheckMate 274 trial demonstrated that adjuvant treatment with nivolumab significantly prolonged disease-free survival in high-risk patients following radical cystectomy.[13] Although the indications and sequencing of PD-1/PD-L1 inhibitors can be complex, immunotherapy remains a critical component of treatment for nearly all patients with mUC at some stage of their disease course. In line with the CheckMate 274 trial, our patient had also received adjuvant nivolumab following radical cystectomy.

Following the favorable responses observed with PD-1/PD-L1 inhibitors and EV, the EV-302/KEYNOTE-A39 trial was conducted to evaluate the efficacy of the combination of EV and pembrolizumab as a first-line therapy in patients with mUC. Compared to standard treatments, the combination demonstrated significant improvements in both PFS and OS, positioning this regimen as a potentially new standard of care.[14]

Although our case demonstrates a favorable response to EV, serving as a positive example for both clinicians and patients, this observation is limited to one patient. Questions remain regarding which subgroups of patients are more likely to benefit from EV therapy. In particular, further research is needed to elucidate the relationship between Nectin-4 expression levels and treatment response and identify novel predictive biomarkers that will refine patient selection and improve prognostic assessment in the future.

4. Conclusion

Although various treatment modalities, such as chemotherapy, immunotherapy, and targeted agents, have expanded in the management of mUC, the overall prognosis remains poor. EV has emerged as a valuable treatment alternative in this aggressive disease, where survival expectations are generally poor. However, questions remain regarding patient selection and the potential correlation between treatment response and nectin-4 expression levels. Addressing these uncertainties will require future studies involving larger patient cohorts and comprehensive subgroup analyses.

Acknowledgments

None.

Funding

None.

Conflict of interest

The authors declare they have no competing interests.

Author contributions

Conceptualization: Ali Kaan Güren

Formal analysis: Osman Köstek
Investigation: Ali Kaan Güren, Murat Sari
Methodology: Murat Sari, Osman Köstek
Writing – original draft: Ali Kaan Güren
Writing – review & editing: Murat Sari, Osman Köstek

Ethics approval and consent to participate

The patient gave written informed consent prior to participation.

Consent for publication

The patient provided written informed consent for the publication of anonymized data collected during the study. For person data included in this manuscript (such as quotes, images, or case details), consent for publication has been obtained. Identifiable information has been removed or anonymized to protect the privacy of participants.

Availability of data

Data will be made available upon reasonable request from the corresponding author.

References

1. Gore JL, Wright P, Shih V, *et al*. Development and optimization of a bladder cancer algorithm using SEER-Medicare claims data. *JCO Clin Cancer Inform.* 2024;8:e2400073.

   doi: 10.1200/CCI.24.00073

2. Reddy AC, Gu JZ, Koo BH, Fruh V, Sax AJ. Urothelial carcinoma: Epidemiology and imaging-based review. *R I Med J (2013).* 2024;107(5):26-32.

3. Lenis AT, Lec PM, Chamie K, Mshs MD. Bladder cancer: A review. *JAMA*. 2020;324(19):1980-1991.

   doi: 10.1001/jama.2020.17598

4. Dobruch J, Oszczudłowski M. Bladder cancer: Current challenges and future directions. *Med (Kaunas).* 2021;57(8):749.

   doi: 10.3390/medicina57080749

5. Challita-Eid PM, Satpayev D, Yang P, *et al*. Enfortumab vedotin antibody-drug conjugate targeting Nectin-4 is a highly potent therapeutic agent in multiple preclinical cancer models. *Cancer Res.* 2016;76(10):3003-3013.

   doi: 10.1158/0008-5472.CAN-15-1313

6. Yu EY, Petrylak DP, O'Donnell PH, *et al*. Enfortumab vedotin after PD-1 or PD-L1 inhibitors in cisplatin-ineligible patients with advanced urothelial carcinoma (EV 201): A multicentre, single-arm, phase 2 trial. *Lancet Oncol.* 2021;22(6):872-882.

   doi: 10.1016/S1470-2045(21)00094-2

7. Rosenberg JE, Powles T, Sonpavde GP, *et al*. EV-301 long-term outcomes: 24-month findings from the phase III trial of enfortumab vedotin versus chemotherapy in patients with previously treated advanced urothelial carcinoma. *Ann Oncol.* 2023;34(11):1047-1054.

   doi: 10.1016/j.annonc.2023.08.016

8. Balar AV, Galsky MD, Rosenberg JE, *et al*. Atezolizumab as first-line treatment in cisplatin-ineligible patients with locally advanced and metastatic urothelial carcinoma: A single-arm, multicentre, phase 2 trial. *Lancet.* 2017;389(10064):67-76.

   doi: 10.1016/S0140-6736(16)32455-2

9. Vuky J, Balar AV, Castellano D, *et al*. Long-term outcomes in KEYNOTE-052: Phase II study investigating first-line pembrolizumab in cisplatin-ineligible patients with locally advanced or metastatic urothelial cancer. *J Clin Oncol.* 2020;38(23):2658-2666.

   doi: 10.1200/JCO.19.01213

10. Fradet Y, Bellmunt J, Vaughn DJ, *et al*. Randomized phase III KEYNOTE-045 trial of pembrolizumab versus paclitaxel, docetaxel, or vinflunine in recurrent advanced urothelial cancer: Results of >2 years of follow-up. *Ann Oncol.* 2019;30(6):970-976.

    doi: 10.1093/annonc/mdz127

11. Sharma P, Retz M, Siefker-Radtke A, *et al*. Nivolumab in metastatic urothelial carcinoma after platinum therapy (CheckMate 275): A multicentre, single-arm, phase 2 trial. *Lancet Oncol.* 2017;18(3):312-322.

    doi: 10.1016/S1470-2045(17)30065-7

12. Grivas P, Park SH, Voog E, *et al*. Avelumab first-line maintenance therapy for advanced urothelial carcinoma: Comprehensive clinical subgroup analyses from the JAVELIN Bladder 100 phase 3 trial. *Eur Urol.* 2023;84(1):95-108.

    doi: 10.1016/j.eururo.2023.03.030

13. Galsky MD, Bajorin DF, Witjes JA, *et al*. Disease-free survival analysis for patients with high-risk muscle-invasive urothelial carcinoma from the randomized CheckMate 274 trial by PD-L1 combined positive score and tumor cell score. *Eur Urol.* 2023;83(5):432-440.

    doi: 10.1016/j.eururo.2023.01.016

14. Powles T, Valderrama BP, Gupta S, *et al*. Enfortumab vedotin and pembrolizumab in untreated advanced urothelial cancer. *N Engl J Med.* 2024;390(10):875-888.

    doi: 10.1056/NEJMoa2312117

ACCSCIENCE PUBLISHING

Tumor Discovery

CASE REPORT

An unusual case of malignant biliary tract obstruction

Sakditad Saowapa[1]*, Chalothorn Wannaphut[2], Hector Jose Garcia Pleitez[1], Andrea Ortiz Maldonado[1], Miriam Alicia Paz Sierra[1], Natchaya Polpichai[3], Pharit Siladech[4], Meenu Sharma[5], and Lukman Tijani[6]

[1]Department of Internal Medicine, Texas Tech University Health Sciences Center at Lubbock, Lubbock, Texas, United States of America

[2]Department of Medicine, John A. Burns School of Medicine, University of Hawaii, Honolulu, Hawaii, United States of America

[3]Department of Internal Medicine, Louis A. Weiss Memorial Hospital, Chicago, Illinois, United States of America

[4]Department of Internal Medicine, Faculty of Medicine Ramathibodi Hospital, Mahidol University, Bangkok, Thailand

[5]Department of Pathology, Texas Tech University Health Sciences Center at Lubbock, Lubbock, Texas, United States of America

[6]Department of Hematology and Oncology, Texas Tech University Health Sciences Center at Lubbock, Lubbock, Texas, United States of America

***Corresponding author:**
Sakditad Saowapa
(sakditad.saowapa@ttuhsc.edu)

Citation: Saowapa S, Wannaphut C, Pleitez HJC, *et al*. An unusual case of malignant biliary tract obstruction. *Tumor Discov*. 2025;4(3):96-99.
doi: 10.36922/TD025070011

Received: February 11, 2025

1st revised: April 18, 2025

2nd revised: May 4, 2025

3rd revised: May 27, 2025

Accepted: June 5, 2025

Published online: June 25, 2025

Abstract

Malignant biliary tract obstruction (MBTO) is most commonly associated with primary hepatobiliary and pancreatic malignancies. Here, we present a rare case of a 65-year-old female who developed obstructive jaundice, which initially raised suspicion for hepatobiliary carcinoma. Cross-sectional imaging, including computed tomography and magnetic resonance imaging, revealed hepatic lesions, and endoscopic retrograde cholangiopancreatography demonstrated a malignant biliary stricture. Histopathological analysis of a liver biopsy unexpectedly confirmed metastatic urothelial carcinoma (UC). Further evaluation with cystoscopy, prompted despite the absence of urinary symptoms, identified a small bladder mass, which was biopsy-proven as the primary UC. UC typically metastasizes to lymph nodes, lungs, or bones, and isolated liver involvement causing MBTO is exceptionally uncommon. This case underscores the importance of maintaining a broad differential diagnosis in patients with malignant biliary obstruction, as atypical metastatic patterns can mimic more common hepatobiliary cancers and delay appropriate management.

Keywords: Malignant biliary tract obstruction; Cholangiocarcinoma; Urothelial carcinoma; Hepato-pancreato-biliary cancer; Bladder cancer

1. Background

Malignant biliary tract obstruction (MBTO) is a common condition that could arise from hepato-pancreato-biliary cancer or metastasis from other primary cancers such as pancreatic adenocarcinoma or cholangiocarcinoma. The common metastatic cancers causing MBTO by extrinsic compression include colon, stomach, breast, lung, and

cervical malignancies.[1] Obstruction from metastatic urothelial cancer rarely occurs. Here, we report a case of obstructive jaundice caused by metastatic urothelial carcinoma (UC).

2. Case presentation

A 65-year-old female with a past medical history of hypertension, rhabdomyolysis, and alcohol abuse presented with progressive abdominal pain for 4 months with new-onset jaundice and anorexia with self-reported recent significant weight loss. Initial examination showed stable vital signs with marked jaundice and distended abdomen and tenderness in the right upper quadrant. Blood work showed elevated total troponin (23.7 mg/dL), alanine transaminase/aspartate transaminase (70/152 IU/L), alkaline phosphatase (623 IU/L), total bilirubin (25 mg/dL), and direct bilirubin (>10 mg/dL), which was suggestive of cholestasis jaundice.

Computed tomography (CT) showed intrahepatic duct dilatation with narrow common bile duct, suggesting possible sclerosing cholangitis or cholangiocarcinoma. She had elevated cancer antigen 19-9 at 456 U/mL (normal: <37 U/mL) and carcinoembryonic antigen at 5.8 ng/mL (normal: 0 – 2.9 ng/mL) but normal alpha-fetoprotein, which lent further support to the possibility of hepatobiliary carcinoma. Further imaging with magnetic resonance imaging (MRI) showed an 8.5 cm hypoenhancing mass within the central aspect of the liver, resulting in intrahepatic biliary dilatation with multiple other satellite liver lesions, which were suggestive of cholangiocarcinoma (Klatskin tumor) (Figure 1). Endoscopic retrograde cholangiopancreatography (ERCP) found a malignant stricture in the bile duct. Endoscopic ultrasound (EUS) with negative brush biopsy results led to a liver biopsy to confirm the diagnosis. Interventional radiology-guided liver biopsy revealed metastatic carcinoma positive for GATA3, CK903, P40, P63, and thrombomodulin, consistent with metastatic UC (Figures 2-4). The patient denied urinary symptoms, and urinalysis was negative.

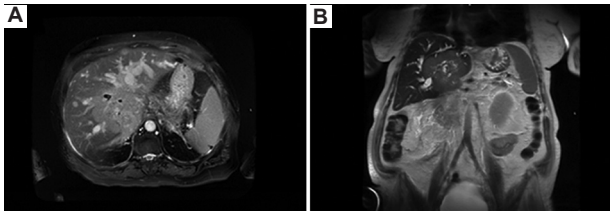

Figure 1. T1-weighted axial view image (A) and T2-weighted coronal view image (B) from the abdominal magnetic resonance imaging scan show an 8.5 cm hypoenhancing mass within the central aspect of the liver, which results in intrahepatic biliary dilatation. Findings are suggestive of cholangiocarcinoma (Klatskin tumor). Smaller satellite lesions are noted in both lobes of the liver.

Cystoscopy performed by the urologist showed a small bladder mass. The mass was resected, and further histopathological test confirmed squamous cell carcinoma invading the bladder wall. Eventually, the oncology team was consulted for appropriate treatment of metastatic bladder cancer.

3. Discussion

MBTO predominantly arises from primary hepatic biliary cancers. Our case illustrates MBTO arising from uncommon metastatic UC that originated from bladder cancer. UC of the bladder commonly metastasizes to various anatomical sites, with lymph nodes being the most prevalent site at 25%, followed by bone metastasis at 24%, involvement of the urinary tract at 23%, pulmonary metastases at 19%, hepatic involvement at 18%, and brain

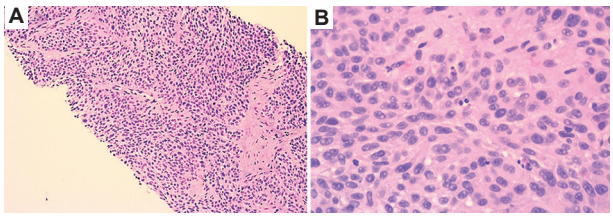

Figure 2. Histopathological images of liver biopsy specimens visualized with hematoxylin and eosin staining. Observations under 20× (A) and 40× (B) magnification show irregularly distributed nests of urothelial cells, which are surrounded by fibrotic stroma. Scale bar: (A) 100 µm. (B) 50 µm.

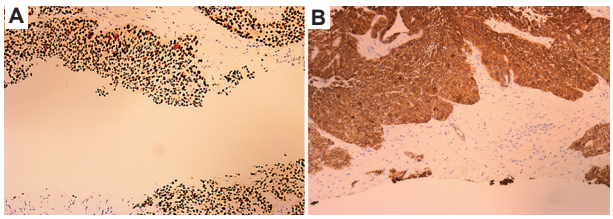

Figure 3. Histopathological images of liver biopsy specimens visualized with immunohistochemical staining for P40 and high-molecular-weight keratin (HMWK). Observations under 2.5× (A) and 10× (B) magnification show cells positive for P40 and HMWK, respectively. Scale bar: (A) 1 mm. (B) 500 µm.

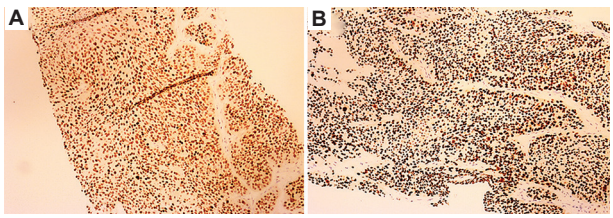

Figure 4. Histopathological observation of liver specimens visualized with immunohistochemistry at ×10 magnification. The images show urothelial cells positive for GATA-3. (A) and p63. (B), respectively. Scale bar: 500 µm for both panels.

metastasis occurring in 3% of cases.[2] Case reports and small case series suggest that MBTO secondary to UC accounts for <1% of all MBTOs, which are most commonly caused by pancreatic, cholangiocarcinoma, or metastatic colorectal cancers.[3]

Initial diagnosis involves distinguishing between benign and malignant conditions, often achieved through magnetic resonance cholangiopancreatography (MRCP) or ERCP. Both MRCP and ERCP are preferred over CT scans due to their higher sensitivity and specificity, with 85% and 71% for MRCP and sensitivity of 75% for ERCP, respectively.[3,4] Recent studies have shown that MRCP's sensitivity exceeds 96% and specificity reaches 85% for differentiating between benign and MBTOs.[2,4] In addition, ERCP's diagnostic accuracy is enhanced by adjunct techniques such as EUS and intraductal ultrasound.[5]

Metastatic UC to the liver typically demonstrates hypovascularity on contrast-enhanced CT, with minimal arterial enhancement and progressive enhancement during the portal venous and delayed phases. On MRI, lesions appear hypointense on T1-weighted images, mildly hyperintense on T2-weighted images, and exhibit restricted diffusion on diffusion-weighted imaging sequences, with delayed progressive contrast enhancement. Unlike hypervascular metastases from neuroendocrine tumors or renal cell carcinoma, urothelial metastases lack early arterial phase enhancement. On EUS, they present as hypoechoic, stiff, and hypovascular lesions, consistent with other adenocarcinoma metastases.[6-9]

When malignancy is suspected, tissue sampling becomes crucial to refine the diagnosis. Brush cytology coupled with forceps or needle biopsy is recommended over brush cytology alone due to its increased sensitivity and specificity. While brush cytology typically exhibits sensitivity rates around or below 50%, its specificity remains notably high at 95%.[10] Forceps or needle biopsy can further elevate sensitivity to 70% and specificity to 100%, respectively.[10] Percutaneous transhepatic cholangiography serves as a secondary diagnostic option when ERCP is unsuccessful or infeasible and the patient has potential bleeding complications.[2] In our case, while the EUS and brush biopsy yielded negative results, the clinical presentation strongly suggested cancer, necessitating a pathology diagnosis to guide appropriate treatment. Consequently, a liver biopsy was performed as the next step.

In addition, positive tumor markers can help diagnose UC. Some tumor markers with high sensitivities (>75%) for UC include uroplakin II, p40, p63, GATA 3, and CK903.[11-13] In addition, there are a variety of histological variants, subtypes, and immunophenotypes of urothelial cancer that determine its risk of progression.[12] In this case, although the patient did not report urinary symptoms, the positive staining for p40, p63, high-molecular-weight keratin, and GATA-3 in the tissues strongly indicates a urothelial origin. Therefore, further investigation for primary urothelial cancer should be the next step.

The most prevalent bladder tumor histologies include UC, characterized by invasion into the muscularis propria and representing the majority of cases in the US and Europe. Squamous cell carcinomas, originating from the urothelium, constitute a small percentage of cases, while adenocarcinomas, exhibiting a glandular phenotype, are rarer still, typically arising from the bladder's urothelium or remnants of the urachus.[13,14]

This case underscores the importance of considering distant metastases, particularly from bladder cancer, in the differential diagnosis of MBTO and emphasizes the significance of comprehensive diagnostic approaches and multidisciplinary collaboration for optimal patient management.

4. Conclusion

MBTO is a common presentation of hepato-pancreato-biliary cancer. However, a distant metastasis could mimic the presentation. Gastrointestinal workup with ERCP and EUS for tissue sampling or cytology has low yield in terms of diagnosing MBTO. Even if the result is negative, further workup of tissue biopsy should be done for the definitive diagnosis. If metastasis is suspected, investigations for primary cancer based on pathology results should be the next step.

Acknowledgments

The authors would like to thank the Department of Pathology, Texas Tech University Health Sciences Center (TTUHSC), for providing the original pathology images used in this manuscript. In addition, we extend our gratitude to Nutthamon Aroonwon for her assistance in editing and formatting the figures.

Funding

None.

Conflict of interest

The authors declare they have no competing interests.

Author contributions

Conceptualization: Sakditad Saowapa, Chalothorn Wannaphut

Formal analysis: Natchaya Polpichai, Pharit Siladech

Investigation: Sakditad Saowapa, Hector Jose Garcia Pleitez, Andrea Ortiz Maldonado, Miriam Alicia Paz Sierra
Methodology: Sakditad Saowapa, Meenu Sharma
Writing – original draft: Sakditad Saowapa
Writing – review & editing: Chalothorn Wannaphut, Hector Jose Garcia Pleitez, Andrea Ortiz Maldonado, Lukman Tijani

Ethics approval and consent to participate

No institutional review board (IRB) approval was required for this single-patient case report in accordance with local guidelines. Written informed consent was obtained from the patient prior to participation. The consent included permission to use relevant clinical information and images for the purpose of this case report.

Consent for publication

Written informed consent was obtained from the patient to publish this report in accordance with the journal's patient consent policy.

Availability of data

The data that support the findings of this study are available from the corresponding author upon reasonable request. However, access to the data is restricted due to patient privacy and ethical considerations.

References

1. Lorenz JM. Management of malignant biliary obstruction. *Semin Interv Radiol*. 2016;33(4):259-267.

   doi: 10.1055/s-0036-1592330

2. Bianchi M, Roghmann F, Becker A, *et al*. Age-stratified distribution of metastatic sites in bladder cancer: A population-based analysis. *Can Urol Assoc J*. 2014;8(3-4):E148-E158.

   doi: 10.5489/cuaj.787

3. Paik WH, Park DH. Endoscopic management of malignant biliary obstruction. *Gastrointest Endosc Clin N Am*. 2024;34(1):127-140.

   doi: 10.1016/j.giec.2023.07.004

4. Suthar M, Purohit S, Bhargav V, Goyal P. Role of MRCP in differentiation of benign and malignant causes of biliary obstruction. *J Clin Diagn Res*. 2015;9(11):TC08-TC12.

   doi: 10.7860/JCDR/2015/14174.6771

5. Canto MI, Hruban RH, Fishman EK, *et al*. Frequent detection of pancreatic lesions in asymptomatic high-risk individuals. *Gastroenterology*. 2012;142(4):796-804; quiz e14-e15.

   doi: 10.1053/j.gastro.2011.12.056

6. Ronot M, Vilgrain V. Imaging of benign and malignant hepatocellular lesions. *Semin Liver Dis*. 2008;28(3):267-282.

   doi: 10.1055/s-0028-1085093

7. Namasivayam S, Martin DR, Saini S. Imaging of liver metastases: MRI. *Cancer Imaging*. 2007;7(1):2-9.

   doi: 10.1102/1470-7330.2007.0002

8. Larsen LP. Role of contrast enhanced ultrasonography in the assessment of hepatic metastases: A review. *World J Hepatol*. 2010;2(1):8-15.

   doi: 10.4254/wjh.v2.i1.8

9. Albiin N. MRI of focal liver lesions. *Curr Med Imaging Rev*. 2012;8(2):107-116.

   doi: 10.2174/157340512800672216

10. Burnett AS, Calvert TJ, Chokshi RJ. Sensitivity of endoscopic retrograde cholangiopancreatography standard cytology: 10-year review of the literature. *J Surg Res*. 2013;184(1):304-311.

    doi: 10.1016/j.jss.2013.03.056

11. McDaniel AS, Chinnaiyan AM, Siddiqui J, McKenney JK, Mehra R. Immunohistochemical staining characteristics of nephrogenic adenoma using the PIN-4 cocktail (p63, AMACR, and CK903) and GATA-3. *Am J Surg Pathol*. 2014;38(12):1664-1671.

    doi: 10.1097/PAS.0000000000000267

12. Hoang LL, Tacha D, Bremer RE, Haas TS, Cheng L. Uroplakin II (UPII), GATA3, and p40 are highly sensitive markers for the differential diagnosis of invasive urothelial carcinoma. *Appl Immunohistochem Mol Morphol*. 2015;23(10):711-716.

    doi: 10.1097/PAI.0000000000000143

13. Takahara T, Murase Y, Tsuzuki T. Urothelial carcinoma: Variant histology, molecular subtyping, and immunophenotyping significant for treatment outcomes. *Pathology*. 2021;53(1):56-66.

    doi: 10.1016/j.pathol.2020.09.004

14. Reuter VE. The pathology of bladder cancer. *Urology*. 2006;67(3 Suppl 1):11-17;discussion 17-18.

    doi: 10.1016/j.urology.2006.01.037

ACCSCIENCE PUBLISHING

Tumor Discovery

CASE REPORT

Challenges and considerations in diagnosing mature teratoma during pregnancy: A case report

Sumaira Siddiqui*

Department of Pathology, Clinilabs and Research, Lucknow, Uttar Pradesh, India

Abstract

The progression of rapidly growing teratomas in pregnancy may be influenced by hormonal and genetic factors. The current report is about a unique case involving a mature teratoma with rapid growth characteristics, yet it did not lead to any complications throughout pregnancy of a primigravida. The benign mature teratoma was identified via antenatal ultrasound during the first trimester. In this case, the patient experienced no adverse effects, and the size of the ovarian teratoma showed a gradual increasing trend during pregnancy without resulting in any complications. In summary, mature teratoma is a benign tumor with a good prognosis, and if fetal distress is detected, cesarean section should be recommended.

Keywords: Mature teratoma; Pregnancy; Fetal distress; Cesarean section

***Corresponding author:**
Sumaira Siddiqui
(sumiimc011@gmail.com)

Citation: Siddiqui S. Challenges and considerations in diagnosing mature teratoma during pregnancy: A case report. *Tumor Discov*. 2025;4(3):100-104.
doi: 10.36922/TD025120022

Received: March 20, 2025

1st revised: April 30, 2025

2nd revised: June 1, 2025

Accepted: June 3, 2025

Published online: June 30, 2025

1. Introduction

Cystic teratomas represent a form of germ-cell tumor distinguished by the presence of mature tissues from all three embryonic layers: ectoderm, mesoderm, and endoderm. Remarkably, evidence of teratomas dates back to 2000 B.C., demonstrating the long-standing recognition of these tumors. The first formally recorded case of a mature cystic teratoma was made by Johannes Scultetus in 1659, who documented the ovarian tumor findings of a young woman during the autopsy, describing it as a "dermoid cyst."[1] Rudolf Virchow introduced the term "teratoma" in 1863, derived from the Greek word "teras," which means monster.[2] Mature cystic teratomas are considered benign, with an average growth rate of 1.8 mm/year, although malignant transformation has been reported in rare cases. The development of mature cystic teratomas is associated with several risk factors, including late menarche with menstrual irregularities, alcohol use, a history of cystic teratomas, fewer pregnancies, infertility, and adolescent's physical activity that may contribute to an anovulatory cycle.[3] Mature teratomas are benign tumors of the ovary that have a generally favorable prognosis and account for <1% of ovarian tumors. Their occurrence during pregnancy is uncommon.[4] Notably, the hormonal changes during pregnancy cause an increase in the size of mature teratoma.

The current report is about a unique case involving a mature teratoma with rapid growth characteristics, yet it did not lead to any complications throughout pregnancy of a primigravida.

2. Case presentation

A 21-year-old primigravida at a gestational age of 37 weeks presented with a complaint of sudden abdominal pain and visited our gynecology department located at the periphery of Uttar Pradesh, a northern state in India. Physical examination was normal. Systemic investigations were carried out, and all were normal. Blood investigation showed mild leukocytosis. Electrolytes, amylase, lipase, liver function, and renal function tests were within normal range. Ultrasonography was conducted during the first trimester of pregnancy, indicating a small dermoid cyst. The patient was followed up upon this clinical discovery. Ultrasonography during the third trimester showed a left-sided well-defined homogeneous hyperechoic mass measuring 9 × 6 cm. Tumor markers such as CA-125, lactate dehydrogenase (LDH), alpha-fetoprotein (AFP), human chorionic gonadotropin (b-hCG), and human epididymis protein 4 were normal. On abdominal examination, left lower quadrant tenderness was observed. A single live intrauterine pregnancy was noted on ultrasonography with a fetal heart rate of 80 bpm. In this case, due to fetal distress, the patient was recommended by a gynecologist to undergo a cesarean section. Interestingly, no complications due to the ovarian mass were found during pregnancy. Then, cesarean section was done, concomitant with left salphingoopherectomy, delivering a live male newborn. Intraoperative findings of the right ovary and the right fallopian tube were normal. The surgical procedure was well tolerated by the patient, and a surgical specimen was sent for histopathological examination. The patient's post-operative course was uneventful.

2.1. Gross examination

Based on the gross examination shown in Figure 1, the external surface of the ovary received, measuring 9.5 × 9 × 5.5 cm, was smooth and glistening. Upon sectioning, a unilocular cyst embedded with pultaceous material, hair, and sebum was identified. A fallopian tube measuring 3 cm was seen but appeared unremarkable.

2.2. Microscopic examination

The tumor mainly consists of mature elements such as squamous epithelium, pseudostratified ciliated columnar epithelium, adnexal structure, hair follicles, and fibroadipose tissue, as shown in Figure 2. The immature component was not seen.

3. Discussion

The reported incidence of ovarian tumors during pregnancy varies between 1% and 4%.[5] During pregnancy, mature cystic teratomas are the most common benign ovarian tumors, comprising 24 – 40% of all cases.[6] It is a benign cystic tumor made up of tissues from the endoderm, mesoderm, and especially the ectoderm, affecting tissues such as teeth, hair, and sebum.[7]

Figure 1. Gross image of ovarian mass with hair follicle, sebum, and pultaceous material. Left: Ovary shows smooth and glistening external surface; right: Cut section shows hair, pultaceous material.

Cystic teratomas are mostly asymptomatic, and benign ovarian tumors are also known as dermoid cysts. In most cases, they are detected incidentally during radiological imaging, routine physical examinations, or pelvic and abdominal surgeries performed for unrelated conditions. When symptoms are present, the most frequently reported one is lower abdominal or pelvic pain. This may be followed by the discovery of a palpable abdominal or pelvic mass during examination. Some patients may notice an increase in abdominal girth due to the growing size of the mass.

As the tumor enlarges, it can exert pressure on surrounding organs, leading to gastrointestinal symptoms such as constipation or bloating, as well as urinary symptoms such as increased frequency or urgency. In more advanced stages, systemic symptoms, including fever, cachexia (severe weight loss and muscle wasting), intense abdominal pain, and abnormal vaginal bleeding may occur, indicating potential complications or malignant transformation.

One of the most critical and common complications is ovarian torsion, where the ovary twists around the supporting ligaments. This leads to an acute onset of intense abdominal pain, often associated with nausea and vomiting. Ovarian torsion is a surgical exigency and requires immediate medical attention.

During the clinical assessment, a thorough history – with a focus on gynecological details – is essential. Physical examination should include a careful bimanual pelvic examination to analyze the size along with the mobility of the uterus and adnexa, as well as any tenderness or masses. Abdominal examination may also reveal distension or localized pain. A comprehensive clinical evaluation is

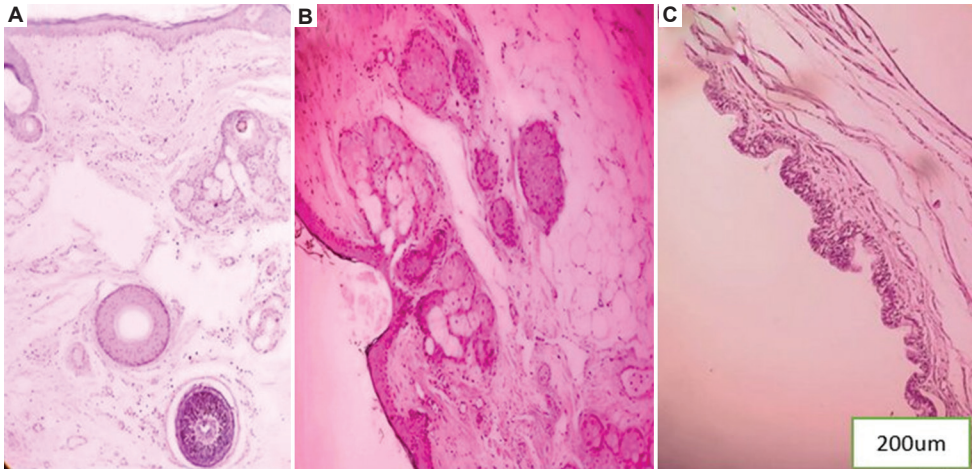

Figure 2. Microscopic examination of the specimen shows a cyst wall, stratified squamous epithelium, adnexal structure, hair follicle, and mucinous epithelium. (A) Section shows stratified squamous epithelium with the hair follicle. (B) Section shows sebaceous gland. (C) Section shows mucinous epithelium. Scale bar: 200 μm; magnification: ×10; staining: Hematoxylin and Eosin.

crucial for early detection, timely intervention, and optimal management of cystic teratomas and their complications.

A definitive tumor marker is unavailable for diagnosing mature cystic teratomas; however, serum markers such as AFP, hCG, LDH, and CA-125 may contribute to diagnostic evaluation and monitoring.[8] Mature cystic teratomas are typically asymptomatic unless complicated or significantly enlarged. Their diagnosis can be difficult, often mimicking other conditions in both clinical and paraclinical assessments.[9,10]

Acute abdominal pain is a common complaint during pregnancy, and its differential diagnosis is broad and often complex. The challenge lies in the wide range of potential etiologies, including appendicitis, diverticulitis, ureteral colic, ectopic pregnancy, degenerating pedunculated fibroids, hemorrhagic ovarian cysts, tubo-ovarian abscesses, polycystic ovaries, simple cysts, endometriomas, cystadenomas, and other ovarian tumors. Although less common, ovarian torsion secondary to ovarian masses should also be considered in the differential diagnosis.[11]

Adnexal torsion is the most significant complication of mature cystic teratomas during pregnancy, occurring in about 8% of cases – primarily in the first and early second trimesters.[12] Although ovarian torsion is more commonly associated with ovarian hyperstimulation syndrome, instances caused by mature teratomas are infrequently reported. Most cases occur in the first trimester, with fewer in the second and rare occurrences in the third.[13]

Ultrasound is the reference standard for evaluating ovarian tumors during pregnancy due to its non-invasive nature and diagnostic reliability. When further assessment is needed, magnetic resonance imaging (MRI) offers superior soft-tissue contrast and additional diagnostic information.[14] On ultrasound, cystic teratomas typically present as heterogeneous masses with echogenic foci and posterior acoustic shadowing caused by components such as calcification, sebum, and hair. Specific findings may include fat-fluid and hair-fluid levels. Characteristic ultrasonographic features include the Rokitansky nodule, iceberg sign, dot-dash pattern (dermoid mesh), and floating balls sign. Transvaginal ultrasound, with a sensitivity of 57.9% and a specificity of 99.7%, outperforms abdominal ultrasound in detection and is as accurate as MRI in identifying and characterizing these tumors.[15,16]

Ovarian cystic teratomas may lead to several complications. Early and precise diagnosis plays a key role in minimizing associated morbidity and mortality. Complications of ovarian cystic teratomas include torsion, rupture, infections, adhesions, malignant transformation, and anti-N-methyl-D-aspartate receptor encephalitis related to ovarian tumors.[17] Mature teratomas are asymptomatic in most affected women; therefore, a proper diagnostic process is required. Since torsion is a common complication among the affected women, surgical intervention is often necessary.

Treatment of mature cystic teratomas is individualized based on the presenting symptoms, radiologic characteristics, risk of malignancy, patient age, and fertility preservation considerations. Surgical excision is the standard of care, with procedures categorized as either ovary-sparing surgery or oophorectomy performed through laparoscopy or laparotomy, depending on the clinical context.[18] Laparoscopic surgery remains the gold standard for the management of mature cystic teratomas. When feasible, cystectomy is the treatment of choice to conserve ovarian parenchyma and preserve reproductive

potential. In cases where the tumor extensively involves the ovary, rendering the parenchyma non-viable, oophorectomy or salpingo-oophorectomy becomes necessary.[19]

Surgery during the first trimester is generally avoided unless the patient presents with acute symptoms suggestive of adnexal torsion, in which case urgent intervention is warranted.[20] For asymptomatic cases, a follow-up ultrasound in the early second trimester is indicated to evaluate the persistence of the lesion. When the mass appears benign, is smaller than 6 cm, and shows no growth, the risk of complications remains low, supporting the use of an expectant management approach. However, any increase in tumor size or change in appearance may prompt consideration for surgical treatment.[4] Younger patients, as well as those having bilateral or large dermoid cysts, should be monitored closely. Taken together, treatment decisions should be individualized, carefully balancing the risks of torsion, rupture, or labor obstruction against the potential for unnecessary surgical intervention and associated risks to both the mother and fetus.[21]

Women presenting with ovarian cysts or tumors during pregnancy should receive counseling about the risk of recurrence, with close ultrasound surveillance recommended throughout gestation. Those with a prior history of ovarian tumors should also be counseled preoperatively on recurrence risks and the potential implications for fertility.[22] Laparoscopic salpingo-oophorectomy, performed with an endoscopic retrieval bag, is considered the standard treatment for post-menopausal and perimenopausal women presenting with a large teratoma. In contrast, laparoscopic cystectomy may be a more suitable and conservative option for younger women, preserving ovarian function when feasible.[23] Women diagnosed with ovarian cysts or tumors during pregnancy should be thoroughly counseled and closely monitored to identify and manage any potential complications.

This case highlights the importance of a comprehensive approach – integrating clinical assessment, laboratory findings, and diagnostic imaging – while making decisions that prioritize the safety of both the mother and the fetus. Despite the final diagnosis being pathological, it is necessary to carefully interpret all parameters to preserve the pregnancy and ultimately ensure the successful delivery of a healthy baby.[24]

4. Conclusion

Mature teratoma is a benign tumor with a good prognosis. To avoid the missed diagnosis of any rare or synchronous malignancies, a gross examination of sufficient specimens containing both solid and suspicious areas of the ovarian cyst is required. Diagnosis of mature teratoma is confirmed through histopathological examination. If a mass is larger, complications, such as ovarian torsion, rupture, malignant transformation, infection, and obstructed labor, may occur, and surgical intervention is generally selected for management if the patient would like to preserve fertility. In this case, cesarean section was recommended as fetal distress was detected, and no complications were reported by or detected in the pregnant patient despite the large ovarian mass.

Acknowledgments

None.

Funding

None.

Conflict of interest

The author declares no conflicts of interest.

Author contributions

This is a single-authored article.

Ethics approval and consent to participate

Patient gave verbal consent before her participation.

Consent for publication

Patient consented on the publication of her data.

Availability of data

Not applicable.

References

1. Peterson WF. Malignant degeneration of benign cystic teratomas of the overy; A collective review of the literature. *Obstet Gynecol Surv*. 1957;12(6):793-830.

   doi: 10.1097/00006254-195712000-00001

2. Pantoja E, Noy MA, Axtmayer RW, Colon FE, Pelegrina I. Ovarian dermoids and their complications. Comprehensive historical review. *Obstet Gynecol Surv*. 1975;30(1):1-20.

   doi: 10.1097/00006254-197501000-00001

3. Westhoff C, Pike M, Vessey M. Benign ovarian teratomas: A population-based case-control study. *Br J Cancer*. 1988;58(1):93-98.

   doi: 10.1038/bjc.1988.171

4. Joudar I, El Abbassi I, Khalloufi C, Jalal M, Lamrissi A, Bouhya S. Mature teratoma during pregnancy: A case report. *J Case Rep Images Obstet Gynecol*. 2023;9(1):70-74.

   doi: 10.5348/100150Z08IJ2023CR

5. Ueda Y, Sekiyama K, Ito M, Egawa H, Tokushige M, Takakura K. Displacement of ovarian mature cystic teratoma following rupture during pregnancy: Case report. *Japanese J Gynecol Obstet Endosc*. 2013;29(1):84-87.

6. Sheng Y, Yuan J, Wang J, Wang L, Li Y, Wang Y. Ovarian mature cystic teratoma is an independent risk factor for the premature rupture of membranes in pregnancy: A single-center retrospective study. *Int J Womens Health*. 2022;14:1477-1487.

doi: 10.2147/IJWH.S381297

7. Osto M, Brooks A, Khan A. Ovarian cystic teratoma in pregnant women: Conservative management or prophylactic oophorectomy? *Cureus*. 2021;13(8):e17354.

doi: 10.7759/cureus.17354

8. Ahmed A, Lotfollahzadeh S. Cystic teratoma. In: *StatPearls*. Treasure Island, FL: StatPearls Publishing; 2025. Available from: https://www.ncbi.nlm.nih.gov/books/NBK564325 [Last accessed on 2023 Jun 03].

9. Bouzoubaa W, Jayi S, Alaoui FZF, Chaara H, Melhouf MA. Immature teratoma of the ovary: About a case. *Pan Afr Med J*. 2017;27:263.

doi: 10.11604/pamj.2017.27.263.6400

10. Chenana A, Kouach J, Moussaoui D, Dehayni M. Tératome immature de l'ovaire et grossesse: A propos d'un cas/ [Immature teratoma of the ovary and pregnancy: A case report]. *Int J Innov Appl Stud*. 2016;15(3):503-514.

11. Tan KH, Chen KC, Wang TL, Chong CF, Chen CC. Ovarian cystic teratoma torsion in pregnancy. *Emerg Med J*. 2010;27:879-880.

doi: 10.1136/emj.2008.063883

12. Tariel O, Huissoud C, Rudigoz RC, Dubernard G. Presumed benign ovarian tumors during pregnancy. *J Gynecol Obstet Biol Reprod* (*Paris*). 2013;42(8):842-855.

doi: 10.1016/j.jgyn.2013.09.038

13. Walid MS, Boddy MG. Bilateral dermoid cysts of the ovary in a pregnant woman: Case report and review of the literature. *Arch Gynecol Obstet*. 2009;279:105-108.

doi: 10.1007/s00404-008-0695-3

14. Haddada S, Selleret L, Fedida B, *et al*. Adnexal masses and pregnancy: Which diagnosis and which imaging? *Imagerie Femme*. 2017;27(2):104-110.

15. Srisajjakul S, Prapaisilp P, Bangchokdee S. Imaging features of unusual lesions and complications associated with ovarian mature cystic teratoma. *Clin Imaging*. 2019;57:115-123.

doi: 10.1016/j.clinimag.2019.05.013

16. Sahin H, Abdullazade S, Sanci M. Mature cystic teratoma of the ovary: A cutting edge overview on imaging features. *Insights Imaging*. 2017;8(2):227-241.

doi: 10.1007/s13244-016-0539-9

17. Nguyen HT, Trinh NB, Tran NH, Nguyen PN. Massive mature cystic teratoma presenting as ovarian cancer grade IIIC in a young Vietnamese woman: A case report. *Oman Med J*. 2025;40:1-8.

doi: 10.5001/omj.2028.17

18. Cong L, Wang S, Yeung SY, Lee JH, Chung JP, Chan DY. Mature cystic teratoma: An integrated review. *Int J Mol Sci*. 2023;24(7):6141.

doi: 10.3390/ijms24076141

19. Aggarwal P, Kehoe S. Ovarian tumours in pregnancy: A literature review. *Eur J Obstet Gynecol Reprod Biol*. 2011;155(2):119-124.

doi: 10.1016/j.ejogrb.2010.11.023

20. Cohen-Herriou K, Semal-Michel S, Lucot JP, Poncelet E, Rubod C. Management of ovarian cysts during pregnancy: Lille's experience and literature review. *Gynecol Obstet Fertil*. 2013;41(1):67-72.

doi: 10.1016/j.gyobfe.2012.12.001

21. Chen LH, Chang SD, Huang HY, Wang HS, Soong YK, Wu HM. Repeated pregnancy with concomitant presence of ovarian teratoma: A case report and literature review. *Taiwan J Obstet Gynecol*. 2017;56(5):694-696.

doi: 10.1016/j.tjog.2017.08.021

22. Schreck AM, Mikdachi HF. Benign ovarian tumors in pregnancy: A case report of metachronous ipsilateral recurrent mucinous cystadenoma in initial pregnancy and mature cystic teratoma in subsequent pregnancy. *Cureus*. 2019;11(1):e3818.

doi: 10.7759/cureus.3818

23. Gbary-Lagaud E, Effoh D, Ehui A, Koffi S, Houphouet-Mwandji C, Adjoby R. Mature ovarian teratoma and pregnancy about a case in Abidjan Cote d'Ivoire. *J Gynecol Obstet*. 2020;8(4):117-121.

doi: 10.11648/j.jgo.20200804.19

24. Spasimir TS. A collision tumor of the ovary during pregnancy-rare combination. *J Med Clin Res Rev*. 2019;3(6):1-3.

ACCSCIENCE PUBLISHING

Tumor Discovery

CASE REPORT

Chemotherapy-induced ileus and gastrointestinal hemorrhage following therapy with BrECADD for Hodgkin lymphoma: A case report

Karl Mayrhofer* and Simon Udovica

Department of Internal Medicine I., Centre for Oncology and Haematology, Vienna Healthcare Group, Ottakring, Vienna, Austria

Abstract

A 62-year-old male with newly diagnosed advanced-stage Hodgkin lymphoma (HL) developed life-threatening gastrointestinal (GI) complications during brentuximab vedotin, etoposide, cyclophosphamide, doxorubicin, dacarbazine, and dexamethasone chemotherapy. He presented with chemotherapy-induced enteritis and jejunal ileus, followed by severe GI bleeding requiring two consecutive laparotomies and segmental jejunal resections. Histology revealed ulcerative jejunitis without signs of lymphoma infiltration. His medical course was further complicated by acute renal failure requiring dialysis. Although the patient temporarily stabilized with intensive care management, he subsequently developed Candida sepsis. At the time of submission, his outcome remains uncertain. This case underscores a rare but serious occurrence of GI toxicity associated with intensive chemotherapy for HL.

Keywords: Ileus; Enteritis; Hemorrhage; BrECADD; Hodgkin lymphoma

***Corresponding author:**
Karl Mayrhofer
(karl.mayrhofer@posteo.de)

Citation: Mayrhofer K, Udovica S. Chemotherapy-induced ileus and gastrointestinal hemorrhage following therapy with BrECADD for Hodgkin lymphoma: A case report. *Tumor Discov*. 2025;4(3):105-109. doi: 10.36922/TD025180033

Received: May 1, 2025

Revised: June 12, 2025

Accepted: July 2, 2025

Published online: July 21, 2025

1. Background

Hodgkin lymphoma (HL) is a highly curable malignancy with a range of effective chemotherapeutic regimens. While hematological and infectious complications are well-documented, gastrointestinal (GI) complications such as chemotherapy-induced ileus remain poorly characterized. This report presents a rare case of enteritis complicated by ileus, GI hemorrhage, and renal failure, following brentuximab vedotin (BV), etoposide, cyclophosphamide, doxorubicin, dacarbazine, and dexamethasone (BrECADD) chemotherapy.[1]

2. Case presentation

A 62-year-old male patient with a medical history of arterial hypertension, obesity, and hypothyroidism presented for evaluation of prolonged coughing. Imaging studies revealed extensive mediastinal tumor mass, bilateral pleural effusions, and a pericardial effusion. A computed tomography-guided biopsy confirmed the diagnosis of HL. The patient was then referred to our oncology department for treatment initiation.

Staging workup revealed advanced-stage HL with a large mediastinal mass and associated pleural and pericardial effusions (Figure 1). Before initiating chemotherapy, right-sided pleural drainage and pericardial drainage were necessary. The patient was then started on systemic therapy according to the BrECADD protocol in accordance with the German Hodgkin Study Group recommendations for patients up to 75 years of age.[2]

On day 5 of chemotherapy, the patient developed diarrhea consistent with chemotherapy-induced enteritis. Stool cultures were negative. Several days later, he experienced abdominal pain and vomiting. Imaging revealed a mechanical ileus caused by jejunal stenosis (Figure 2). The patient had no prior history of abdominal surgery, and there was no radiological evidence of abdominal lymphoma involvement. Although surgical intervention was indicated, it was not performed as it was deemed unfeasible due to chemotherapy-induced aplasia. Conservative management with a nasogastric tube, prokinetic agents (neostigmine and metoclopramide), fluid replacement, parenteral nutrition, and antibiotic therapy (meropenem) led to resolution of the ileus over the next several days.

Subsequently, the patient experienced acute GI bleeding resulting in hemorrhagic shock. The patient had to be transferred to the intensive care unit for vasopressor support. Emergency laparoscopy identified a bleeding jejunal ulcer, requiring segmental small bowel resection. A second laparotomy with additional jejunal resection was necessary a few days later due to recurrent bleeding. Histopathological analysis of the resected jejunal segments revealed severe ulcerative jejunitis without evidence of lymphoma infiltration.

The patient also developed dialysis-dependent acute tubular necrosis and transient hyperbilirubinemia. The renal failure was attributed to both the cytotoxic effects of chemotherapy and the neutropenic enteritis.

Following a prolonged intensive care unit stay, the patient was eventually transferred to the general ward. After a brief period of recovery, he unfortunately developed Candida sepsis, requiring catecholamine support and endotracheal intubation. At the time of manuscript submission, his outcome remains uncertain. In the event of sufficient recovery, a de-escalated treatment regimen for his HL is planned, most likely incorporating nivolumab.

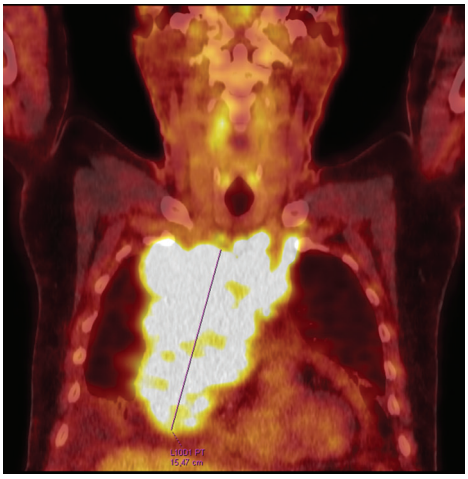

Figure 1. Positron emission tomography scan showing the large mediastinal tumor mass

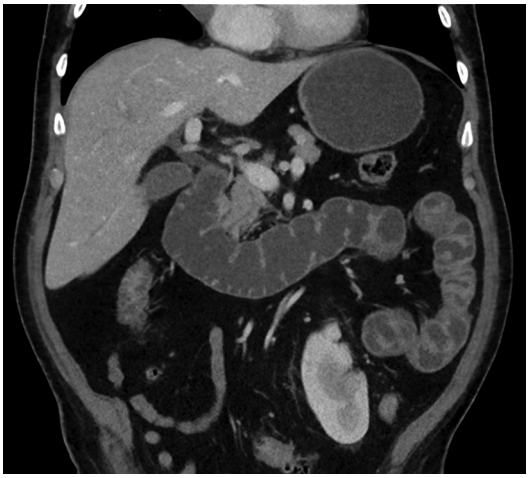

Figure 2. Computed tomography scan showing high ileus with distention of the stomach and a jejunal bowel segment

3. Discussion

3.1. Chemotherapy-induced ileus

Chemotherapy-induced (GI) toxicity encompasses a spectrum of adverse effects, including nausea, vomiting, diarrhea, constipation, and mucositis. Among these, bowel obstruction is a rare but potentially life-threatening complication. The pathophysiology involves direct cytotoxic effects on enteric neurons and smooth muscle cells, leading to impaired motility. In addition, chemotherapy-induced mucosal injury can disrupt the gut barrier, promoting bacterial translocation and systemic inflammation, which may exacerbate ileus and contribute to sepsis.[3]

Reports of chemotherapy-induced ileus are quite rare in the scientific literature. Published case reports exist for a variety of chemotherapeutic agents and most patients were successfully managed without surgery.[4-9]

BV has been associated with a range of GI complications, including intestinal obstruction, (neutropenic) enterocolitis, erosion, ulceration, perforation, and hemorrhage, some of which have resulted in patient deaths.[10] A meta-analysis of four lymphoma trials involving over 2,000 patients found an increased incidence of GI adverse events in the

BV treatment group.[11] In addition, a review of the Food and Drug Administration adverse event reporting system indicated that antibody-drug conjugates, including BV, may elevate the risk of a broad spectrum of GI adverse events.[12]

In our patient, neutropenic enteritis likely led to mucosal compromise, stenosis, and eventual bleeding. The absence of prior surgeries and lymphoma involvement suggests a direct link to chemotherapy toxicity. Our patient was initially managed conservatively with nasogastric decompression, prokinetic agents, intravenous fluids, parenteral nutrition, and antibiotics. Despite initial resolution, the patient experienced severe GI bleeding, necessitating surgical intervention and intensive care support.

3.2. Chemotherapy-associated GI hemorrhage

GI bleeding is a well-recognized complication in cancer patients undergoing chemotherapy. However, massive GI hemorrhage resulting in hemodynamic compromise is a rare and serious event. The management of GI bleeding in this population involves a multidisciplinary approach that combines supportive care with targeted interventional procedures.[13]

Initial treatment typically includes transfusion of blood products such as red blood cells, platelets, fresh frozen plasma, and coagulation factors to stabilize the patient and correct any underlying coagulopathies. Endoscopic techniques play a central role in controlling bleeding and may include argon plasma coagulation, hemoclipping, or epinephrine injection, depending on the source and severity of the hemorrhage.[13]

In cases where endoscopic therapy is either unsuccessful or not feasible, trans-arterial embolization has emerged as an effective alternative.[14] Surgical intervention remains a last resort, reserved for refractory cases, but it is associated with a significantly higher risk – particularly in patients with advanced malignancies or poor performance status.

A retrospective analysis of 156 patients with pancreatic cancer undergoing chemoradiation found that approximately 25% experienced GI bleeding, most commonly from the upper GI tract. Among these, there were eight fatal cases. Management strategies in that cohort included transfusion support, pharmacologic measures, and endoscopic therapy, which demonstrated a high success rate in most patients.[15]

3.3. Contemporary treatment strategies for advanced-stage HL: Spotlight on BrECADD and Nivo-AVD

The BrECADD regimen – comprising BV, etoposide, cyclophosphamide, doxorubicin, dacarbazine, and dexamethasone – was developed to improve the treatment of advanced-stage classical HL (AS-cHL) by enhancing efficacy while reducing toxicity. The phase 3 HD21 trial, a multicenter, open-label, randomized study, compared BrECADD with the escalated bleomycin, etoposide, doxorubicin, cyclophosphamide, vincristine, procarbazine, and prednisone (BEACOPP) regimen in patients aged 18 – 60 years with newly diagnosed AS-cHL.[1] The trial demonstrated that BrECADD was superior to BEACOPP in terms of progression-free survival (PFS) and had a more favorable safety profile. At a median follow-up of 48 months, the 4-year PFS was 94.3% for BrECADD compared to 90.9% for BEACOPP (hazard ratio: 0.66; p=0.035). Furthermore, treatment-related morbidity was significantly lower in the BrECADD group (42%) compared to the BEACOPP group (59%; p<0.0001). Notably, the BrECADD regimen was associated with a lower incidence of severe sensory polyneuropathy and improved recovery rates of gonadal function compared to BEACOPP. The reported rate of severe GI adverse events was 8% for the BrECADD cohort, apparently without any cases of bowel obstruction.

A single-arm cohort within the phase II HD21 trial, examining the BrECADD protocol in adults up to 75 years of age, concluded that the regimen is feasible and safe in older patients, although it requires more frequent dose adjustments.[16]

Historically, patients older than 60 years received ABVD (doxorubicin, bleomycin, vinblastine, and dacarbazine) therapy.[2] This treatment standard has since evolved – first to BV, doxorubicin, vinblastine, and dacarbazine (BV-AVD) and more recently to nivolumab, doxorubicin, vinblastine, and dacarbazine (Nivo-AVD).[17,18] The phase III S1826 study demonstrated significantly improved outcomes and a more favorable safety profile with six cycles of Nivo-AVD compared to BV-AVD.[18] The complete remission rate at the end of treatment with Nivo-AVD was 83.1%, which is similar to the 82% reported with BrECADD. After a median follow-up of 2.1 years, the 2-year PFS for the overall cohort, as well as for the subgroup of patients aged 18 – 60 years, was 92%. Although numerically slightly lower than the PFS reported for BrECADD, direct comparison of these results is not appropriate due to significant differences in trial design and populations. For instance, the S1826 trial included patients younger than 18 years and those aged 60 and above, and enrolled a racially and ethnically diverse population. Nevertheless, the safety profile of Nivo-AVD is clearly more favorable, with fewer severe adverse events and treatment discontinuations due to toxicity compared to BrECADD.[1,18]

3.4. Clinical considerations of chemotherapy selection in our patient

In our patient, we opted to administer BrECADD due to the highly aggressive and symptomatic nature of the disease. Before diagnosis, the patient was in excellent

physical condition, with an ECOG performance status of 0. His comorbidities were considered clinically insignificant. Therefore, despite his age being over 60 years, we elected to proceed with the more intensive BrECADD regimen.

As this case illustrates, careful patient selection is critical when considering intensive chemotherapy in older or comorbid individuals, to minimize the risk of excessive toxicity, as was unfortunately observed in our patient. Based on this experience, we will adopt a more conservative approach moving forward, reserving intensive regimens such as BrECADD for younger patients with adequate performance status and minimal comorbidity burden.

4. Conclusion

This case report highlights the rare but potentially life-threatening complication of chemotherapy-induced ileus in a patient with AS-cHL treated with the BrECADD regimen. Although GI toxicity, including diarrhea and mucositis, is well documented in chemotherapy, bowel obstruction remains an uncommon manifestation. In this case, chemotherapy-induced enteritis likely triggered ileus, which was further complicated by GI hemorrhage and acute renal failure. Despite initial conservative management, the patient required surgical intervention due to recurrent bleeding. Our case demonstrates that careful patient selection is essential when considering intensive chemotherapy regimens such as BrECADD. Close monitoring for GI symptoms is crucial during treatment.

Acknowledgments

None.

Funding

None.

Conflict of interest

The authors declare they have no competing interests.

Author contributions

Conceptualization: Karl Mayrhofer
Investigation: Karl Mayrhofer
Writing – original draft: Karl Mayrhofer
Writing – review & editing: Simon Udovica

Ethics approval and consent to participate

Not applicable.

Consent for publication

Informed consent was obtained from the patient for the publication of this case report and any accompanying images. The patient agreed to the use of clinical details for academic and publication purposes. All data have been fully anonymized to protect the patient's identity.

Availability of data

Not applicable.

References

1. Borchmann P, Ferdinandus J, Schneider G, *et al*. Assessing the efficacy and tolerability of PET-guided BrECADD versus eBEACOPP in advanced-stage, classical Hodgkin lymphoma (HD21): A randomised, multicentre, parallel, open-label, phase 3 trial. *Lancet*. 2024;404(10450):341-352.

   doi: 10.1016/S0140-6736(24)01315-1

2. German Hodgkin Study Group. *Therapy - GHSG*. Available from: https://en.ghsg.org/treatment [Last accessed on 2025 Jun 08].

3. Akbarali HI, Muchhala KH, Jessup DK, Cheatham S. Chemotherapy induced gastrointestinal toxicities. *Adv Cancer Res*. 2022;155:131-166.

   doi: 10.1016/bs.acr.2022.02.007

4. Carraro F, Rivetti E, Romano E, Fagioli F. Two cases of paralitic ileus in onco-hematologic patients. *Pediatr Rep*. 2012;4(1):e3.

   doi: 10.4081/pr.2012.e3

5. Mourad AP, De Robles MS. Chemoimmunotherapy-related enteritis resulting in a mechanical small bowel obstruction - a case report. *Int J Surg Case Rep*. 2021;79:131-134.

   doi: 10.1016/j.ijscr.2020.12.096

6. Jiao XD, Luo X, Qin WX, Yuan LY, Zang YS. Paralytic ileus due to a novel anticancer drug, nab-paclitaxel: A case report. *Mol Clin Oncol*. 2016;4(5):824-826.

   doi: 10.3892/mco.2016.782

7. Roy R, Sarkar S. Paralytic ileus - a rare but serious side-effect of oral capecitabine. *Int J Anat Radiol Surg*. 2022;11(1):SC01-SC02.

   doi: 10.7860/IJARS/2022/56456.2843

8. Kumar KS, Balaji P, Muppa L. Paralytic ileus as a rare complication of vincristine therapy: A case report. *Ind J Pharm Pract*. 2024;14(4):396-399.

   doi: 10.5530/ijopp.17.4.65

9. Balu A, Nagarajan T, Mudawi H. Chemotherapy induced small bowel obstruction in small cell lung cancer. *Arab J Gastroenterol*. 2021;22(3):246-248.

   doi: 10.1016/j.ajg.2021.07.001

10. European Medicines Agency. *Adcetris: EPAR - Product Information*. Amsterdam: EMA; 2024. Available from: https://www.ema.europa.eu/en/documents/product-

information/adcetris-epar-product-information_en.pdf [Last accessed on 2025 Jun 08].

11. Gao S, Zhang M, Wu K, *et al*. Risk of adverse events in lymphoma patients treated with brentuximab vedotin: A systematic review and meta-analysis. *Expert Opin Drug Saf*. 2020;19(5):617-623.

    doi: 10.1080/14740338.2020.1718103

12. Shi Y, Yao K, Zhao J, Yue Y, Wu H. Gastrointestinal toxicity of antibody-drug conjugates: A pharmacovigilance study using the FAERS database. *BMC Pharmacol Toxicol*. 2025;26:50.

    doi: 10.1186/s40360-025-00877-4

13. O'Brien JW, Rogers M, Gallagher M, Rockall T. Management of massive gastrointestinal haemorrhage. *Surgery (Oxford)*. 2022;40(9):582-592.

14. Hall T, Temperley HC, Mac Curtain BM, *et al*. Transcatheter arterial embolisation (TAE) to treat acute upper gastrointestinal bleeding secondary to gastric cancer: A systematic review and meta-analysis. *Surgeon*. 2024;22(6):e213-e220.

    doi: 10.1016/j.surge.2024.09.009

15. Lee KJ, Kim HM, Jung JW, *et al*. Gastrointestinal hemorrhage after concurrent chemoradiotherapy in locally advanced pancreatic cancer. *Gut Liver*. 2013;7(1):106-111.

    doi: 10.5009/gnl.2013.7.1.106

16. Ferdinandus J, Kaul H, Fosså A, *et al*. PET-guided brecadd in older patients with advanced-stage classic hodgkin lymphoma: Results of the phase 2 part of the GHSG HD21 trial. *Blood*. 2024;144 Suppl 1:568–568.

17. Connors JM, Jurczak W, Straus DJ, *et al*. Brentuximab vedotin with chemotherapy for stage III or IV hodgkin's lymphoma. *N Engl J Med*. 2018;378(4):331-344.

    doi: 10.1056/NEJMoa1708984

18. Herrera AF, LeBlanc M, Castellino SM, *et al*. Nivolumab+AVD in advanced-stage classic hodgkin's lymphoma. *N Engl J Med*. 2024;391(15):1379-1389.

    doi: 10.1056/NEJMoa2405888

ACCSCIENCE PUBLISHING

Tumor Discovery

LETTER TO EDITOR

Redefining the role of radiation oncologists in the AI era

Melek Yakar*

Department of Radiation Oncology, Faculty of Medicine, Osmangazi University, Eskişehir, Turkey

Dear Editor,

Recent years have seen significant acceleration in the integration of artificial intelligence (AI) into radiation oncology practice. From automated contouring to treatment planning optimization and big data analytics, AI offers remarkable advantages in terms of efficiency and accuracy. However, this rapid transformation has also begun to redefine the role of radiation oncologists in clinical decision-making. In this letter, I aim to highlight the potential risk of physicians becoming distanced from critical decisions – and even professionally isolated – as AI assumes a larger role, while also emphasizing the importance of preserving core values such as ethics, autonomy, and empathy throughout this transition.

While AI-driven systems have demonstrated superior performance in several aspects of radiation oncology – such as patient assessment, clinical decision-making, segmentation, dose prediction, and outcome modeling – it is essential to recognize that these tools are only as reliable as the data they are trained on. Radiation oncologists must continue to utilize their expertise in clinical guidelines, patient data, and multidisciplinary assessments to make the best treatment decisions. Each individual's situation is unique, and the decision-making process requires both big data analysis and clinical experience due to disease-specific factors. AI-powered systems can accelerate and support doctors' decisions by providing recommendations based on clinical guidelines. The advantages of clinical decision support systems are that they reduce the margin of error by assisting doctors, analyzing complex patient data more effectively, and recommending the best treatment options for each patient, all while accelerating decision-making in multidisciplinary workflows. However, clinical decisions should not be left entirely to AI. Human oversight is essential to ensure the best outcomes and further validation is needed for clinical acceptance.[1,2]

One of the most time-consuming steps in treatment planning is organ and target volume segmentation. AI-based methods, such as U-Net/TransU-Net convolutional neural network models, have been utilized to reduce segmentation time, making it much faster than manual processes, which can take hours.[3-6] Despite these advancements, full automation is still not possible. Clinical validation is required, and manual corrections may still be necessary in certain cases, such as low-contrast tumors. In addition, clinical integration of these systems requires time, training, and standardization of evaluation criteria.[7]

Synthetic computed tomography (CT) images, generated from magnetic resonance imaging data using AI-based algorithms, are becoming increasingly utilized in radiotherapy planning. Synthetic CT provides an alternative to conventional CT by offering accurate electron density information, which reduces radiation exposure and improves workflow efficiency. However, challenges such as inter-vendor variability and

***Corresponding author:**
Melek Yakar
(myakar@ogu.edu.tr)

Citation: Yakar M. Redefining the role of radiation oncologists in the AI era. *Tumor Discov*. 2025;4(3):110-112.
doi: 10.36922/TD025200039

Received: May 15, 2025

Accepted: May 22, 2025

Published online: June 10, 2025

anatomical accuracy still remain key areas for further research and standardization. The generative adversarial networks algorithm has shown promise in generating clearer, more detailed synthetic images, offering an advantage in image clarity compared to traditional methods.[8,9]

AI-assisted adaptive radiotherapy offers significant advantages for patients with frequent anatomical changes, such as those with head and neck, lung, or gynecological cancers. Daily cone beam CT imaging allows real-time evaluation, while AI-based auto-contouring enables rapid delineation of tumors and organs at risk. Treatment plans can be updated instantly based on anatomical shifts. However, limitations such as suboptimal image quality and the need for expert validation of AI-generated contours highlight the continued importance of human oversight in clinical decision-making.[10]

Prognostic estimations in radiation oncology have traditionally relied on clinical and anatomical data. However, AI-based models now enable more precise predictions by integrating biological, clinical, dosimetric, treatment, and imaging data.[11,12] Toxicity prediction is equally crucial for developing personalized treatment plans, minimizing both acute and late side effects, and ultimately improving patient quality of life.[13,14] Predictive models, especially those using hybrid approaches, combine radiomic/dosiomic features with clinical and dosimetric parameters to improve both prognosis and toxicity prediction. Challenges include ensuring clinically acceptable model accuracy, ensuring data diversity, and navigating regulatory requirements, such as Food and Drug Administration approval.

As AI continues to reshape the landscape of radiation oncology, it is clear that the role of the radiation oncologist will evolve.[15] With AI automating routine tasks, clinicians are expected to focus more on patient monitoring and complex decision-making. This shift necessitates new competencies, including understanding AI algorithms, interpreting data, and considering ethical implications. Radiation oncologists will need to collaborate with multidisciplinary teams and develop skills in data literacy and clinical validation of AI tools.

As AI becomes increasingly integrated into radiation oncology, several ethical challenges must be addressed. These include ensuring patient privacy through data anonymization and cybersecurity, defining accountability in AI-assisted clinical decisions, and mitigating bias arising from non-representative training datasets. Equitable access to AI tools is a concern, as is the potential erosion of physicians' decision-making autonomy. It is crucial to maintain a strong patient–physician relationship, ensure informed consent for AI use, and respect patients' rights to refuse AI-based interventions. In addition, the environmental impact of AI systems, including energy consumption and e-waste, must be considered.[16,17]

In conclusion, AI is expected to play a central role in shaping the future of radiation oncology. Personalized treatment protocols, biomarker-driven dose adaptation, and even fully autonomous treatment planning may become the norm. However, strong ethical oversight, legal frameworks, and sustainable implementation models will be essential for this integration. Radiation oncologists will need not only medical expertise but also a solid understanding of AI technologies. As the field evolves, the focus will shift from technical tasks to clinical decision-making and patient-centered care, making it essential for radiation oncologists to redefine their roles and actively integrate into multidisciplinary care teams to remain indispensable in an increasingly automated landscape.

Conflict of interest

The author declares that she has no conflict of interest.

References

1. Wang L, Chen X, Zhang L, *et al*. Artificial intelligence in clinical decision support systems for oncology. *Int J Med Sci*. 2023;20(1):79-86.

   doi: 10.7150/ijms.77205

2. Nafees A, Khan M, Chow R, *et al*. Evaluation of clinical decision support systems in oncology: An updated systematic review. *Crit Rev Oncol Hematol*. 2023;192:104143.

   doi: 10.1016/j.critrevonc.2023.104143

3. Erden MB, Cansiz S, Caki O, *et al*. FourierLoss: Shape-aware l function with Fourier descriptors. *Neurocomputing*. 2025;638:130155.

   doi: 10.1016/j.neucom.2025.130155

4. Chen M, Wu S, Zhao W, Zhou Y, Zhou Y, Wang G. Application of deep learning to auto-delineation of target volumes and organs at risk in radiotherapy. *Cancer Radiother*. 2022;26(3):494-501.

   doi: 10.1016/j.canrad.2021.08.020

5. Matoska T, Patel M, Liu H, Beriwal S. Review of deep learning based autosegmentation for clinical target volume: Current status and future directions. *Adv Radiat Oncol*. 2024;9(5):101470.

   doi: 10.1016/j.adro.2024.101470

6. Wang TW, Hong JS, Huang JW, Liao CY, Lu CF, Wu YT. Systematic review and meta-analysis of deep learning applications in computed tomography lung cancer segmentation. *Radiother Oncol*. 2024;197:110344.

doi: 10.1016/j.radonc.2024.110344

7. Mackay K, Bernstein D, Glocker B, Kamnitsas K, Taylor A. A review of the metrics used to assess auto-contouring systems in radiotherapy. *Clin Oncol (R Coll Radiol)*. 2023;35(6):354-369.

   doi: 10.1016/j.clon.2023.01.016

8. Bahloul MA, Jabeen S, Benoumhani S, Alsaleh HA, Belkhatir Z, Al-Wabil A. Advancements in synthetic CT generation from MRI: A review of techniques, and trends in radiation therapy planning. *J Appl Clin Med Phys*. 2024;25(11):e14499.

   doi: 10.1002/acm2.14499

9. Giraud P, Bibault JE. Artificial intelligence in radiotherapy: Current applications and future trends. *Diagn Interv Imaging*. 2024;105(12):475-480.

   doi: 10.1016/j.diii.2024.06.001

10. Byrne M, Archibald-Heeren B, Hu Y, *et al*. Varian ethos online adaptive radiotherapy for prostate cancer: Early results of contouring accuracy, treatment plan quality, and treatment time. *J Appl Clin Med Phys*. 2022;23(1):e13479.

    doi: 10.1002/acm2.13479

11. Zwanenburg A, Price G, Löck S. Artificial intelligence for response prediction and personalisation in radiation oncology. *Strahlenther Onkol*. 2025;201(3):266-273.

    doi: 10.1007/s00066-024-02281-z

12. Akcay M, Etiz D, Celik O. Prediction of survival and recurrence patterns by machine learning in gastric cancer cases undergoing radiation therapy and chemotherapy. *Adv Radiat Oncol*. 2020;5(6):1179-1187.

    doi: 10.1016/j.adro.2020.07.007

13. Kraus KM, Oreshko M, Schnabel JA, Bernhardt D, Combs SE, Peeken JC. Dosiomics and radiomics-based prediction of pneumonitis after radiotherapy and immune checkpoint inhibition: The relevance of fractionation. *Lung Cancer*. 2024;189:107507.

    doi: 10.1016/j.lungcan.2024.107507

14. Isaksson LJ, Pepa M, Zaffaroni M, *et al*. Machine learning-based models for prediction of toxicity outcomes in radiotherapy. *Front Oncol*. 2020;10:790.

    doi: 10.3389/fonc.2020.00790

15. Bitterman DS, Miller TA, Mak RH, Savova GK. Clinical natural language processing for radiation oncology: A review and practical primer. *Int J Radiat Oncol Biol Phys*. 2021;110(3):641-655.

    doi: 10.1016/j.ijrobp.2021.01.044

16. Naik N, Hameed BMZ, Shetty DK, *et al*. Legal and ethical consideration in artificial intelligence in healthcare: Who takes responsibility? *Front Surg*. 2022;9:862322.

    doi: 10.3389/fsurg.2022.862322

17. Lahmi L, Mamzer MF, Burgun A, Durdux C, Bibault JE. Ethical aspects of artificial intelligence in radiation oncology. *Semin Radiat Oncol*. 2022;32(4):442-448.

    doi: 10.1016/j.semradonc.2022.06.013

Our Journals

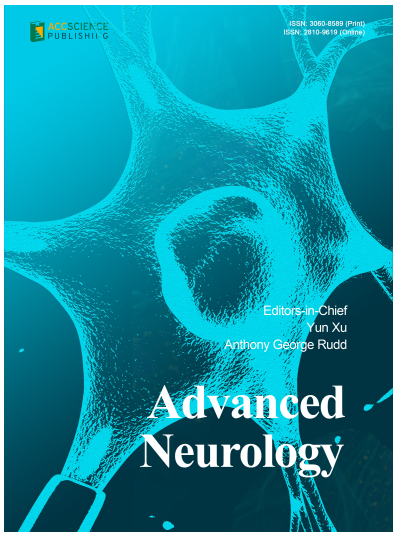

Advanced Neurology is a peer-reviewed and open-access journal that aims to publish and disseminate novel research in the breadth of neurology and neuroscience. The journal aims to advance our understanding in the nervous system and provide a platform to neuroscientists and physicians to showcase their findings in original fundamental and clinical research as well as to present new ideas that highlight the changes in the neurological clinical practice.

Advanced Neurology covers subject areas, including but not limited to the following:

- Neurological disorders
- Neurodegenerative disease
- Cerebrovascular disease
- Epilepsy and movement disorders
- Neuroimmune disease
- Neurological infections
- Muscle disease
- Molecular and cellular neuroscience
- Systems neuroscience
- Cognitive neuroscience
- Computational modeling of nervous system

Global Translational Medicine is a quarterly journal that focuses on medicine, biological sciences, and biomaterials engineering. The goal of *Global Translational Medicine* is to provide a platform to researchers for showcasing their latest research works in translational medicine so as to advance the field towards the betterment of human health. Despite the advancement of omics and new technologies, the process of transforming these technologies and scientific research results into effective therapies and putting them into clinical use still has a long way to go. *Global Translational Medicine* provides a platform to fill the gaps in preclinical and inter-disciplinary research, to promote clinical translation of scientific research results, and to contribute to the conception of new and improved preventive measures as well as diagnostic and therapeutic techniques of diseases.

Global Translational Medicine covers the following themes: cardiovascular disease, metabolism/diabetes/obesity, neuroscience/neurology, cancer, biomaterials and their applications in medicine, proteomics/metabolomics, pharmacogenomics, biomarkers, bioinformatics and data mining, animal and clinical research, and medical methods arising from interdisciplinary crossover.

Start a new journal

Write to us via email if you are interested to start a new journal with AccScience Publishing. Please attach your CV, professional profile page and a brief pitch proposal in your email. We shall inform you of our decision whether we are interested to collaborate in starting a new journal.

Contact: info@accscience.com

https://accscience.com/journal/TD

Contact

www.accscience.com

9 Raffles Place, Republic Plaza 1 #06-00 Singapore 048619

Email: editorial@accscience.com

Phone: +65 8182 1586